The University of Nottingham
UNITED KINGDOM · CHINA · MALAYSIA

Shermado, Fairouz M. (2014) Molecular characterization of cannabinoids and free fatty acid receptors in human and rat skeletal muscle. PhD thesis, University of Nottingham.

Access from the University of Nottingham repository:
http://eprints.nottingham.ac.uk/14145/1/Fairouz_Shermado.pdf

Copyright and reuse:

The Nottingham ePrints service makes this work by researchers of the University of Nottingham available open access under the following conditions.

- Copyright and all moral rights to the version of the paper presented here belong to the individual author(s) and/or other copyright owners.
- To the extent reasonable and practicable the material made available in Nottingham ePrints has been checked for eligibility before being made available.
- Copies of full items can be used for personal research or study, educational, or not-for-profit purposes without prior permission or charge provided that the authors, title and full bibliographic details are credited, a hyperlink and/or URL is given for the original metadata page and the content is not changed in any way.
- Quotations or similar reproductions must be sufficiently acknowledged.

Please see our full end user licence at:
http://eprints.nottingham.ac.uk/end_user_agreement.pdf

A note on versions:

The version presented here may differ from the published version or from the version of record. If you wish to cite this item you are advised to consult the publisher's version. Please see the repository url above for details on accessing the published version and note that access may require a subscription.

For more information, please contact eprints@nottingham.ac.uk

MOLECULAR CHARACTERISATION OF CANNABINOID AND FREE FATTY ACID RECEPTORS IN HUMAN AND RAT SKELETAL MUSCLE

Fairouz M. Shermaddo, MBChB, MSc

Thesis submitted to the University of Nottingham for the degree of Doctor of Philosophy

September 2013

Abstract

The mechanisms underlying the development of insulin resistance in skeletal muscle are very complex and are not completely understood. Insulin resistance in skeletal muscle is of particular importance because muscle is the major site of insulin stimulated glucose uptake. Skeletal muscle is one of the major insulin sensitive organs and it is responsible for 80% of insulin stimulated glucose disposal as well as fatty acid oxidation. Elevated circulating free fatty acids (FFAs) and their derivatives such as endocannabinoids (ECs) have been described in obesity and are thought to be influential in the development of muscle insulin resistance. While several hypotheses have been put forward to explain the mechanisms by which FFAs and ECs may cause insulin resistance, there are still many potential signalling pathways which may be involved that have not yet been examined. The main aim of this thesis was to characterize the role of the cannabinoid receptors and free fatty acid receptor 1 (GPR40) in cell signalling in human and rat skeletal muscle tissue and primary cultured myotubes. Gene expression profiling of human skeletal muscle and cultured myotubes and myoblasts indicated that the cannabinoid receptor CB1 and GPR40 were expressed at low levels and these results were confirmed using Taqman QRTPCR. CB2 receptor expression was only detected in rat tissue and as a result was not further studied in cell culture systems. When global gene expression profiles were further examined it was evident that whilst cultured myotubes retained many characteristics of skeletal muscle tissue, the phenotype appeared to be closer to fetal than adult muscle. Furthermore, when metabolic gene expression networks were analysed using pathway based analysis, it was apparent that expression of genes involved in oxidative phosphorylation, insulin signalling and glucose transport were markedly reduced in cultured cells. The most striking example being GLUT4 which was expressed at approximately 3000-fold lower levels in cell culture as compared to tissue.

The functionality of CB1 and GPR40 receptors was demonstrated using selective agonists and antagonists. CB1 activation by both synthetic and endogenous ligands was confirmed using phosphorylation of ERK1 and 2 as was the presence of functional GPR40 protein in myotubes. Neither agonists nor antagonists of CB1 or GPR40 receptors were found to modulate insulin signalling as determined by phosphorylation of downstream targets Akt and GSK3α/β.

Global expression profiling was also carried out on myotubes treated with GPR40 agonists and antagonists obtained from AstraZeneca. No changes in metabolic or insulin signalling genes were observed. Rather, antagonists of GPR40 appear to activate gene expression networks involved in cell proliferation – in particular an elevation in the ERBB2 signalling pathway.

Poster presentation

Fairouz Shermado, Kostas Tsintzas and Andrew J. Bennett. Cannabinoid Receptors in Human and Rat (Wistar and Zucker) Skeletal Muscle. 6th European Workshop on Cannabinoid Research, 2013, Dublin, Ireland.

Fairouz Shermado, Kostas Tsintzas and Andrew J. Bennett. Characterization and Functional Significance of Cannabinoid Receptors in Skeletal Muscle. BPS, Winter meeting, 2012, London, UK

Acknowledgements

Praise be to Allah

I would like to thank my primary supervisor Dr Andrew Bennett for the expert guidance, and support throughout my PhD studies. I am also grateful to Dr Kostas Tsintzas for the additional supervisory support and encouragment.

Thanks also to Dr. Steve Alexander for readily offering help and advice whenever called upon. I am eternally grateful for the help and support from friends and colleagues in the FRAME lab. Special thanks to Monika Owen and Roya Jaddi for the technical and social support.

I recognize that this research would not have been possible without the financial assistance of Libyan Higher Education.

To my mother, sisters and brothers I say, thanks for believing in me. Your prayers, words of encouragement and support have been very helpful in getting me here. You kept me going when the going seemed tough and insurmountable. I continue to realize and appreciate in new ways how fortunate I am to have such family.

To my husband, thanks for your immense help, love and solid support, without your encouragement and immeasurable assistance I would not have finished this thesis. I wish you the best for your PhD study. To my adorable daughters (Alla and Asma) and sons (Mohamed and Ahmed) I say, sorry for not spending much time with you, breaking my promises (occasionally!) and thanks for your love. I now hope we can enjoy our family life and I will do my best to be "a real mum who cares about her children more than her work" as you wished once.

I would like to dedicate this thesis to the soul of my father who had always been, and continue to be, my inspiration. I could never adequately express all that he has given to me, or all that he has meant to me.

Above all, glory and honour go to God almighty, for granting me the strength, the will to succeed even in the face of adversity, and for his abundant mercies and blessings upon my life.

Declaration

I hereby declare that the work presented in this thesis, has not been submitted for any degree or diploma, at this, or any other university, and that all of the experiments, unless otherwise stated, were performed by me.

Dr. Fairouz M. Shermado

Contents

List of Figures

List of Tables

List of Abbreviations

AA: Arachidonic acid

ACC: Acetyl-CoA carboxylase

ACEA: Arachidonyl-2-chloroethylamide

Actb: Beta-actin

AEA: N-arachidonoylethanolamine (anandamide)

2-AG: 2-Arachidonoylglycerol

AKT: Serine threonine kinase/protein kinase B

AM251: 1-(2, 4-dichlorophenyl)-5-(4-iodophenyl)-4-methyl-N-(1-piperidyl) pyrazole-3-carboxamide

ANOVA: Analysis of variance

APS: Ammonium persulphate

AZ: Astra Zeneca

BMI: Body mass index

cAMP: Cyclic-adenosine monophosphate

CBI: Cannabinoid receptor 1

CB2: Cannabinoid receptor 2

cDNA: Complementary DNA

CPT1: Carnitine palmitoyl transferase 1

CT: Cycle threshold

DAG: Diacylglycerol

DAGL: Diacylglycerol lipase

DGK: Diacylglycerol kinase

DMSO: Dimethyl sulfoxide

EC: Endocannabinoids

EDL: Extensor digitorum longus

FA: fatty acid

FAAH: Fatty acid amide hydrolase

FAS/FASN: Fatty acid synthase

FFA: Free fatty acid

FOXO: Forkhead box

Fura-22AM: L-[2-(carboysyloxazol-2-yl)-6-amino-benzofuran-5-oxy]-2-(2'-amino-5'methylphenoxy) ethane-N,N,N,N-tetraacetic acid pentaacetoxymethyl ester; fura 2-acetoxymethyl ester.

GLUT4: Glucose transporter-4

GR: Gastrocnemius red portion

GSK3: Glycogen synthase kinase 3

GW: Gastrocnemius white portion

HGD: High fat diet

HSL: Hormone sensitive lipase

IKKβ: IκB kinase β

IL-6: Interleukin-6

IPA: Ingenuity Pathways Analysis

IR: Insulin receptor

IRS: Insulin receptor substrate

JNK: c-Jun N-terminal kinases

LPC: Lysophosphatidylcholine

LTCC: L-Type Calcium Channel

MAGL: Monoacylglycerol lipase

MAPK38: Mitogen activated protein kinase **(p38 MAPK)**

MB: Myoblast

MCD: Malonyl-CoAdecarboxylase

MHC: myosin heavy chain

mRNA: Messenger ribonucleic acid

MT: Myotube

MRS2179: 2'-Deoxy-N6-methyladenosine 3', 5'-bisphosphate

NAPE: N-arachidonoyl-phosphatidylethanolamine

NECA: 5'-N-ethylcarboxamidoadenosine

OEA: N-oleoylethanolamine

pAKT: Phospho-AKT

PBS: Phosphate buffered saline

PCA: principle component analysis

PCR: Polymerase chain reaction

PDK1: 3'-phosphoinositide-dependent kinase 1

PFA: parafomaldehyde

PGC-1: Peroxisome proliferator-acitvated receptor y coactivator 1a

PH: Pleckstrin-homology

PI-3 kinase: Phosphatidylinosito1-3 kinase

PKA: cAMP-dependant protein kinase

PKC: Protein kinase C

PLC: Phospholipase C

PLD: Phospholipase D

PPAR: Peroxisome proliferator-activated receptor

PTX: Pertussis toxin

P-value: Probability

r: Pearson correlation

RIM: 5-(4-Cholorophenyl)-1-(2, 4-dichloro-phenyl)-4-methyl-N-(piperidin-1-yl)-1H-pyrazole-3-carboxamide; rimonabant

ROS: Reactive Oxygen Species

RT-PCR: Reverse transcription polymerase chain reaction

SDS-PAGE: Sodium dodecyl sulphate polyacrylamide gel electrophoresis

SEM: Standard error of the mean

SHC: Src homology 2 domain containing

Skeletal muscle: skeletal muscle

SOL: Soleus

SREBPs: Sterol regulatory element-binding proteins

TAG: Triacylglycerol

TBE: Tris/Borate/EDTA

TBS: Tri-Borate/EDTA

TBS: Tri-Buffered saline

TEMED: (N,N,N',N'-Tetramethylethylenediamine)

TG: triglyceride

TIS: tissue

UCP3: Uncoupling protein 3

VL: Vastus Lateralis

WHO: World Health Organisation

WR: Wistar rat

ZFR: Zucker fat rat

ZLR: Zucker lean rat

CHAPTER ONE

GENERAL INTRODUCTION

CHAPTER 1. General Introduction

1.1. Insulin resistance in skeletal muscle

1.1.1. Introduction

Diabetes is a chronic disease that occurs either when the pancreas does not produce enough insulin or when the body cannot effectively use the insulin it produces. The World Health Organization (WHO) in March 2013 reported that 347 million people worldwide have diabetes. Type 2 diabetes comprises 90% of people with diabetes around the world and is largely the result of excess body weight and physical inactivity. Obesity is now considered as an epidemic disease, decreasing life expectancy because of adverse consequences such as type 2 diabetes. In 2008, 10% of men and 14% of women in the world were obese (BMI ≥30 kg/m2), compared with 5% for men and 8% for women in 1980. In fact, 80% of diabetes cases can be attributed to weight gain. Obesity causes a predisposition to developing diabetes because a high body mass index of >40 is associated with an almost 100% risk for the disease (Sell et al. 2006). The pathophysiology of type 2 diabetes involves defects in tissue sensitivity to insulin and decreased insulin secretion. Insulin resistance starts with an inability of peripheral target tissues (liver, adipose and skeletal muscle) to respond properly to insulin which is followed by a compensation state through increasing insulin secretion and ended by pancreatic β cell failure resulting in decreased insulin secretion. Insulin resistance precedes the onset of overt diabetes by 1 to 2 decades (Dipl-Pharm & Zierath 2005). Communication between the tissues responsible for insulin resistance (particularly adipose tissue and skeletal muscle) occurs through metabolic mediators of Free Fatty acids (FFAs) and their metabolites and endocrine mediators in the form of adipokines and possibly myokines.

Insulin resistance especially in skeletal muscle which is responsible for 70-80% of peripheral glucose disposal, is an early sign and cause of type two diabetes (Di-Marzo & Matias 2005; Edfalk et al. 2008). Skeletal muscle is the primary site of insulin-mediated glucose uptake defects in insulin action on glucose uptake and metabolism. Skeletal muscle insulin resistance precedes the manifestation of type 2 diabetes. Circulating levels of FFAs, which are markedly increased in obesity and associated-diseases, has a core role in the development of skeletal muscle insulin resistance. Among the different types of fatty acids, saturated long-chain fatty acids such as palmitic and stearic acids were demonstrated to be potent inducers of insulin resistance. Several mechanisms have been suggested to explain the mechanism through which saturated fatty acids impair insulin actions such as the Randle cycle, accumulation of intracellular lipid derivatives, defect in insulin signalling, oxidative stress, modulation of gene transcription, inflammation and mitochondrial dysfunction.

1.1.2. Mechanisms underlying the insulin resistance induced by saturated fatty acids

1.1.2.1. The Randle cycle

Around 50 years ago Randle and his colleagues hypothesised that increased fatty acid oxidation raises the production of acetyl-CoA resulting in inhibition of pyruvate dehydrogenase activity and elevation of citrate levels at the tricarboxylic acid cycle (**Error! Reference source not found.**) (Samuel et al. 2010; Randle 1998). Citrate together with an increased ATP/ADP ratio reduces the activity of phosphofructokinase and consequently glucose flux through the glycolytic pathway, resulting in glucose 6-phosphate accumulation, hexokinase II inhibition, increase in intracellular glucose content and, consequently, reduction in glucose uptake (Petersen & Shulman 2002; Boden & Shulman 2002).

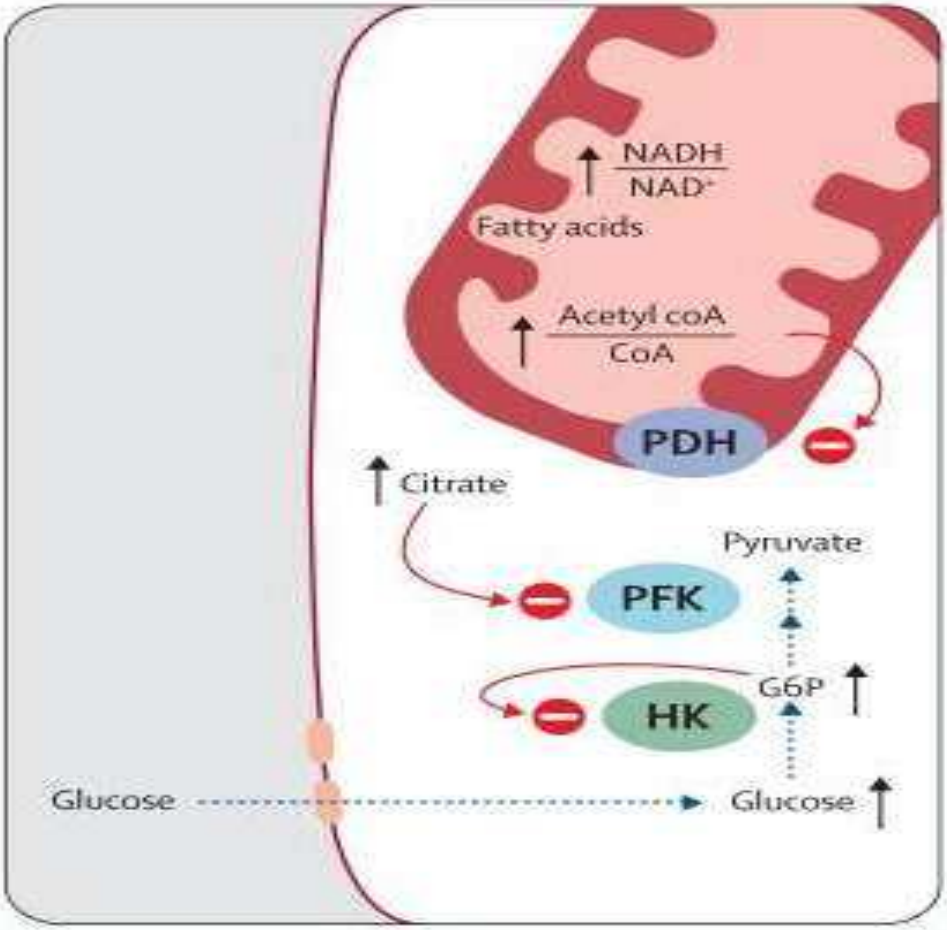

Figure 1-1: Glucose-fatty-acid cycle proposed by Randle and colleagues CoA=coenzyme A. PDH=pyruvate dehydrogenase. PFK=phosphofructokinase. G6P=glucose-6-phosphate. HK=hexokinase. Red circle with minus sign represents inhibition. Black line with arrowhead represents increase or accumulation of substrate. Blue dotted line with arrowhead indicates a pathway that is inhibited. Adapted from Pender et al. (2005)

Further studies demonstrated that the insulin resistance induced by fatty acids is primarily associated with impaired glucose uptake rather than changes in hexose metabolism (Arner 2002). Roden et al. (1996) demonstrated that the reduction in muscle glycogen synthesis is preceded by a decrease in intramuscular glucose 6-phosphate, suggesting that inhibition of glucose transport or its phosphorylation are the main reasons of insulin resistance. Other studies also demonstrated that lipid infusion decreases intracellular glucose and glucose 6-phosphate content, due to inhibition of glucose uptake by skeletal muscle (Petersen & Shulman 2002). However, Tsintzas et al. (2007) demonstrated that lipid induced decrease in insulin-stimulated glucose uptake

happened after a reduction in carbohydrate oxidation. Thompson et al. (2000) reported that the reduction of basal and insulin stimulated glucose uptake by palmitate in rat muscle occurred after reduction in glycogen synthesis. Moreover, the role of PDK4 in skeletal muscle insulin resistance induced by high FFA was addressed by Tsintzas et al. (2007) and Chokkalingam et al. (2007). They observed an early upregulation of PDK4 content in skeletal muscle biopsy from healthy humans after 6 days of high fat diet, which was associated with a reduction in skeletal muscle PDC activation and hence glucose oxidation but not glucose disposal mediated skeletal muscle insulin resistance. A high level of muscle PDK4 protein expression was observed in starved and diabetic rats (Wu et al. 1999). Upregulation of muscle PDK4 protein and mRNA expression in starved humans may mediate the insulin resistance induced by the high fatty acids level in fasting (Tsintzas et al. 2006).

1.1.2.2. Inhibition of skeletal muscle insulin signalling

Under physiological conditions, insulin activates glucose uptake by stimulating the canonical IRS-PI3K-Akt pathway and by phosphorylating and inactivating Akt substrate 160 (AS160), a protein that, when activated, prevents glucose transporter (GLUT) 4 translocation to the membrane (Martins et al. 2012) (Figure 1-2). Saturated fatty acids were demonstrated to affect insulin intracellular signalling pathways in skeletal muscle and myocytes. Thompson et al. (2000) and Yu et al. (2002) have demonstrated a marked reduction in IRS-1 tyrosine phosphorylation, PI3-kinase activity and Akt phosphorylation and activity in skeletal muscle after lipid infusion in euglycemic hyperinsulinemic clamp. However, Tsintzas et al. (2007) did not observe any alteration in muscle Akt after lipid infusion. As reviewed by Schmitz-Peiffer (2000), palmitic acid was shown to decrease insulin receptor expression and activity and phosphorylation

of IRS-1 and -2 at tyrosine residues, Akt and GSK-3 in isolated soleus muscle, primary culture of rat myocytes, pmi28 myotubes, C2C12 and L6 myocytes. Activation of various kinases by FFAs such as PKCs, JNK and p38 MAP kinase catalyse the phosphorylation of serine residues in IRS-1 instead of tyrosine phosphorylation leading to blocking of its downstream signal transduction. Ruiz-Alcaraz et al. (2013) observed a significantly reduced insulin-induced activation of p42/44 MAP kinase in volunteers with poor insulin sensitivity. It is now known that FFAs interfere with insulin signaling in skeletal muscle at the level of IRS-1 serine phosphorylation, involving the activation of protein kinase C. Various PKC isoforms have been shown to be involved in lipid-induced insulin resistance in skeletal muscle (Griffin et al. 1999).

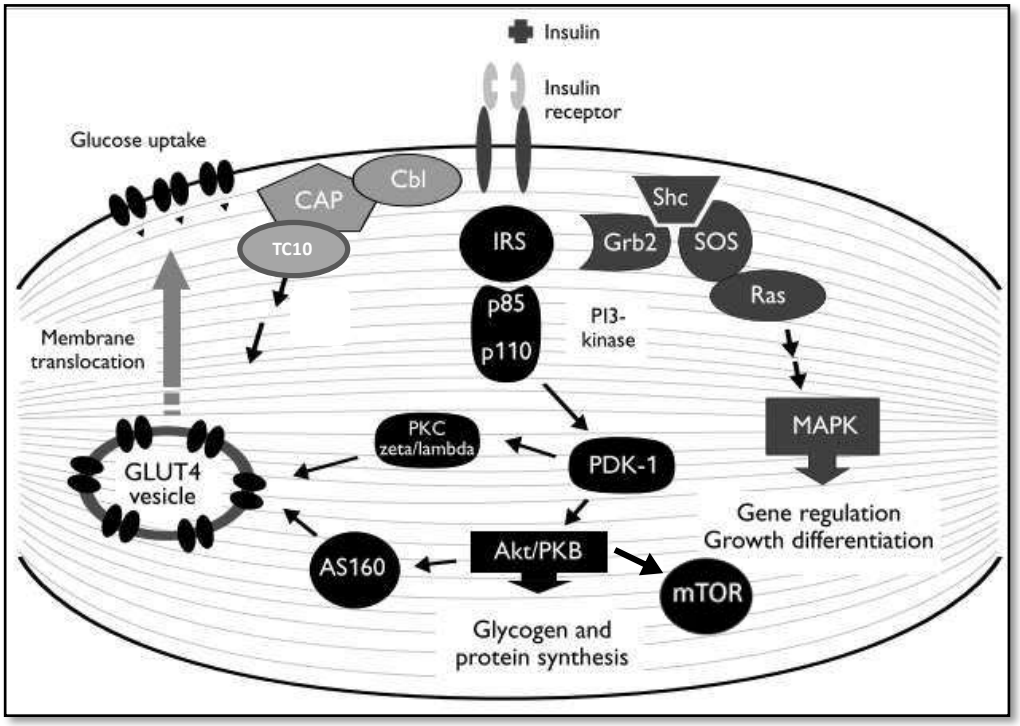

Figure 1-2: Overview of insulin signalling pathways downstream of the insulin receptor in skeletal muscle.
Activation of insulin receptor leads to tyrosine phosphorylation of IRS family, SHC and Cbl. Tyrosine phosphorylation of IRS results in the activation of a variety of signalling pathways; the RAS/ MAPK pathway which involved in gene regulation, CAP/ Cbl pathway which participate in insulin mediated glucose transporter through activation of TC10 and PI3-kinase which phosphorylate AKT (PDK1 dependent) and in turn phosphorylate GSK3, activate the mTOR and glucose uptake. AS160 = 160-kDa Akt substrate, CAP = Cbl-associated protein, GLUT4 = glucose transporter 4, GSK3 =glycogen synthase kinase 3 Grb2 = growth factor receptor-bound protein 2, IRS = insulin receptor substrate, MAPK = mitogen-activated protein kinase, PDK-1 = 3-phosphoinositide-dependent protein kinase-1, PI3 = phosphatidylinositol 3, PKC zeta/lambda = protein kinase C zeta/lambda, RAS = retrovirus-associated DNA sequences, Shc = Src homology 2 domain-containing protein, SOS = son-of-sevenless protein. Adapted with modification from (Dipl-Pharm & Zierath 2005)

1.1.2.3. Lipotoxic intramyocellular lipid accumulation

Elevation of plasma FFAs and its metabolites leads to ectopic fat stores which have lipotoxic effects on skeletal muscle and other peripheral tissues (Martins et al. 2012). Genetic deletion of lipoprotein lipase, fatty acid transporters, and diacylglycerol acyl transferase-1 inhibited the accumulation of intramyocellular diacylglycerol and triacylglycerol induced by high fat diet (Wang et al. 2009). Diacylglycerol directly activates PKCθ that catalyzes the phosphorylation of serine-307 residue at IRS-1, reducing its tyrosine phosphorylation and activation by insulin (Schmitz-Peiffer C et al. 1997). Increased production of ceramide and sphingosines in skeletal muscle cells due to high fat diet is associated with glucose intolerance and insulin resistance (Chavez et al. 2005). In addition, Han et al. (2011) demonstrated that increased lysophosphatidylcholine content in myocytes leads to serine phosphorylation IRS-1 and induce insulin resistance.

1.1.2.4. Activation of inflammatory signaling pathways

A close relationship between chronic inflammation and skeletal muscle insulin resistance has recently been established. Saturated fatty acids activate inflammatory signaling pathways directly through interaction with members of Toll-like receptor (TLR) family and indirectly through the secretion of cytokines including TNFα,IL-1β and IL-6 (Sell et al. 2006; Martins et al. 2012). This is supported by increased macrophages and increased inflammatory molecules. Activation of JNK and IKKβ by saturated fatty acids is associated with a marked inhibition of insulin action due to serine phosphorylation IRS-1(Wei et al. 2008). Diabetic and obese mice have increased skeletal muscle IKK and JNK activities, whose pharmacological and genetic inhibition leads to an improvement in insulin sensitivity and glucose tolerance (Solinas et al. 2006). Skeletal muscle generates and secretes several inflammatory cytokines named myokines including TNFα,

IL-6, IL-1, IL-1Rα, IL-8, IL-10, IL-15, and monocyte chemotatic protein (MCP)-1 which possibly modulate insulin sensitivity (Pedersen et al. 2007). The role of IL6 in insulin sensitivity is controversial. Increased levels of IL6 after exercise or after short-term treatment increase insulin sensitivity, whereas chronically increased levels are associated with insulin resistance (Weigert et al. 2005). Increased levels of TNFα have been noted in skeletal muscle tissue and cultured skeletal muscle cells from humans and animals with insulin resistance and/or diabetes (Saghizadeh & Ong 1996). Genetic deletion of TNFα and suppression of TNFα by anti-TNFα antibodies or TNFα converting enzyme inhibitors improves insulin sensitivity in obese or nonobese insulin-resistant models (Wei et al. 2008). TNFα decreases tyrosine phosphorylation of IRS-1 and increases IRS-1 serine phosphorylation (Eckardt et al. 2008). It is worth mentioning that Petersen et al. (2007) and Dietze et al. (2002) found that insulin resistance was independent of TNFα and IL-6 in insulin resistance subjects and Storz et al. (1999) observed that TNFα did not interfere with AKT kinase signalling and it increased GLUT1 content suggesting a protective mechanism by increasing basal glucose uptake. Overfeeding in healthy humans resulted in significantly increased in peripheral insulin resistance without changes in inflammatory gene expression (IL6) (Tam et al. 2010).

1.1.2.5. Oxidative stress and mitochondrial dysfunction

Type 2 diabetes mellitus, obesity and the metabolic syndrome are strongly correlated with increased skeletal muscle content of reactive oxygen species (ROS) (Abdul-Ghani et al. 2008). Chronic elevation in plasma lipids levels and excessive accumulation of intramyocellular lipid content are characterized by increased reactive oxygen species (ROS) and reactive nitrogen species (RNS) production. ROS lead to impaired insulin response by inducing IRS serine/threonine phosphorylation, decreasing GLUT4 gene transcription, and decreasing mitochondrial activity. Several studies have shown that mitochondrial

content, mitochondrial function, and oxidative capacity are decreased in insulin-resistant obese and type 2 diabetic individuals (Holloway et al. 2007; Martins et al. 2012). Impaired mitochondrial function and reduced fatty acid oxidative capacity were found in isolated primary myocytes from insulin resistant obese and type 2 diabetic patients (B et al. 2005). High fatty acid availability in type 2 diabetes myotubes caused an impaired mitochondrial capacity for fatty acid oxidation and glucose due to defects of fatty acid β oxidation (AJ et al. 2009). Exposure of rat L6 myotubes to high fatty acid levels lead to excessive but incomplete β oxidation which lead to mitochondrial stress and ultimately to insulin resistance in skeletal muscle (Koves et al. 2008).

A decrease in succinate dehydrogenase (a mitochondrial dysfunction marker) activity in insulin-resistant and diabetic patients skeletal muscle cells indicates a possible role of decreased oxidative capacity in the initiation of adipocyte-derived muscle insulin resistance (Sell et al. 2006). Impairment of mitochondrial function leads to production of ROS and accumulation of fatty acid-derived metabolites which lead to insulin resistance through activation of several kinases, such as NF kB, p38 MAP kinase, JNK, PKC-ζ and PKC-ε and subsequently serine phosphorylation in IRS-1 (Hirabara et al. 2010) (Figure 1-3). However, the role of mitochondria dysfunction in skeletal muscle insulin resistance is still debatable as recently Galgani et al. (2013) found no evidence of impaired muscle mitochondrial oxidative capacity in insulin-resistant vs insulin-sensitive individuals. Induction of skeletal muscle insulin resistance by overfeeding in healthy individuals without a reduction in mitochondrial content was observed by Samocha-Bonet et al. (2012).

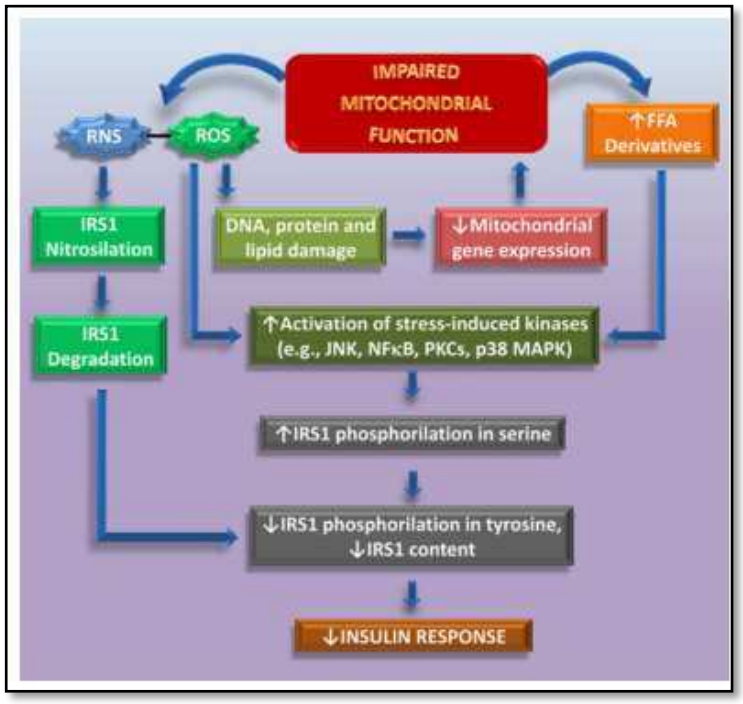

Figure 1-3: Mechanisms underlying insulin resistance by impaired mitochondrial function as suggested by Martins et al. (2012).
Mitochondria dysfunction leads to increase in FFAs derivatives, reactive oxygen species (ROS) and reactive nitrogen species (RNS) which lead to decrease in IRS1 serine phosphorylation and content and eventually lead to insulin resistance adapted from Martins et al. (2012).

1.1.2.6. Skeletal muscle fibre types and insulin resistance

Skeletal muscle contains a unique composition of different muscle fibres referred to as ''slow-twitch'' and ''fast-twitch''. On the basis of metabolic and contractile properties and myosin heavy chain (MyHC) isoforms, muscle fibres can be broadly classified as type I, oxidative, slow-twitch fibres and type II, fast-twitch fibres which can be further classified into type IIa, type IIx and IIb fibres, (Shi et al. 2007). Generally, type I and type IIa fibres utilize oxidative phosphorylation as their primary metabolic activity, whereas type IIx and IIb fibres primarily harness glycolysis to generate ATP. In response to environmental signals such as aging, atrophy, exercise, and diabetes, however, muscle can modify its functional characteristics by changing its fibre type (Pette & Staron 2001). Conversion of fibre type happens both in vivo and in vitro (Zebedin et al. 2004). An association between muscle fibres types and insulin resistance has been reported. Patients with central obesity, which is associated with insulin

resistance, had higher proportions of type IIb fibres (Lillioja et al. 1987). Layne et al. (2011) observed diminished type I fibre content in muscle biopsies from patients with type 2 diabetes and nondiabetic subjects with the metabolic syndrome. Skeletal muscle from obese patients also contains a smaller number of mitochondria because of a lower ratio of type I to type II muscle fibres (Martins et al. 2012).

The reason that a higher proportion of type I fibres leads to better insulin responsiveness or higher utilization of oxygen during exercise remains elusive. Shi et al. (2008) and Shi et al. (2007) suggested that ERK1/2 pathway may play an important role in the maintenance of fast fibre phenotype and ERK1/2 activity was more than 2-fold higher in fast-twitch muscles than in slow-twitch muscle. In contrast, Murgia et al. (2000) and Higginson et al (2002) reported that Ras/MEK/ERK play a pivotal role in re-establishing the slow muscle programming as ablation of the ERK1/2 pathway increases MyHC IIx and IIb transcripts, whereas it decreases MyHC I expression in cultured rat fetal myocytes. Interestingly, Stuart et al. (2013) found a 21% fewer Type I muscle fibres, but a more than two-fold increase in the mixed Type IIa fibres in men and women with central obesity and a family history of type 2 diabetes. Moreover, down-regulation of myogenin (transcription factor mainly found in type I) and IL-6 (mainly expressed in type I fibres) in condition media treated myotubes might be indicative of the formation of less oxidative myotubes more similar to type II fibres in the presence of high concentration of fatty acids (Eckardt et al. 2008).

Thus, the full explanation of the mechanism of insulin resistance in skeletal muscle remains elusive, but the search may be narrowed by examining the role of free fatty receptors and cannabinoid receptors.

1.2. The endocannabinoid system

1.2.1. Introduction

The endocannabinoid system is a complex endogenous signalling system which influences multiple metabolic pathways and takes its name from the cannabis plant. Even though the use of compounds containing cannabinoids to stimulate appetite and increase body weight is a traditional treatment, the understanding of their metabolism and action is quiet recent (Kunos 2007; Bellocchio et al. 2008). The psychotropic compound of marijuana Δ9-tetrahydrocannabinol (THC) was identified in 1964. Since then considerable research has been carried out to clarify the mechanisms of cannabinoid action.

In the 1990s, receptors for THC were identified. The receptors CB1 and CB2 are G protein coupled membrane receptors (GPCR), the Gi/o family (Matias et al. 2008) which act through the adenyl cyclase pathway (Di-Marzo & Matias 2005). CB1 receptors are the most common GPCR in the brain while CB2 receptors are predominantly found in the immune system. In 2003 Cota et al. identified the presence of CB1 receptors in peripheral tissues such as adipose tissue, liver, pancreas and skeletal muscle, which are the major organs involved in energy metabolism. Even though most research has demonstrated the presence of CB2 in immune system solely, Engeli (2008b) has also found them in brain stem and Rajesh et al. (2008) found them in human myocardium and skeletal muscle.

1.2.2. Endocannabinoids synthesis and degradation

A number of ligands (ECs) for these receptors have been identified such as N-arachidononyl ethanolamine (anandamide) and 2 arachidonoyl glycerol (2AG) which are arachidonic acid derivatives. They are produced on demand as metabolic stress and cellular damage lead to an increase in EC synthesis (Bellocchio et al. 2008; Engeli 2008b; Matias et al. 2008). Enzymes for EC

biosynthesis have been identified; ethanolamine-selective phospholipase D for anandamide formation and Sn-1-selective diacylglycerol lipase for 2AG formation. EC are highly lipophilic compounds and they are rapidly hydrolyzed by fatty acid amide hydrolase (FAAH) and monoacylglycerol lipase (MAGL) into arachidonic acid (Burstein 2005; Bellocchio et al. 2008).

The formation of anandamide involves a calcium dependent mechanism and occurs through the cleavage of NAPE, the precursor for anandamide, by a specific phospholipase D (NAPE-PLD). The activity of PLD is regulated by the activation of G protein coupled receptors, ionotropic receptors such as glutamate, N methyl-D aspartate and metabotropic receptors such as glutamate and acetylcholine (Piomelli 2003; Eckardt et al. 2008) (Figure 1-4).

The formation of 2AG is also a calcium dependent process. First, diacylglycerol is formed through the action of phosphatidylinositol specific PLC and then by the action of DAGL, 2AG is formed. The activation of metabotropic P2Y receptors as well as ionotropic P2X receptors, for example, facilitates 2 AG formation as the activation of these receptors leads to an increase in calcium entry into the cell, activation of DAGL and inhibition of MAGL (Eckardt et al. 2008) (Figure 1-4).

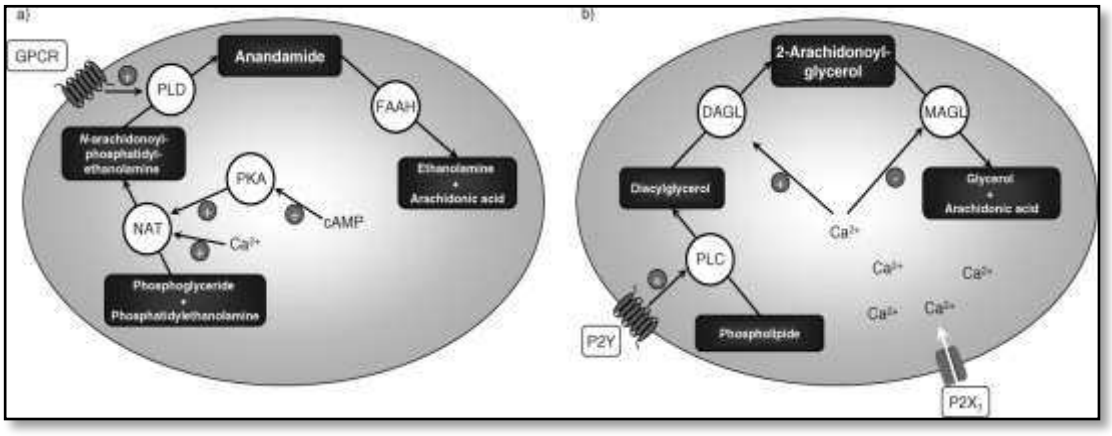

Figure 1-4: Factors regulating ECs synthesis.
(a) The formation of anandamide occurs through the activation of the Calcium dependent N-acyltransferas (NAT) and Phospholipase D, the former activity increases by the phosphorylation of cAMP protein kinase A (PKA). The degradation of anandamide is mediated by fatty acid amide hydrolase (FAAH). (b) The activation of metabotropic purinergic P2Y and ionotropic purinergic P2X receptors lead to the activation of phospholipase C (PLC) and diacylglycerol lipase (DAGL) and inhibition of monoacylglycerol lipase (MAGL), respectively. (Adapted from Eckardt K, 2008)

1.2.3. Mechanism of action of endocannabinoids

The endogenous binding activity of EC to CB receptors is different. Anandamide is a partial agonist at CB1 and CB2 receptors with higher affinity for CB1 receptors, while 2AG is a full agonist at both receptors. Similar to anandamide, 2AG has higher affinity for CB1 receptors. CB1 and CB2 receptors activation lead to inhibition of adenyl cyclase and decrease in PKA. CB1 receptor activation is also associated with activation of K influx and inhibition of voltage-Ca channels Figure 1-5. However, CB2 receptors activation is not associated with the modulation of ion channel functions. CB receptors activation:

- Leads to phosphorylation of p42 & p44 MAPK, p38 MAPK and JNK which regulate nuclear transport factor (Howlett 2005).
- and is coupled to phospotidylinositol 3 kinase and Focal adhesion kinase (Rodríguez de Fonseca et al. 2005)

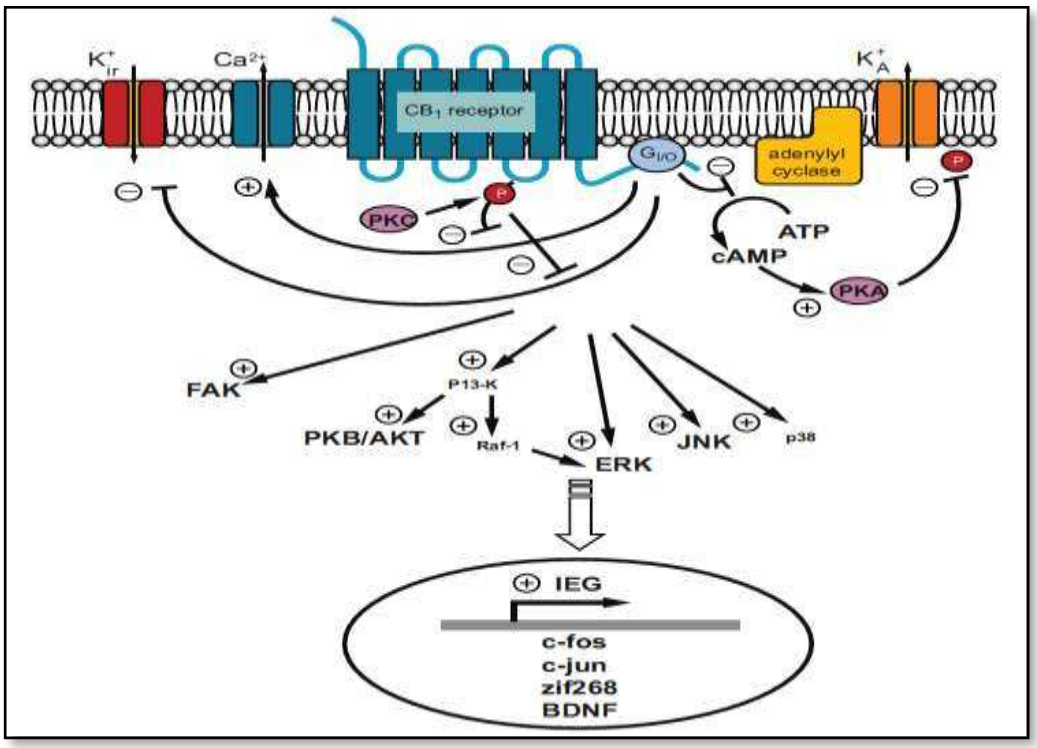

Figure 1-5: CB1 receptor intracellular signalling cascades.
Activation of CB1 receptors leads to inhibition of adenyl cyclase and decrease in cAMP which stimulates K^+_A through inactivation of PKA. Through modulation of PKC, CB1 activation leads to inhibition of Ca^{++} channel and activation of inward rectifying of K^+ ion channels. Activation of PKC will phosphorylate CB1 and prevent its effect on ion channels. CB1 activation also stimulates intracellular kinases, such as Focal Adhesion Kinase (FAK), Phosphatidyl inositol 3-kinase (PI3-K), Protein Kinase B (PKB), extracellular signal-regulated kinase (ERK), C-jun N-terminal Kinase (c-JNK) and p38 MAPK (p38). Adapted from Pagotto et al. (2006)

1.2.4. Other Potential endocannabinoid receptors:

Not all ECs actions can be explained through activation of CB1 and CB2 receptor-mediated pathways. Using CB1 and CB2 receptor antagonists, researchers have suggested the presence of other non CB receptors (Rodríguez de Fonseca et al. 2005) such as the nuclear receptor PPAR, Transmitter gated channel transient receptors vanilloid (TRPV1) and GPR55 which may also be activated by ECs.

1.2.4.1. GPR 119

GPR119 is thought to play an important role in metabolic disease and its modulators may influence parameters related to both diabetes and obesity. GPR119 is GPCR (class I rhodopsin-type) which increases cAMP levels (Overton et al. 2008). The major sites of expression in humans are pancreas, fetal liver and GIT as reported by Overton et al. (2008) while Bonini et al. (2001) & Bonini et al. (2002) reported that it is present in most rat tissues including brain.

Oleoylethanolamide (OEA), a structural analogue of the cannabinoid anandamide, is a potent natural agonist for GPR119. Anandamide, Lysophosphotidyl choline (LPC) also activates GPR119. PSN375693 and PSN632408 are synthetic GPR119 agonists which stimulate insulin secretion in a glucose-dependent manner. The latter also decreases food intake and body weight in rats (Overton et al. 2008).

In the β cell of pancreas GPR119 activation stimulates insulin secretion as well as that of glucagon like peptide (GLP) and gastric inhibitory polypeptide (GIP) in a glucose dependent manner (Figure 1-6). GPR119 controls glucose homeostasis in two ways; firstly by stimulating insulin release from the β cells of the pancreas and secondly through the release of antihyperglycaemic agents such as GIP from enteroendocrine cells (Drucker 2001; Meier et al. 2002; Gromada et al. 2004).

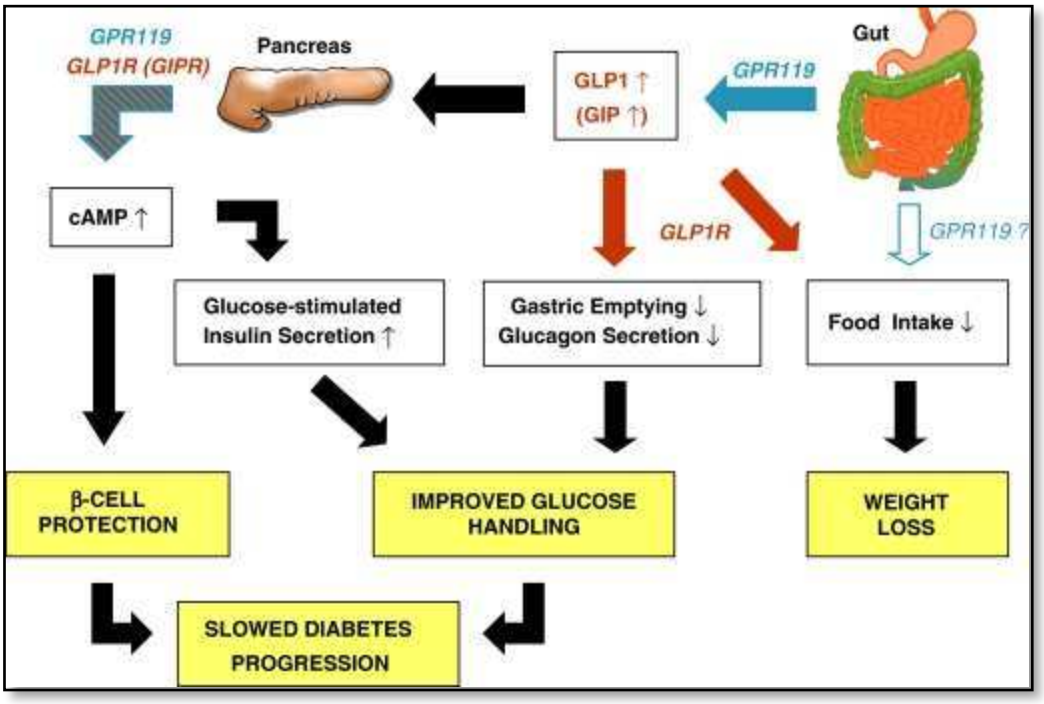

Figure 1-6: Proposed mechanisms of GPR119 agonist action.
GPR119 agonists may affect food intake through direct action or by increase the concentration of Glucagon Like peptide 1 (GLp1) and Gastric Inhibitory polypeptide (GIP). GPR119 also lead to β cell protection and prevention of diabetes. (Adapted from Overton HA et al 2008)

1.2.4.2. Nuclear receptor PPAR;

O'Sullivan (2007) reported that inflammation, feeding behaviour and analgesic roles of ECs can be mediated through nuclear receptors. O'Sullivan (2007) also reported that the synthetic CB1 and CB2 receptor agonist, Win55212, binds to PPARα, whereas anandamide binds to PPARγ directly and stimulates differentiation of pre-adipocytes into adipocytes. It has been found that 2AG and Ajulemic acid activate PPARγ which exhibits similar action to the CB1 and CB2 agonist (Burstein 2005).

1.2.4.3. Transmitter gated channel transient receptors Vanilloid 1 (TRPV1)

TRPV1 was cloned in 1997 (Cavuoto et al. 2007). Anandamide stimulates TRPV1 and causes calcium influx which leads to neurotransmitter release. Burstein (2005) suggested that the vasodilation effect of anandamide is

mediated through these receptors as it was not inhibited by a CB receptor antagonist (rimonabant), whereas the use of a selective TRPV1 antagonist abolished vasodilation.

1.2.4.4. GPR55;

Recently, GPR55 has been considered as a cannabinoid receptor. GPR55 is only 13.5% identical to CB1 and 14.4% identical to CB2, and its mRNA is present in the brain and peripheral tissues. Lauckner et al. (2008) reported that GPR55 is an additional cannabinoid receptor that activates signaling pathways distinct from CB1 or CB2, and that it may increase neuronal excitability. Anandamide and virodhamine activate GTPγS binding via GPR55 and ligands such as cannabidiol and abnormal cannabidiol which exhibit no CB1 or CB2 activity are believed to function through GPR55 (Ryberg et al. 2007)

1.2.5. The roles of Endocannabinoids

1.2.5.1. Central mechanisms.

The presence of CB1 receptors has been established and they are the most abundant GPCR in the brain. The presence of CB2 receptor is still under investigation even though Van Sickle et al. (2005) demonstrated their presence in rat and ferret brainstem neurons. The production of ECs in the brain is under tight control as endocannabinoid levels are regulated by both synthesis and degradation. Leptin, which is a known negative regulator of orexigenic peptides, decreases the ECs level while ghrelin increases their level (Di-Marzo & Matias 2005).

The main role of ECs in brain is mediated through retrograde signalling (Figure 1-7) and the subsequent inhibition of neurotransmitters such as GABA, serotonin, acetylcholine and other neuropeptides. This might be one of ECs possible mechanism in controlling food intake as inhibition of GABA leads to

stimulation of MCH (Bellocchio et al. 2008). Another possible explanation for ECs action on the central nervous system is through the dopaminergic system, as dopamine receptors antagonists reduce the orexigenic stimulation of THC (Liu et al. 2005). CB1 can form a heterodimer with dopamine D2 receptor and this complex, unlike CB1, stimulates adenyl cyclase.

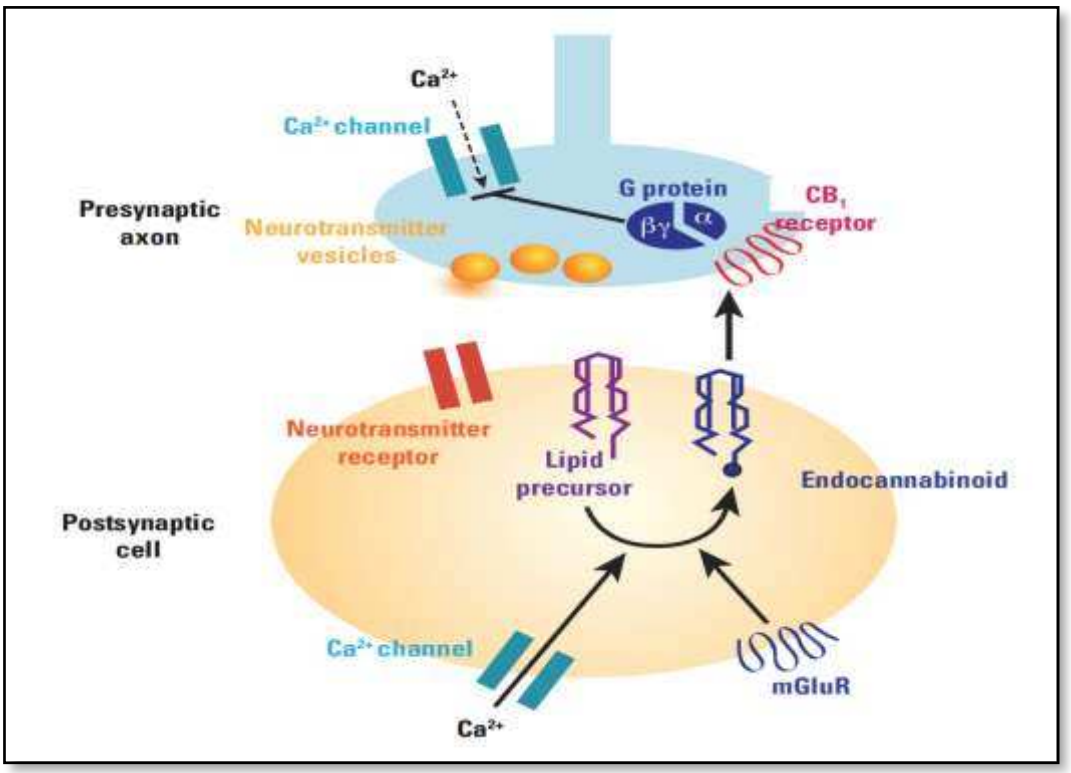

Figure 1-7: Retrograde signalling by endocannabinoids.
Depolarization of postsynaptic cell leads to opening of calcium channels and activation of metabotropic glutamate receptors (mGluR) which leads to increased endocannabinoid synthesis. Presynapticly, the activation of CB1 receptor liberates Gβγ which blocks Ca^{++} channel and subsequently results in a decrease in intracellular calcium and the release of neurotransmitters. (Adapted from Wilson & Nicoll (2002))

In the brain, ECs control feeding behaviour in both human and animals by increasing appetite (Figure 1-8). It has been found that stimulation of cannabinoid receptors leads to an increase in food consumption and the blockade of CB1 receptors by antagonists such as Rimonabant leads to a decrease in appetite (Di-Marzo & Matias 2005). The effect of ECs on food intake starts from the early stages of life. Chan (2004) found that blockade of CB1 receptors in newborn mice leads to decrease in the suckling of milk. Similar findings were

reported in young rodents by Cota et al. (2003). Cannabinoid receptors are overactivated in animal models of genetic- and diet-induced obesity (Kunos 2007; Liu et al. 2005). Bellocchio et al. (2008) reported that Cannabinoid receptor stimulation in the brain leads to an increase in FA synthase gene expression. ECs also affect emotional state, motor function and pain perception. In addition they play a role in the control of neurexcitability, neuroprotection, nausea and emisis (Van Sickle et al. 2005).

1.2.5.2. Peripheral effects

It has been reported that the effect of ECs is mediated not only through central but also through peripheral mechanisms. ECs functions in adipose tissue, liver, pancreas and skeletal muscle are an attractive field for research (Figure 1-8).

1.2.5.2.1. Liver

CB1 receptors are present in mouse liver and their expression increases in response to a high fat diet. An increase in anandamide and a decrease in FAAH activity with no change in 2AG were also observed after a high fat diet (Eckardt et al. 2008). ECs stimulate adipogenesis through the activation of PPARγ which leads to maturation of adipocytes, inhibition of adenylate cyclase (Bellocchio et al. 2008) and upregulation of LPL and SREBP-1C expression (Rajesh et al. 2008; Engeli 2008b). Activation of CB1 receptors in liver leads to inhibition of AMPK and stimulation of acetyl co-enzyme A carboxylase {ACC1} along with an increase in de novo fatty acid synthesis (Eckardt et al. 2008). Blocking of CB1 receptors in cirrhotic liver, which exhibits a high level of CB1 expression, leads to a decrease in the fibrotic activity of hepatic myofibroblasts which may be due to the decrease in transforming growth factors β expression (Engeli 2008b).

1.2.5.2.2. Adipose tissue

All genes responsible for biosynthesis and degradation of ECs are present

in adipocytes. The presence of CB2 receptors is not fully confirmed yet even though Pagano et al. (2007) reported the presence of both CB1 and CB2 receptors. The enzymes NAPE-PLD, DAGL, FAAH, and MAGL have been found in adipose tissue (Roche et al. 2006). In addition adipocytes have the ability to synthesize 2AG and anandamide (Gonthier et al. 2007). High fat diets increase tissue levels of ECs (Artmann et al. 2008). Di Marzo & Matias (2005) found that ECs have a role in fat accumulation independent of the amount of dietary fat intake by acting directly on adipose tissue. ECs stimulate de novo FA synthesis through stimulation of glucose uptake, LPL activation and glycolysis (Eckardt et al. 2008) and upregulation of SREBP-1C, acetyl COA carboxylase and fatty acid synthase gene expression (Matias et al. 2008). In cultured mouse adipocytes there is a 3-4 fold increase in CB1 protein content during differentiation and an increase in 2AG, DAGL, anandamide and NAPE-PLD in the first four days (Matias et al. 2006).

The blockade of CB1 receptors by the antagonist (RIM) leads to stimulation of lipolysis and a release of FFA into the circulation and an increase in energy expenditure (Liu et al. 2005), a reduction of body weight and an increase in adiponectin expression (Eckardt et al. 2008). It has been noticed that stimulation and inhibition of adiponectin gene expression occurs after the use of CB1 receptor antagonist and agonist, respectively (Hollander 2007).

1.2.5.2.3. Pancreas

The expression of CB receptors in pancreas is species specific. In human pancreas, CB1 receptors are present in β cells and in small amount in β cells, whereas CB2 are present in α cells and exocrine pancreas. DAGL and MAGL are present in islet cells while FAAH in β cells (Eckardt et al. 2008). Mouse CB1 receptors are present in α cells and CB2 present in α and β cells (Engeli 2008b). In rat both CB1 and CB2 receptors are present in beta- and non-beta-cells and

the endocannabinoid system modulates glucose homeostasis through the coordinated actions of cannabinoid CB1 and CB2 receptors (Bermudez-Silva et al. 2007). Increased levels of 2AG and anandamide were observed in obese mice. Stimulation of CB1 and CB2 receptors leads to inhibition of insulin secretion by reduction of glucose-induced calcium oscillation (Eckardt et al. 2008). High glucose levels appear to induce ECs production. Indeed, when rat insulinoma (RIN- m5F) β-cells were cultured in low glucose medium, insulin led to inhibition of glucose induction of ECs, whereas incubation with high glucose medium blocked the effect of insulin and increased the level of anandamide and 2 AG (Matias et al. 2006).

1.2.5.2.4. Skeletal muscle

Skeletal muscle is one of the major insulin sensitive organs and it is responsible for 80% of insulin-stimulated glucose disposal as well as fatty acid oxidation (Di Marzo & Matias 2005; Engeli 2008). The role of ECs and the presence of their receptors in muscle is still under investigation. Engeli (2008) reported the presence of CB1, FAAH and MGL in human skeletal muscle. Cavuoto et al. (2007) also found CB1 receptors in human skeletal muscle myotubes with a similar amount of mRNA expression in obese and lean subjects and they also reported the presence of CB2 in human and rodent skeletal muscle. Despite these reports, the expression of cannabinoid receptors in primary skeletal muscle cells needs more confirmation because human CB1 and CB2 are single exon genes in human. The variation in the level of expression in slow, fast and mixed muscle fibres in different stages of muscle cell development also needs evaluation.

Insulin resistance in skeletal muscle may be due to impaired insulin signalling, lower mitochondrial capacity, increase ceramide content and abnormal secretion of myokines (Eckardt et al. 2008). The role of ECs in insulin signalling needs

further investigation. A decrease in insulin sensitivity in skeletal muscle, which is a primary cause for diabetes, has been linked to an increase in 2AG (Engeli 2008). The effect of CB1 activation or inactivation in cell signalling cascades in skeletal muscle is still under investigation. CB1 receptor blockade enhances AMP-kinase mRNA expression in myotubes in both obese and lean subjects (Eckardt et al. 2008; Cavuoto et al. 2007). Furthermore, ECs modulate energy utilization in skeletal muscle as it has been found that Rimonabant increased glucose uptake, oxygen consumption and decrease fatty acid oxidation in mouse soleus muscle (Cavuoto et al. 2007).

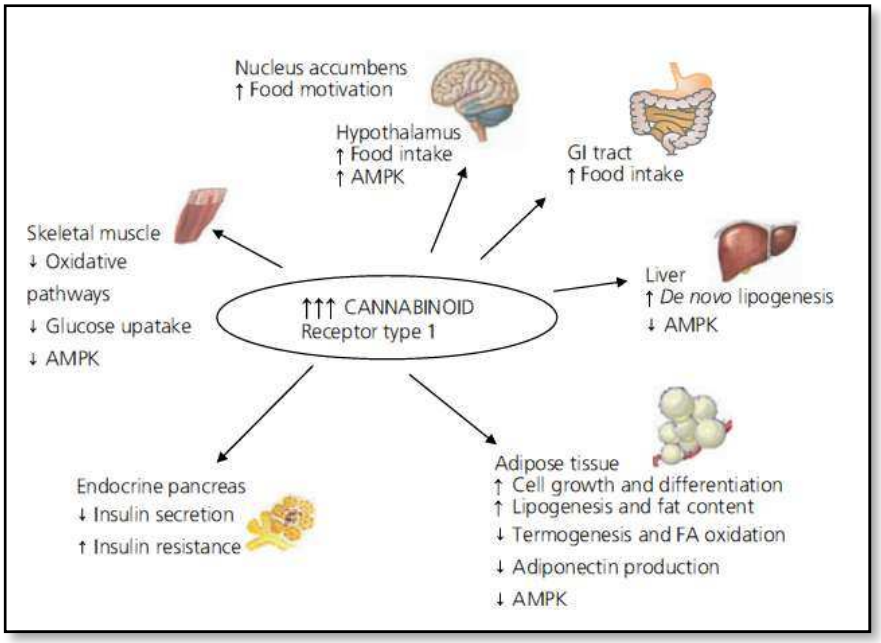

Figure 1-8: Effect of CB1 activation in various tissues.
In general, endocannabinoid activation leads to an increase in food intake and lipogenesis and a decrease in glucose uptake and insulin secretion. (Adapted from Bellocchio L et al 2008)

1.2.6. Role of endocannabinoids in obesity and type 2 diabetes mellitus (T2D).

The continuous increase in the prevalence of obesity has led to enormous amount of research to understand the underlying causes. Obese people have an inability to increase fatty acid oxidation in response to high fat intake, which is associated with a decrease in insulin sensitivity (Cavuoto et al. 2007). Obesity

plays a major role in the development of insulin resistance and subsequently T2D. T2D which is due to beta cell dysfunction and/or peripheral insulin resistance affect 150 million people worldwide (Esposito et al. 2008). It is expected that the prevalence of T2D will be 4.4% in 2030 worldwide (Hollander 2007). Genetic and functional abnormalities found in obesity are quite similar to those abnormalities found in T2D, therefore the possibility of similar underlying molecular mechanisms is under investigation and the focus of much contemporary research.

1.2.6.1. Endocannabinoids in obesity.

High levels of ECs in both central and peripheral tissues in obese people have been found (Engeli 2008). Endogenous and exogenous ECs lead to an increase in food intake and weight gain, whereas the use of rimonabant leads to a decrease in body weight and an improvement in lipid profiles. High fat diet promotes a pathological production of ECs and an increase in the expression of ECs receptors in different organs that leads to obesity-associated metabolic changes (Engeli 2008; Bellocchio et al. 2008). Engeli (2008) found a higher circulating level of ECs in obese women compared with lean subjects. Kunos (2007) also found a 3-4 fold increase in CB1 receptor expression in adipose tissue, liver and skeletal muscle of obese people. An increase in mRNA expression of CB1 in adipose tissue, skeletal muscle and liver of diet induced obese rodents was also reported by Eckardt et al. (2008) (Figure 1-9). Matias et al. (2006) reported high levels of 2AG and anandamide in visceral adipose tissue of obese and diabetic individuals. Besides the abnormal CB1 receptor expression, a relation between FAAH and obesity has also been reported by Osei-hyiaman et al. (2005) who found an 80% reduction in FAAH and unchanged levels of AEA in mice maintained on a high fat diet. Cavuoto et al. (2007) reported a reduction in FAAH, an increase in AEA and a polymorphism in the gene encoding FAAH in human obesity.

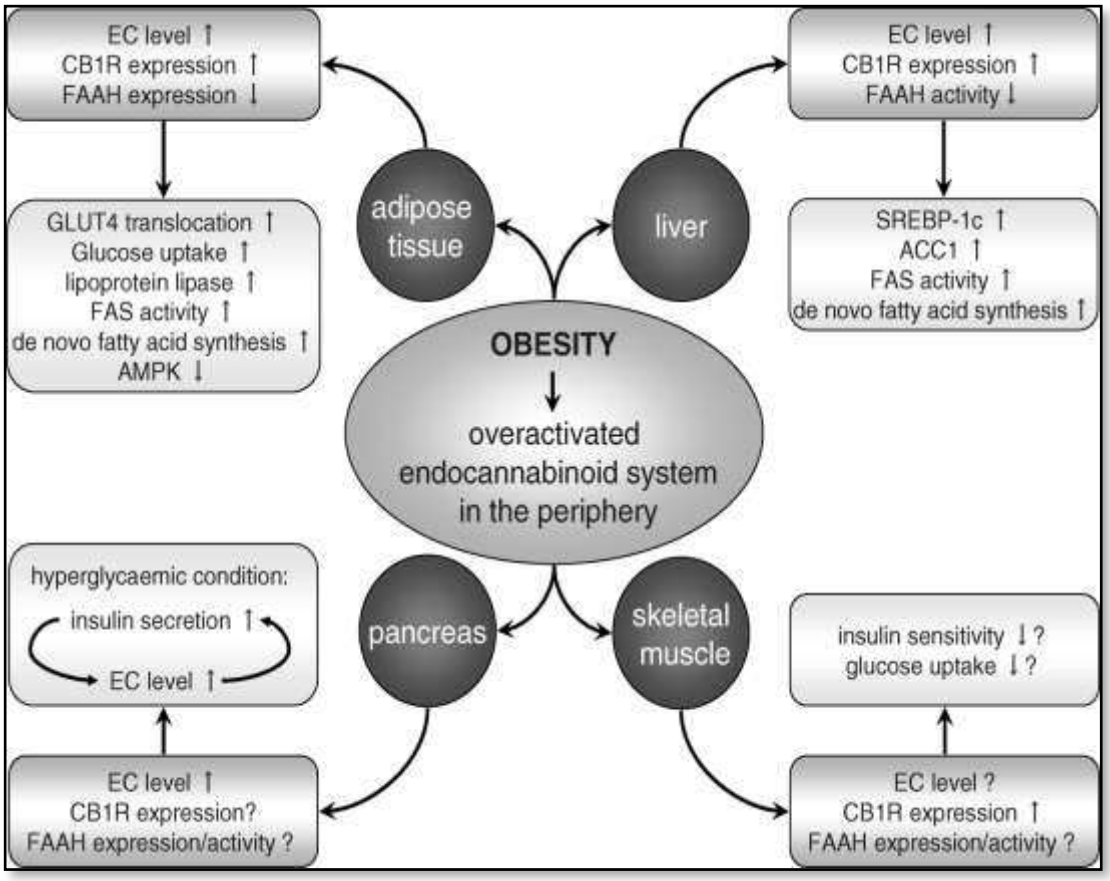

Figure 1-9: Consequences of obesity-related overactivation of the endocannabinoid system in peripheral tissues.
In obesity, ECs level usually increase in most tissues. The role of ECs in skeletal muscle is under investigation and its role in the development of insulin resistance in obesity is still debatable. (Adapted from Eckardt K etal, 2008)

1.2.6.2. Type 2 diabetes.

ECs play a major role in controlling glucose uptake by peripheral tissues and blockade of CB1 leads to reduction in blood glucose levels (Hollander 2007). High levels of ECs and a decrease in insulin sensitivity in T2D. An increase in AEA and 2AG in β cell cultured in hyperglycemic conditions have been reported by Bellocchio et al. (2008). ECs also modulate glucagon and insulin secretion from pancreas. The role of ECs in glucose homeostasis has been studied with the use of the CB1 antagonist rimonabant. Liu et al. (2005) reported a significant increase in glucose uptake in mouse soleus muscle treated with rimonabant even in the presence of low insulin concentrations and Engeli (2008) observed that rimonabant leads to the preservation of β cell integrity and cell mass in animal

models of T2D. Esposito et al. (2008) reported that in a skeletal muscle culture cell model (L6), pharmacological blockade of ECs controls insulin stimulated glucose uptake at the level of PI3K as rimonabant increased the expression of the regulatory units of PI3k (P85 &110 alpha) with no changes in IRS, PI3 kinase, protein kinase C, lipid phosphatase and glucose transporter 1 or 4. Esposito et al. (2008) also illustrated the role of CB1 receptors in glucose uptake in skeletal muscle as they found that the blockade of CB1, but not CB2 or TRVI, stimulated 2 deoxyglucose uptakes. The use of rimonabant in diabetes (RIO Diabetes) concluded that rimonabant significantly reduced weight, HBA1c, lipid profiles and associated metabolic dysfunction in obese and overweight diabetic patients (Scheen et al. 2006).

The use of CB1 antagonists in treatment of diabetes is still under consideration, as obesity is usually associated with psychological problems and CB receptor antagonists might exaggerate these symptoms. However, studies in north America RIO (rimonabant in obesity) which used rimonabant to control obesity and the metabolic syndrome, as well as other studies (RIO-Europe, RIO Diabetes and RIO-lipid), reported no significant association between rimonabant administration and psychiatric illness. A significant weight loss, improvement in lipid profile (decrease in TG and increase in HDL cholesterol) and decrease in fasting insulin after one year of treatment and a further increase in HDL cholesterol without a further reduction in body weight were reported after 2 years of treatment (RIO America). Despite this, the use of rimonabant has been stopped in most countries and the search for antidiabetic drugs without side effects is continuing.

1.3. FREE FATTY ACID RECEPTORS

1.3.1. Introduction

Obesity-driven type 2 diabetes has become a major health problem. Understanding of the molecular abnormalities leading to obesity and T2D is under intense research investigation. The search for drugs which overcome the current antidiabetic drugs side effects and prevent diabetic complication is also continuing. The role of free fatty acids in insulin secretion from the β cells of the pancreas and their association with insulin resistance in liver, adipose tissue and skeletal muscle is a fertile area of research as the underlying molecular mechanisms remain elusive. It is well known that FFAs not only are a fuel for cell metabolism but also function as extracellular messengers to activate intracellular signalling pathways through membrane receptors (Wang et al. 2011). In the last decade de-orphanization of free fatty acid receptors which belong to class A (rhodopsin-like) G protein coupled receptors highlighted the importance of FFAs in health and disease (Swaminath 2008). The gene encoding the FFAs receptors GPR40, GPR43 and GPR41 (also called FFAR1, FFAR2 & FFAR3) were identified by Sawzdargo et al. (1997) as intronless genes coded in tandem and located, in human, at chromosome 19q13.1. These receptors represent a family of receptors because they are more closely related to each other than to any other known GPCR. Despite this, this family exhibits somewhat limited similarity: 43% between FFAR2 and FFAR3 and 33 and 34% when FFAR1 is compared with FFAR2 and FFAR3, respectively (Stoddart et al. 2008). The FFAR2 and FFAR3 are activated by short chain fatty acids while FFAR1 is activated by medium and long chain saturated and unsaturated fatty acids. Other FFA receptors which are activated by medium and long chain fatty acids are GPR120 (Costanzi et al. 2008) and GPR84 (Pu & Liu 2012). Table 1-1 illustrates some biological functions of the FFA receptors. GPR40 (FFAR1) is the only receptor that will be discussed in more detail.

Table 1-1: Characterization of Free Fatty Acid Receptors

Protein	Tissue Expression	Ligand	Function	Synthetic Agonist	G protein-coupling
GPR 40 (FFAR1)	Pancreatic β –cell intestinal tract, muscle, brain, monocytes	Medium- and long- C9-C22	Insulin secretion; incretin secretion	Thiazolidinedione, GW9508, MEDICA16	$G_{q/11}$, G_i
GPR41 (FFAR3)	Adipose tissue, sympathetic, ganglia, enteroendocrine, cells	Short C2-C4	Leptin secretion; PYY secretion	/	$G_{i/o}$
GPR 43 (FFAR2)	Leukocyte, spleen, bone marrow, adipose tissue	Short C2-C4	5-HT secretion; PYY secretion; inhibition of lipolysis	/	$G_{q/11}$, $G_{i/o}$
GPR 48	Immune cell, bone marrow, leukocyte, lung, lymph node, spleen	Medium C9-14C	Amplify IL-12 p40	/	$G_{i/o}$
GPR 120	Intestinal tract, Macrophage, lung, adipose tissue	Medium- and long- C10-C22	GLP-1 secretion	NCG21; GW9508	$G_{q/11}$

Adapted from (Stoddart et al. 2008 & Swaminath 2008)

1.3.2. The free fatty receptor 1 (GPR40)

1.3.2.1. Structure and Phylogenetic Analysis

GPR40 is an intronless gene located on CD22 on chromosome 19q13 (Briscoe et al. 2006). Hydropathy analysis indicates that it contains seven hydrophobic regions, consistent with transmembrane (TM) spanning helices and is classified as class A GPCR that belongs to the rhodopsin family (Stoddart et al. 2008) (Figure 1-10). Phylogenetic analysis has clustered GPR40 into a branch of class A that contains receptors for lipids and nucleotides (Costanzi et al. 2008). The GPR40 receptor contains cysteine residues in the first and second extracellular loops that are likely to contribute to structure, proline residues in TM domains 5, 6, and 7, an asparagine in TM1, and an aspartate in TM2. It also contains an arginine at the bottom of TM3, which is within the highly conserved

motif Glu-Arg-Tyr. The arginine is known to bind to a carboxylic group of GPR40 agonists (Costanzi et al. 2008)(Mancini & Poitout 2013). Two N-glycosylation consensus sequences (Asn-x-Ser/Thr) were identified in extracellular loop 2 (Swaminath 2008). The key structural features of FFA1 are exemplified in Fig. 1.10. At the protein level, human GPR40 is 82%, 83% and 88% similar to rat, mouse and dog GPR40, respectively. At the DNA level, rat and mouse GPR40 are 94% identical to each other and 75% and 76% to human GPR40, respectively.

Polymorphisms in the open-reading frame of human GPR40 have been reported (Milligan et al. 2006; Costanzi et al. 2008). Two nucleotide substitutions were found, a replacement of Arg211 by His in the third intracellular loop and a second, relatively rare polymorphism, characterised by replacement of Asp175 by Asn in the second extracellular loop (Ichimura et al. 2009). The functional significance of these polymorphisms remains unclear; a Japanese study has suggested they are linked to variability in insulin-secretory capacity (Hirasawa et al. 2008). Another GPR40 variant, Gly180Ser, was reported by Vettor et al. (2008) and it is associated with reduced β cell ability to sense lipid as an insulin secretory stimulus. The pharmacological consequences of these variations remain to be studied in detail using a range of FFAs.

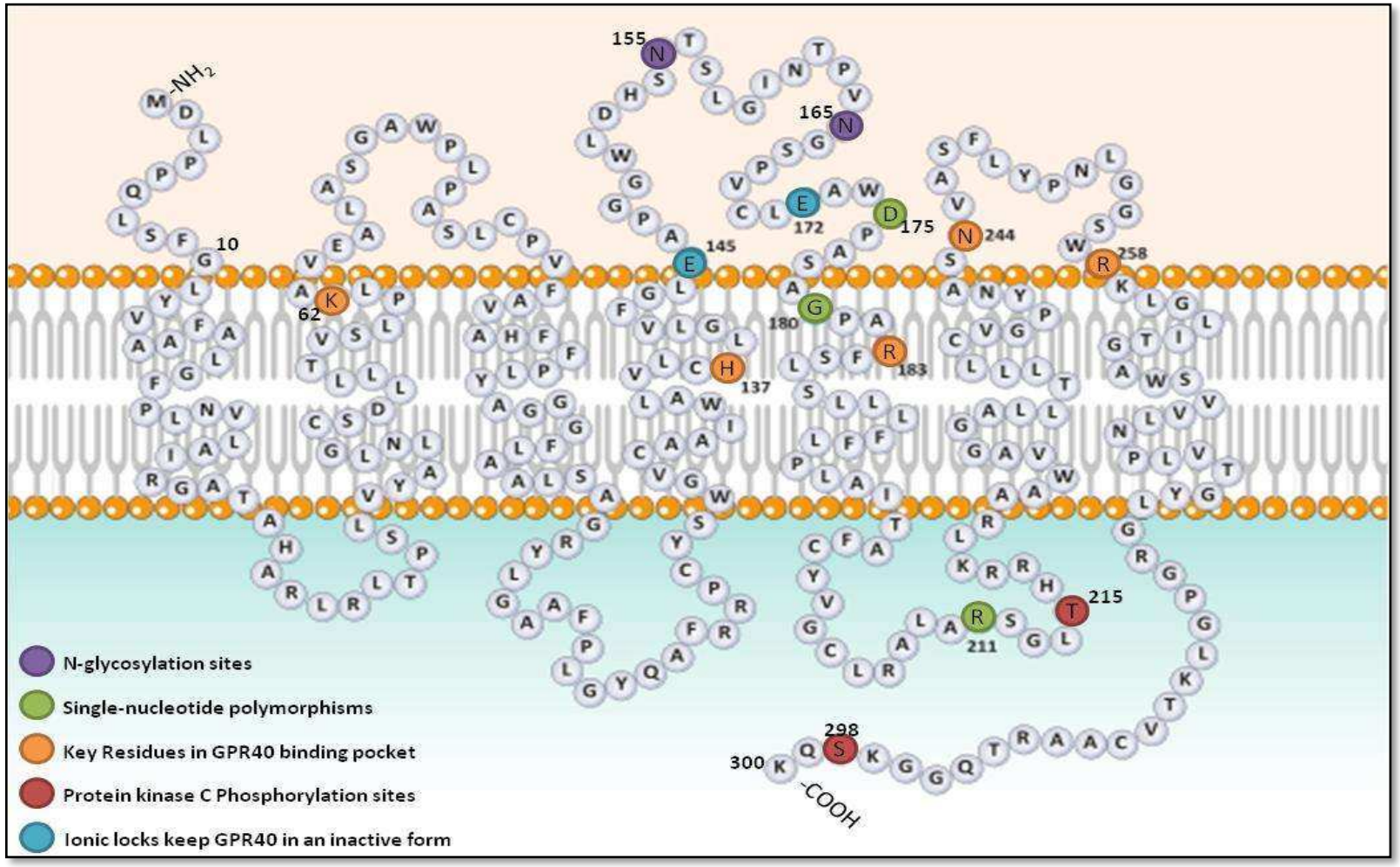

Figure 1-10: Predicted topology of human GPR40.
The figure shows the important functional residues in different colours as indicated in the legend.(Adapted with modification from Stoddart et al. (2008) and Mancini & Poitout (2013)

1.3.2.2. Tissue Distribution

Expression analysis of GPR40 using RT-PCR, Western Blot, Northern blot and immunohistochemistry revealed a high level of GPR40 receptor mRNA and protein in the pancreas (Briscoe & Tadayyon 2003; Itoh et al. 2003; Kotarsky et al. 2003; Ichimura et al. 2009). Closer analysis of the distribution of GPR40 expression in the pancreas showed high levels in the insulin-producing-cells compared to the whole pancreas (Briscoe & Tadayyon 2003; Itoh et al. 2003). GPR40 expression has also been found in pancreas-derived cell lines, including MIN6, TC-3, HIT-T15, and INS-1E (Shapiro et al. 2005; Briscoe & Tadayyon 2003; Itoh et al. 2003; Kotarsky et al. 2003). Expression has also been detected in rat islets (Salehi et al. 2005; Feng et al. 2006) and mouse β cells (Schnell et al. 2007). The expression of the GPR40 receptor in glucagon-producing cell was also reported in some studies (Flodgren et al. 2007; Wang et al. 2011) but not all studies (Itoh et al. 2003).

The expression of GPR40 is controversial and not well documented in other tissues. GPR40 expression is not only tissue specific but also species specific. Kotarsky et al. (2003) and Briscoe et al. (2003) reported the expression of GPR40 in human skeletal muscle using Northern blot and RT-PCR, respectively. However, Steneberg et al. (2005) using PCR and Itoh et al. (2003) using RT-PCR failed to detect the presence of GPR40 in mouse and rat skeletal muscle tissue, respectively. The expression of GPR40 in human brain appears to be ubiquitously expressed with the highest expression in the substantia nigra and medulla oblongata (Briscoe & Tadayyon 2003), although Itoh et al. (2003) were unable to detect GPR40 mRNA in rat brain. Brownlie et al. (2008) also reported the presence of GPR40 in human brain but not in rat brain. The expression of GPR40 in monkey brain was also reported by Ma et al. (2007). Kotarsky et al.

(2003) detected expression of GPR40 in the human liver and heart, but specific expression could not be seen in any of these areas in human or rat tissue by Briscoe et al. (2003) or by Itoh et al. (2003). GPR40 expression has also been reported in human immune cells, with the highest levels of mRNA detected in monocytes (Briscoe & Tadayyon 2003). Hidalgo et al. (2011) detected GPR40 mRNAin bovine neutrophils. In cultured cell lines, functional GPR40 has been detected in human breast cancer cell lines, MCF-7 (Yonezawa et al. 2004) and in bovine mammary epithelial cells and lactating mammary glands (Yonezawa et al. 2008). Expression of GPR40 has been demonstrated within the enteroendocrine cells of mice (Edfalk et al. 2008), hypothalamic ventromedial nucleus (Le Foll et al. 2009), human bronchial epithelial cells (Gras et al. 2009a), mouse bone cells (Wauquier et al. 2013), primary chicken hepatocytes (Suh et al. 2008), mouse keratinocytes (Fujita et al. 2011) and human spleen (Ichimura et al. 2009).

1.3.2.3. Deorphanization of Free Fatty Acid Receptor1 (GPR40)

GPR40 remained classified as an orphan receptor until 2003 when Briscoe et al. (2003); Itoh et al. (2003) and Kotarsky et al. (2003) identified a range of medium and long chain saturated and unsaturated fatty acids as ligands for GPR40. Briscoe et al. (2003) demonstrated that more than 40 different medium and long chain fatty acids (LCFAs) were able to activate GPR40 with micromolar range potency and this result was confirmed by Itoh et al. (2003) who also reported the importance of the carboxyl group in the agonist function. Interestingly, the potency of the saturated fatty acids was dependent on chain length, whereas chain length and degree of saturation did not correlate with the potency of unsaturated fatty acids (Briscoe & Tadayyon 2003).

1.3.2.4. Free Fatty Acid Receptor 1 (GPR40) Synthetic Agonists and Antagonists

The first discovered and most commonly used GPR40 agonist is **GW9508**. It is an arylalkyl derivative of propanoic acid and was identified by GlaxoSmithKline as a potent GPR40 agonist that has a potency in the nanomolar range compared with the micromolar potencies of LCFAs (Briscoe et al., 2006). Costanzi et al. (2008) reported that a carboxylic acid moiety was not essential for agonist action although the presence of such a feature resulted in more efficacious compounds. The same group also identified the FFA1-selective antagonist, **GW1100**. Table 2.1 illustrates some other available agonists and antagonists.

Table 1-2: List of synthetic GPR40 agonists and antagonists

Compound	Property	Reference
Rosiglitazone	Agonist	Kotarsky et al. (2003)
MEDICA 16*	Agonist	Kotarsky et al. (2003)
TAK-875* *	Agonist	Tsujihata et al. (2011)
AMG 837	Agonist	Lin et al. (2011)
TUG469	Agonist	Wagner R et al. (2013)
AM-1638	Agonist	Luo et al. (2012)
AM-6226	Agonist	Luo et al. (2012)
DC260126	Antagonist	Hu et al. (2009); Zhang et al. (2010)
ANT203	Antagonist	Brownlie et al. (2008)

* Antiobesity compound
**A novel and orally available selective GPR40 agonist which is in use in clinical trials. [(3S)-6-({2_,6_-dimethyl-4_-[3-(methylsulfonyl)propoxy]biphenyl-3-yl}meth-oxy)-2, 3-dihydro-1-benzofuran-3-yl]acetic acid hemihydrate)"

1.3.2.5. Signalling mechanisms downstream of GPR40

The initial studies on FFA1 suggested that the GPR40 receptor couples to

the G protein subunit Gαq/11 (Tan et al. 2008; Itoh et al. 2003; Kotarsky et al. 2003) (Schnell et al. 2007) which in turn is predicted to catalyze the phospholipase C (PLC) mediated hydrolysis of phosphatidylinositol 4,5-bisphosphate into diacylglycerol (DAG) and inositol trisphosphate (IP3). DAG and IP3 subsequently serve as second messenger molecules to activate protein kinase C (PKC) and mobilize ER Ca2+ stores, respectively. Latour et al. (2007) and Shapiro et al. (2005) reported that inhibition of Gαq/11 or PLC blocks the FFA-mediated potentiation of GSIS in vitro, whereas IP3 generation in response to FFA in islets was shown to be GPR40 dependent (Alquier et al. 2009). Multiple lines of evidence favour a model in which FFA activation of GPR40 leads to influx of extracellular Ca^{2+} with minimal cytosolic ingress from ER Ca^{2+} stores (Fujiwara et al. 2005). Activation of GPR40 modulates K_{ATP} channel and L-type calcium channel (LTCC) activity, whereas pharmacological inhibition of LTCC or opening of K_{ATP} channels attenuates FFA-induced increases in intracellular Ca^{2+} (Zhao et al. 2008) (Figure 1-11). GPR40 activation increases intracellular Ca^{2+} levels primarily via the coordinated enhancement of extracellular Ca^{2+} influx through LTCC and inhibition of both K^{ATP} and delayed rectifier K^{+} channels (Feng et al. 2006; Shapiro et al. 2005). Furthermore, although the balance of currently available data on GPR40 signal transduction suggests that the IP3 signalling is likely to play a minor role in the control of intracellular Ca^{2+} concentrations (and insulin secretion) in response to FFAs. Recent studies have attempted to unravel the GPR40 mediated, Gαq/11/PLC-dependent signalling mechanisms responsible for FFA augmentation of 2nd phase GSIS. Ferdaoussi et al. (2012) showed that both oleate and exogenous DAG promote the activation/phosphorylation of the serine/threonine protein kinase D1 (PKD1). FFA activation of GPR40 results in the generation of DAG via PLC-mediated hydrolysis of membrane phospholipids, activation of PKD1, cortical actin depolymerization, and potentiation of 2nd phase GSIS (Figure 1-12).

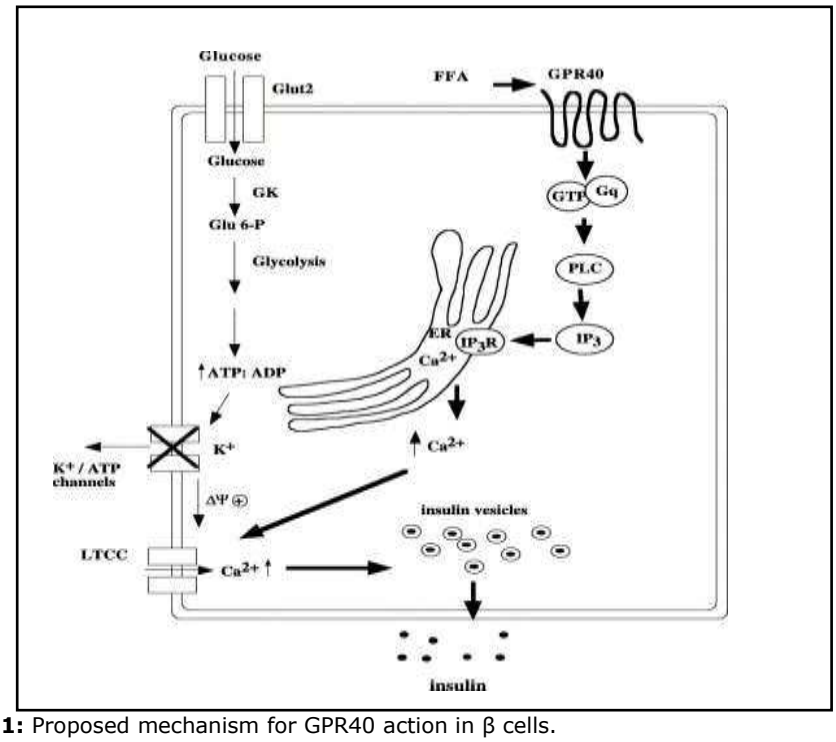

Figure 1-11: Proposed mechanism for GPR40 action in β cells.
Activation of GPR40 leads to calcium release from endoplasmic stores through Gq-PLC signalling pathway.Elevated glucose leads to stimulation of LTCC channel and further increases in intracelluar calcium and insulin release. (Adapted from Shapiro H 2005)

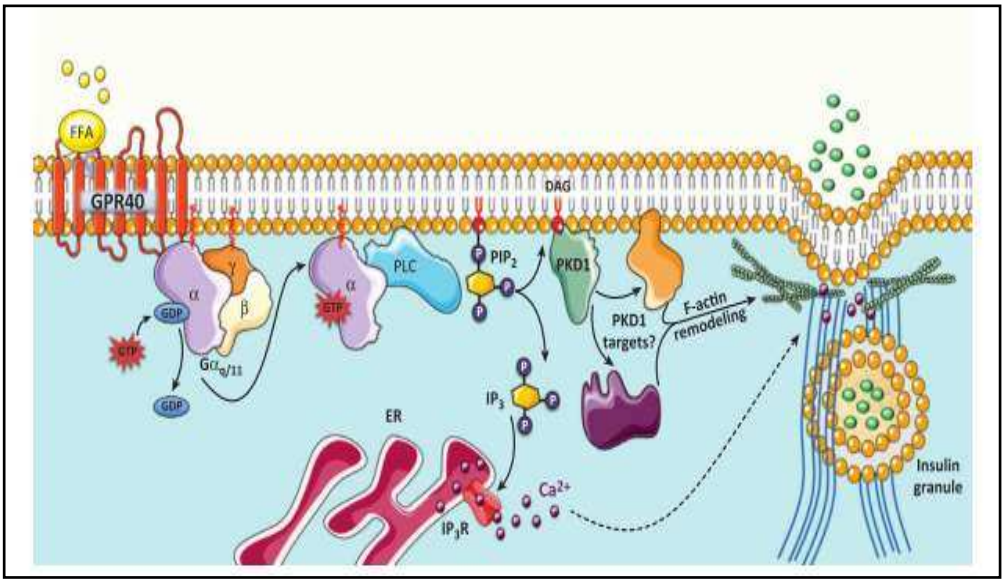

Figure 1-12: Potentiation of glucose-stimulated insulin secretion (GSIS) via GPR40.
Protein kinase D1 (PKD1) mediates free fatty acid (FFA) potentiation of glucose-stimulated insulin secretion (GSIS) via GPR40. Following FFA stimulation of GPR40, the GTP-bound (active) α subunit activates phospholipase C (PLC), which cleaves phosphatidylinositol-4,5-bisphosphate (PIP2) to produce inositol-1,4,5-trisphosphate (IP3) and diacylglycerol (DAG). IP3 triggers Ca^{2+} efflux from the endoplasmic reticulum (ER). DAG promotes the phosphorylation and activation of PKD1 which facilitate (F)-actin filamentous remodelling. Adapted from (Mancini & Poitout 2013)

Data from Itoh et al. 2003 suggested that GPR40 could couple to Gαi, although these findings were not confirmed by Briscoe et al. (2006). Support for the ability of FFA1 to couple weakly to Gi/o comes from studies on the breast cancer cell line, MCF-7, in which treatment with pertussis toxin blocked the LCFA induced elevation of [Ca^{2+}] (Yonezawa et al. 2004). Yonezawa et al. (2008) reported that GPR40 agonists (oleate and linoleate) decreased cAMP production. Fujita et al. (2011) reported that GW9508 inhibited CCL17 and CCL5 expression in a pertussis toxin-sensitive manner in keratinocytes. To our knowledge, the only report that provided evidence for coupling between GPR40 and Gαs is by Feng et al. (2006) who suggested that FFAs may act on GPR40 to activate Gs protein through cAMP/PKA signalling in rat β cell. Linoleic acid significantly enhanced cAMP accumulation when combined with IBMX (phosphodiesterase inhibitor) or forskolin (adeno cyclase stimulator). A recent interesting finding was reported by Mancini & Poitout (2013) who stated that "7 transmembranes receptor can couple to multiple heterotrimeric G proteins as well as to G protein-independent, β-arrestin-dependent pathways to promote the activation of numerous (potentially cross talking) signalling cascades in a ligand and context dependent manner". Whether this can be applied or not to the GPR40 receptors requires further investigation.

1.3.2.6. Regulation of GPR40 expression

A physiologically important property of GPCRs is their tendency to desensitize during exposure to agonists. Desensitization mechanisms include "down-regulation" or reduction of receptor number, apparent shielding of the receptors from interacting ligands and uncoupling from G-proteins (Kaplamadzhiev et al. 2010; Xiao et al. 1999). Addition of a GPR40 ligand for 14 days led to a significant down-regulation of GPR40, i.e., G protein-coupled

receptor-specific internalization (Kaplamadzhiev et al. 2010). A decreased level of GPR40 mRNA expression in the islets of mice kept on a high fat diet for several months and in islet cultured in medium containing high concentrations of FFAs for 18h were observed by (Flodgren et al. 2007). A decrease in GPR40 mRNA after 6 hours treatment with oleic acid was also observed by Hu et al. (2009). Interestingly, GPR40 transcripts and protein were significantly upregulated in bone marrow cell cultured with fibroblast growth factors (Kaplamadzhiev et al. 2010). Expression of the GPR40 gene is reduced under glucolipotoxic conditions in rats (Fontés et al. 2010) and in islets from T2D patients (Del Guerra et al. 2010). However, Briscoe et al. (2003) detected high levels of GPR40 mRNA expression in islets from obese mice (ob/ob) and more recently Kebede et al. (2012) detected an upreguation of GPR40 mRNA expression in mice and human β cells cultured in medium containing high glucose for 6 or 24 hours, respectively.

The transcription factor pancreatic duodenum homobox-1 (PDX1) is highly expressed in β cells and the endocrine cells of the gastrointestinal tract. PDX1 controls key aspects of β cell function by regulating the expression of genes involved in glucose sensing, insulin gene expression, and insulin secretion. Loss or perturbation of PDX1 function leads to impaired GSIS and consequently diabetes or glucose intolerance in both mice and humans (Ahlgren et al. 1998). PDX1 is a transcription regulator for GPR40 and it binds to an enhancer element within the 5-flanking region of GPR40 (Bartoov-Shifman et al. 2007). Studying the mechanism through which glucose regulates the GPR40 gene expression in β cell, Kebede et al. (2012) established that glucose stimulates GPR40 gene transcription in pancreatic β-cells via increasing the binding of PDX1 to the A-box in the HR2 region of the GPR40 promoter. Moreover, they demonstrated that

mutation of the PDX1 binding site abolishes glucose activation of GPR40 promoter activity. This observation is supported by Edfalk et al. (2008) who observed no GPR40 expression in the endocrine cells of PDX1 knockout mice.

1.3.2.7. Potential role of GPR40 Receptor in pancreas and glucose homeostasis

A large number of in vivo and in vitro studies have now conclusively confirmed the importance of GPR40 in mediating the acute stimulatory effects of long chain FFAs on GSIS. GPR40 loss of function via small interfering RNA (Itoh et al. 2003; Shapiro et al. 2005), antisense oligonucleotides (Salehi et al. 2005), pharmacological inhibition (Briscoe et al. 2006), pharmacological activation (. Doshi et al. 2009) or gene deletion in mice (Kebede et al. 2008; Latour et al. 2007; Steneberg et al. 2005) consistently resulted in a significant decrease in FFA-mediated potentiation of GSIS. Interestingly, Vettor et al. (2008) identified a low-frequency mutation in human GPR40 that is associated with a decrease in lipid-mediated enhancement of GSIS. Conversely, transgenic overexpression of the human GPR40 gene prevented the development of hyperglycemia in high-fat diet (HFD) fed mice, and improved insulin secretion and glucose tolerance in genetically diabetic (KK) mice (Nagasumi et al. 2007).

Acutely, FFAs amplify GSIS, but chronically elevated FFAs promote β cell dysfunction and glucolipotoxicity. The potential involvement of GPR40 in β cell glucolipotoxicity has been studied in GPR40$^{-/-}$ and GPR40 transgenic overexpression mice but the result was controversial. Steneberg et al. (2005) demonstrated that HFD fed GPR40$^{-/-}$ mice were protected from insulin resistance, whereas, conversely, transgenic overexpression of GPR40 exhibited disrupted islet morphology and impaired β cell function. They proposed that GPR40 antagonists, rather than agonists, should be developed for therapeutic

use. Brownlie et al. (2008) and Duttaroy et al. (2008) also found that GPR40$^{-/-}$ mice were protected from the effects of HFD on glucose tolerance and had an enhancement in insulin sensitivity. In contrast, Nagasumi et al. (2007), Latour et al. (2007) and Tsujihata et al. (2011) concluded that chronic treatment with GPR40 agonist improved GSIS and hence a reduction in GPR40 signalling may be mechanistically linked to the development of T2D. Authors referred these discrepancies to the GPR40−/− mouse derivation, type of food and duration of feeding. Moreover, Brownlie et al. (2008), Wu et al. (2010) and Tan et al. (2008) reported that GPR40 does not mediate the chronic toxic effects of FFAs on islet function. Accordingly, chronic activation of GPR40 should produce beneficial effects on glucose homeostasis. Indeed, administration of synthetic GPR40 agonists improved glycaemic control in diabetic rodents (Tan et al. 2008; Doshi et al. 2009) and in T2D patients (TAK-875 Phase II trials). TAK-875 significantly improved glycaemic control in patients with type 2 diabetes with minimum risk of hypoglycaemia (Burant et al. 2012). However, the picture has become less clear with a recent study using GPR40 knockout mice conducted by Matsuda-Nagasumi1 et al. (2013) who reported that even though GPR40/FFAR1 has a major role in regulating fatty-acid-mediated insulin secretion; the lack of GPR40 does not induce diabetes even under insulin resistance conditions induced by high fat diet or diabetogenic KK gene. It is worth mentioning that GPR40 receptors have a role in glucagon secretion. Flodgren et al. (2007) reported that knockdown of GPR40 receptors significantly reduced the ability of linoleic acid to increase glucagon exocytosis. In support of this, Wang et al. (2011) reported that FFA-induced secretion of glucagon from isolated islets is GPR40 dependent. Consistent with these *in vitro* observations, Lan et al. (2008) found that FFA1-/- mice secrete significantly less glucagon than wild-type mice in response to elevated plasma fatty acid levels.

1.3.2.8. Potential role of GPR40 in tissues involved in energy homeostasis

GPR40 expression has been found in several tissues including enteroendocrine cells, the brain and skeletal muscle, all of which contribute to glucose homeostasis. Luo et al. (2012) and Edfalk et al. (2008) reported that GPR40 induces secretion of gut hormones and GPR40 null mice displayed reduced plasma incretin levels in response to high fat feeding. Luo et al. (2012) developed GPR40 full agonists that have insulinogenic and incretinogenic properties. Collectively, GPR40 modulates FFAs stimulated insulin secretion not only directly from β cells but also indirectly via regulation of incretin secretion from enteroendocrine cells. Moreover, the expression of GPR40 in hypothalamus could possibly influence the regulation of energy balance (Ma et al. 2007). Interestingly, GPR40 is expressed in taste buds and mediate taste preference to fatty acids (Cartoni et al. 2010). Even though skeletal muscle has a vital role in glucose homeostasis surprisingly no previous reports have described the role of GPR40 in skeletal muscle.

1.3.2.9. Other potential roles of GPR40

Skin. GPR40 suppresses immune inflammation in the skin similar to other Gi-coupled GPCR such as cannabinoid receptors. GPR40 agonist (GW9508) attenuate the induction of critical cytokines (CCL5 and CCL17) by proinflammatory cytokines (TNFα) in keratinocytes and suppresses allergic inflammation in the skin (Fujita et al. 2011).

Bone. Cornish et al. (2008) demonstrated the expression of GPR40 in osteoblasts and osteoclasts, and suggested that activation of GPR40 might mediate the antiosteoclastogenic effects of FFAs. GPR40 receptors might play a

role in the induction of osteocyte apoptosis (Mieczkowska A et al. 2012). Wauguier et al. (2013) confirmed that GPR40-null mice have lower bone density and that GPR40 mediates the FFA-mediated inhibition of osteoclastogenesis.

Cell proliferation. Currently it is well documented that obesity which is accompanied with hyperlipidaemia and elevated circulating free fatty acids is associated with increased risk of cancer (Pirgon et al. 2013). A link between free fatty acids and incidence of breast cancer has also been reported (Rose 1997). GPR40 is expressed in human breast cancer cell line (MCF-7) and its expression is significantly higher at the beginning and at the end of proliferation indicating that LCFA might play a role in cell proliferation (Yonezawa et al. 2004). Hardy et al. (2005) established that oleic acid-induced proliferation is mediated through the GPR40 receptor. In mammary epithelial cells GPR40 mediates LCFA signalling and plays an important role in cell proliferation and survival (Yonezawa et al. 2008). In addition, downregulation of GPR40 by small-interfering RNA led to a significant inhibition in the proliferative effect of the anti-diabetic drugs TZDs in nonmalignant human bronchial epithelial cells. Whether or not chronic GPR40 activation might have carcinogenic effects warrants further investigation as this might hold the key to the use of GPR40 agonists in near future.

1.4. Aim of thesis

Obesity and diabetes are major health problems worldwide. One of the underlying causes of diabetes is insulin resistance and its development appears years or even decades before manifestation of diabetes. Skeletal muscle has a core role in insulin resistance associated with high levels of circulating free fatty acids. The search for safe drugs without side effects to treat diabetic patients has been an attractive field for decades.

The aim of this thesis is to investigate two possible targets for the treatment of insulin resistance (cannabinoid receptors specifically CB1 and free fatty receptor 1) and downstream signalling in human and rat (Wistar and the diabetic model, Zucker) skeletal muscle tissue and cultured cells. The major objectives of this thesis are:

1. To analyse the transcriptional profiles of skeletal muscle tissues and cultured cells in order to assess the suitability of using cell culture to model skeletal muscle metabolism and signalling.
2. To investigate the expression of the cannabinoid receptors and GPR40 in different stages of muscle development as well as in different muscle fibre types.
3. To examine the influence of cannabinoid receptors and GPR40 (GPR40) on insulin signalling and skeletal muscle glucose metabolism.
4. To study the effects of activation and inhibition of GPR40 upon global gene expression profiles in human primary skeletal muscle cells.

CHAPTER TWO

GENERAL MATERIALS AND METHODS

CHAPTER 2. GENERAL MATERIALS AND METHODS

2.1. Tissue collection

Human muscle samples were obtained from the mixed muscle fibre Vastus lateralis (VL). The samples were taken from 19 healthy male volunteers with a age of 22.78±3.02 (Mean±SDV) and BMI of 24.69±2.52 using the needle biopsy technique (Bergstrom needles) under local anaesthetic with medical school ethical approval (G/5/2009).

Rat muscle samples were obtained from Wistar and Zucker fat and Zucker lean rats. Zucker rats were generously provided by Professor Michael Randall. Rat muscle samples were taken from fast muscle fibres Soleus (SOL) and the red portion of gastrocnemius (GR), slow muscle fibre the white portion of gastrocnemius (GW) and the Extensor digitorum longus (EDL) and the mixed muscle fibres Vastus Lateralis (VL). The rats were killed by cervical dislocation without anaesthesia, a method approved by the University of Nottingham and the Animal Scientific Procedures Act (ASPA) and the muscles were carefully excised within 10 minutes of death.

Table 2-1: Rat parameters

	WR	ZFR	ZLR	ZFR	ZLR
Age (wks)	4-6	12	12	20	20
Weight(g)	180-200	342	292	408	401
Blood Glucose(mM)		24	6	28	8.5

WR=Wistar Rat, ZFR=Zucker Fat Rat, ZLR=Zucker Lean Rat

2.2. Reagents

Fetal Bovine Serum (FBS) and Ham's F 10 medium for cell culture were purchased from Sigma and PAA laboratories (Somerset, UK). CB1 agonist ACEA,

GPR40 agonist GW9508, Anandamide (AEA) and PPAR antagonist T0070907 were from Tocris Biosience. Epidermal growth factor (EGF), horse serum and RNA clean up kit were from Invitrogen and MAP kinase inhibitor (U0126) from Promega. Oleic acid, Palmitic acid, Rimonabant (Rim) and fatty-acid-free BSA were from Sigma. Rim was obtained from the NIMA Chemical Synthesis program, via Dr Stephen ALexander. GPR40 agonist and antagonist (AZ921, AZ915, AZ836 and AZ468) were provided by Astra Zeneca. Human brain and spleen Poly A+ RNA were from Clontech (catalogue numbers 636102 and 636121, respectively)

2.3. Muscle cell culture

Satellite cell isolation and culture were carried out according to the method of Blau & Webster (1981) with some modifications. The muscle samples were divided into two pieces, one piece was flash frozen in liquid nitrogen for RNA and Protein extraction. The second piece was put in ice cold phosphate buffer saline (PBS) for primary tissue culture. Under sterilized condition, the sample was washed with PBS and minced finely in a Petri dish by using a scalpel (no.22 blade). The tissue was then transferred to a 50ml Falcon tube containing a magnetic stirrer and 5 ml trypsin (0.05% trypsin, 0.02% EDTA in PBS) and stirred gently for 15 minutes at 37°C. The supernatant was neutralized by adding an equal amount of growth media (Ham's F10 supplement with 20% FBS, 50 iu/ml penicillin and 50µg/ml streptomycin). After removal of tissue debris by filtering through 100µm pore size Nylon mesh the supernatant was transferred to a new falcon tube and centrifuged for 10 min at 1700rpm at room temperature. The cell pellets were re-suspended in 2 ml of Ham's F10 containing 20% FBS media, allowed to adhere to tissue culture plastic for 10mins, to minimize fibroblast contamination, and subsequently transferred to culture in

T25 flasks coated with 0.2% gelatin (W/V).

The cells were grown in 5% CO_2 at 37°C. Feeding of the cells was as follows; after 24 hours the cells were washed with PBS and new Hams F10 media containing 20% FBS were added. The media were then changed every 2 days, in the first 3 weeks with Ham's F10 media containing 20% FBS. Once myoblast cultures reached approximately 80% confluence, they were induced to differentiate by reducing the serum concentration to 10% for 3 days followed by changing into 6% horse serum-containing media until the cells had differentiated into a fused multinucleated myotube network at which point they were treated.

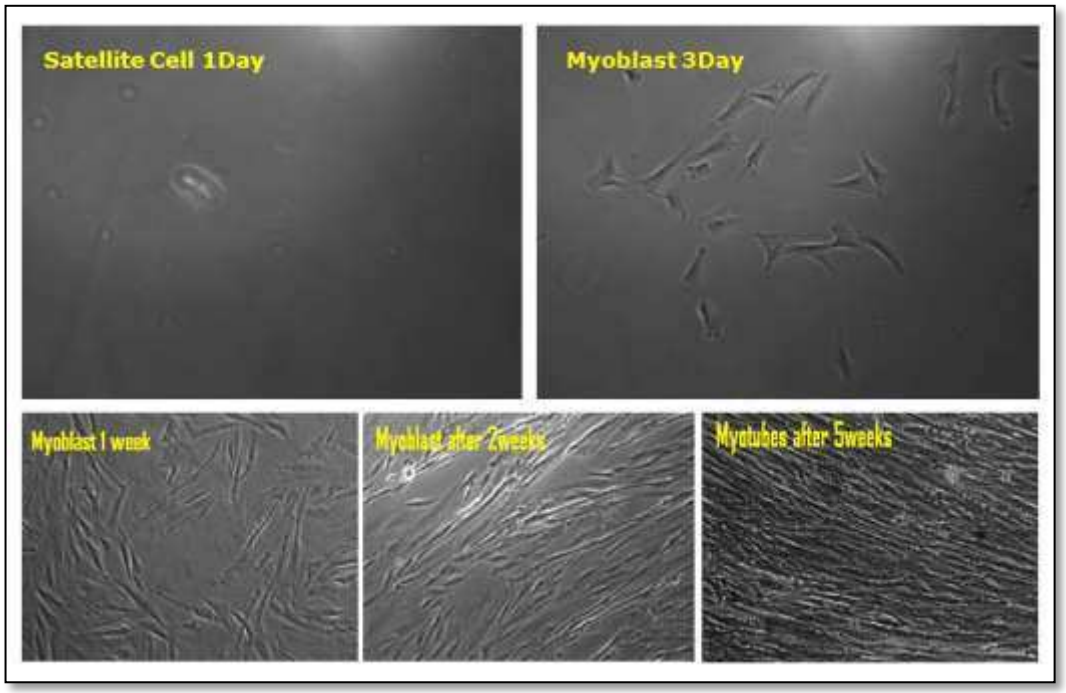

Figure 2-1: Representative pictures for human satellites, myoblasts and myotubes derived from human skeletal muscle

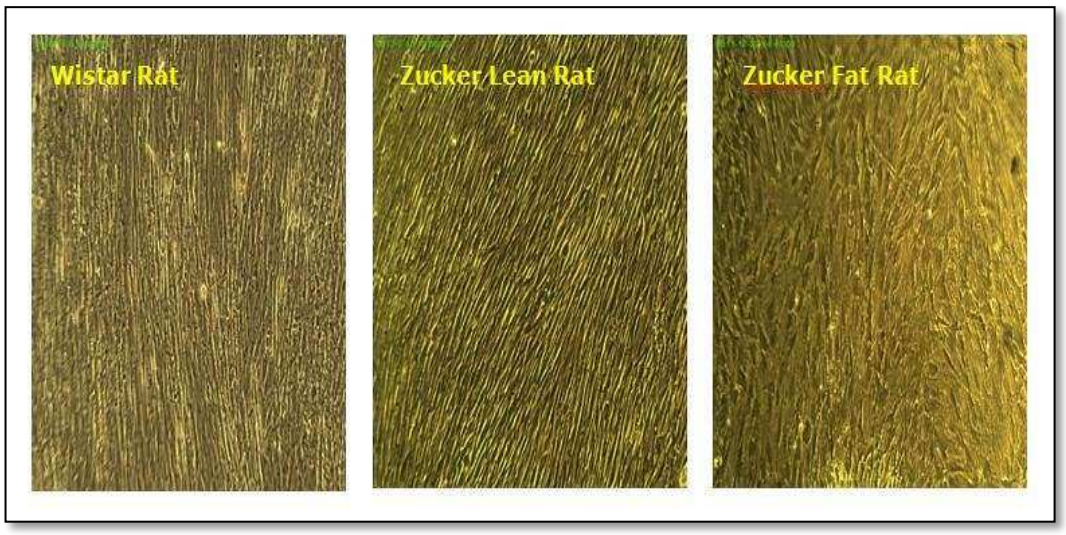

Figure 2-2: Representative picture of Wistar and Zuckers rat myotubes (5 weeks).

Important observation from skeletal muscle culture:

- First, serum plays an important role for successful human cell primary culture as cells were unable to proliferate properly when PAA serum was used and that lead to culture failure in 4 samples . From our experience in muscle culture, we recommended the use of Thermo Scientific Hyclone serum (cat no HYC-001-406B). The serum is sterile filtered, not heat inactivated, Bovine growth serum and US origin.
- Second, there were no observed differences between cells cultured from different muscle types (slow and fast) or rat origin (Wistar and Zucker).
- Third, rat muscle cells proliferate more rapidly than human cells due to the smaller number of satellite cells isolated from the small size human samples.
- Fourth, the maximum time for serum starvation is two hours and we do not recommend serum starvation as cells appear stress.
- Fifth, the appearance of scatter myoblast in day two is a sign of a successful culture.

2.4. Delipidation of foetal bovine serum

Fatty-acid-free serum was prepared according to the method described in Hannah et al, (2001). Briefly, 125ml of FBS was mixed with 40:60 volume ratio of 100 ml N-butanol and 150ml Di-isopropyl ether. The solutions were mixed thoroughly by end to end rotation on a daisy-wheel for 20 minutes followed by incubation on ice for another 20 minutes. Separation of the aqueous phase from the organic phase was achieved by 5 minutes centrifugation at 2500 rpm. The extraction of the aqueous phase (the straw coloured bottom layer) was carefully done by pipette. A second solvent extraction step was carried out by adding 50ml Di-isopropyl ether only. The mixing, centrifugation and extraction was repeated and then with the aqueous phase was placed under a gentle stream of nitrogen for 30 min in order to remove any remaining solvent. Delipidated serums was transferred to a pear shaped flask and freeze dried for at least 24 hours. The freeze dried serum was dissolved in 50ml HPLC water, dialyzed with 3 changes of PBS for 12 hours each and finally filter sterilised using 0.2 μm crodisk syringe filter.

2.5. Preparation of Fatty Acids in Complex with BSA

The 24% (w/v) bovine serum albumin (BSA) was prepared by gradually adding 6g of fatty-acid-free BSA (cat. No. A6003; Sigma) into 17.5ml 150mM NaCl in a beaker, over a slow period of time at room temperature with stirring. The pH was adjusted to 7.4 with 5M NaOH, and the volume made up to 25ml with 150mM NaCl. This solution was filtered through a 0.45μm filter and frozen in aliquots at –20°C.

The fatty acid/BSA solution was then prepared by a modification of the method of Van Harken and Dixon (1969). Briefly, 39.6 mg Sodium Oleate or

36mg palmitic acid was transferred to a glass beaker containing 0.5ml ethanol, and the ethanol was evaporated under a stream of nitrogen. Then 7 ml 24% (w/v) ice-cold BSA and 48µl of 5M NaOH were added. The solution heated gently with stirring on a hot plate until an emulsion is formed then the fatty acids were stored at –20°C until use.

2.6. Analysis of Gene Expression at the mRNA level

2.6.1. Total RNA extraction

Tissue RNA was extracted using Tri-reagent® (Ambion). Frozen ~50 mg of tissues were homogenized in 2ml tri reagent using a Janke & Kunkel Ultra-Turrax T25 homogenizer. The RNA from cell culture samples was extracted by scraping the cells in 1ml Tri reagent. The homogenate was allowed to stand for 5 minutes at room temperature then 200µl of BCP (1-Bromo-3-chloropropane, Sigma) was added per ml of Tri-reagent used. The solution was vortexed and centrifuged at 10,000 rpm for 15 minutes at 4°C. RNA was precipitated from the upper aqueous phase by the addition of 250µl of 2M sodium acetate and 700µl 2-isopropanol per ml of solution. After mixing, the solution was chilled at -20^{o}C for at least an hour, followed by centrifugation at 10000g for 10 minutes at 4^{o}C. The supernatant was discarded and the pellet washed twice with 500µl 70% ethanol solution. The supernatant was then removed, and the pellet air dried for 5 minutes and then re-suspended in 50µl RNAse free water.

2.6.2. RNA clean up, quantification and quality measurement

Total RNA clean up and on-column DNAse digestion were performed using RNeasy purification kit (Qiagen) by following the manufacturer's instructions. The quality of RNA was initially determined by subjecting samples to agarose gel electrophoresis (1.5%). briefly, 1 µg of RNA were mixed with 10 µL of glyoxal

reaction mixture (1x BPTE buffer,1M deionised glyoxal ,4.8% (v/v) glycerol, 60% (v/v) DMSO and 20% (w/v) ethidium bromide), incubated at 55°C for 1 hour and then placed on ice for 10 minutes. Prior to loading into the gel 2µL of loading dye was added to the sample. The gel was run at 90 V (5 V/cm). The RNA 18S and 28S bands were visualised with a UV transilluminator, and the photograph recorded using Genesnap software. Un-degraded RNA samples showed two intact and distinct ribosomal subunits- 28S and 18S. The RNA and purity and concentration were further measured on a nanodrop spectrophotometer (Nanodrop technologies, USA). The ratio of absorbances between 1.8-2.0 at both 260/280 and 260/230 was taken as an indication of acceptance of RNA purity.

For microarray studies, RNA quality was also measured by Agilent bioanalyzer 2100 which provides concentration, visual inspection of RNA integrity, generates a ribosomal ratio and an RNA Integrity number (RIN). RIN is a comprehensive estimation of RNA integrity, as it takes the entire electrophoretic trace into account (Mueller & Schroeder, 2004). Samples were deemed acceptable for microarray studies if they had a RIN value more than 7.5 (see Figure 2-3 & appendix 1).

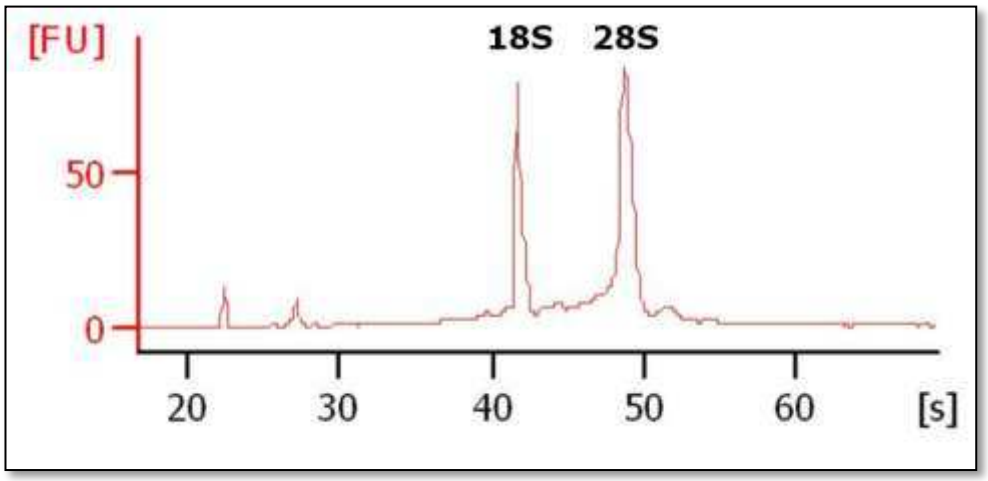

Figure 2-3: Electrophoretogram showing 18S and 28S peaks in one sample with RIN=9.5.

2.6.3. mRNA purification from total RNA

Dynabeads® mRNA purification kit (Invitrogen) was used to extract mRNA from total RNA to overcome the problem of genomic DNA contamination following the manufacturers' instructions. As suggested for low total RNA concentrations, the amount of reagents used were reduced according to the concentration of total RNA used (3.5 to 7.5 µg were used). mRNA was eluted from the dynabeads using 11µl 10mM Tris-HCl (pH 7.5) and heating for 2 min at 70^{o}C. Dynabeads were reconditioned and used for subsequent mRNA extraction according to the manufacturers' protocol.

2.6.4. cDNA synthesis

cDNA was produced by the reverse transcription of 500ng of total RNA or 10 µL of mRNA prepared from at least 3.5 µg total RNA. The following were added into 0.5 ml PCR tubes: the total RNA or mRNA, 1µL random primers (100ng), 1µl of dNTP's (10 mM) along with RNase-free water was added to give a total volume of 13 µL. The tubes were briefly vortexed and centrifuged before being placed into a thermocycler (MWG-Biotech Primus 96 Plus) at 65°C for 5 minutes followed by a rapid chill on ice. Whilst on ice 4µL of 5 X First-strand buffer, 1 µL of 0.1M DTT, 1µL of RNaseOUT (40u/µL) and 1µL of Superscript™ III RT (200u/µL) were mixed and then added to the primer:RNA mix. The contents of the tube were mixed and incubated at 25°C for 5 minutes, 50°C for 1 hour, 70°C for 15 minutes and then cooled to 4°C. cDNA was then stored at -20°C until RT-QPCR analysis.

2.6.5. Analysis of mRNA expression by TaqMan® real-time quantitative PCR

The mRNA expression levels of selected genes were quantified using the

step one plus real –time PCR system (Applied Biosystems) based on Taqman standard curve method. The Taqman RT-PCR is a very selective and useful assay for the amplification of specific sequences encoding the gene of interest. It employs the use of a Probe where its ends are labelled with a fluorophore and a quencher respectively. During the RT-PCR reaction, the Probe identifies amplified targets and binds to them. The intensity of light emitted, which is due to the release of the probe, is measured in real time which reflects the expression levels of the gene in the sample being analysed. For a reaction with a total volume 25µL the following reagents were added to 5µl of cDNA;

Table 2-2: Sample preparation for QRT-PCR reaction.

TaqMan® Universal PCR Mastermix Applied Biosystems (4304437)	12.5µL
Forward primer (10 µM)	0.75µL
Reverse primer (10 µM)	0.75µL
Probe (dual labelled) (10 µM)	0.5µL
Water (molecular grade)	5.5µL

A negative/No Template Control (NTC) was also included by replacing 5µL of cDNA with 5µL RNase-free water. Thermo-cycling parameters were 50°C for 2 minutes, 95°C for 10 minutes (melting temperature) followed by 40 x (95°C for 15 seconds, 60°C for 1 minute) (annealing temperature). The standard curve consisted of two-fold serial dilutions of cDNA reverse transcribed from a known quantity of RNA (NEAT). All standards, samples and negative controls were assayed in triplicate to ensure accurate results. The threshold cycle (Ct Value) is the point at which fluorescence rises to a point considered statistically significant above the baseline values. A standard curve was then constructed by plotting Ct values versus the logarithm of the serial cDNA dilutions. Any assay which did not have a standard curve with a slope between -3.0 and -3.6 (90-100% efficient)

was rejected as were any results where the values for the triplicates had a range greater than 0.5 Ct Figure 2-4. Maintenance genes were used where appropriate.

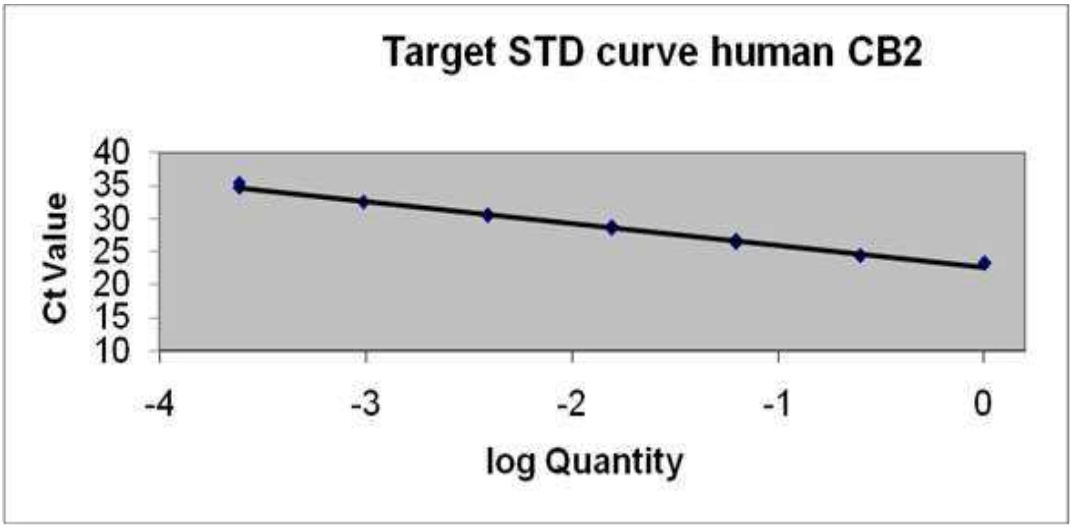

Figure 2-4: Serial standard curve with slop of -3.33 and r2 of -0.99

The primers and probes (Table 2-3) were designed using Primer Express 3 software and analysed by NCBI blast.

Table 2-3: Oligonucleotide sequences for probes and primers

Type	Forward Primer (5'?3')	Reverse Primer (5'?3')	Probe
18S	CGGCTACCACATCCAAGGAA	GCTGGAATTACCGCG	TGCTGGCACCAGACTTGCCCTC
Human *β-actin*	CCTGGCACCCAGCACAAT	GCCGATCCACACGGAGTACT	ATCAAGATCATTGCTCCTCCTGAGCGC
Human CB1	GCCCATGTGGCTAAAAAAGC	CAATGCCAAGTGTATCGGTTCTT	AGACAGTGGATGAGACACACAACGGCA
Human CB2	GCAGCGTGACTATGACCTTCAC	GAGCTTTGTAGGAAGGTGGATAGC	TGACCGCCATTGACCGATACCTCTG
Human EGR1	CCGCAGAGTCTTTTCCTGACA	CCACAAGGTGTTGCCACTGT	TGGAGACCAGTTACCCCAGCCAAACC
Human GPR 119	GCGGATGGCATTTGTCACTT	GTACCTGTCAAAGGTGATCAGCAT	CTCCGCAGCTGCCTCTGTCCTCAC
Human GPR 55	AATGACATCTCTCAGCCCTCTCA	CAGCAATTCATGCCCATTGA	TGCACCGGACCACCAACAGTTGTG
Human GPR 40	GCCCGCTTCAGCCTCTCT	GAGGCAGCCCACGTAGCA	CCTGCTCTTTTTTCTGCCCTTGGCC
Human IL6	GGCGCTTGTGGAGAAGGAG	CGGGAACGAAAGAGAAGCTCTA	TCCCCTCCAGGAGCCCAGCTATGA
Human PDK4	CAAGGATGCTCTGTGATCAGTATTATTT	TGTGAATTGGTTGGTCTGGAAA	CATCTCCAGAATTAAAGCTTACACAAGTGAATGGA
Human TBP	GGAGCTGTGATGTGAAGTTTCCTA	CCAGGAAATAACTCTGGCTCATAAC	TAGAAGGCCTTGTGCTCACCCACCA
Human TNFa	CCCAGGGACCTCTCTCTAATCA	GGTTTGCTACAACATGGGCTACA	CTCTGGCCCAGGCAGTCAGATCATCT
RAT *β-actin*	AGCCATGTACGTAGCCATCCA	TCTCCGGAGTCCATCACAATG	TCTCCCTGTATGCCTCTGGTCGTACCAC
Rat CB1	CCAAAAGTGGAGAGCGACAAC	CGTCTCGAAGGTCCCAATGT	CATCCAGATCACCATGCCGTTCACA
Rat CB2	TTGGCCGGAGCTGACTTC	CACACCGTGAAAGACATGGAA	CGTGATCTTTGCCTGCAACTTCGTCA
Rat GPR 119	TCCATATTCCAGCAGACCACCTA	GCACAAACCTTGGGTGAAACA	CATGGGCCCTGCACCTTCTTTGC
Rat GPR 40	CCTGCCCGACTCAGTTTCTC	CGGAGGCAGCCCACATAG	TTCTGCTCTTCTTTCTGCCCTTGGTTATCA
Rat GPR 55	CGCCATCCAGTACCCTCTTC	ATGCAGCAGATCCCAAAGGT	TCAATCACTTCCGGTCCCCCAGG
RAT IL6	TCAGGAACAGCTATGAAGTTTCTCTCCG	CGAAACTGGCTGGAAGTCTCT	GGCAACTGGCTGGAAGTCTCT
Rat PDK4	GCTCACACAAGTCAATGGAAAATT	ATGTGGTGAAGGTGTGAAGGAA	CCAGGCCAACCAATCCACATCGTG

2.6.6. One-Color Agilent Microarray:

Agilent's Quick Amp Labelling Kit protocol was followed; briefly, cDNA was generated from 500ng of total RNA mixed with Agilent RNA spike-in positive control in the presence of T7 promoter primer. Fluorescent cRNA (complementary RNA) was generated by using T7 RNA polymerase, which simultaneously amplifies target material (approximately 100-fold) and incorporates cyanine 3'-labeled CTP. According to the manufacturers recommendation, RNeasy Mini Kit (Qiagen) was used for cRNA purification and NanoDrop spectrophotometer for quantification of of cRNA (ng/µL) and cyanine 3 (pmol/µL) concentrations to determine the specific activity and cRNA yield. Recommended cRNA yields and specific activities for hybridization are ≥1.65 and ≥9, respectively. For hybridization, equal amounts of cRNA were hybridized to Agilent Human Whole Genome Oligo Microarray for 17 hours at 65^{o}C with rotation (10 rpm) in a hybridization oven. The hybridized microarrays were subjected to washing as recommended by Agilent protocol. Scanning and feature extraction were done using Agilent scanner.

2.6.7. Affymetrix microarray

Whole-genome Human GeneChip HT PM Array (HG_U133+PM_(HT_HG-U133_Plus_PM) was used. The RNA was isolated from human myotubes after being subjected to different treatments. The labelling and hybridization steps were performed at the Nottingham Arabidopsis Stock Centre (NASC).

2.6.8. Taqman® Low-Density Array

Taqman® Low-Density Custom Array Micro Fluidic cards (ABI Applied Biosystems, UK) were used for the quantification of expression of 48 key metabolic genes in human skeletal muscle. Each card allowed for 8 samples to

be run in parallel for 48 Taqman gene expression assay targets that were pre-loaded into each of the wells on the card. Briefly, 55 µl of Taqman Universal PCR master mix (2x) (ABI Applied Biosystems, UK) was added to 500 ng RNA equivalent of 30 µl cDNA into an Eppendorf RNAse free tube. RNAse free water (25 µl) was then added to make the total volume of the reaction mixture up to 110 µl. The reaction mixture was then vortexed, centrifuged and loaded into one of the fill reservoirs of the Micro Fluidic card. The cards were then centrifuged (MULTIFUGE 3 S-R, Heraeus) and run on a 7900HT Fast Real-Time PCR System (ABI Applied Biosystems, UK). The expression of hydroxymethylbilane synthase (HMBS) was used to normalise the data to minimize variations in the expression of individual housekeeping genes. Gene expression was measured using the 2-ΔΔCt method.

2.7. Protein Expression Experiments:

2.7.1. Protein gel electrophoresis and Western blotting

Reagents

10% Ammonium persulfate (APS)

0.1g of Ammonium persulfate was dissolved in 1ml of distilled water immediately prior to use

4x Separation Buffer (pH 8.8)

1.5 M Tris.Cl

0.4%SDS

4x Stacking Buffer (pH 6.8)

0.5 M Tris.Cl

0.4%SDS

SDS-PAGE Separating Gel (12% for 2 gels)

30% Acrylamide/bisacrylamide: 8 ml

4x separation buffer: 5ml

Distilled water: 6.8ml

10% APS: 200 µL

TEMED: 20 µL

SDS-PAGE Stacking gel (10ml)

30% Acrylamide/bisacrylamide: 1 ml

4x stacking buffer: 2.5ml

Distilled water: 6.5ml

10% APS: 120 µL

TEMED: 12µL

5x Protein sample loading buffer (50ml)

1 M Tris (pH 6.8) :4.5 ml (90mM)

5% (v/v) beta-mercaptoethanol

4% (w/v) SDS:2g

Bromophenol blue (0.01% w/v)

7M deionized urea (dissolved in water and deionized by incubation with Amberlite Monobed resin for 30 min with gentle stirring)

SDS-PAGE running buffer (500ml 10x)

1.92 M Glycine: 72g

0.25 M Tris base: 15g

10% (w/v) SDS: 5g

Transfer buffer (500ml 10x)

1.92 M Glycine: 72g

0.25 M Tris base: 15g

Tris-Buffered Saline (10xTBS PH 7.4)

Tris Base: 15g

NaCl: 4.4g

KCL: 1.0g

pH adjusted to 7.4 and made up to 500 mL with distilled H_2O

TBS-T

10xTBS 1:10

0.1% (v/v) Tween™20

Blocking buffer

3% fish gelatine in TBS-T

Stripping buffer (pH 2.0)

0.25 M glycine

2% SDS

Ponceau Red

0.1% (w/v) Ponceau S (3-hydroxy-4[2-sulpho-4-(4-sulphophenylazo)-phenyl-azo]-2, 7-napthalenedisulphoric acid) in 5% (v/v) acetic acid.

2.7.2. Protein extraction and quantification

Proteins were precipitated by adding isopropanol to the organic bottom layer following the RNA extraction with trizol method, and centrifuging at 5000rpm for 10 minutes at 4O^{o}C. After removal of supernatant, the pellet was washed with 0.3M guanidine HCl/ 95% ethanol and then stored in 2 ml 70% ethanol (-20^{o}C). The pellets were dissolved in SDS (Sodium Dodecyl Sulfate)-Urea sample buffer. For complete dissolving of the proteins, 3x 10 second sonication was performed.

Proteins in RIPA buffer (Radio Immuno Precipitation Assay) [150mM NaCl 25mM Tris-HCl pH 7.6, Triton X-100, 1% Sodium deoxycholate 0.1% SDS, 1mM Na_3VO_4, 10mM NaF, and stock 25 × Complete Protease inhibitor (Roche)], were dissolved by sonicating 3 times for 10 seconds and rotating the homogenate for

45 minutes on a daisy wheel in cold room followed by centrifugation at 15000g for 10 minutes. The supernatant was then separated from the pellet and assayed for total protein concentration was determined using the BCA Protein Assay Kit (Pierce, Rockford, IL). Sample loading buffer was used before heating and loading of the sample in the polyacrylamide gels for electrophoresis.

2.7.3. Sodium dodecyl sulphate polyacrylamide gel electrophoresis (SDS-PAGE)

Protein (25 to 45µg/ml) in RIPA buffer was mixed with 5X denaturing buffer boiled for 5 minutes and then resolved on 12% SDS-Polyacrylamide gel for about an hour under a constant current of 150mA. Proteins were then transferred onto pre-soaked nitrocellulose membrane at 105mA, after which the membrane was blocked for 1 hour in blocking buffer (3% fish gelatine in 0.1%TBST) in order to reduce non specific binding to the primary antibody. The membrane was subsequently incubated with appropriate polyclonal or monoclonal antibodies as listed in table below overnight at 4^{o}C. Blots were washed three times for 15 minutes duration each in TBST buffer and incubated with IRDye® conjugated anti-rabbit or anti-mouse secondary antibodies (LI-COR® biosciences) for an hour at room temperature. After subsequent washing (3 times 5mins in TBST) the blots were scanning by using a LI-COR® Odyssey infrared imaging system (LI-COR® Biosciences, Lincoln, NE/USA). Densitometric analysis of protein bands were performed on Odyssey version 3 software.

Table 2-4: List of primary and secondary antibodies used in Western Blot experiments

Antibody (Catalog number)	Company	Species raised in	Concentration	Condition	Secondary	Approx Weight (kDa)
Monoclonal—phospho-p44/42 MAPK (ERK1/2)—(#4370)	Cell Signalling	Rabbits	1/1500	Overnight incubation	1/10000	44
Monoclonal—p44/42 MAPK (ERK1/2)—(#9107)	Cell Signalling	Mice	1/1500	Overnight incubation	1/10000	42
Monclonal--phospho-GSK-3α/β--(#9327)	Cell Signalling	Rabbits	1/500	Overnight incubation	1/10000	51 α 46 β
Monoclonal--GSK-3α/β--(sc-7291)	Santa Cruz Biotechonology	Mice	1/1000	Overnight incubation	1/10000	51 α 47 β
Monoclonal--phospho-AKT--(#4051)	Cell Signalling	Mice	1/500	overnight incubation using bags	1/10000	60
Polyclonal--AKT--(#9272)	Cell Signalling	Rabbits	1/1000	overnight incubation using bags	1/10000	60
Monoclonal--P38--(#9107)	Cell Signalling	mouse	1/1000	Overnight incubation	1/10000	40
Monoclonal--phospho-P38--(9215)	Cell Signalling	Rabbits	1/500	Overnight incubation	1/10000	43
Monoclonal--cyclophilin--(ab74173)	Abcam	mouse	1/1500	Overnight incubation	1/10000	21
Polyclonal CB1 (10006590)	Cayman	Rabbits	1/500	Overnight incubation	1/10000	
Polyclonal CB2 (101550)	Cayman	Rabbits	1/500	Overnight incubation	1/10000	

2.7.4. Immunocytochemistry

Rat myoblast cells were grown on a coated cover slip and fixed with 3-4% PAF (paraformaldehyde in PBS pH 7.4) for 15 min at room temperature. The cells were then washed twice with ice cold PBS. Permeabilization was done by incubation of the samples PBS containing 0.25% Triton X-100 for 10 min and cells were then washed in PBS three times for 5 min. To block unspecific binding of the antibodies cells were incubated with 1% BSA in PBST for 30 min. Overnight incubation with the primary antibodies was done at 4°C. The solution

was then decanted and the cell washed three times in PBS (5min each) before incubation with the secondary antibody in 1% BSA, PBS for 1 hr at room temperature in the dark. The cells were then washed three times with PBS for 5 min each in the dark. Before mounting the cover slip on a slide the nuclei were stained with DAPI for 1 min. Images were obtained using a Leica DMRB fluorescent microscope with an oil or glycerol immersion lens at 40x and 64x magnification, respectively. Images were captured using Openlab software (Improvision-Perkin Elmer, UK).

Table 2-5: List of primary and secondary antibodies used in immunoflourescence experiments

Primary antibody (source)	Dilution/conditions	Secondary antibody/wavelength	Dilution/conditions
Rabbit polyclonal anti- GLUT 4 (Abcam 33780)	1:100, O/N, 4°C	Goat anti-rabbit Alexa Fluoro 488	1:750, 1hrs, RT
Mouse monoclonal anti- PKC β (P-2584 Sigma, UK)	1:500, O/N, 4°C	Anti-mouse Alexa fluoro 568	1:750, 1hrs, RT
Rabbit monoclonal anti Ki67 (Abcam, UK)	1:200, O/N, 4°C	Goat anti-rabbit Alexa Fluoro 488	1:750, 1hrs, RT
Rabbit polyclonal anti- PKC δ (P-8333 Sigma, UK)	1:500, O/N, 4°C	Goat anti-rabbit Alexa Fluoro 488	1:750, 1hrs, RT
Rabbit polyclonal anti- PKC ζ (P-0713 Sigma, UK)	1:500, O/N, 4°C	Goat anti-rabbit Alexa Fluoro 488	1:750, 2hrs, RT

2.8. Calcium imaging

Single cell intracellular [Ca^{2+}] was quantified in myoblast and myotube clusters by using Ca^{2+} sensitive fluorescent dye fura-2AM (Cambridge Bioscience, Cambridge, UK) and an Andors IQ imaging system. The cells were seeded in 19 mm glass coverslips (0.2% gelatine coated). Cells were washed 3 times with Ca^{2+}buffer (NaCl 145mM, KCl 5mM, $CaCl_2$ 2mM, $MgSO_4$ $7H_2O$ 1mM, HEPES 10mM and Glucose 10mM with or without 2g BSA) and then loaded with 10μM Fura-2-AM for 30 minutes in the dark at 37°C followed by wash and another 15 min incubation with buffer. The cover slips were fixed to a Perspex chamber and the

pictures were taken by Retiga chilled digital intensified charge-coupled device (CCD) camera. Images were obtained every 5 sec up to 30 min by exciting the preparations at 340 and 380 nm. Excitation wavelengths were used to obtain the ratio 340/380 with excitation wavelengths set to 500 nm.

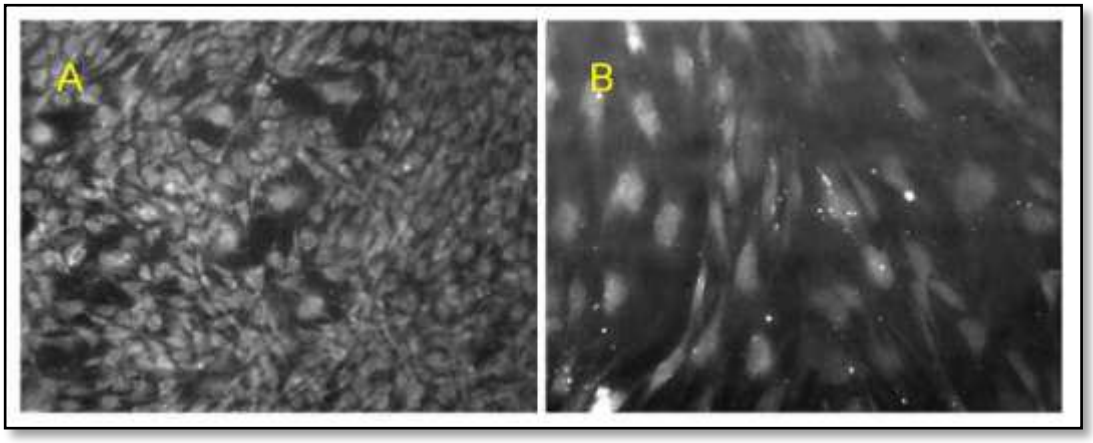

Figure 2-5: Myotubes (A) and Myoblasts (B) loaded with fura-2

CHAPTER THREE

MICROARRAY STUDY OF MUSCLE DEVELOPMENT, MYOGENESIS

CHAPTER 3. MICROARRAY STUDY OF MUSCLE DEVELOPMENT, MYOGENESIS

3.1. Introduction

Myogenesis, skeletal muscle development, is a multistep process that involves commitment of multipotential, mesodermal precursors to a muscle cell fate, followed by myoblast proliferation, activation of muscle specific genes, and fusion to form multinucleated muscle fibres (Shen et al. 2003). This complex process is a highly ordered cascade and is under strict transcriptional control. In myogenesis, proliferation of mononucleate myoblasts is followed by irreversible cell-cycle withdrawal, cell fusion to form multinucleate myotubes and subsequent maturation of myotubes into various classes of myofibres. Myogenic differentiation is under the control of two major families of transcription factors; the myogenic regulatory factor (MRF) family which includes (Myf5, MyoD, myogenin and MRF4) and the myocyte enhancer factor 2 (MEF2) family which consists of MEF2A, MEF2B, MEF2C and MEF2D (Tomczak et al. 2004; Wang et al. 2004). It is well known that the quiescent satellite cells are activated after muscle injury as well as severe exercise, however the fate of these cells is either to myogenesis or to a mesenchymal alternative differentiation program (Shefer et al. 2004; Yablonka-Reuveni 1988; Beauchamp et al. 1999; Zammit et al. 2006). Different molecular markers (Pax7, Pax3 & MYOD) have been identified which can be used to characterize muscle satellite cells (Parker et al. 2003; Siegel et al. 2011; Seale et al. 2000). However, (Shefer et al. 2004) reported that Pax7 is initially expressed in both myogenic and non-myogenic clones and (Yablonka-Reuveni et al. 2008) reported that Pax3 is only present in certain muscles such as diaphragm and limb muscles. The activated satellite cells and

proliferating myoblasts tend to co-express Pax7 and MyoD, whereas the differentiating myocytes start to express myogenin with concomitant downregulation of Pax7 (Wang et al. 2008 and Zammit et al. 2006). It has been found that insulin-like growth factors, hepatocyte growth factors, fibroblast growth factors (Kudla et al. 1998 and Bhasker & Friedmann 2008) and the p38 mitogen-activated protein kinase (MAPK) pathway are required for myogenesis. The extracellular signal-regulated kinase (ERK) pathway plays dual roles: it inhibits differentiation at the onset of differentiation and promotes myocyte fusion at the late stage of differentiation (Wang et al. 2008). Although myogenesis has been widely described, this complex cascade, which involves many steps and interactions between various genes is not fully understood. Furthermore, there are many genes involved in muscle cell proliferation/differentiation that are not yet known. The rapid development of expression microarray technology has provided new possibilities to view myogenesis in a genome-wide perspective. In skeletal muscle the use of microarray studies has focused on the identification of gene expression differences between normal and diseased muscle (Haslett & Kunkel 2002; Baker et al. 2006; Gonzalez de Aguilar et al. 2008; Han et al. 2003). The transcriptional profile differences between myoblasts and myotubes were studied in C2C12 mouse cells at limited time points in the glycogenome only (Moran et al. 2002 and Janot et al. 2009). In this study microarray was used not only to focus on gene expression differences between proliferating and fully differentiated stages but also to highlight the importance of the identification of suitable reference genes as well as searching for G protein coupled-receptors which might have a role in skeletal muscle development. Changes in mRNA transcription levels are crucial during developmental processes. Ideally the reference genes should not be regulated or influenced by the experimental

procedure, should be resistant to cell cycle fluctuations or nutrient status and be expressed early in fetal development and throughout adulthood (Radonić et al. 2004 and Warrington et al. 2000).

The superfamily of Gprotein-coupled receptors (GPCRs) is one of the largest families of proteins in the mammalian genome which play a key role in cellular communication, mediating the efficient coordination of a cell's responses to extracellular stimuli (Lander et al. 2001; New & Wong 2007). GPCRs share a common structural signature of seven hydrophobic trans membrane (7 TM) segments, with an extracellular amino terminus and an intracellular carboxyl terminus (Kobilka 2007). These receptors can be clustered into 5 families: the rhodopsin family, the adhesion family, the frizzled/ taste family, the glutamate family, and the secretin family (Fredriksson et al. 2003). When stimulated these receptors modulate the activity of a wide range of intracellular signalling pathways that facilitate cellular development, cell migration, differentiation, proliferation, and survival (Wang et al. 2007). GPCRs transduce signals across the plasma membrane through their ability to stimulate guanine nucleotide exchange by heterotrimeric G proteins which are grouped into four classes, known as Gαq/11, Gαi/o, Gαs and Gα12/13 (New & Wong 2007). This promotes the release of free Gα and Gβγ subunits, which then initiate intracellular signal transduction. Members of all four classes of Gα subunit have been shown to be involved in the regulation of cell growth and proliferation. Depending on the type of G protein to which the receptor is coupled, a variety of downstream signalling pathways can be activated. GPCR-mediated proliferation activate via activation of PI3Ks, MAPKs , NF-kB or transactivating of RTKs (Receptor Tyrosine Kinase) which is integral to second messenger regulation (Milligan & Kostenis 2006; Schäfer et al. 2004; Wang et al. 2007). Signalling is then attenuated

(desensitized) by GPCR internalization, which is facilitated by arrestin dependent or arrestin independent pathways (Kroeze et al. 2003; Luttrell & Lefkowitz 2002). Very little is known regarding the possible roles of GPCRs in regulating the development of skeletal muscle and most studies have used myogenic cell lines C2C12 and L6 as models for studying skeletal muscle development (Jean-Baptiste et al. 2005; Weiss et al. 2010).

Skeletal muscle primary cell culture provides a well-established model for studying myogenesis as well as the metabolic and molecular functions of skeletal muscle. The drawback of cell culture in general is that cells change their phenotype and remain relatively immature (Raymond et al. 2010; Baker et al. 2006).The availability of microarray technology makes it possible to investigate the gene expression differences between human myotubes and skeletal muscle tissues.

3.2. Aims

The objectives of this study are:

- To address the gene expression difference during muscle development.
- To recognize suitable and stable reference genes during skeletal muscle development.
- To identify GPCRs that might have a role in skeletal muscle development.
- To study the differences in the global gene expression profiles between myotubes and skeletal muscle tissue.

3.3. Experiment design and methods

3.3.1. Sample collection and preparation

Human skeletal muscle tissues from vastuis lateralis were collected from three subjects and samples were divided into two parts, the first part snap frozen in liquid nitrogen and the second part was used for isolation and culture of satellite cells in gelatinized flasks.

Total RNA, mRNA, cDNA and protein preparation was performed as described in chapter 2 section 2.6.

3.3.2. One-Color Microarray:

Agilent one color whole genome microarrays (4*44K DNA) were used to measure the mRNA expression level of 41078 entities in human skeletal muscle tissues, myoblasts and myotubes. The microarray experiment was carried out as described in chapter 2 section 2.6.6 .Data were extracted using Agilent Feature Extraction Software. Data from arrays which passed the Agilent QC report were loaded onto GeneSpring GX 11 software (Appendix 2).

3.3.3. Pre-processing and normalization of microarray data

Pre-processing of raw probe intensities is an essential procedure in the analysis of gene expression microarray data. Generally, background correction and normalization are used to reduce the impact of variations in experimental conditions (Gyorffy et al. 2009).

Normalization requires adjustment of microarray data for effects which arise from variation in the technology rather than from biological differences between the RNA samples or between the printed probes (Smyth et al. 2003). Background Subtraction is an important step in this process as fluorescence of a

spot is due not only to spot signal intensity but also background noise which is due to a variety of technical factors. The processed signal was generated after background subtraction by setting all data with a value of less than 1.0 to 1.0 to avoid bias in estimation.

In order to produce similar scales for fold changes in both the up and down directions as well as to produce normal distribution of expression, raw data were transformed to log to base 2 followed by 75% quantile normalization. Quality control was performed as a first step to identify potential outliers; two unsupervised methods were used, Pearson correlation and Principal Component Analysis (PCA).

Ranking of genes involves either ranking the genes in order of expression from strongest to weakest or choosing a critical-value above which any value is considered to be significant. Agilent flagging rules were applied and all the marginal and absent features were sited to be missing before ranking. Two-way Hierarchical clustering was performed on the 3 experimental conditions according to their gene expression. A fold change, with a cut off value of plus or minus two was also calculated to assess the level and direction of changes in gene expression between skeletal muscle tissues, myoblast and myotubes. This was followed by applying the Gene ontology (GO) classification system. In GO, GeneSpring computes a p value to quantify the significance in the GO by applying the Benjamini-Yekutieli correction to quantify the significance and apply correction for the large number of hypotheses tested.

Data were interpreted using Ingenuity Pathways Analysis (IPA) (Ingenuity Systems, Redwood City, CA, USA) http://www.ingenuity.com. The list of differentially expressed genes selected by the microarray analysis described above was loaded onto IPA using the following criteria: Direct and Indirect

relationships were included; data were filtered by species (human), and subsequently by tissue (skeletal muscle). Then IPA generated lists of genes that were associated with particular biological functions, diseases, and molecular processes. The IPA output also showed the canonical pathways active in the different samples.

3.3.3.1. Evaluation of microarray data

To confirm the validity of the microarray data, evaluation was performed as follows;

1) An estimate of the concordance was provided by the percentage of genes defined as present (expressed at above marginal levels) between biological replicates.
2) Pearson correlation was used to correlate the normalized expression intensity of present entities between biological replicates.

3.4. Results

3.4.1. Principle Component Analysis (PCA) and Hierarchal Clustering.

PCA analysis indicated that the samples separated according to tissue/cell type and not to the volunteer subject they were obtained from i.e the tissues clustered together whereas myobasts and myotubes formed another group (Figure 3-1). Two-way hierarchal clustering also showed that tissues were clearly separated from culture cells based on their gene expression profile (Figure 3-2). Samples that did not pass the agilent QC report and the quality metrics were removed from further analysis. The final analysis was performed between two biological replicates.

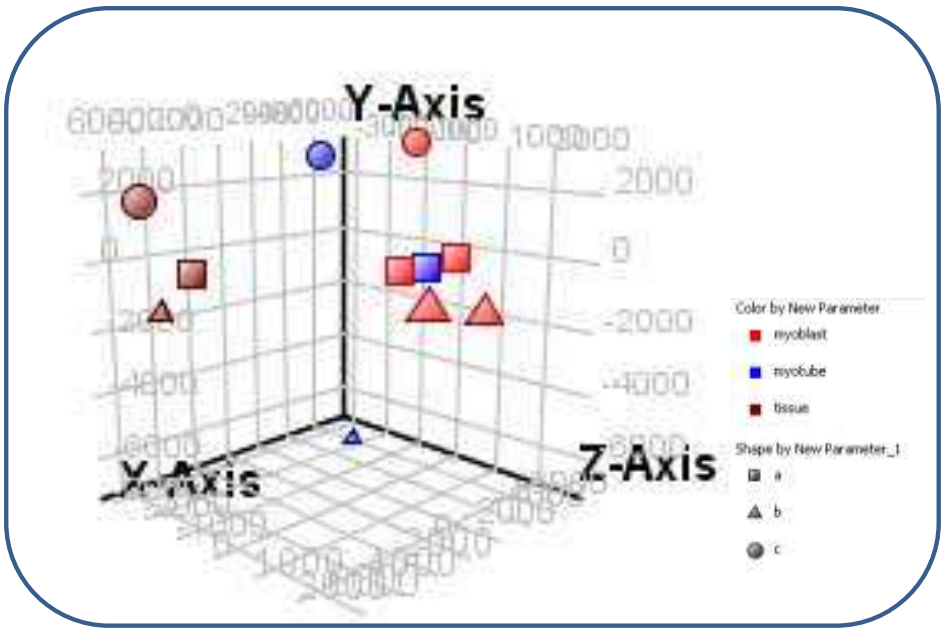

Figure 3-1: PCA analysis of human muscle arrays from three biological samples.
The figure shows the distribution of tissue and cultured cells (myoblasts and myotubes).The distribution of subjects along 3 eigenvectors. The samples separated according to tissue/cell type and not to the volunteer subject they were obtained from. New parameter = the average.

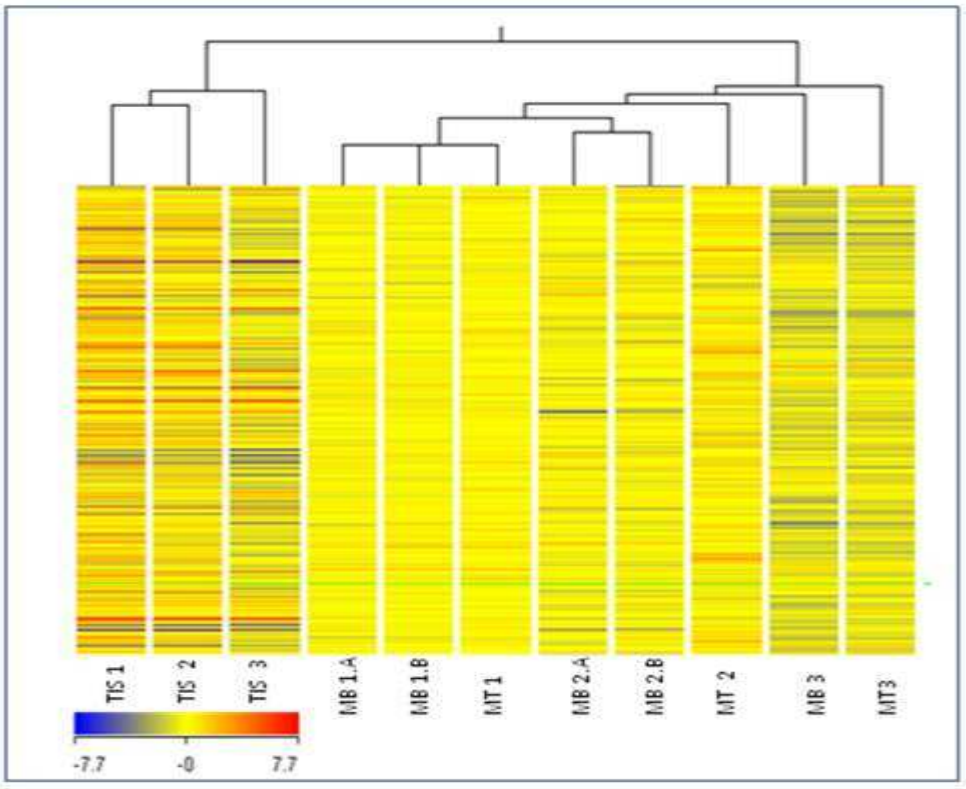

Figure 3-2: Dendrogram of hierarchal clustering from 3 biological samples.
The figure shows separation of human muscle tissues (TIS) from myoblasts (MB) and myotubes (MT). Tissues were clearly separated from culture cells based on their gene expression profile

3.4.2. Reproducibility.

Pearson correlation analysis showed high correlation between two biological replicates from whole tissues, myoblasts and myotubes (r=0.92, r=0.93, r=0.95, respectively). Technical replicates e.g. two myoblast replicates from the same human tissue had a high correlation coefficient (r=0.98) (Figure 3-3).

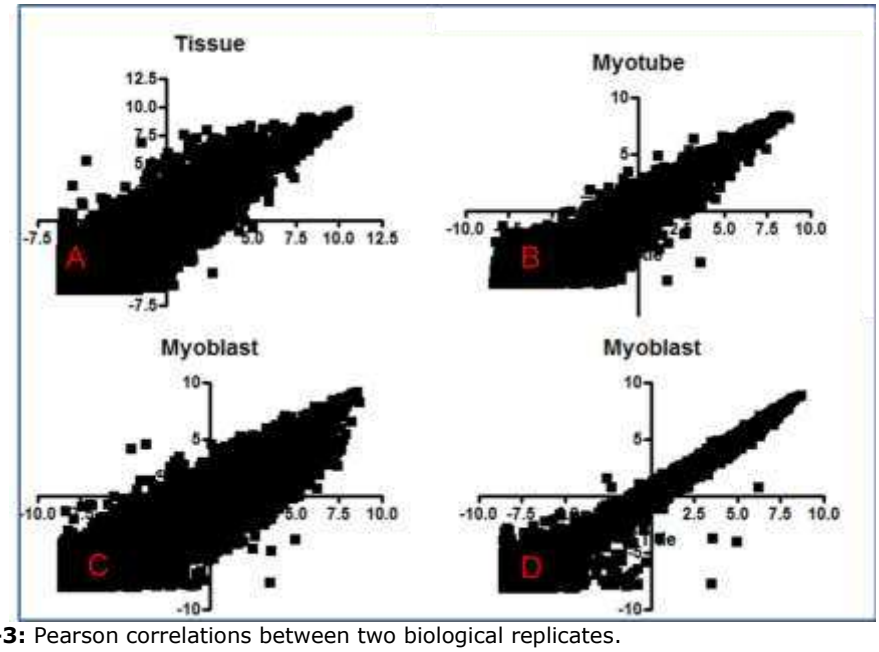

Figure 3-3: Pearson correlations between two biological replicates.
A (r=0.92), B (r=0.95) & C (r=0.93) and two technical replicates D (r=0.98).

3.4.3. Concordance.

Using only the entities called as Flag present, it was found that out of 41,078 entities; tissues displayed 23,772, myotubes 27,861 and myoblast 29,090 entities. Concordance rates among biological replicates were 79% in tissues (Figure 3-4), 84% in myoblast and 88% in myotube. Technical replicates e.g. myoblasts from the same human had a 93% concordance rate.

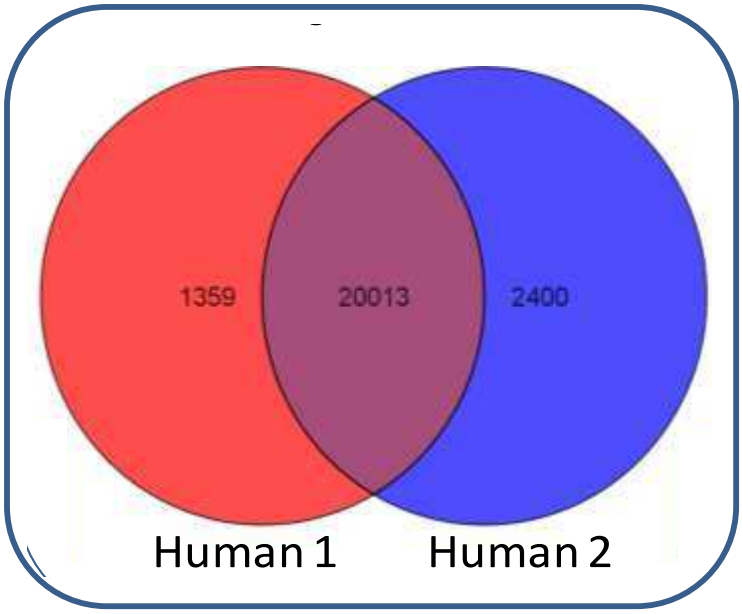

Figure 3-4: Venn diagram showing concordance, the number of similar entities between two human muscle tissue samples.

3.4.4. Ranking.

According to the expression intensity, genes were ranked in a descending order. A similar rank order for most genes was observed between two biological replicates (Table 3-1).

Table 3-1: List of some genes ranking in myoblast, myotube and skeletal muscle tissue.

GeneSymbol	Myoblast 1	Myoblast 2	GeneSymbol	Myotube 1	Myotube 2	GeneSymbol	Tissue 1	Tissue 2
MAT2A	313	313	OAZ1	2	2	MYH7	1	1
NDUFB10	1955	1955	ACTB	29	28	ENO3	3	2
OAZ1	2	1	SOX8	2734	2733	MB	4	5
EIF1	25	24	UBC	15	13	ERBB2IP	4383	4384
FBL	664	662	SLC35E4	265	263	SLC15A2	34600	34601
UBC	13	10	RPLP0	23	20	TNNI2	5	7
CCT7	1347	1343	ITGB5	1754	1750	ACTA1	8	6
UBB	73	78	TPM1	188	183	TNNC2	6	3
ENO1	970	976	RBP4	24119	24112	IL19	35532	35535
RPS4Y1	916	907	TTC3	3622	3613	CCL2	13570	13574

Among the three biological replicates, two replicates only passed the quality control. As the validation of the data was highly acceptable and comparative, ranking, intensity value and a fold-change cut off point of ≥ 2.0 was computed to identify transcriptome differences between muscle tissue and cultured myotubes and cultured myoblasts

3.4.5. Genes involved in myogenesis

The comparison was carried out using ranking from high to low expression when comparing between myoblasts and myotubes, while ranking and fold change were used when comparing cultured cell and muscle tissue (Table 3-2). The transcriptional regulators MYOD1, MYF5, CDK6 and MYOG were all higher in cultured cells than tissue. MYOD1, MYF5 and CDK6 were also higher in myoblasts than myotubes, whereas MYOG was higher in myotubes than myoblasts. In contrast to transcriptional regulators, the myocyte enhancer family had higher expression in tissue compared to cultured cells. Comparison between myoblasts and myotubes revealed that expression of MEF2a and MEF2b was higher in myoblasts, whereas MEF2c and MEF2d were higher in myotubes. Genes that have a role in adhesion (MGAT1, HES6, ITGb1, ITGa1, ITGb7, ITGa4, NCAM1 and VCAM1) were higher in myotubes compared to myoblasts. Furthermore, STAT1, STAT2 and STAT4, genes that have a role in differentiation, were slightly higher in myotubes than myoblasts, whereas the growth factors FGFR2, IGFbp3 and IGFbp4 were higher in myoblasts compared to myotubes. Not surprisingly, genes responsible for muscle structure proteins and phenotypes (Desmin, Tropomyosin, Troponin, Tropomodulin and myosin light and heavy chain) were higher (fold change ≥ 2) in tissue than cultured cells. It is worth mentioning that the embryonic type myosin heavy chain gene (MYH3) was higher in myotubes compared to skeletal muscle tissue. Interestingly, most genes associated with both slow and fast muscle fibres phenotype were lower in cultured cells than muscle tissue.

Table 3-2: List of genes involved in myogenesis

Gene Symbol	Rank MYOBLAST	Rank MYOTUBE	Rank TISSUE	Description
ACTA1	1000	256	7	Homo sapiens actin, alpha 1, skeletal muscle (ACTA1), mRNA [NM_001100]
CDH15	489	809	1958	Homo sapiens cadherin 15, M-cadherin (myotubule) (CDH15), mRNA [NM_004933]
CDK6	1490	1929	7824	Homo sapiens cyclin-dependent kinase 6 (CDK6), mRNA [NM_001259]
CKMT2	17904	17846	191	Homo sapiens creatine kinase, mitochondrial 2 (sarcomeric) (CKMT2), nuclear gene encoding mitochondrial protein, mRNA [NM_001825]
DES	760	542	48	Homo sapiens desmin (DES), mRNA [NM_001927]
DMD	4779	4069	1671	Homo sapiens dystrophin transcript variant Dp427p2, mRNA [NM_004010]
FGFR2	14141	16309	27743	Homo sapiens fibroblast growth factor receptor 2 transcript variant 2, mRNA [NM_022970]
HES6	10731	8055	20607	Homo sapiens hairy and enhancer of split 6 (Drosophila) (HES6), mRNA [NM_018645]
IGF2	825	682	977	Homo sapiens insulin-like growth factor 2 (somatomedin A) (IGF2), transcript variant 2, mRNA [NM_001007139]
IGFBP3	355	331	11078	Homo sapiens insulin-like growth factor binding protein 3 (IGFBP3), transcript variant 1, mRNA [NM_001013398]
IGFBP4	6697	5800	16045	Homo sapiens insulin-like growth factor binding protein 4 (IGFBP4), mRNA [NM_001552]
INSR	25948	22471	24169	Homo sapiens insulin receptor (INSR), transcript variant 1, mRNA [NM_000208]
ITGA3	10364	9354	20617	Homo sapiens integrin, alpha 3 (ITGA3), transcript variant a, mRNA [NM_002204]
ITGA4	17660	15852	28149	Homo sapiens integrin, alpha 4 (ITGA4), mRNA [NM_000885]
ITGB1	48	29	674	Homo sapiens integrin, beta 1 (ITGB1), transcript variant 1A, mRNA [NM_002211]
ITGB7	8626	13513	16076	Homo sapiens integrin, beta 7 (ITGB7), mRNA [NM_000889]
JAK1	7794	6946	8376	Homo sapiens Janus kinase 1 (a protein tyrosine kinase) (JAK1), mRNA [NM_002227]
JAK2	15326	14802	12002	Homo sapiens Janus kinase 2 (a protein tyrosine kinase) (JAK2), mRNA [NM_004972]
JAK3	11160	9856	14610	Homo sapiens Janus kinase 3, mRNA (cDNA clone MGC:39993 IMAGE:5212575), complete cds. [BC028068]
LEPR	12573	8131	25386	Homo sapiens leptin receptor (LEPR), transcript variant 2, mRNA [NM_001003679]
MAPK1	10202	10565	9613	Homo sapiens mitogen-activated protein kinase 1 (MAPK1), transcript variant 1, mRNA [NM_002745]
MEF2A	15349	15563	13714	Homo sapiens MADS box transcription enhancer factor 2, polypeptide A (MEF2A), mRNA [NM_005587]
MEF2B	7341	9312	9338	Homo sapiens MADS box transcription enhancer factor 2, polypeptide B mRNA (cDNA clone IMAGE:4280324), complete cds. [BC010931]
MEF2C	4267	2944	1001	Homo sapiens MADS box transcription enhancer factor 2, polypeptide C (MEF2C), mRNA [NM_002397]
MEF2D	9103	7058	8045	Homo sapiens MADS box transcription enhancer factor 2, polypeptide D (MEF2D), mRNA [NM_005920]
MYBPC1	31944	31122	107	Homo sapiens myosin binding protein C, slow type (MYBPC1), transcript variant 2, mRNA [NM_206819]
MYF5	2548	2888	10407	Homo sapiens myogenic factor 5 (MYF5), mRNA [NM_005593]
MYH1	4893	3394	521	Homo sapiens myosin, heavy chain 1, skeletal muscle, adult (MYH1), mRNA [NM_005963]
MYH2	3057	1721	13	Homo sapiens myosin, heavy chain 2, skeletal muscle, adult (MYH2), mRNA [NM_017534]
MYH3	1265	322	8166	Homo sapiens myosin, heavy chain 3, skeletal muscle, embryonic (MYH3), mRNA [NM_002470]
MYH7	1905	303	1	Homo sapiens myosin, heavy chain 7, cardiac muscle, beta (MYH7), mRNA [NM_000257]

Table 3-2: (Continued)

Gene Symbol	Rank MYOBLAST	Rank MYOTUBE	Rank TISSUE	Description
MYL1	3510	1668	56	Homo sapiens myosin, light chain 1, alkali; skeletal, fast (MYL1), transcript variant 3f, mRNA [NM_079422]
MYL2	6040	3111	27	Homo sapiens myosin, light chain 2, regulatory, cardiac, slow (MYL2), mRNA [NM_000432]
MYL3	10717	7054	827	Homo sapiens myosin, light chain 3, alkali; ventricular, skeletal, slow (MYL3), mRNA [NM_000258]
MYLK2	21057	24226	161	Homo sapiens myosin light chain kinase 2, skeletal muscle (MYLK2), mRNA [NM_033118]
MYOD1	8456	8734	12377	Homo sapiens myogenic differentiation 1 (MYOD1), mRNA [NM_002478]
MYOG	10756	8997	12531	Homo sapiens myogenin (myogenic factor 4) (MYOG), mRNA [NM_002479]
MYOZ1	25911	28386	275	Homo sapiens myozenin 1 (MYOZ1), mRNA [NM_021245]
MYOZ3	21309	21329	412	Homo sapiens myozenin 3 (MYOZ3), mRNA [NM_133371]
NCAM1	16479	13133	28905	Homo sapiens neural cell adhesion molecule 1 (NCAM1), transcript variant 3, mRNA [NM_001076682]
PAX3	16647	20649	15077	Homo sapiens paired box gene 7 (PAX7), transcript variant 2, mRNA [NM_013945]
PAX7	15503	16575	22617	Homo sapiens paired box gene 7 (PAX7), transcript variant 2, mRNA [NM_013945]
RYR1	12680	11523	1261	Homo sapiens ryanodine receptor 1 (skeletal) (RYR1), transcript variant 1, mRNA [NM_000540]
RYR2	31602	32575	31553	Homo sapiens ryanodine receptor 2 (cardiac) (RYR2), mRNA [NM_001035]
RYR3	18317	26195	9456	Homo sapiens ryanodine receptor 3 (RYR3), mRNA [NM_001036]
STAT1	6561	6118	10188	Homo sapiens signal transducer and activator of transcription 1, 91kDa (STAT1), transcript variant alpha, mRNA [NM_007315]
STAT2	17191	15859	23891	Homo sapiens signal transducer and activator of transcription 2, 113kDa (STAT2), mRNA [NM_005419]
STAT3	16223	15053	14539	Homo sapiens signal transducer and activator of transcription 3 (STAT3), transcript variant 3, mRNA [NM_213662]
STAT4	19467	16823	21558	Homo sapiens signal transducer and activator of transcription 4 (STAT4), mRNA [NM_003151]
STAT6	2232	2354	5638	Homo sapiens signal transducer and activator of transcription 6, interleukin-4 induced (STAT6), mRNA [NM_003153]
TCEAL7	8147	9514	15268	Homo sapiens transcription elongation factor A (SII)-like 7 (TCEAL7), mRNA [NM_152278]
TMOD4	21647	23413	193	Homo sapiens tropomodulin 4 (muscle) (TMOD4), mRNA [NM_013353]
TMOD4	21647	23413	193	Homo sapiens tropomodulin 4 (muscle) (TMOD4), mRNA [NM_013353]
TNNC1	3339	1402	39	Homo sapiens troponin C type 1 (slow) (TNNC1), mRNA [NM_003280]
TNNC2	1944	747	5	Homo sapiens troponin C type 2 (fast) (TNNC2), mRNA [NM_003279]
TNNI1	10099	5781	1962	Homo sapiens troponin I type 1 (skeletal, slow) (TNNI1), mRNA [NM_003281]
TNNI2	5868	3512	6	Homo sapiens troponin I type 2 (skeletal, fast) (TNNI2), mRNA [NM_003282]
TNNT1	691	701	18	Homo sapiens troponin T type 1 (skeletal, slow), mRNA (cDNA clone MGC:104241 IMAGE:4247379), complete cds. [BC107798]
TNNT3	3185	1265	39	Homo sapiens troponin T type 3 (skeletal, fast) (TNNT3), transcript variant 2, mRNA [NM_006757]
TPM1	119	175	42	Homo sapiens tropomyosin 1 (alpha) (TPM1), transcript variant 5, mRNA [NM_000366]
TPM3	1870	1956	98	Homo sapiens tropomyosin 3 (TPM3), transcript variant 2, mRNA [NM_153649]
VCAM1	11760	7113	20836	Homo sapiens vascular cell adhesion molecule 1 (VCAM1), transcript variant 1, mRNA [NM_001078]

3.4.6. Reference genes

The reference genes must be expressed at a constant level between individuals and different samples, and have amplification efficiency and abundance similar to that of the genes of interest. In this study a list of common reference genes were chosen according to Eisenberg & Levanon (2003). TBP was found to be the most stable gene as it had a similar rank and intensity at all stages of development in agreement with Stern-Straeter et al. (2009) (Table 3-3).

Table 3-3: List of reference genes in skeletal muscle tissue and cultured cells.

Gene Symbol	Rank			Intensity			Description
	MB	MT	TIS	MB	MT	TIS	
ACTB	17	29	368	8.19	7.87	6.90	Homo sapiens actin, beta (ACTB), mRNA [NM_001101]
GAPDH	367	242	76	6.33	6.69	8.39	Homo sapiens glyceraldehyde-3-phosphate dehydrogenase (GAPDH), mRNA [NM_002046]
RPS18	107	101	230	7.38	7.33	7.49	Homo sapiens ribosomal protein S18 (RPS18), mRNA [NM_022551]
TBP	13154	13198	12816	-0.91	-0.90	-0.80	Homo sapiens TATA box binding protein (TBP), mRNA [NM_003194]
TAPBP	6882	6114	7200	1.20	1.49	1.12	Homo sapiens TAP binding protein (tapasin) (TAPBP), transcript variant 1, mRNA [NM_003190]
RPL18	338	269	647	6.38	6.59	6.17	Homo sapiens ribosomal protein L18 (RPL18), mRNA [NM_000979]
TUBB	2108	1904	5144	3.85	3.95	2.03	Homo sapiens tubulin, beta (TUBB), mRNA [NM_178014]
TRFP	10262	10915	10492	0.01	-0.20	-0.08	Homo sapiens Trf (TATA binding protein-related factor)-proximal homolog (Drosophila) (TRFP), mRNA [NM_004275]
UBC	12	14	18	8.24	8.04	9.22	Homo sapiens ubiquitin C (UBC), mRNA [NM_021009]
ALDOA	787	605	74	5.38	5.67	8.55	Homo sapiens aldolase A, fructose-bisphosphate (ALDOA), transcript variant 1, mRNA [NM_000034]
PGK1	439	491	442	6.14	5.96	6.69	Homo sapiens phosphoglycerate kinase 1 (PGK1), mRNA [NM_000291]
LDHA	604	680	604	5.75	5.53	6.28	Homo sapiens lactate dehydrogenase A (LDHA), mRNA [NM_005566]
ENSA	13013	14248	10636	-0.87	-1.21	-0.07	Homo sapiens endosulfine alpha (ENSA), transcript variant 3, mRNA [NM_004436]
BTF3	361	367	494	6.30	6.29	6.56	Homo sapiens basic transcription factor 3 (BTF3), transcript variant 2, mRNA [NM_001207]
YARS	11185	9266	15731	-0.32	0.33	-1.66	Homo sapiens tyrosyl-tRNA synthetase (YARS), mRNA [NM_003680]
CSTB	2297	2266	3115	3.65	3.62	3.20	Homo sapiens cystatin B (stefin B) (CSTB), mRNA [NM_000100]
RAB1A	2848	2740	5464	3.24	3.26	1.86	Homo sapiens RAB1A, member RAS oncogene family (RAB1A), mRNA [NM_004161]
TKT	2511	2281	7860	3.49	3.65	0.87	Homo sapiens transketolase (Wernicke-Korsakoff syndrome) (TKT), mRNA [NM_001064]
YARS	11185	9266	15731	-0.32	0.33	-1.66	Homo sapiens tyrosyl-tRNA synthetase (YARS), mRNA [NM_003680]
ZFP36L1	722	582	1703	5.49	5.75	4.47	Homo sapiens zinc finger protein 36, C3H type-like 1 (ZFP36L1), mRNA [NM_004926]
BTBD2	13963	12689	11090	-1.17	-0.74	-0.26	Homo sapiens BTB (POZ) domain containing 2 (BTBD2), mRNA [NM_017797]
CDC2L2	24256	23909	23652	-4.62	-4.33	-4.03	Homo sapiens cell division cycle 2-like 2 (PITSLRE proteins) (CDC2L2), transcript variant 6, mRNA [NM_033532]
HYOU1	16368	14825	23718	-1.91	-1.39	-4.04	Homo sapiens hypoxia up-regulated 1 (HYOU1), mRNA [NM_006389]
GSK3A	1705	1940	1335	4.18	3.90	4.99	Homo sapiens glycogen synthase kinase 3 alpha (GSK3A), mRNA [NM_019884]
ATP5H	399	460	117	6.22	6.04	8.11	Homo sapiens ATP synthase, H+ transporting, mitochondrial F0 complex, subunit d (ATP5H), transcript variant 1, mRNA [NM_006356]
NDUFA7	2077	2277	711	3.83	3.61	6.00	Homo sapiens NADH dehydrogenase (ubiquinone) 1 alpha subcomplex, 7, 14.5kDa (NDUFA7), mRNA [NM_005001]
CLSTN1	4990	4937	7687	2.04	2.01	0.93	Homo sapiens calsyntenin 1 (CLSTN1), transcript variant 1, mRNA [NM_001009566]
NDUFV2	1893	1793	359	4.01	4.04	6.98	Homo sapiens NADH dehydrogenase (ubiquinone) flavoprotein 2, 24kDa (NDUFV2), mRNA [NM_021074]
NDUFS5	308	336	137	6.52	6.42	7.98	Homo sapiens NADH dehydrogenase (ubiquinone) Fe-S protein 5, 15kDa ((NDUFS5), mRNA [NM_004552]
B2M	518	453	536	5.92	6.06	6.47	Homo sapiens beta-2-microglobulin (B2M), mRNA [NM_004048]

MB=myoblast, MT=myotube, TIS=tissue, FC=fold change & N/A=no difference

3.4.7. GPR receptors and Endoannabinoid metabolism genes.

Targeting of G-protein coupled receptors (cannabinoid and free fatty acids receptors in particular) in different tissues has been the focus of recent research in an attempt to discover new therapies for metabolic diseases (Fredriksson et al. 2003). The expression of CB1, CB2, GPR55 and GPR119 were observed in both culture skeletal muscle cells and skeletal muscle tissue. The gene expression for most of the enzymes responsible for endocannabinoid synthesis and degradation (FAAH, MGLL, DAGLA & NAPE-PLD) was higher in skeletal muscle tissue than cultured cells. DAGLB was the only enzyme for which the gene expression was higher in myotubes than skeletal muscle tissue (Table 3-4). The expression of the free fatty acid receptors (GPR40, GPR120, GPR84 and GPR43) was also observed. A considerable number (87 out of 329, taken from The International Union of Basic and Clinical Pharmacology) of GPCR receptors in tissue were observed and 72 had a fold change of >± 2 when skeletal muscle tissue was compared to cultured cells. Among the 87 GPCR receptors observed, only 4 transcripts were higher in cultured cells when compared to skeletal muscle tissue (ADRA2A, ADRA2C, HRT2B and GPR126) (Table 3-5).

Table 3-4: Cannabinoid receptors and Endoannabinoid metabolism genes.

Gene Symbol	Rank			Intensity			Fold Change			Description
	MB	MT	TIS	MB	MT	TIS	MB vs MT	MT vs TIS	MB VS TIS	
CNR1	34339	32628	28149	-7.51	-6.72	-5.82	#N/A	-6.40	-8.09	Homo sapiens cannabinoid receptor 1 (brain) (CNR1), mRNA [NM_033181]
CNR2	31846	30571	28967	-7.00	-6.68	-5.50	#N/A	-2.31	-2.37	Homo sapiens cannabinoid receptor 2 (macrophage) (CNR2), mRNA [NM_001841]
GPR119	25291	24315	21455	-4.88	-4.44	-3.35	#N/A	-2.13	-2.89	Homo sapiens G protein-coupled receptor 119 (GPR119), mRNA [NM_178471]
GPR55	34813	32689	30692	-7.78	-6.83	-5.62	#N/A	-2.31	-4.46	Homo sapiens G protein-coupled receptor 55 (GPR55), mRNA [NM_005683]
FAAH	31349	30314	23612	-7.10	-6.68	-4.00	#N/A	-6.40	-8.53	Homo sapiens fatty acid amide hydrolase (FAAH), mRNA [NM_001441]
MGLL	3757	3570	2086	2.66	2.73	4.06	#N/A	-2.51	-2.63	Homo sapiens monoglyceride lipase (MGLL), mRNA [NM_007283]
DAGLB	15932	13985	17888	-1.78	-1.12	-2.28	#N/A	2.24	#N/A	Homo sapiens diacylglycerol lipase, beta (DAGLB), mRNA [NM_139179]
DAGLA	25539	24691	23579	-4.95	-4.59	-4.00	#N/A	#N/A	#N/A	Homo sapiens diacylglycerol lipase, alpha (DAGLA), mRNA [NM_006133]
NAPE-PLD	11207	10147	8119	-0.32	0.04	0.78	#N/A	#N/A	#N/A	N-acyl-phosphatidylethanolamine-hydrolyzing phospholipase D [RefSeq_peptide;Acc:NP_945341]

MB=myoblast, MT=myotube, TIS=tissue, FC=fold change & N/A=no difference

Table 3-5: List of GPCR receptors in cultured cells and skeletal muscle tissue. The genes are arranged according to tissue ranking

Gene Symbol	Rank MB	Rank MT	Rank TIS	FC MB VS MT	FC MT VS TIS	FC MB VS TIS	Description
GPRc5c	7666	3348	1384	-3.1	-4.9	-9.6	Homo sapiens G protein-coupled receptor, family C, group 5, member C (GPRC5C), transcript variant 1, mRNA [NM_022036]
P2RY2	18349	21274	1938	#N/A	-201	-108.1	Homo sapiens purinergic receptor P2Y, G-protein coupled, 2 (P2RY2), transcript variant 1, mRNA [NM_176072]
GPR125	2863	3576	2404	#N/A	-2.2	-4.5	Homo sapiens G protein-coupled receptor 125 (GPR125), mRNA [NM_145290]
GPR153	5675	931	2464	-5.9	#N/A	-3.3	Homo sapiens G protein-coupled receptor 153 (GPR153), mRNA [NM_207370]
GPR56	3573	2838	3387	#N/A	#N/A	#N/A	Homo sapiens G protein-coupled receptor 56 (GPR56), transcript variant 3, mRNA [NM_201525]
ADRB2	7692	8928	4628	#N/A	-3.7	-2.7	Homo sapiens adrenergic, beta-2-, receptor, surface (ADRB2), mRNA [NM_000024]
GPRC5B	8034	9967	5922	#N/A	-3.0	#N/A	Homo sapiens G protein-coupled receptor, family C, group 5, member B (GPRC5B), mRNA [NM_016235]
LGR4	5356	6085	6715	-2.3	#N/A	#N/A	Homo sapiens leucine-rich repeat-containing G protein-coupled receptor 4 (LGR4), mRNA [NM_018490]
ADRA2C	1988	4348	7062	3.1	2.2	6.9	Homo sapiens adrenergic, alpha-2C-, receptor (ADRA2C), mRNA [NM_000683]
MRGPRF	11655	9634	7298	#N/A	2.6	-2.9	Homo sapiens MAS-related GPR, member F (MRGPRF), mRNA [NM_145015]
P2RY14	35436	38374	10482	#N/A	-140.1	-169.9	Homo sapiens purinergic receptor P2Y, G-protein coupled, 14 (P2RY14), transcript variant 2, mRNA [NM_014879]
GPR157	18386	19218	10560	#N/A	-18.1	-13.2	Homo sapiens G protein-coupled receptor 157, mRNA (cDNA clone IMAGE:4720622), complete cds. [BC018691]
ADRA1D	20282	19561	10632	#N/A	-6.9	-8.3	Homo sapiens adrenergic, alpha-1D-, receptor (ADRA1D), mRNA [NM_000678]
Lphn1	9353	7814	10665	#N/A	#N/A	#N/A	Homo sapiens latrophilin 1 (LPHN1), transcript variant 1, mRNA [NM_001008701]
TBXA2R	13694	16716	11085	#N/A	-3.4	-2.0	Homo sapiens thromboxane A2 receptor (TBXA2R), transcript variant 1, mRNA [NM_201636]
Gpr18	36277	34545	32714	-2.6	#N/A	-4.8	Homo sapiens G protein-coupled receptor 18 (GPR18), mRNA [NM_005292]
Gpr84	31977	29064	29610	-2.1	#N/A	-3.4	Homo sapiens G protein-coupled receptor 84 (GPR84), mRNA [NM_020370]
Gpr120	32499	30315	26555	#N/A	#N/A	#N/A	Homo sapiens G protein-coupled receptor 120 (GPR120), mRNA [NM_181745]
CXCR4	5510	8883	11353	2.7	#N/A	4.7	Homo sapiens chemokine (C-X-C motif) receptor 4 (CXCR4), transcript variant 1, mRNA [NM_001008540]
EDNRB	16815	20018	11467	#N/A	-6.2	-3.2	Homo sapiens endothelin receptor type B (EDNRB), transcript variant 2, mRNA [NM_003991]
Gpr116	35032	35411	11739	#N/A	-106.8	-173.3	Homo sapiens G protein-coupled receptor 116 (GPR116), mRNA [NM_015234]
EDG6	27201	31771	12924	#N/A	#N/A	#N/A	Homo sapiens endothelial differentiation, lysophosphatidic acid G-protein-coupled receptor, 6 (EDG6), mRNA [NM_003775]
P2RY1	33830	33221	13035	#N/A	-64.1	-114.4	Homo sapiens purinergic receptor P2Y, G-protein coupled, 1 (P2RY1), mRNA [NM_002563]
Eltd1	17101	16911	13206	#N/A	-2.1	-2.3	Homo sapiens EGF, latrophilin and seven transmembrane domain containing 1, mRNA (cDNA clone MGC:34204 IMAGE:5229055), complete cds. [BC025721]
VIPR2	27981	28850	13404	#N/A	-5.0	-5.5	Homo sapiens vasoactive intestinal peptide receptor 2 (VIPR2), mRNA [NM_003382]
AVPR2	14236	19094	13748	2.6	-2.1	#N/A	Homo sapiens arginine vasopressin receptor 2 (nephrogenic diabetes insipidus) (AVPR2), mRNA [NM_000054]
GPR20	17363	13769	14023	-2.3	-10.0	-8.2	Homo sapiens G protein-coupled receptor 20 (GPR20), mRNA [NM_005293]
GPR4	29738	31124	14184	#N/A	-9.6	-18.6	Homo sapiens G protein-coupled receptor 4 (GPR4), mRNA [NM_005282]
EDG5	10463	8907	16106	#N/A	#N/A	#N/A	Homo sapiens endothelial differentiation, sphingolipid G-protein-coupled receptor, 5 (EDG5), mRNA [NM_004230]
GPR162	23523	23779	16962	#N/A	-4.8	-3.4	Homo sapiens G protein-coupled receptor 162 (GPR162), transcript variant A-2, mRNA [NM_019858]
ADRA2B	25557	30826	17290	3.2	-24.5	-7.6	Homo sapiens adrenergic, alpha-2B-, receptor (ADRA2B), mRNA [NM_000682]
ADORA2A	21563	20315	17310	#N/A	#N/A	-2.7	Homo sapiens adenosine A2a receptor (ADORA2A), mRNA [NM_000675]

Table 3-5: (Continued)

Gene Symbol	Rank MB	Rank MT	Rank TIS	FC MB VS MT	FC MT VS TIS	FC MB VS TIS	Description
ADORA2A	21563	20315	17310	#N/A	#N/A	-2.7	Homo sapiens adenosine A2a receptor (ADORA2A), mRNA [NM_000675]
HTR7	9775	10758	17343	#N/A	3.9	4.9	Homo sapiens 5-hydroxytryptamine (serotonin) receptor 7 (adenylate cyclase-coupled) (HTR7), transcript variant d, mRNA [NM_019859]
CALCR	34753	35559	17906	#N/A	-22.6	-37.5	Homo sapiens calcitonin receptor (CALCR), mRNA [NM_001742]
BDKRB2	6570	6580	17999	#N/A	13.2	12.8	Homo sapiens bradykinin receptor B2 (BDKRB2), mRNA [NM_000623]
GPR68	5493	5153	18338	#N/A	21.0	-2.1	Homo sapiens G protein-coupled receptor 68 (GPR68), mRNA [NM_003485]
CCRL2	24161	25064	18852	#N/A	-4.5	-3.7	Homo sapiens chemokine (C-C motif) receptor-like 2 (CCRL2), mRNA [NM_003965]
LPHN2	13142	11933	19745	#N/A	4.9	3.8	Homo sapiens latrophilin 2 (LPHN2), mRNA [NM_012302]
TACR2	22237	21701	20120	#N/A	#N/A	#N/A	Homo sapiens tachykinin receptor 2 (TACR2), mRNA [NM_001057]
CCR1	33102	31669	20472	#N/A	-13.3	-24.4	Homo sapiens chemokine (C-C motif) receptor 1 (CCR1), mRNA [NM_001295]
GABBR1	21716	21340	21410	#N/A	#N/A	#N/A	Homo sapiens gamma-aminobutyric acid (GABA) B receptor, 1 (GABBR1), transcript variant 1, mRNA [NM_001470]
NPY1R	32643	33382	21728	#N/A	-10.8	-16.8	Homo sapiens neuropeptide Y receptor Y1 (NPY1R), mRNA [NM_000909]
ADORA2B	11428	11369	21815	#N/A	8.6	8.4	Homo sapiens adenosine A2b receptor (ADORA2B), mRNA [NM_000676]
GPR126	18236	16073	21988	#N/A	3.4	2.0	Homo sapiens G protein-coupled receptor 126 (GPR126), transcript variant b1, mRNA [NM_198569]
ADRA2A	10860	11718	22464	#N/A	9.6	12.6	Homo sapiens adrenergic, alpha-2A-, receptor (ADRA2A), mRNA [NM_000681]
GPR114	21105	19708	22763	#N/A	-2.4	-3.6	Homo sapiens G protein-coupled receptor 114 (GPR114), mRNA [NM_153837]
PTAFR	35488	33848	22895	#N/A	-3.3	-6.6	Homo sapiens platelet-activating factor receptor (PTAFR), mRNA [NM_000952]
PTHR1	20355	19752	22934	#N/A	#N/A	#N/A	Homo sapiens parathyroid hormone receptor 1 (PTHR1), mRNA [NM_000316]
P2RY6	17981	17176	23661	#N/A	3.9	3.0	Homo sapiens pyrimidinergic receptor P2Y, G-protein coupled, 6 (P2RY6), transcript variant 2, mRNA [NM_176798]
GPR3	28878	33144	24208	#N/A	-4.2	-3.7	Homo sapiens G protein-coupled receptor 3 (GPR3), mRNA [NM_005281]
Edg2	12958	12767	24625	#N/A	#N/A	#N/A	Homo sapiens endothelial differentiation, lysophosphatidic acid G-protein-coupled receptor, 2 (EDG2), transcript variant 2, mRNA [NM_057159]
AGTRL1	33644	34763	24951	#N/A	#N/A	#N/A	Homo sapiens angiotensin II receptor-like 1 (AGTRL1), mRNA [NM_005161]
GPR45	30585	28962	26475	#N/A	-2.5	-3.7	Homo sapiens G protein-coupled receptor 45 (GPR45), mRNA [NM_007227]
GPR120	32499	30315	26555	#N/A	#N/A	#N/A	Homo sapiens G protein-coupled receptor 120 (GPR120), mRNA [NM_181745]
AVPR1A	38504	37645	27556	#N/A	-4.4	-8.5	Homo sapiens arginine vasopressin receptor 1A (AVPR1A), mRNA [NM_000706]
GABBR2	30663	30561	28416	#N/A	-2.3	-2.7	Homo sapiens gamma-aminobutyric acid (GABA) B receptor, 2 (GABBR2), mRNA [NM_005458]
DRD3	31541	30430	28600	#N/A	-2.3	-2.9	Homo sapiens dopamine receptor D3 (DRD3), transcript variant e, mRNA [NM_033663]
GCGR	19872	27908	29167	7.0	#N/A	5.5	Homo sapiens glucagon receptor (GCGR), mRNA [NM_000160]
FFAR2	33532	31388	29225	#N/A	-2.3	-4.5	Homo sapiens free fatty acid receptor 2 (FFAR2), mRNA [NM_005306]
CRHR2	31621	29060	29314	-2.1	#N/A	-3.2	Homo sapiens corticotropin releasing hormone receptor 2 (CRHR2), mRNA [NM_001883]
GPR84	31977	29064	29610	-2.1	#N/A	-3.4	Homo sapiens G protein-coupled receptor 84 (GPR84), mRNA [NM_020370]
NTSR2	33927	32038	29882	#N/A	-2.3	-4.4	Homo sapiens neurotensin receptor 2 (NTSR2), mRNA [NM_012344]

Table 3-5: (Continued)

Gene Symbol	Rank MB	Rank MT	Rank TIS	FC MB VS MT	FC MT VS TIS	FC MB VS TIS	Description
GALR2	33763	31728	30620	#N/A	-2.2	-4.3	Homo sapiens galanin receptor 2 (GALR2), mRNA [NM_003857]
PTGER1	22896	22946	30695	#N/A	2.7	2.6	Homo sapiens prostaglandin E receptor 1 (subtype EP1), 42kDa (PTGER1), mRNA [NM_000955]
FFAR1	28375	29027	32595	#N/A	#N/A	#N/A	Homo sapiens free fatty acid receptor 1 (FFAR1), mRNA [NM_005303]
SSTR3	27175	27011	32810	#N/A	#N/A	#N/A	Homo sapiens somatostatin receptor 3 (SSTR3), mRNA [NM_001051]
ADRB1	33509	33588	33017	#N/A	-2.2	-3.6	Homo sapiens adrenergic, beta-1-, receptor (ADRB1), mRNA [NM_000684]
MRGPRD	36324	34856	33799	#N/A	-2.3	-4.4	Homo sapiens MAS-related GPR, member D (MRGPRD), mRNA [NM_198923]
SSTR5	31132	34979	33921	#N/A	-2.3	-2.6	Homo sapiens somatostatin receptor 5 (SSTR5), mRNA [NM_001053]
ADORA1	21595	15364	33977	-4.6	18.5	4.0	Homo sapiens adenosine A1 receptor (ADORA1), transcript variant 1, mRNA [NM_000674]
CELSR3	24863	29218	34552	#N/A	#N/A	2.1	Homo sapiens cadherin, EGF LAG seven-pass G-type receptor 3 (flamingo homolog, Drosophila) (CELSR3), mRNA [NM_001407]
P2RY12	37667	36463	35323	#N/A	-2.3	-4.4	Homo sapiens purinergic receptor P2Y, G-protein coupled, 12 (P2RY12), transcript variant 1, mRNA [NM_022788]
OPRD1	27534	31714	35687	#N/A	#N/A	#N/A	Homo sapiens opioid receptor, delta 1 (OPRD1), mRNA [NM_000911]
HRH4	38027	37115	35846	#N/A	-2.3	-4.4	Homo sapiens histamine receptor H4 (HRH4), mRNA [NM_021624]
DRD5	24648	36868	36431	3.2	-2.3	-2.8	Homo sapiens dopamine receptor D5 (DRD5), mRNA [NM_000798]
CHRM3	28874	30983	37040	#N/A	-2.3	-2.2	Homo sapiens cholinergic receptor, muscarinic 3 (CHRM3), mRNA [NM_000740]
EMR1	38131	36041	37418	-2.0	-2.1	-4.3	Homo sapiens egf-like module containing, mucin-like, hormone receptor-like 1 (EMR1), mRNA [NM_001974]
BAI2	18027	15226	37626	#N/A	21.8	11.4	Homo sapiens brain-specific angiogenesis inhibitor 2 (BAI2), mRNA [NM_001703]
GPR19	25556	32913	37781	2.2	#N/A	#N/A	Homo sapiens G protein-coupled receptor 19 (GPR19), mRNA [NM_006143]
GPR149	38288	39089	38077	#N/A	-2.4	-4.2	Homo sapiens G protein-coupled receptor 149 (GPR149), mRNA [NM_001038705]
ADMR	37097	40733	40586	#N/A	#N/A	#N/A	Homo sapiens adrenomedullin receptor (ADMR), mRNA [NM_007264]
HTR2B	22553	19637	40838	-2.1	9.4	4.4	Homo sapiens 5-hydroxytryptamine (serotonin) receptor 2B (HTR2B), mRNA [NM_000867]

Further analysis of the data was performed using GeneSpring and Ingenuity Pathway Analysis (IPA) to examine the differences between myotubes and tissue; myoblasts and myotubes; myoblasts and tissue.

3.4.8. Cultured Myotubes vs. Muscle Tissue

Close examination of the fold-change ratio between myotubes vs muscle tissue showed that 12,851 entities out of 41,078 had a fold change of ≥ 2; there was a considerable number (2,417) of genes whose annotation was unidentified.

The number of downregulated genes was almost twice the number of upregulated genes (8,363 & 4,489 respectively). These genes were further analysed with the GO classification system, in which the genes were divided into three categories (cellular component, biological process and molecular function). Most genes that were downregulated in cultured myotubes compared to skeletal muscle tissue (Figure 3-5) were in cellular component (41.9%) mainly associated with cytoplasm and mitochondria (43.7%). With respect to biological processes (39.9% of all downregulated genes), a significant number of genes was associated with cellular metabolic processes (19.4%), response to stimulus (18.2%) and biological regulation (13.7%). The molecular function category (18.2% of all downregulated genes), included genes involved in receptor activity (28.7%) and membrane transducer activity (25.6%). Among the genes that were upregulated (Figure 3-5) in cultured myotubes, genes in the cellular components category (35.3% of all upregulated genes) were primarily associated with endoplasmic reticulum (57.7%). In the molecular function category (containing 31.4% of all upregulated genes) most genes were in associated with binding (64.5%), mainly protein binding. The augmented biological processes category (33.7% of all upregulated genes) included genes involved in cellular processes (21.2%), biological regulation (15.7%) and metabolic processes (12.1%). Overall, the over-represented GO annotations were associated with cytoskeletal protein binding (molecular function); fatty acid beta oxidation and organic acid metabolism-related terms (metabolic processes); and muscle development (biological process).

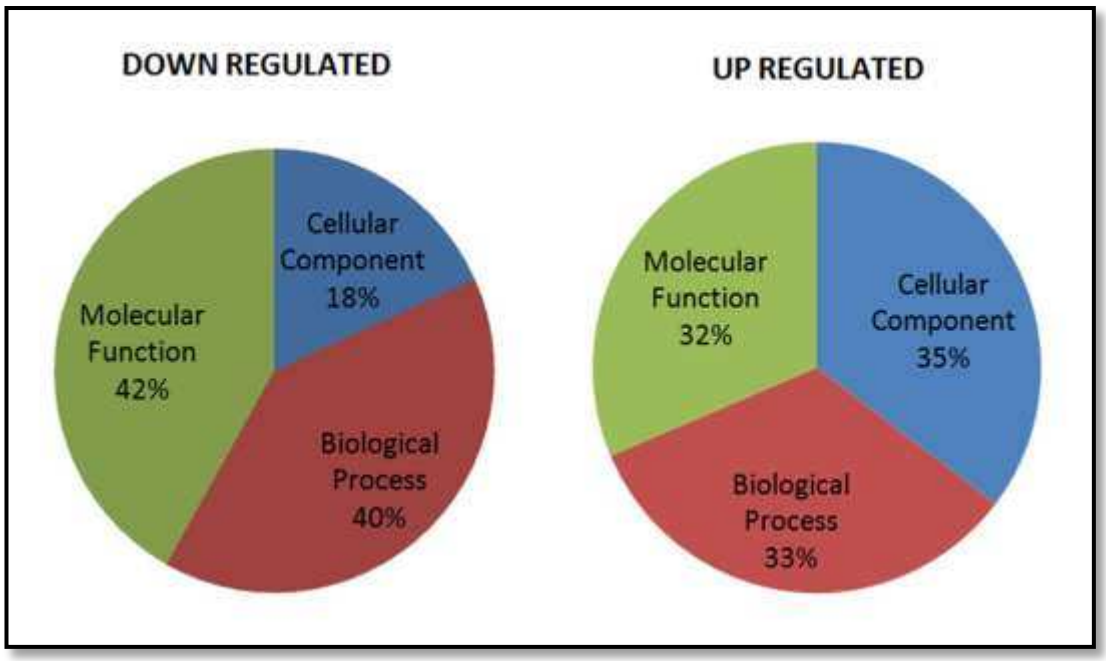

Figure 3-5: Gene Ontology analysis in skeletal muscle Tissue vs. Myotubes.
The figure shows that the molecular functions and cellular components categories had the highest percentage of downregulated and upregulated genes, respectively.

3.4.8.1. Downregulated genes.

IPA analysis was used for further analysis of the low expressed (downregulated) genes in myotubes vs skeletal muscle tissue. Interestingly, the low expressed genes were associated with carbohydrate, protein and lipid metabolism as well as energy production and molecular transport. Genes encoding metabolic proteins were included in this group: phosphorylase, glycogen, muscle (PYGM), citrate synthase (CS), lipoprotein lipase (LPL), carnitine palmitoyltransferase 1B (muscle) (CPT1B), phosphoglycerate mutase 2 (muscle)(PGAM2), fatty acid binding protein 3, muscle and heart (FABP3), adenosine monophosphate deaminase 1 (AMPD1), and fructose-1,6-bisphosphatase 2 (FBP2) (see Appendix 3 tables 1, 2 and 3). Mitochondrial dysfunction, TCA Cycle and calcium signalling were among the top canonical pathways. Interestingly, all the enzymes in TCA Cycle (Figure 3-6) as well as

genes responsible for β oxidation (Figure 3-7) were downregulated in myotubes. Furthermore, genes that are involved in transcriptional control of fatty acid oxidation and glucose homeostasis such as PPARα, PPARβ, PPARδ, PPARGCIα & PPARGC1β were also low expressed in myotubes. IPA analysis showed these transcription factors were among the upstream regulators and as most of downstream transcripts were low expressed, they are predicted to be inhibited. The prediction of inhibition is due to the fact that the genes controlled by these transcription factors are inhibited in the database. This indicates that the genes involved in fatty acid and glucose oxidation were decreased in myotubes compared to skeletal muscle tissue. For example, the downstream transcripts of PPARGC1β (Figure 3-8) are responsible for; Glucose Transport [solute carrier family 2 member 4 (SLC2A4)]; Glucogenogesis [phosphoenolpyruvate carboxykinase 1 (PCK1)]; Glucogenogesis and Glycogenolysis [glucose-6-phosphatase (G6PC)]; cholesterol synthesis [farnesyl-diphosphatefarnesyltransferase 1 (FDFT1)] and [acetyl-CoA carboxylase beta (ABCA1)]; Triglyceride synthesis [diacylglycerol O-acyltransferase 1 (DGAT1)]; TCA cycle [citrate synthase (CS); β oxidation [carnitine palmitoyltransferase 1B (CPT1B)], [acyl-CoA dehydrogenase very long, long and medium chains (ACADVL, ACADM ACAADL)] and [acetyl-CoA carboxylase beta (ACACB)] ; Oxidative Phosphorylation [cytochrome c oxidase (COX5A & COX4II)] and [ATP synthase, H+ transporting, mitochondrial complex (ATP512 & ATP5B)].

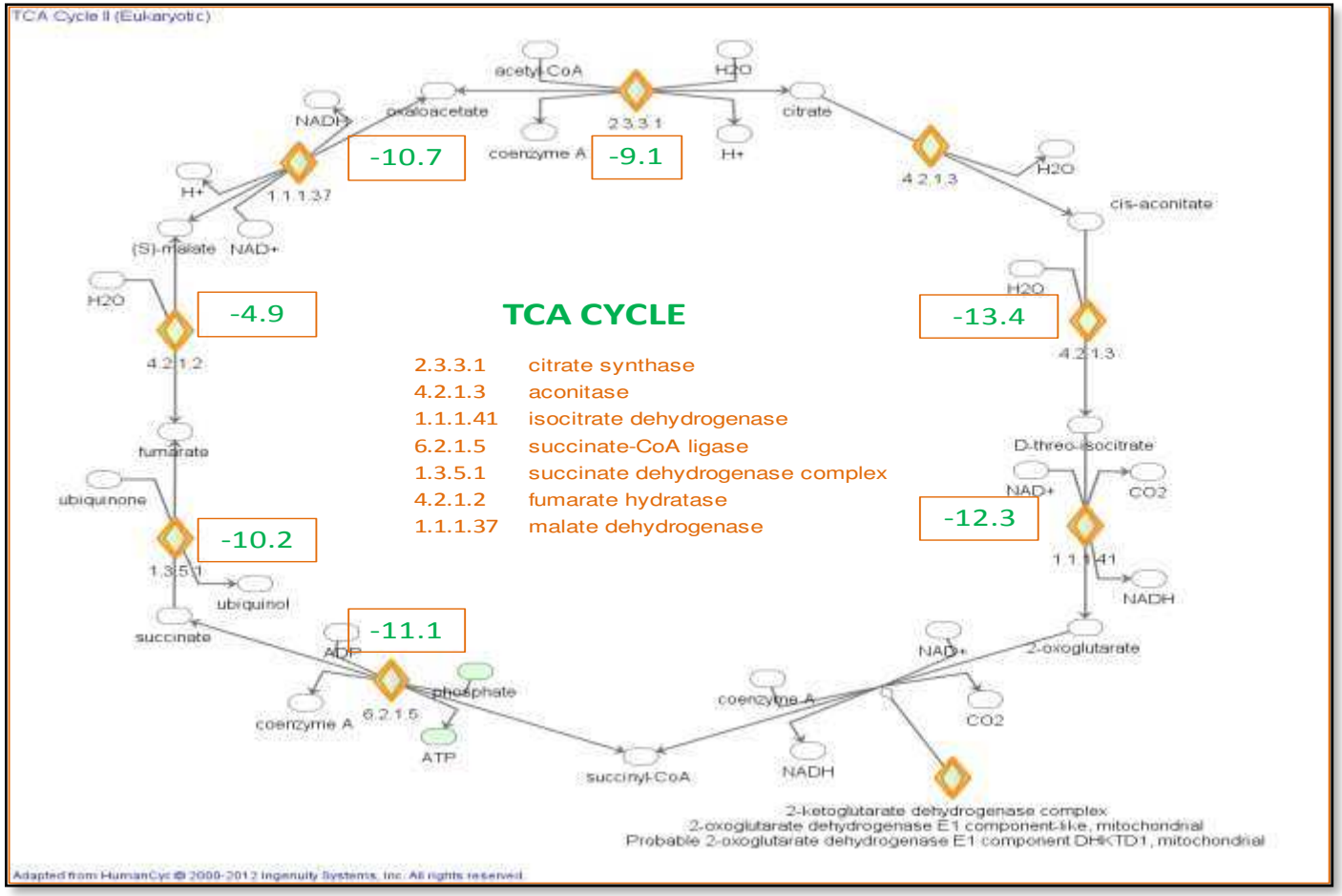

Figure 3-6: TCA CYCLE, Graphical representation of the downregulated genes in cultured myotubes compared to SM tissue and their molecular relationships. Genes are represented as green diamond shapes. The colour intensity corresponds to the magnitude of change. The fold changes appear in green numbers. The pathway image was created using the IPA software.

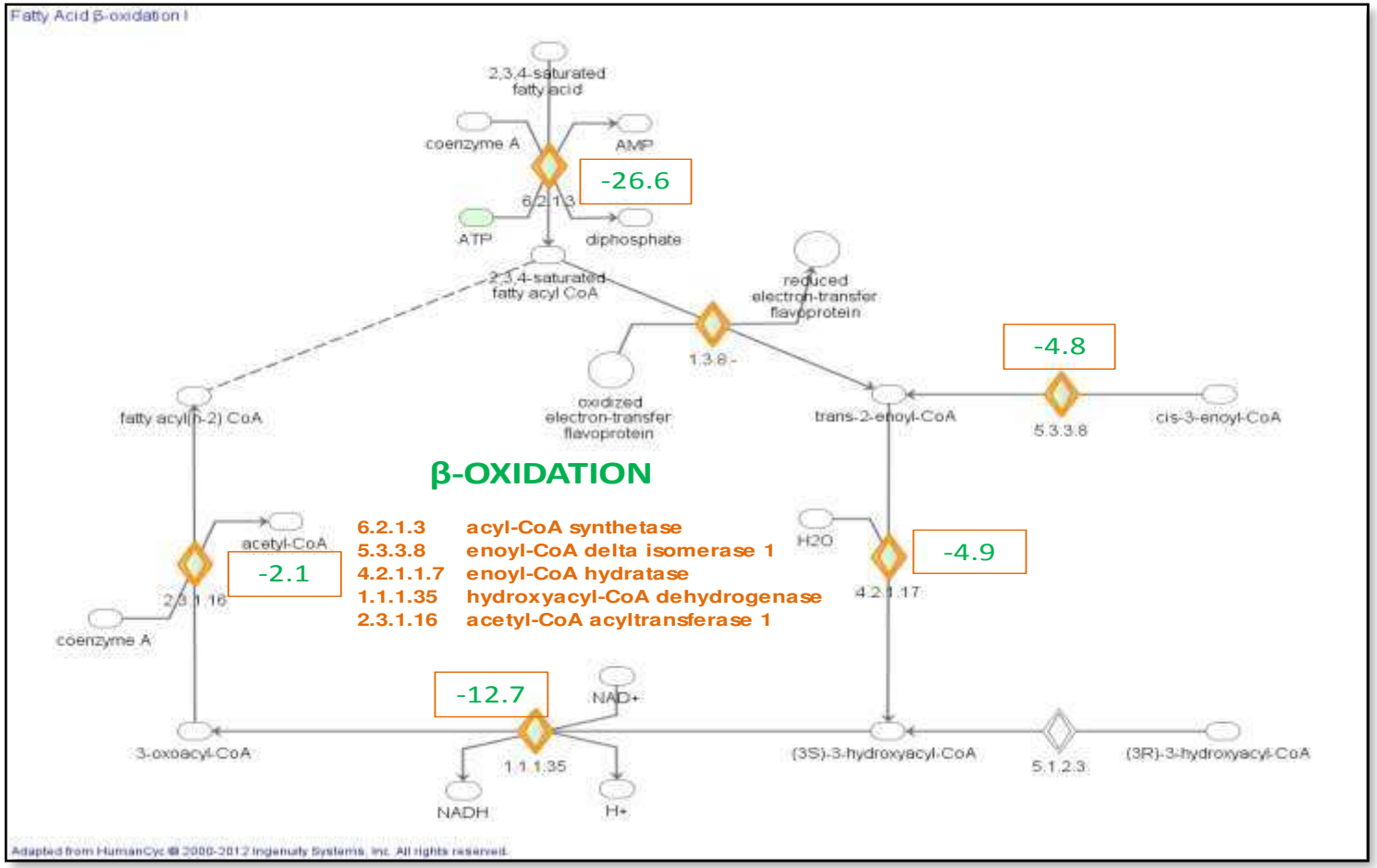

Figure 3-7: β-oxidation, Graphical representation of the downregulated genes in cultured myotubes compared to SM tissue and their molecular relationships. Genes are represented as green diamond shapes. The colour intensity corresponds to the magnitude of change. The fold changes appear in green numbers. The pathway image was created using the IPA software.

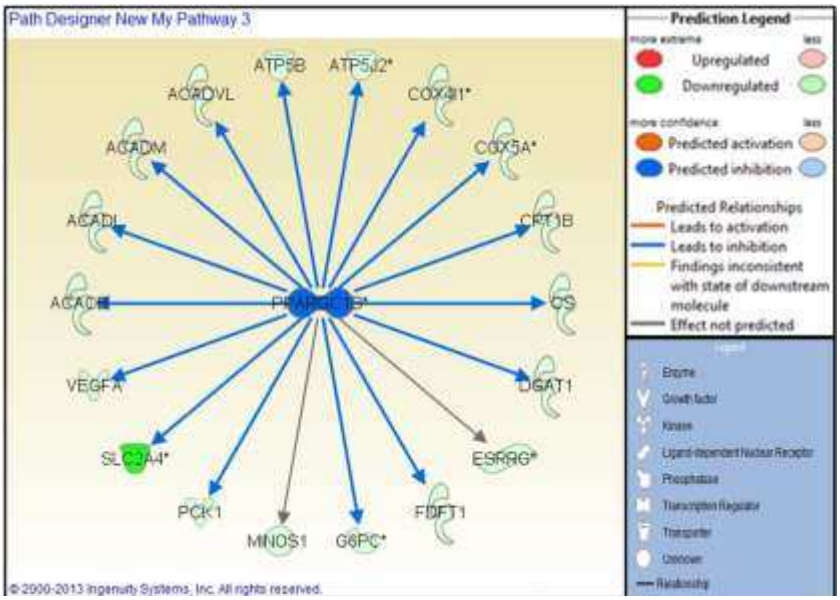

Figure 3-8: Graphical representation of the transcriptional regulator PPARGC1β and the downstream genes in cultured myotubes compared to skeletal muscle tissue.
Genes are represented in green colour. The colour intensity corresponds to the magnitude of change. The lines in between genes represent known interactions. The downstream transcripts of PPARGC1B are responsible for; Glucose Transport (SLC2A4); Glucogenogesis (PCK1); Glucogenogesis and Glycogenolysis (G6PC); cholesterol synthesis (FDFT1) and (ABCA1); Triglyceride synthesis (DGAT1); TCA cycle (CS); β oxidation (CPT1B, ACADVL, ACADM ACAADL and (ACACB); Oxidative Phosphorylation (COX5A & COX4II) and [ATP (ATP512 & ATP5B). The pathway image was created using the IPA software. For genes symbol and fold change see appendix 3.

Moreover, most genes for the insulin signalling pathway had lower expression in myotubes compare to skeletal muscle tissue. As illustrated in Figure 3-9 the MAPKs pathway was not affected whereas the PI3K/AKT pathway and GLUT4 translocation were affected. Interestingly, most of the negative regulators of insulin transduction pathway had higher expression in myotubes compare to skeletal muscle tissue such as PTEN, SHIP2, SOSC3 and LAR. It is worth mentioning that not only the expression of GLUT4 (SLC2A4) but also genes responsible for GLUT4 trafficking, such as VAMP2 and TC10 had lower expression in myotubes than skeletal muscle tissue Table 3-6. Mitochondria dysfunction was also among the top canonical pathways as most complexes enzymes (NADH dehydrogenase, succinate dehydrogenase), cytochromes (CYC1, CYTB, COX1 & COX7A1) and monoamine oxidase (MAOB & MAOA) were downregulated (Figure 3-10) (Appendix 3 table 5).

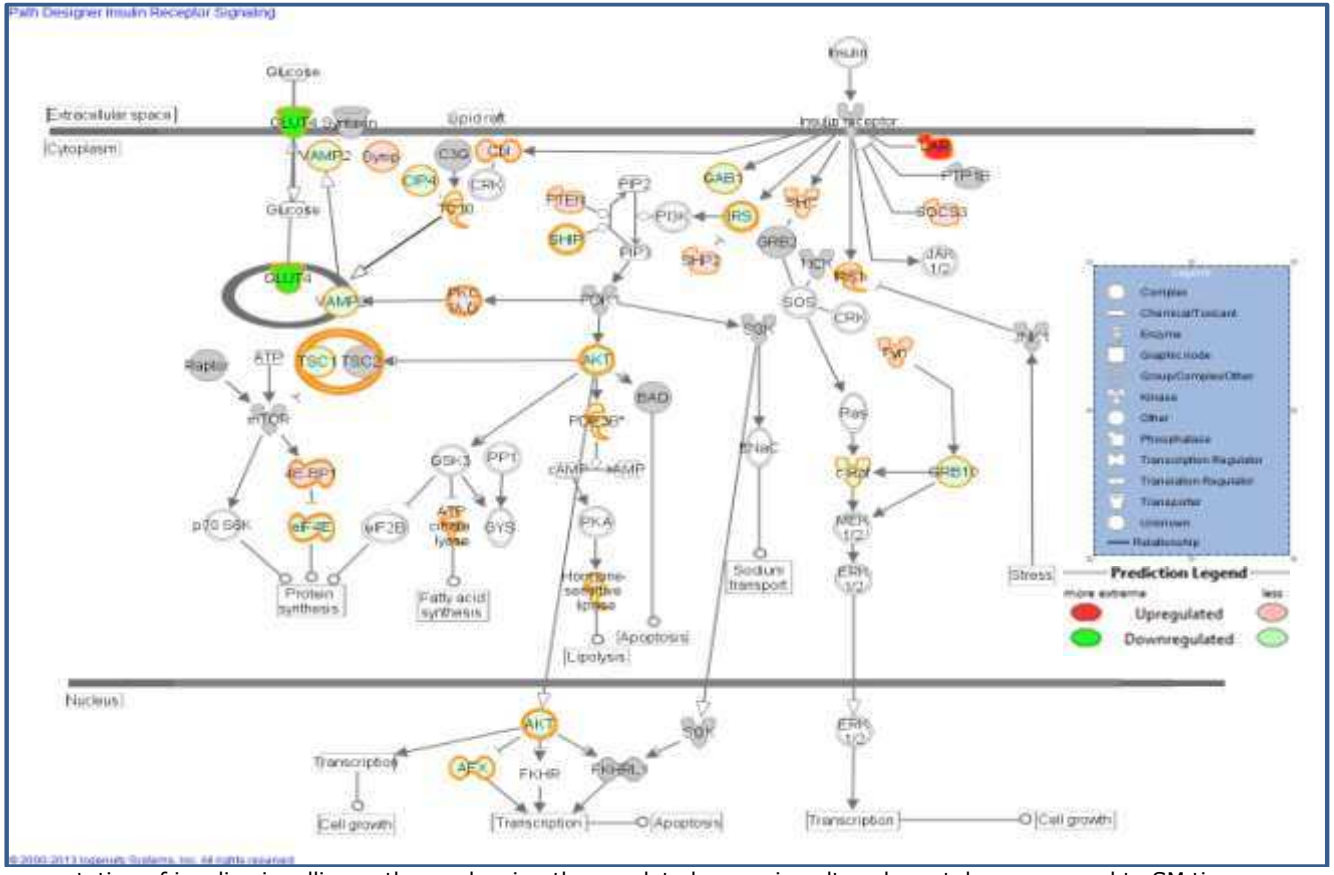

Figure 3-9: Graphical representation of insulin signalling pathway showing the regulated genes in cultured myotubes compared to SM tissue.
An expression is shown using green (down regulated) and red (up regulated). All transcripts shown had a fold-change ≥±2. The colour intensity corresponds to the magnitude of change. The MAPKs pathway was not affected whereas the PI3K/AKT pathway, the GLUT4 and genes responsible for GLUT4 trafficking such as VAM2 and TC10 had lower expression in myotubes than skeletal muscle tissue. Most of the negative regulators of insulin transduction pathway (PTEN, SHIP2, SOSC3 and LAR) had higher expression in myotubes compare to skeletal muscle tissue. The pathway image was created by IPA software with modification. For genes name and fold changes see Table 3-6

Table 3-6: List of genes involved in insulin signalling pathway.

Symbol	Entrez Gene Name	Fold Change
ACLY	ATP citrate lyase	6.427
AKT2	v-akt murine thymoma viral oncogene homolog 2	-2.477
CBL	Cbl proto-oncogene, E3 ubiquitin protein ligase	3.523
EIF4E	eukaryotic translation initiation factor 4E	-2.373
EIF4EBP1	eukaryotic translation initiation factor 4E binding protein 1	3.339
FOXO4	forkhead box O4	-2.324
FYN	FYN oncogene related to SRC, FGR, YES	7.054
GAB1	GRB2-associated binding protein 1	-4.888
GRB10	growth factor receptor-bound protein 10	-2.316
INPP5D	inositol polyphosphate-5-phosphatase, 145kDa	-12.031
IRS1	insulin receptor substrate 1	2.429
IRS2	insulin receptor substrate 2	-2.787
IRS4	insulin receptor substrate 4	-2.372
LIPE	lipase, hormone-sensitive	-10.644
PDE3B	phosphodiesterase 3B, cGMP-inhibited	-2.471
PRKCZ	protein kinase C, zeta	3.100
PTEN	phosphatase and tensin homolog	2.048
PTPN11	protein tyrosine phosphatase, non-receptor type 11	2.485
PTPRF (LAR)	protein tyrosine phosphatase, receptor type, F	35.321
RAF1	v-raf-1 murine leukemia viral oncogene homolog 1	-3.125
RHOQ	ras homolog family member Q	-4.767
SHC1	SHC (Src homology 2 domain containing) transforming protein 1	5.685
SLC2A4	solute carrier family 2 (facilitated glucose transporter), member 4	-3329.000
SOCS3	suppressor of cytokine signaling 3	5.694
STXBP4	syntaxin binding protein 4	3.458
TRIP10	thyroid hormone receptor interactor 10	-6.084
TSC1	tuberous sclerosis 1	-2.541
VAMP2	vesicle-associated membrane protein 2 (synaptobrevin 2)	-3.036

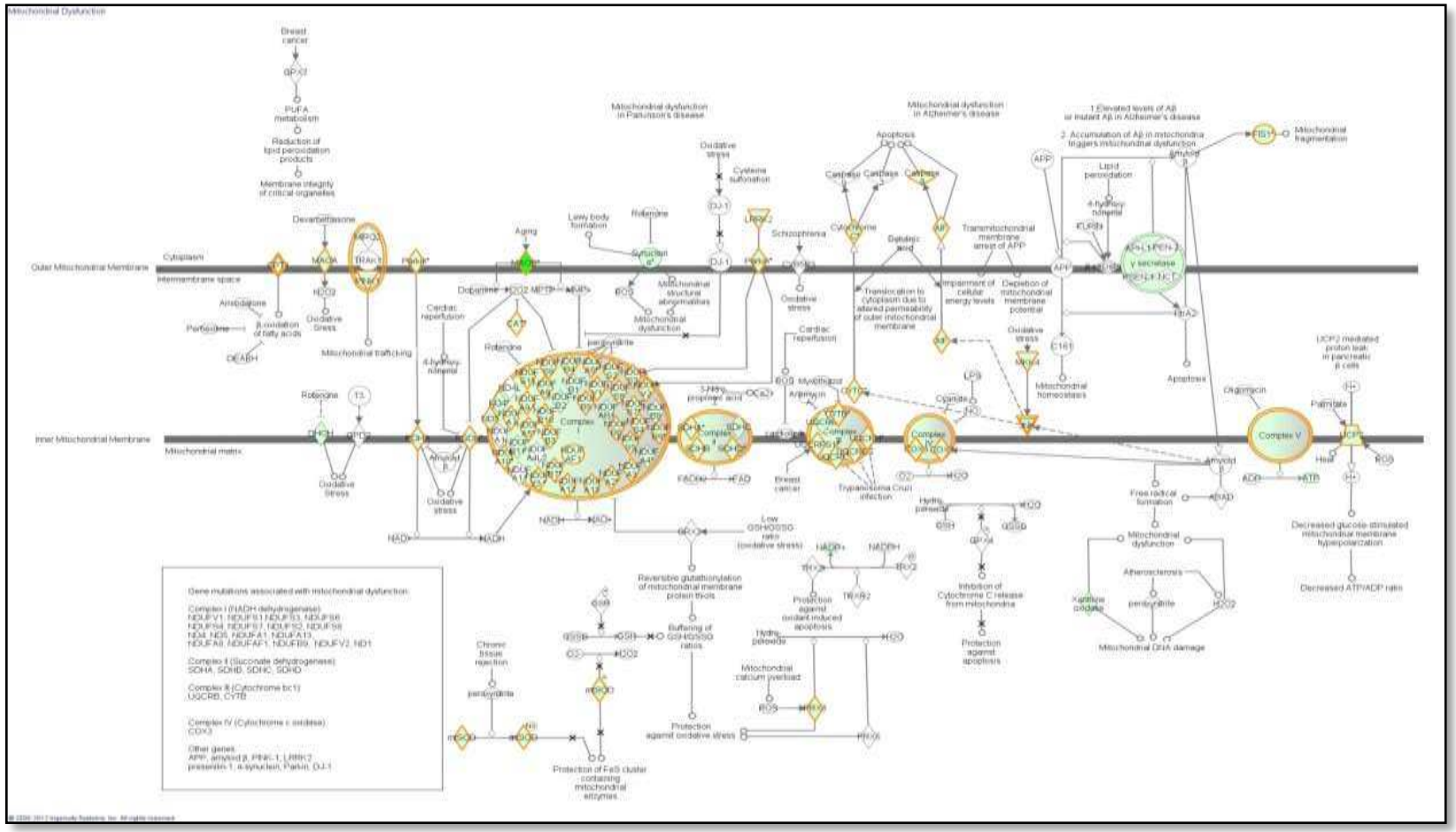

Figure 3-10: Mitochondria dysfunction. Graphical representation of the downregulated genes in cultured myotubes compared to SM tissue and their molecular relationships. Genes are represented in green colour and.the colour intensity corresponds to the magnitude of change. All genes has a Fold change of ≥ -2 with a range from -2 for PPP3CA to -2485 for MAOB The lines in between genes represent known interactions. The pathway image was created using the IPA software. For genes symbol and fold change see appendix 3 table 5.

The genes responsible for calcium signalling and muscle contraction and relaxation were also downregulated (including SERCA, CASQ, RYR, TROPONIN, TROPMYOSIN, MYOSIN, CALM & CREB) (Figure 3-11) (Appendix 3 table 6). A closer examination of the downregulated groups revealed several genes encoding proteins of myofilaments MYL3; associated/regulatory proteins TMOD4, MYBPC1, and XIRP2; the regulator of the muscle sarcomere CAPN3 and skeletal muscle phenotypes (MYL3, TNNC1, TNNI1 & TNNT1 for slow phenotype and MYL1, TNNC2, TNNI2, and TNNT3 for fast phenotype). The top downregulated genes were myoglobin (MB-29166), myosin binding protein ,slow type (MYBPC1 -25444), fructose1,6 biosphosphate 2 (FBP2 -6480), adenosine monophosphate deaminase 1 (AMPD1 -6150), myozenin 1 (MYOZ1 -4595), phosphorylase glycogen muscle (PYGM -4374) and solute carrier family 2 , member 4 (SLC2A4 {GLUT4} -3329). This indicates that genes involved in various highly regulated biological functions (energy metabolism and muscle contraction) were the most downregulated genes.

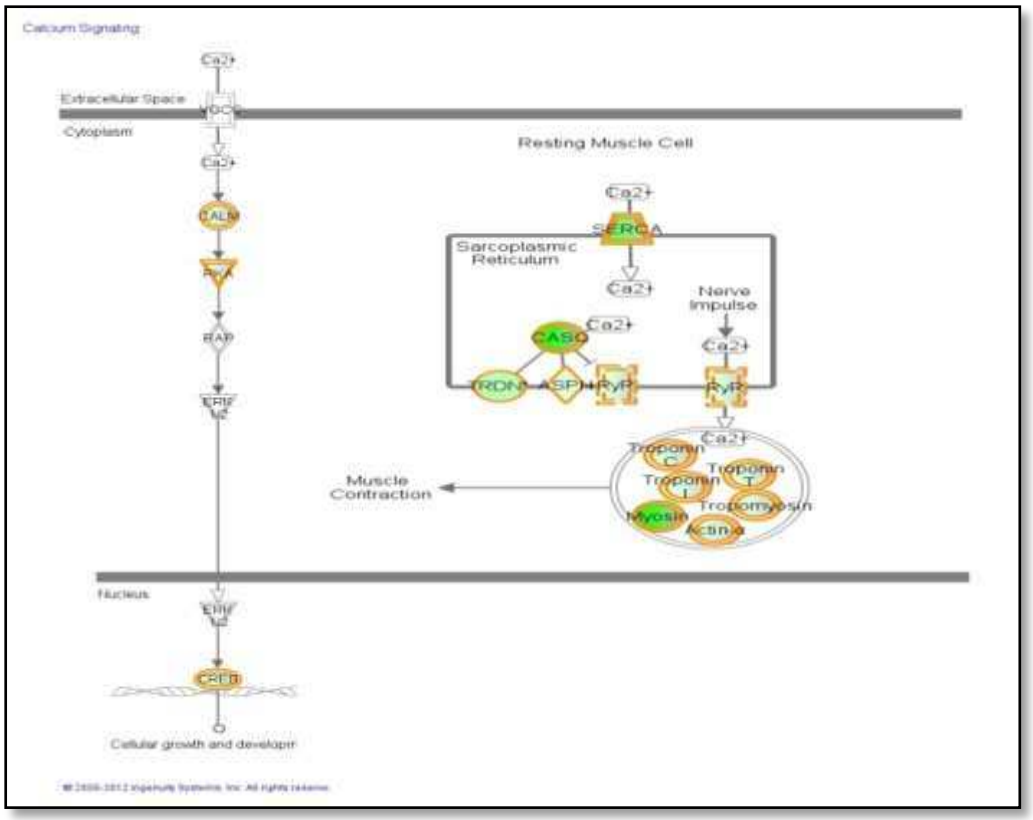

Figure 3-11: Calcium signalling. Graphical representation of the downregulated genes in cultured myotubes compared to SM tissue and their molecular relationships.
Genes are represented as green diamond shapes. The intensity corresponds to the magnitude of change. The lines in between genes represent known interactions. The pathway image was created using the IPA software. For gene symbol see appendix 3 table 6.

3.4.8.2. Upregulated genes.

As expected, the top biological functions in the upregulated genes were associated with Cellular Movement, Cellular Growth and Proliferation, Cellular Development, Cellular Assembly and Organization and Cellular Function and Maintenance. Table 3-7 shows the most important functions annotation of the upregulated genes. Among the upregulated genes detected in skeletal muscle proliferation and differentiation category were well-known regulatory factors such as MYOD1, MYOG, MYF5, FGFR2, ITGB1, CDKN, TOP2A, and HIF1A (Appendix 4). The top canonical pathway includes the Epithelial Adherens Junction Signalling and the Remodelling of Epithelial Adherence. Several genes that have a regulatory function in cell attachment and adherence were included

in the upregulated category such as CDH2 (Cadherin2) & POSTN (Periostin/ Osteoclast Specific Factor) with fold-changes of 167 and 2,432 respectively. Other genes such as ABL1, ANTXR1, CCND1, PTBP1 had a fold change less than 20 and were also involved in cell adherence. Interestingly, around 200 genes were related to extracellular matrix, such as those encoding: isoforms of lysyl hydroxylase (PLOD3, PLOD2) , an enzyme that catalyzes the formation of hydroxylysine in collagens; CSGlcA-T, which is involved in the synthesis of chondroitin sulphate as a glucuronyltransferase ; the metalloproteinase MMP14; TIMP2, an inhibitor of the metalloproteinase type IV; the protease inhibitor SERPINE2; insulin like growth factor IGFBP; connective tissue growth factor CTGF; growth differentiation factor GDF1s and interleukin 6 (IL6). The upregulated metabolic genes are involved in accumulation of glycosaminoglycan & hyaluronic acid and the release of ATP. The most elevated genes included PTX3 (Pentraxin) which has a role in phagocytosis and inflammatory response; POSTN (Periostin) which has a role in cell adhesion and migration; DMBT1 (Deleted in malignant brain tumors) that plays a role in cell differentiation and migration; IL6 (Interleukin 6) an important cytokine which has a role in cell proliferation, differentiation, apoptosis and growth; FOXD1 (Forkhead box D1) that plays a role in cell activation; GERM1 (Germlin 1) that has a role in proliferation, differentiation, growth and assembly; TNNT2 (Cardiac troponin) that has a role in abnormal morphology and relaxation. It is worth mentioning that cyclin-dependent kinase inhibitor which has an important role in cell proliferation, cell cycle arrest and initiation of differentiation was also among the upstream regulators. TNFα was another upstream regulator and its activation through the TNFR1 leads to induction of cell survival and the activation of the NF-κB pathway (Figure 3-12). Overall, upregulated genes were associated with an increase in cell movement and proliferation.

Table 3-7: Top up regulatory functions in myotubes compared to skeletal muscle tissue.

Category	Functions Annotation	Predicted Activation State
Carbohydrate Metabolism	accumulation of glycosaminoglycan &hyaluronic acid	Increased
Cell Death and Survival	apoptosis of embryonic cell lines, epithelial cell lines & macrophafes	Increased
Cell Death and Survival	cell viability	Increased
Cell Death and Survival	cell death & apoptosis	Decreased
Cell Signaling	hydrolysis of GTP	Increased
Cell-To-Cell Signaling and Interaction	adhesion & attachment of cells (blood , immune & connective tissue	Increased
Cellular Assembly and Organization	development of cytoplasm & formation of cytoskeletonformation of	Increased
Cellular Development	differentiation of cells	Increased
Cellular Growth and Proliferation	formation of cells	Increased
Cellular Movement	cell movement	Increased
Connective Tissue Disorders	congenital anomaly of skeletal bone	Decreased
DNA Replication, Recombination, and Repair	synthesis of DNA	Increased
Hematological System Development and Function	accumulation of leukocytes, myeloid cells, neutrophils &	Increased
Hematological System Development and Function	aggregation of blood platelets	Increased
Inflammatory Response	accumulation of granulocytes	Increased
Molecular Transport	release of ATP	Increased
Organismal Injury and Abnormalities	Bleeding	Decreased
Organismal Survival	organismal death	Decreased
Skeletal and Muscular Disorders	congenital anomaly of musculoskeletal system	Decreased
Small Molecule Biochemistry	quantity of glycosphingolipid, ceramide & sphingolipid	Increased
Tissue Morphology	quantity of blood cells	Increased
Tissue Morphology	quantity of blood platelets	Increased
Tumor Morphology	proliferation of cancer cells	Increased

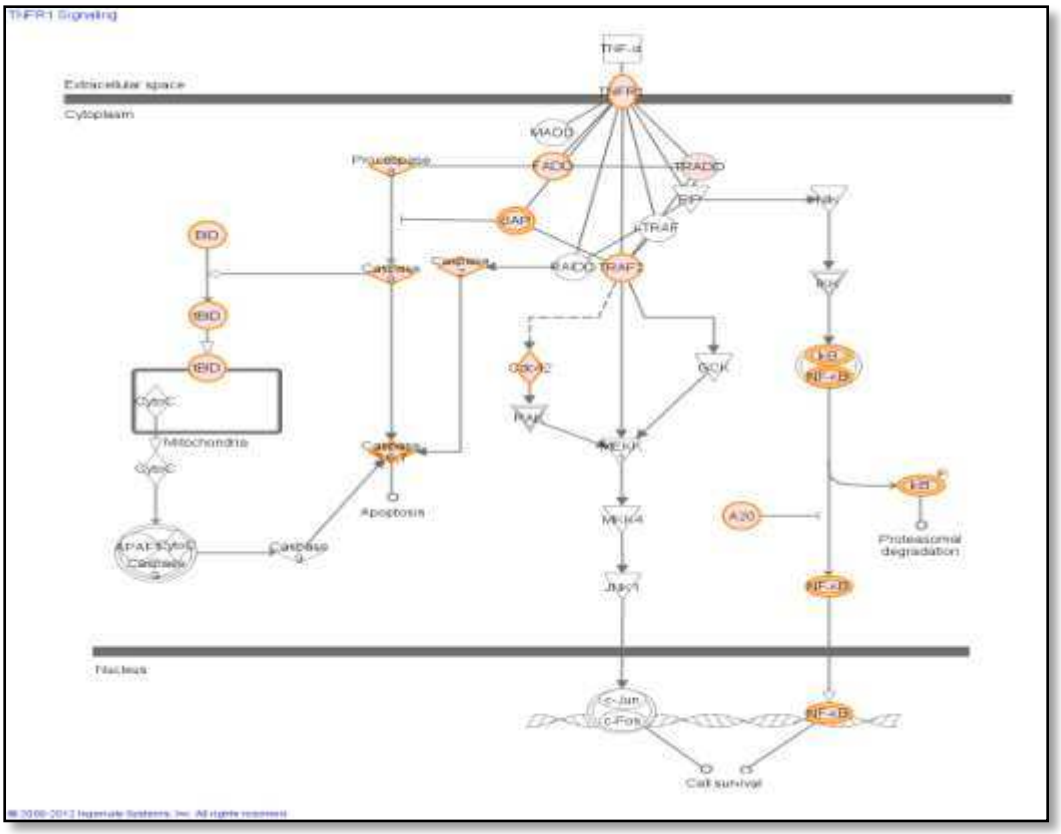

Figure 3-12: TNFR1 signalling. Graphical representation of the unregulated genes in cultured myotubes compared to SM tissue and their molecular relationships.
The red colour intensity corresponds to the magnitude of change. The lines in between genes represent known interactions. The pathway image was created using the IPA software. For gene symbol see appendix 4.

3.4.9. Myoblast versus myotubes.

Comparison of the gene expression differences between myoblasts and myotubes in culture, showed 2,774 entities with a fold change range greater than two. 2,091 were expressed at a lower level whereas 683 genes were increased in myoblasts. GO analysis of the low expressed genes showed a high percentage of those genes to be associated with biological processes (43.3%) followed by cellular components (36.4%) and molecular function (20.7%). The genes expressed at higher levels in myotubes had a similar pattern of distribution across the 3 categories; 54, 4% were associated with biological processes, 43.5% with cellular components and 2.1% with molecular functions (Figure 3-13).

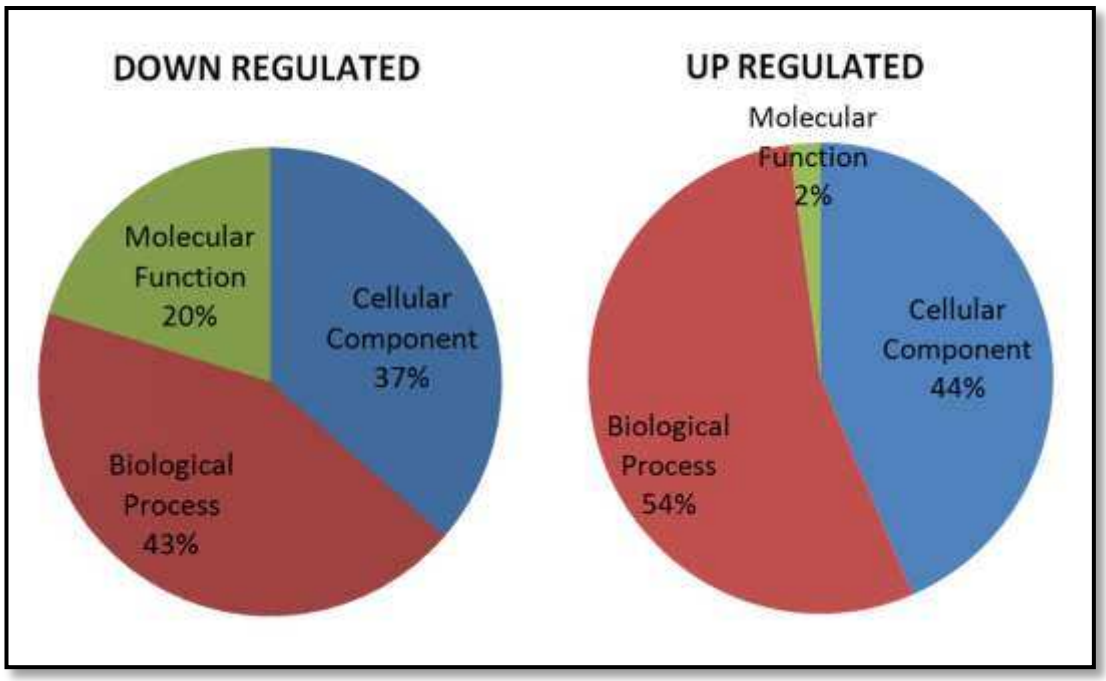

Figure 3-13: Gene Ontology analysis in Myoblasts vs. Myotubes.
The figure showed that the biological processes category had the highest percentage of downregulated and upregulated genes.

Closer inspection of the biological function category revealed a decrease in genes responsible for muscle contraction and cytoskeletal organization (CASQ2, MYLPF, TNNT2, CACNG1, MYH3, MYH8, TNNT3, CSRP3 & ANK1), a decrease in carbohydrates and lipid metabolism genes (ABCB4, ACADS, CD36, CEBPA, CRAT, EGFR, INSR, PDK4, PPARG, SLC2A1 & UCP3), a decrease in cell movement and binding (ACHE, CASP1, CCBP2, CCL11 ,CCL5, CD74, CMKLR1, FOS, IGF1, IKBKB, IL16, IL1B, IL1RL1, NCAM1 & VCAM1) and an increase in organismal death

Table **3-8**) in myoblast compared to myotubes. Among the top upregulated genes were protein disulphide isomerase family A member 3 (PDIA3 FC 16.9) that has a role in apoptosis and folding in; Solute carrier family 24 member 4 (SLC24A4 FC 10.5) that has a role in Na+, Ca2+, K+ binding and transport; Fms-related tyrosine Kinase 4 (FLT4 FC 7.17) that is a growth factor receptor

and has a role in proliferation, migration, apoptosis and growth; ryanodine receptor 3 (RYR3 FC 6.5), a calcium ion transport; chemokine (C-X-C motif) ligand 14 cytokine (CXCL14 FC 6.4) that has a role in signalling, proliferation & mobilization; cell adhesion molecule 1 (CADM1 FC 5.9) that plays a role in abnormal morphology, cell-cell adhesion, & apoptosis. The top downregulated genes include Sarcolipin (SLN FC -8.2) which plays a role in calcium ion transport and relaxation; (C-C motif) ligand 11 (CCL11 FC -8.1) that has a role in migration, adhesion & chemokine; tumor necrosis factor receptor superfamily, member 13C (TNFRSF13C FC -7.1) that has a role in development, proliferation and differentiation; Sema domain (SEMA6A FC -6.4) that plays a role in protein binding, migration, growth; and cell differentiation and (sex determining region Y)-box 17 (SOX FC -5.8) that has a role in cell growth, differentiation and proliferation. LXR/RXR (retinoid X receptors) and FXR/RXR (farnesoid X receptor) pathways were among the top canonical pathways. Most of genes in these patways were down regulated (Figure 3-14). LXR/RXR and FXR/RXR pathways play an important role in lipid metabolism and molecular transport.

Table 3-8: Top regulatory functions in myoblasts compared to myotubes

Category	Functions Annotation	Predicted Activation State
Cellular Movement	cell movement	Decreased
Cell-To-Cell Signaling and Interaction	binding of cells	Decreased
Cell-To-Cell Signaling and Interaction	activation of cells	Decreased
Cellular Movement	leukocyte migration	Decreased
Molecular Transport	quantity of metal ion	Decreased
Cell-To-Cell Signaling and Interaction	interaction of cells	Decreased
Molecular Transport	quantity of Ca2+	Decreased
Cellular Development	differentiation of cells	Decreased
Carbohydrate Metabolism	uptake of carbohydrate	Decreased
Cellular Movement	migration of cells	Decreased
Molecular Transport	concentration of lipid	Decreased
Cellular Movement	recruitment of cells	Decreased
Inflammatory Response	inflammatory response	Decreased
Molecular Transport	uptake of 2-deoxyglucose	Decreased
Cellular Growth and Proliferation	proliferation of cells	Decreased
Cell Cycle	mitogenesis	Decreased
Molecular Transport	release of Ca2+	Decreased
Lipid Metabolism	fatty acid metabolism	Decreased
Cell-To-Cell Signaling and Interaction	binding of blood cells	Decreased
Molecular Transport	secretion of lipid	Decreased
Connective Tissue Development and Function	adipogenesis	Decreased
Organismal Survival	organismal death	Increased
Cell Morphology	mineralization of cells	Increased

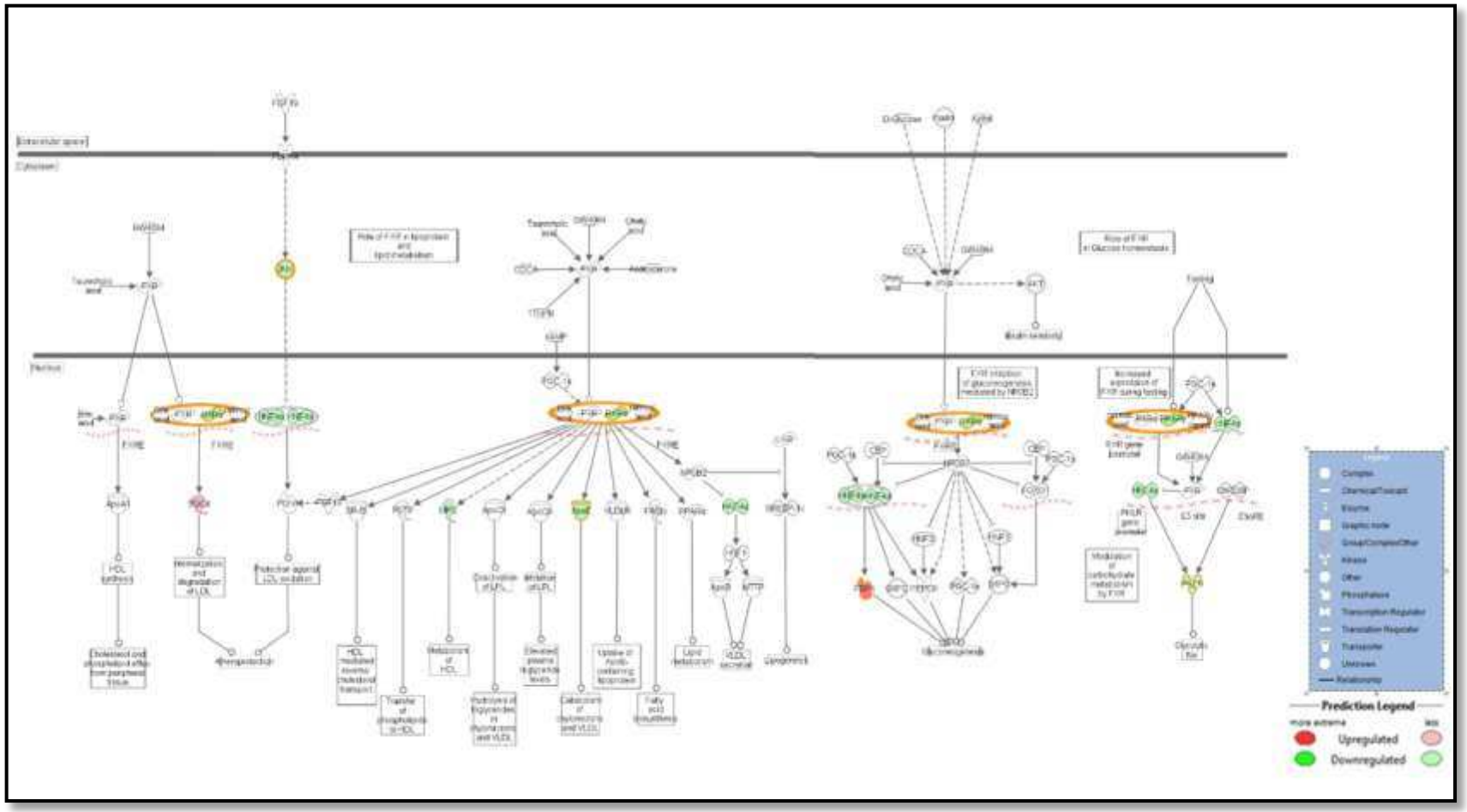

Figure 3-14: Graphical representation of FXR/RXR signalling pathway showing the regulated genes in cultured myoblasts compared to myotubes related to glucose and lipid metabolism.
An expression is shown using green (down regulated) and red (up regulated). All transcripts shown had a fold-change ≥±2. The colour intensity corresponds to the magnitude of change. The pathway image was created with modification by using the IPA software.

3.5. Discussion

Myogenesis is a complex cascade of discrete developmental steps that are under strict transcriptional control. Successful myogenic differentiation requires numerous interactions between diverse cellular processes involving growth factors, hormones, receptors and transcription factors. Although myogenesis has been widely described, there are certainly many genes involved in muscle cell proliferation/differentiation that are not yet known. The use of microarrays to identify genes involved in skeletal muscle function and pathology has been limited to studies investigating disease states and myogenesis in cell lines. In the present study high-density oligonucleotide arrays were used to (a) characterize changes in global mRNA expression patterns during human myogenesis, (b) investigate potential differences in the expression of metabolic genes and GPCR receptors between skeletal muscle tissue and primary cultured cells in a genome-wide perspective and (c) identify suitable reference genes for each developmental stage. The use of primary cell cultures and other cell models provides a well-established and reproducible model in myogenesis. However their use in studying insulin signalling is controversial. Human skeletal muscle cell culture has been used extensively for the investigation of the biochemical and genetic basis of peripheral insulin resistance in type 2 diabetes. Importantly, cultured human muscle cells appear to maintain the biochemical and metabolic properties of skeletal muscle tissue (Jackson et al. 2000; Henry & Ciaraldi 1996; Halse & Bonavaud 2001). Interestingly, Brozinick et al. (2003), Eckardt et al. (2008), Pender et al. (2005) and Berggren et al. (2005) have shown that insulin resistance disappears in cultured skeletal muscle cells obtained from biopsies from obese, insulin-resistant patients demonstrating that insulin resistance might be a reversible feature that can be acquired with obesity. Previous studies indicate that the genetic basis of muscle function and metabolism for each

individual is maintained in cell culture however, muscle from obese or diabetic individuals cease to be insulin resistant and this is because the cells are no longer being subjected to the external signals such as increased FFA and inflammatory cytokines that are present in obese and diabetic subjects.

This study investigated the global gene expression changes in human skeletal muscle tissue compared to cells in culture. The high levels of reproducibility, concordance and correlation between replicates confirmed the reliability of the microarray data. Moreover, the findings were found to be in general agreement with the findings from the published literature. PAX7, a molecular marker for muscle satellite cells, had higher expression in myoblasts than myotubes and showed very low expression in skeletal muscle tissue (Parker et al. 2003; Siegel et al. 2011; Seale et al. 2000; Wang et al. 2008). The transcriptional elongated factors Tceal was higher in myotubes compared to tissue in line with previous observations (Shi & Garry 2010). The expression of the THY1 gene, which is mainly expressed in human fibroblasts, neurons and endothelial cells, was higher in cultured cells than skeletal muscle tissue in agreement with (Raymond et al. 2010). The contamination with fibroblasts can be improved by using Percoll density centrifugation as reported by (Yablonka-Reuveni & Nameroff 1987) culturing satellite cell from a living single fibre (Rosenblatt & Lunt 1995) however, nonmyogenic differentiation of satellite cell commonly happens and 100% pure myogenic cell is almost impossible (Duguez et al. 2003; Shefer et al. 2004; Rosenblatt & Lunt 1995).The glucose transporter GLUT1 (SLC2A1) was also higher in skeletal muscle cultured cells than skeletal muscle tissue (Al-Khalili et al. 2003; Jackson et al. 2000). In line with Guigal et al. (2002), uncoupling protein-3 (UCP3), which is a mitochondrial membrane protein in human skeletal muscle, showed a low expression in cultured muscle cells. Collectively, these observations confirmed the validity of

the microarray data.

Skeletal muscle differentiation is a complex, highly coordinated process that relies on precise temporal gene expression patterns (Tomczak et al. 2004). In order to provide a useful database of genes that are differentially expressed throughout the myogenic process, all the genes described in the present study were compared and were found to be in general agreement with findings from previous studies (Kislinger et al. 2005; Janot et al. 2009; Moran et al. 2002; Shen et al. 2003; Tomczak et al. 2004; Raymond et al. 2010). The expression of the transcriptional regulators MYOD1, MYF5, CDK6 and Myogenin was higher in cultured cells than tissue (Yablonka-Reuveni 1988; Yablonka-Reuveni et al. 2008). Higher expression of MYOD1 and MYF5 were found in myoblasts; differentiating myocytes start to express myogenin with concomitant downregulation of MYOD1 (Tomczak et al. 2004; Wang et al. 2004). MyoD and MEF2 are known to be involved in myogenin induction at the start of differentiation (Wang et al. 2008). In this study MEF2a and MEF2b were higher in myoblasts whereas MEF2c and MEF2d were higher in myotubes indicating that not all members of the MEF family have a role in differentiation (Biressi et al. 2007). Cyclin-dependent kinase, CDK is a cell cycle inhibitor that has a role in normal cell growth during myocyte development as it inhibits proliferation and helps in the initiation of differentation (Shen et al. 2003). The level of CDK was high in myoblasts and then gradually decreased indicating that after 3 weeks cultured myoblasts are at the stage of starting differentiation. Genes encoding cell adhesion molecules are highly expressed in early myotubes providing a clearer indication of how the plasma membrane and extracellular matrix may be modified prior to cell fusion and suggesting their potential role during the initial steps of myogenic differentiation (Janot et al. 2009). In line with Janot et al., (2009) and Shen et al. (2003), we found higher expression of genes involved in

adhesion (MGAT1, HES6, ITGb1, ITGa1, ITGb7, ITGa4, NCAM1 and VCAM1) in myotubes compared to myoblasts and whole tissue. Furthermore, STAT1, STAT2 and STAT4 that play a role in differentiation (Wang et al. 2008) were also slightly higher in myotubes than myoblasts whereas genes for the growth factors FGFR2, IGFbp3 and IGFbp4 were higher in myoblasts compared to myotubes. Skeletal muscle differentiation is regulated by fibroblast growth factors in most skeletal muscle cell lines and in skeletal muscle primary cultures (Kudla et al. 1998). IGF-1 influences the development and maintenance of muscle cells at least partly through the induction of specific transcription factors and knockout of the IGF-IR gene causes severe skeletal muscle growth impairment (Kuninger et al. 2004; Bhasker & Friedmann 2008).

Not surprisingly, genes responsible for muscle structure subunit and phenotypes (Desmin, Tropomyosin, Troponin, Tropomodulin and myosin light and heavy chain) were higher in tissue than cultured cells with a fold change≥ 2 in agreement with previously published data (Raymond et al. 2010). It is worth mentioning that the embryonic type myosin heavy chain (MYH3) was higher in myotubes compared to skeletal muscle tissue. Myofibres are not fixed units but are capable of responding to functional demands by changing their phenotypic profile. Variation between the fibre-type phenotype of myotube cultures and that of the muscle tissue from which they were derived occurs through the increased expression of slow phenotype, Myosin heavy 7 (Myh7) (Chemello et al. 2011; Baker et al. 2006). In this study we used a mixed type muscle (VL) that expresses both slow and fast genes. Interestingly, the expression of genes associated with both slow and fast muscle fibre phenotypes was decreased in cultured cells when compared to skeletal muscle tissue. These data suggest that specific transcriptional programs generating mature muscle phenotype are activated in vivo but not in cultured muscle cells. Collectively, these data are

broadly consistent with the findings reported in previous microarray-based studies of myogenic gene expression in skeletal muscle cell lines and confirm that human skeletal muscle cultured cells is a valuable cell model in studying myogenesis.

The role of G-protein coupled receptors in different tissues has been the focus of intense research in an attempt to discover new therapies for metabolic diseases. The microarray data revealed the presence of cannabinoid and potential cannabinoid receptors and most of the enzymes responsible for endocannabinoid synthesis and degradation in both skeletal muscle cultured cells and skeletal muscle tissue. The expression of most receptors (CB1, CB2, GPR55 and GPR119) and enzymes (FAAH, MGLL, DAGLA & NAPE-PLD) was higher in skeletal muscle tissue than cultured cells. GPCR in tissue were found to have a fold change of + 2 when compared to culture cells, however, 4 transcripts were higher in cultured cell compared to skeletal muscle tissue [ADRA2A, ADRA2C, HRT2B (serotonin) and GPR126]. Serotonin (HRT2B) is another possible target in skeletal muscle proliferation and glucose homeostasis. Identification and localization of a functional skeletal muscle serotonin 5-HT2A receptor in rat fetal myoblasts was reported by Guillet-Deniau (1997) who also observed an upregulation of the transcription factor myogenin by serotonin. Both rat and human skeletal muscle express the 5-HT2A receptor and 5-HT2B and specific 5-HT2A agonists can rapidly stimulate glucose uptake in skeletal muscle (Wappler et al. 2001; Hajduch 1999). Fischer et al., (1995) reported a 1.8 and 1.5-fold increase in the amounts of glucose transporters GLUTI and GLUT4 at the cell surface of the cardiomyocytes with 90min treatment with 5HT. Guillet-Deniau (1997) demonstrated a 2–3-fold increase in GLUT3 mRNA level at 1.5 h, maximal level at 3 h and decreased to reach the control level after 9h after addition of serotonin to the cultured rat myoblast. Interestingly, microarray data

revealed the presence of GLUT3 (SLC2A3) with a rank order 17684 (myoblast), 17082 (myotube) and 28829 (tissue). The 5HT2b (HTR2b) receptor had a fold change of +9.41 (myotubes vs. tissue) and +4.39 (myoblasts vs. tissue).The orphan GPR126, has an essential role in muscle development (Soranzo et al. 2009; Waller-Evans et al. 2010), has been isolated from human umbilical vein endothelial cell cultures and whole-genome association studies have identified genetic variation at the GPR126 locus as a determinant of trunk length and body height in the human population (Waller-Evans et al. 2010).

Based on these interesting data regarding the differences in transcript expression between tissue and cultured cells, further analysis of the data by Genespring and IPA was carried out. IPA computed the data to generate significant networks and canonical pathways

The fold-change ratio between myotubes and muscle tissue showed that more than 12 thousand genes displayed differential expression between cultured myotubes and SM tissue. The number of genes with low expression was almost twice the number of genes with high expression genes (8,363 & 4,489 respectively). Ontology analysis of regulated genes in SM cultures revealed that with regard to cellular components a large number of genes encoding mitochondrial proteins were expressed at a lower level and endoplasmic reticulum components at a higher level in myotubes as compared to tissue. The downregulated genes in myotubes when compared to skeletal muscle tissue were genes associated with carbohydrate, protein and lipid metabolism as well as energy production. The genes that had the lowest expression included those encoding key regulators of glycogenolysis (PYGM), fatty acid oxidation (CPT1B) and ATP production. Various genes involved in glycolysis and oxidative phosphorylation (complexes I, II, III and IV) were also repressed. Mitochondrial dysfunction, TCA Cycle and calcium signalling were among the top canonical

pathways and all the enzymes in TCA Cycle as well as β oxidation had a low expression in myotubes compare to skeletal muscle tissue. Interestingly, genes that are involved in the transcriptional control of fatty acid oxidation and glucose homeostasis (such as PPARA, PPARG, PPARGCIA & PPARGC1B) (Semple 2006; Wahli & Michalik 2012; Lefebvre & Chinetti 2006) were decreased in myotubes compared to skeletal muscle tissue. Moreover, most fatty acid and glucose transporters were lower in cultured cells compared to skeletal muscle tissues. The GLUT4 (SLC2A4) was one of the most downregulated genes (FC -3329) however, GLUT1 was upregulated (FC 87). A decrease in protein and mRNA expression of GLUT4 and an increase in GlUT1 expression in cultured muscle cells was also reported by Michael et al. (2001), Jackson et al. (2000) and Al-Khalili et al. (2003). In this study, decreases in proteins involved in translocation of GLUT4 (VAMP2 and TC10) were also found. The importance of VAMP2 in trafficking of GLUT4 in 3T3 L1 adipocyte and rat cultured skeletal muscle cells was reported by Martin et al., (1996) and Braiman et al., (2001), respectively. JeBailey et al., (2004), Chang, Chiang, & Saltiel, (2005) and (Chiang et al. 2006) reported that TC10 plays an important role in actin remodelling process which is required for GLUT4 translocation to the plasma membrane in response to insulin. Collectively, a decrease in PI3k/AKT pathway was seen with an increase in negative regulator of insulin signal transduction pathway (SHIP2, PTEN and SOCS). Giving that there was little or no GLUT4 and higher levels of GLUT1 may indicate (in cultured cell) there is little insulin stimulated glucose uptake. Human skeletal muscle culture has been used extensively for the investigation of the biochemical and genetic basis of peripheral insulin resistance. However, its use in studying insulin-stimulated glucose transport must be interpreted with caution as a decrease in insulin induced GLUT4 translocation in cultured cell compare to insulin responsiveness typically observed in human forearm muscle balance studies has also been reported (Perriott et al. 2001).

Genes that encode myofilaments and calcium-binding proteins were also expressed at a lower level in cultured cells. Slow type isoforms such as MYL3, MYBPC1 and MYOZ1 and isoforms that are expressed in fast type muscle fibres such as TMOD4, CASQ1 and MYOZ3 showed decreased expression. Vastus lateralis (VL) muscle in humans is described as containing a mixture of type I (slow) and type II (fast) fibres. In contrast, Baker et al. (2006) observed upregulation of slow muscle genes only in cell culture. It can be seen that muscle cell cultures in general remain relatively immature, in terms of their phenotype in line with previous observations by Raymond et al. (2010). As genes responsible for skeletal muscle development and function were also decreased in cultured cells, pathways involving skeletal muscle disorders and muscle myopathies were identified by Ingenuity analysis as being elevated in cultured cells. The decrease in metabolic genes and genes involved in muscle contraction in cultured cells, also indicated a phenotype associated with disuse atrophy and Duchenne muscular dystrophy (Noguchi et al. 2003; Chen et al. 2007; Baker et al. 2006).

As expected, genes showing elevated expression in myotubes compared to skeletal muscle tissue were associated with Cellular Movement, Cellular Growth and Proliferation, Cellular Function and Maintenance. Among the upregulated genes detected in skeletal muscle proliferation and differentiation category were the regulatory factors MYOD1, MYOG, MYF5, FGFR2, ITGB1, CDKN, TOP2A, and HIF1A. Moreover, several genes that have a regulatory function in cell attachment and adherence as well as around 200 genes related to extracellular matrix such as those encoding for accumulation of glycosaminoglycan and hyaluronic acid were also included in this list. This provides an indication of how the plasma membrane and extracellular matrix may be modified prior to cell maturation. Growth related genes were also upregulated in myotubes compared to skeletal muscle tissue (including insulin like growth factor, connective tissue

growth factor and growth differentiation factor). Overall, upregulated genes were associated with an increase in cell movement, adhesion, inflammation and proliferation. Gene expression changes during myoblast differentiation were previously studied in mouse C2C12 cells (Janot et al. 2009; Moran et al. 2002; Kislinger et al. 2005; Shen et al. 2003; Tomczak et al. 2004). The present study is the first study using human primary cultured cells. When myoblasts were compared to myotubes, 2,774 entities had fold change of ± 2 and among them around a thousand genes (1,091) were downregulated. IPA analysis showed that the top biological functions were Cellular Movement, Cell-To-Cell Signalling and Interaction. Close examination of the regulated functions revealed a decrease in genes responsible for muscle contraction and cytoskeletal organization in myoblasts compared to myotubes, which was also reported by Moran et al. (2002), a decrease in carbohydrate and lipid metabolism genes, a decrease in cell movement and binding indicating a modification changes prior to cells fusion in line with (Shen et al. 2003). LXR/RXR (retinoid X receptors) and FXR/RXR (farnesoid X receptor) pathways were among the top canonical pathways and was predicted to be inhibited, as most genes in the networks had lower expression in myoblast than myotubes. Even though It is well known that LXR/RXR and FXR/RXR play a crucial role in the regulation of bile acid catabolism (Goodwin et al. 2000) other studies reported their role in lipid and glucose metabolism. Ma et al. (2006) reported that FXR is a key regulator of glucose metabolism as they observed that FXR-null mice developed severe fatty liver and elevated circulating FFAs, which was associated with elevated serum glucose and impaired glucose and insulin tolerance. FXR also plays an important role in lipoprotein metabolism. Lambert et al., (2003) observed an elevated plasma cholesterol and triglyceride levels and excessive accumulation of fat in the liver in FXR−/− mice. Collectively, the higher level of metabolic genes in myotubes is an essential modification changes (i.e cell are differentiation and gaining muscle

phenotype) prior to cells fusion.

In conclusion, these data indicate that whilst primary human skeletal muscle myotube culture is at present the most physiologically relevant cell model for studying skeletal muscle development and metabolism, at the transcriptional level there are many differences between cell culture and muscle tissue. The decrease in expression of genes in the insulin signalling cascade, glucose metabolism, oxidative phosphorylation and beta oxidation suggests that primary myotube cell culture may be at least partially compromised in terms of being a cellular model for intermediary metabolism.

The expression of GPR40, 55, 119 and CB1 & CB2 were detected at the mRNA level by microarray, but the levels of expression were low. In fact all of these receptors were found to be expressed at levels below that of marginally expressed genes. However, this was also true of other receptors expressed at low levels, such as the insulin receptor, which has been definitively shown to be both present and functional in skeletal muscle. Thus microarray technology, whilst effective as a tool for analysis of global gene expression changes, can lack the sensitivity to detect transcripts expressed at low but functional levels.

In the next chapters, the expression of GPCRs will be further investigated using QRTPCR which is a more sensitive technique for the detection of mRNA. The functionality of these receptors in terms of activation of signal transduction pathways and effects upon metabolic pathways will also be described.

CHAPTER FOUR

MOLECULAR CHARACTERISATION OF CANNABINOID RECEPTORS IN SKELETAL MUSCLE

CHAPTER 4. MOLECULAR CHARACTERISATION OF CANNABINOID RECEPTORS IN SKELETAL MUSCLE

4.1. Introduction

Insulin resistance, especially in skeletal muscle which is responsible for 70-80% of peripheral glucose disposal, is an early sign and cause of type two diabetes. As insulin resistance develops years before overt diabetes, many researchers have focused on understanding the underlying molecular mechanisms with a view to identify targets for future antidiabetic therapies. GProtein-Coupled Receptors (GPCRs) activation or inhibition in skeletal muscle is a fertile area of research to achieve this goal as they may be involved in cross talk with various tyrosine receptors including the insulin receptor (Seale et al. 2000).

The cannabinoid receptors are GPCRs that are coupled to the Gi/o family predominantly and act through the adenyl cyclase pathway (Di-Marzo & Matias 2005; Matias et al. 2008; Engeli 2008a). CB1 and CB2 receptor activation by endogenous endocannabinoids such as N-arachidononyl ethanolamine (anandamide) and 2 arachidonoyl glycerol (2AG) lead to a decrease in cAMP and subsequent PKA, phosphorylation of p42 & p44 MAPK, p38 MAPK and JNK (Howlett 2005). They are also coupled to phosphotidylinositol 3 kinase and Focal adhesion kinase (Rodríguez de Fonseca et al. 2005). CB1 receptor only is associated with K^+ influx and inhibition of voltage-gated Ca^{+2} channels. Although CB1 and CB2 receptors are most highly expressed in brain and spleen, respectively, their presence in other tissues such as liver, pancreas, adipose tissue, myocardium and skeletal muscle has been reported (Engeli 2008a; Rajesh et al. 2008; Paul Cavuoto et al. 2007). The role of endcannabinoids and the potential presence of functional CB receptors in skeletal muscle is still under

investigation. Cavuoto et al. (2007)reported the presence of CB1 and CB2 mRNA in human and rodent skeletal muscle, respectively. CB1 (human and rat) and CB2 (human) open reading frames contain a single exon and Cavuoto et al. (2007) used DNAse treated total RNA (not mRNA) for cDNA synthsis and 10 times over the standard loading amount for RT-PCR were used for CB2.

A growing body of evidence shows that obese and diabetic patients have high levels of circulating endocannabinoids (Engeli 2008b; Bellocchio et al. 2008; Kunos 2007; Matias et al. 2006; O'Sullivan 2007; Osei-Hyiaman 2005). However their role in glucose homeostasis in skeletal muscle is still controversial and requires further investigation. An increase in glucose uptake has been reported with the use of CB1 antagonist Rimonabant (Cavuoto et al. 2007; Esposito et al. 2008; Liu et al. 2005), whereas Eckardt et al. (2009) observed an increase in glucose uptake with Anandamide (AEA), a CB1 agonist. A decrease in skeletal muscle insulin sensitivity as a result of an increase in 2AG in obesity and diabetes was reported by Engeli (2008b) and by (Bellocchio et al. 2008), which might be due to an increase in IRS-1 (Ser307) phosphorylation and a decrease in Akt (Ser473) phosphorylation as observed by Eckardt et al. (2009). The same authors also reported an activation of ERK1/2 and MAPK p38 which are downstream targets of insulin signalling. Furthermore, Esposito et al. (2008) reported that CB1 antagonist (RIM) induced insulin stimulated glucose uptake in mice primary cultured cells and L6 cell module . As slow twitch skeletal muscle fibres are more sensitive to insulin and changing of muscle phenotype from fast to slow improves glycemic control (Kubis et al. 2003; Lillioja et al. 1987; Wang et al. 2004), the role of CB1 and CB2 in insulin signalling in slow and fast muscle requires further investigation.

In addition to the classical cannabinoid receptors, there is a suggestion that GPR55 and GPR119 are potential cannabinoid receptors and may play a role

in glucose homeostasis. GPR55 is coupled to the Gs family and acts through a signalling pathway distinct from CB1 and CB2; for example it does not lead to ERK1/2 phosphorylation or an increase in calcium release (Lauckner et al. 2008; Ryberg et al. 2007). GPR119 is a GPCR (class I rhodopsin-type) that increases cAMP levels (Overton et al. 2008). GPR119 activation stimulates insulin secretion from the pancreas and glucagon like peptide (GLP) and gastric inhibitory polypeptide (GIP) secretion from enteroendocrine cells in a glucose dependent manner (Drucker 2001; Meier et al. 2002; Gromada et al. 2004). Chu et al. (2007) reported that the use of GPR119 agonists such as oleoylethanolamine do not decrease circulating glucose in GPR119 deficient mice. Again, their role in skeletal muscle has not been explored yet.

Another attractive area for research in GPCR biology is their association with cell development and differentiation (such as neurons, red blood cell, neutrophil, osteoblast and smooth muscle cell) (Wang et al. 2004). The role of CB1 in adipogenesis and neurogenesis has been reported by Matias et al. (2008), Pagano et al. (2007). The role of cannabinoid receptors in myogenesis remains to be elucidated.

4.2. Aims

The main objectives of this study are:

- To investigate and confirm the presence of CB1, CB2, GPR55 and GPR119 in human and rat skeletal muscle tissues and primary skeletal muscle cells culture.
- To compare the level of cannabinoid receptor mRNA expression between human and rat skeletal muscle.
- To compare the level of cannabinoid receptor mRNA expression in different muscle types at various stages of differentiation.

- To compare the level of cannabinoid receptors mRNA expression between Zucker Fat Rat (ZFR), Zucker Lean Rat (ZLR) and Wistar rat (WR) in different muscle types, heart, spleen, adipose tissue and liver.
- To assess the functionality of these GPCRs and determine whether their activation or inhibition may have a role to play in the control of blood glucose homeostasis.

4.3. Experiment design and methods

4.3.1. Sample collection and preparation

Human skeletal muscle tissues from vastus lateralis were collected from 8 subjects. Each sample was divided into two parts; the first part was snap frozen in liquid nitrogen and stored at -80^{o}C and the second part was used for isolation and culture of satellite cells in gelatinized flasks.

Slow (SOL & GR), fast (EDL & GW) and mixed (VL) muscle tissue was collected from Wistar, Zucker lean and fat rats. Liver, epididymal adipose, spleen, pancreas and heart tissues were also collected and snap frozen in liquid nitrogen. Isolation and culture of satellite cells was performed from all 3 muscle types obtained from both Wistar and Zucker rats.

Total RNA, mRNA, cDNA and protein preparation was performed as described in chapter 2 section 2.6.

4.3.2. Determination of GPCR mRNA expression levels

4.3.2.1. QRT-PCR

Quantitative Taqman RTPCR was performed using the step one plus real–time PCR system (Applied Biosystems). A standard protocol as described in chapter 2 was followed. In the initial experiments, in both human and rat (myoblasts and myotubes), the results were analysed using the absolute mean

values. The reason for this was the significant differences observed in the reference gene (β-actin and 18s) values between different tissues (brain, muscle, spleen and pancreas) as well as the various stages of muscle development (myoblasts, myotubes and tissues) (Tables 4.1 and 4.2). This result was similar to the microarray analysis described in Chapter 3 and to previous results reported by Stern-Straeter et al. (2009). Radonić et al. (2004) mentioned that the 18s gene cannot to be used as a reference gene when mRNA instead of total RNA is used in cDNA synthesis. Habets et al. (1999) observed a difference in total RNA and 28S rRNA between slow and fast muscles; in slow muscle the 28S rRNA was 5-6 fold higher than fast muscle. In later experiments, normalization was performed using TATA binding protein (TBP) as a reference gene (microarray data showed no significant differences in gene ranking between tissue and cultured cells). Stern-Straeter et al. (2009) & Warrington et al. (2000) reported that TBP is a suitable gene to use as a reference gene in cell development studies.

Table 4-1: Human reference gene CT values

HUMAN	β-actin	18s
50%MB	25	28
100%MB	17	23
MT	15	24
MTIS	15	24
BRAIN	22	31
SPLEEN		27

MB=Myoblast, MT=Myotube, M TIS =muscle tissue. % values describe the confluence of myoblast cells in culture

Table 4-2: Rat β actin CT values

RAT βactin	GR	GW	EDL	SOL
MB	16	22	18	20
MT	17	14	16	14
MTIS	16	21	20	20

MB=Myoblast, MT=Myotube, M TIS =muscle tissue, GR=Gastrocnemius Red, GW= Gastrocnemius White, SOL=Soleus, VL= Vastus Lateralis, EDL= Extensor Digitorum Longus

4.3.3. Protein phosphorylation experiments

Western blotting was used to study the effect of CB1 agonists and antagonists, MEK inhibitor and pertussis toxin on the phosphorylation state and total content of selected cell signalling proteins using procedures described in detail in Chapter 2 section 2.7.

4.3.3.1. ERK1/2 and MAPK38

Human and rat (Wistar and Zucker) myotubes were treated with either 10 nM ACEA, 10nM EGF (Epidermal Growth Factor) or 10μM AEA for 5, 10 and 15 min. Myotubes were also pretreated with either 100nM RIM, 10 μM U0126 or 50nM PTX 30min prior to the addition of ACEA, AEA or EGF for 10min. Wistar rat myotubes were also treated with ACEA and/or RIM for 24 hours in the absence or presence of 100 nM insulin. After treatments, cells were washed with ice-cold PBS and lysed with RIPA buffer. Densitometry was used to measure the degree of phosphorylation.

4.3.3.2. AKT and GSK3α/β

Wistar rat myotubes were cultured in fatty acid free serum and treated with 100nM ACEA or 100nM RIM for 24hrs followed by 10 min stimulation of AKT and GSK3 α/β with 100nM insulin. After treatments, cells were washed with ice-cold PBS and lysed with RIPA buffer.

4.3.4. Protein expression experiments

Western blotting was used to examine the expression of CB1 and CB2. Immunocytochemistry was used to examine the expression of Ki67 and GLUT4.

4.3.4.1. Ki67

Wistar rat myoblasts were cultured in fatty acid free serum for 24 hrs

followed by 24hrs incubation with vehicle (0.01% ethanol) or 10nM ACEA.

4.3.4.2. GLUT4

Wistar rat myotubes were cultured in fatty acid free serum for 24 hrs followed by 24hrs incubation with vehicle (0.01% ethanol) or 100nM ACEA. Cells were also treated with 100nM insulin (5, 10, 30 min) in presence or absence of 100nM ACEA (24hrs before).

4.4. Statistical analysis

Statistical analysis was performed using GraphPad Prism software. RT-PCR and Western blot values were expressed as mean ± S.E.M. Statistical comparisons of different groups were made by one-way analysis of variance (ANOVA) and Bonferroni's multiple comparison post-hoc test Unpaired two-tailed t-test was also used to compare between two variable. A P value <0.05 was taken as the level of significance.

4.5. Results

4.5.1. CB1 mRNA expression

4.5.1.1. Human

The microarray data (chapter 3) revealed very low level expression of CB1 in skeletal muscle tissue and cultured cells Figure 4-1. The expression of CB1 in human skeletal muscle tissue and cultured myoblast and myotubes was assessed by Taqman QRT-PCR. Compared with the level of CB1 expression in the brain, the expression of CB1 in human skeletal muscle is very low (Figure 4-2). Skeletal muscle tissues and 100% myoblasts had significantly higher CB1 mRNA levels than 50% myoblast ($P<0.001$) and myotubes ($P<0.01$) (Figure 4-3).

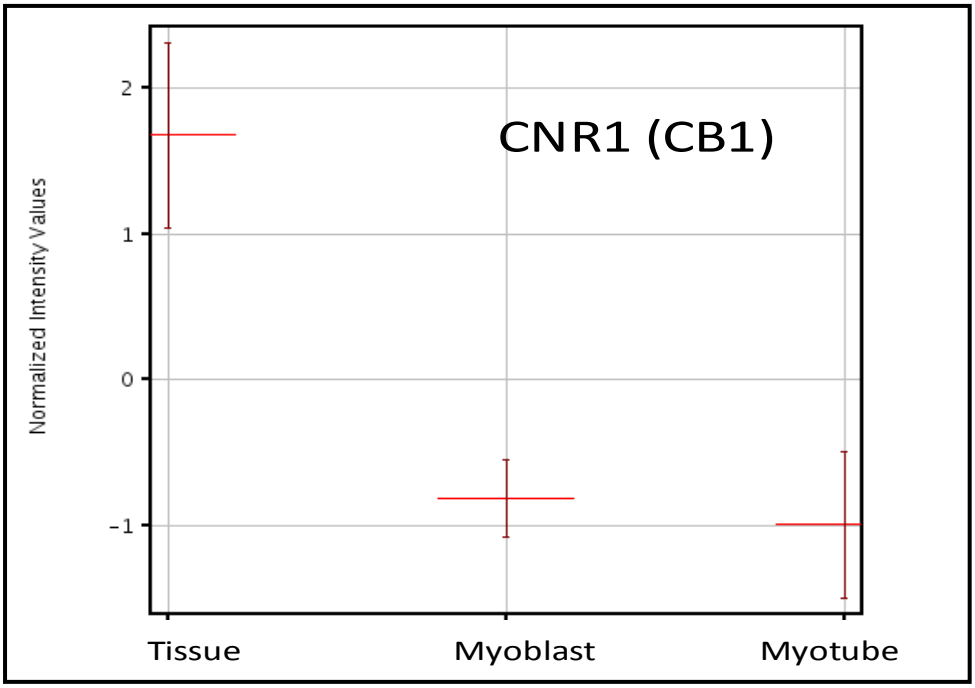

Figure 4-1: Microarray normalized intensity value (Log base 2) of CB1 mRNA expression in human skeletal muscle Tissue, Myoblast and Myotube (data from chapter 3).

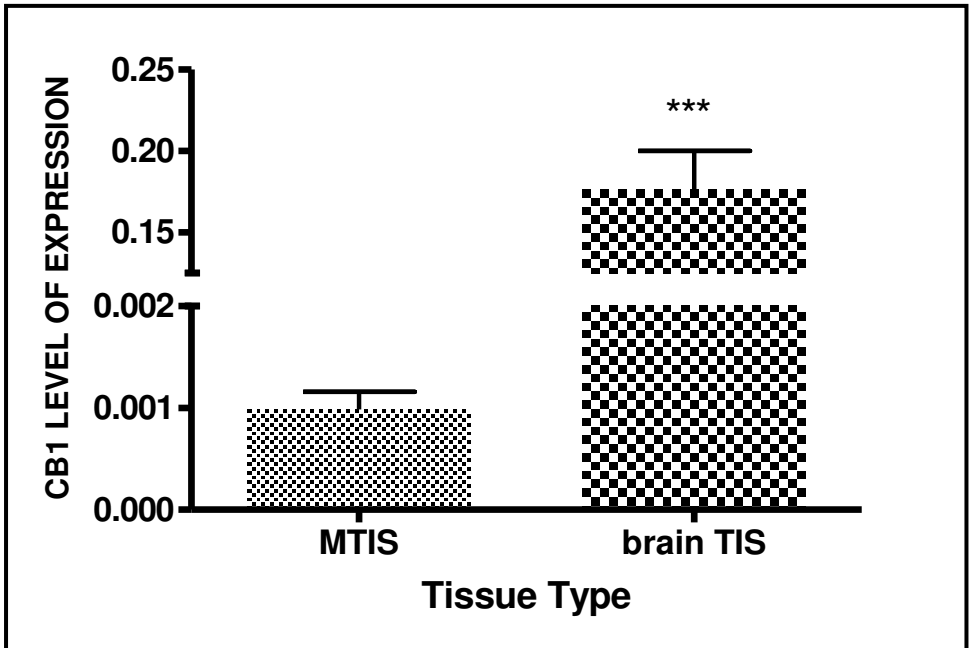

Figure 4-2: QRT-PCR analysis of CB1 expression in human skeletal muscle and brain tissues. Values are mean±SEM; data are non-normalized and just uses CB1 standard curve for quantification (n= 3 subjects for skeletal muscle tissue and brain mRNA were from Clontech). MTIS=muscle tissue, brainTIS= brain tissue. ***denotes P<0.0001.

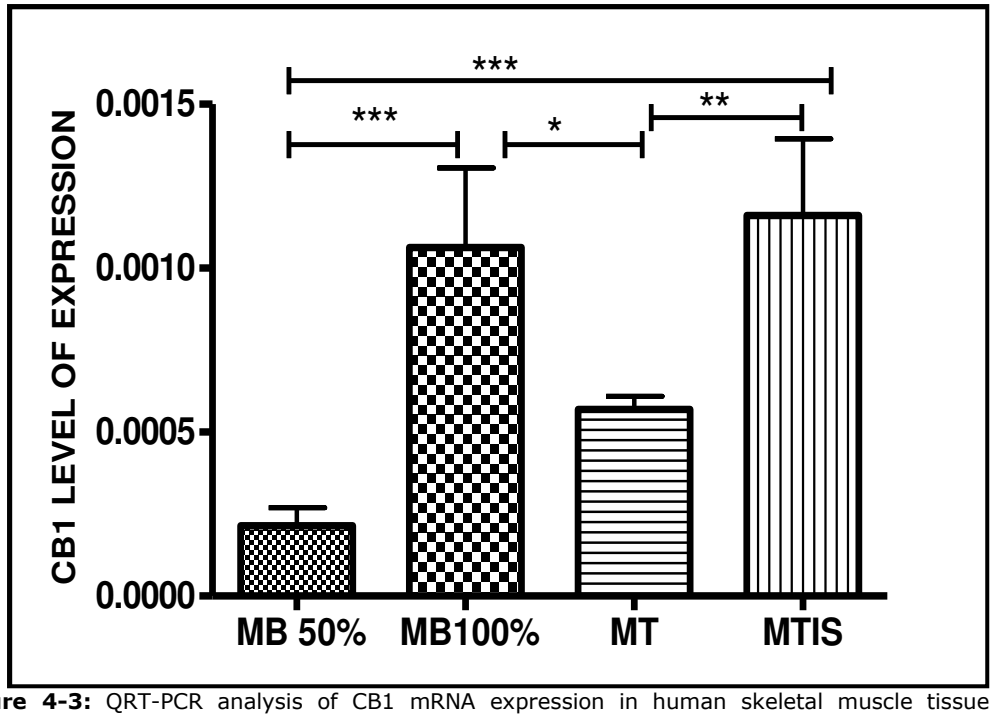

Figure 4-3: QRT-PCR analysis of CB1 mRNA expression in human skeletal muscle tissue and cultured cells.
Values are mean±SEM data is non-normalized and just uses CB1 standard curve for quantification (n=3 human). MB=Myoblast, MT=Myotube, MTIS =muscle tissue. * denotes P<0.05, ** denotes P<0.01, *** denotes P<0.0001.

4.5.1.2. Wistar rat

QRT-PCR was used to characterize gene expression differences between fast and slow skeletal muscle fibres in rat at different stages of differentiation in cell culture. CB1 was expressed in all rat tissues and cells tested. Rat skeletal muscle tissue had a higher CB1 mRNA expression than cultured cells in all muscle types tested (Table 4-3). Brain tissue had a significantly higher level of CB1 mRNA than muscle tissues (P<0.01) but the difference between brain and muscle was much less pronounced than in human samples (Figure 4-4). In both tissue and cultured cells, with the exception of GW myoblasts, the fast muscles (GW & EDL) had a trend for higher CB1 expression than slow muscles (GR & SOL) but the difference was only significant between GR and GW myotubes (P <0.05) (Figure 4-5). Furthermore, skeletal muscle tissues (slow and fast) had a higher level of expression than cultured myoblasts and myotubes (Table 4-3).

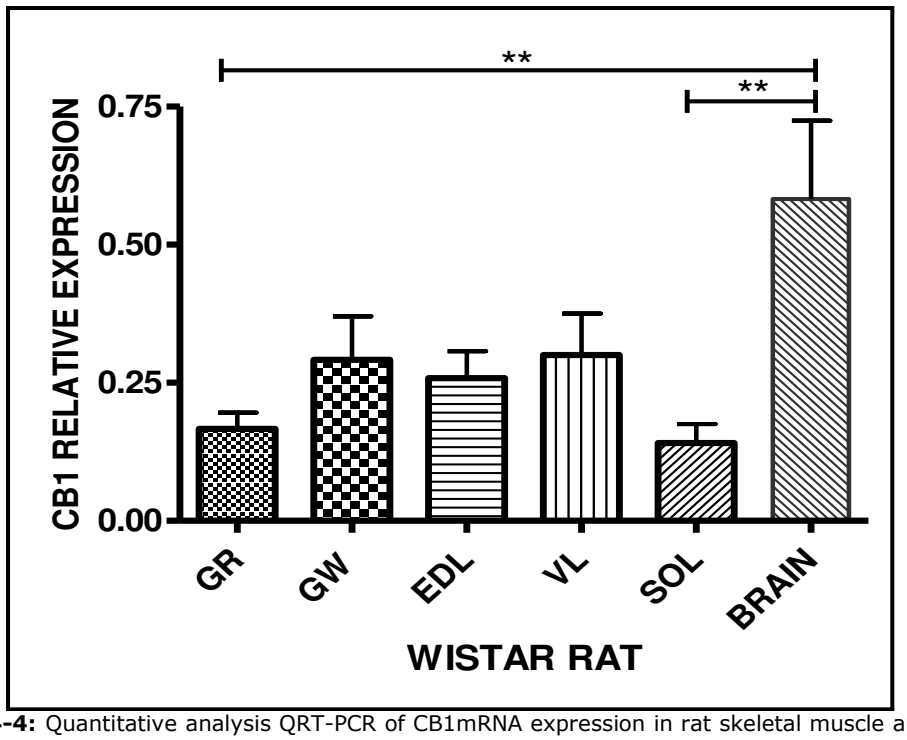

Figure 4-4: Quantitative analysis QRT-PCR of CB1mRNA expression in rat skeletal muscle and brain tissues.
** denote P<0.01 of brain compare to GR and SOL. Values are mean±SEM. Data were normalized to TBP (n=6). GR=Gastrocnemius Red, GW= Gastrocnemius White, SOL=Soleus, VL= Vastus Lateralis, EDL= Extensor Digitorum Longus.

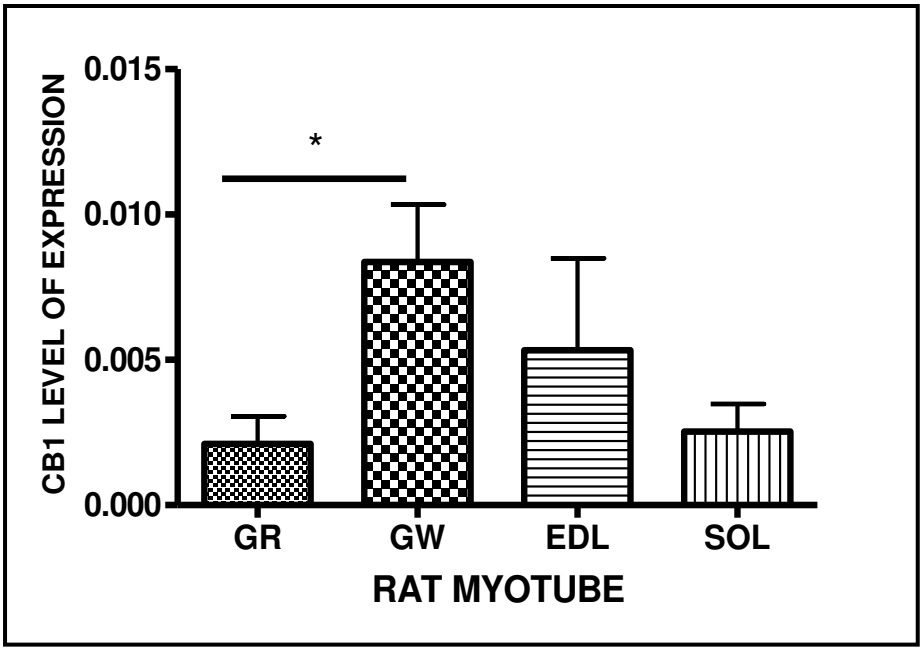

Figure 4-5: QRT-PCR analysis of CB1 mRNA expression in rat myotubes.
* denotes P<0.05. Values are mean±SEM, data are non-normalized and just uses CB1 standard curve for quantification (n= 6 rats) GR=Gastrocnemius Red, GW= Gastrocnemius White, SOL=Soleus, VL= Vastus Lateralis, EDL= Extensor Digitorum Longus.

Table 4-3: Rat skeletal muscle tissue and cultured cell CB1 mRNA expression

	GR	GW	EDL	SOL
Tissue	0.0309±0.0235	0.0947±0.0526	0.1084±0.0803	0.0302±0.0172
Myotube	0.0021±0.0009	0.0084±0.0020	0.0111±0.0061	0.0025±0.0010
Myoblast	0.0068±0.0038	0.0002±0.0001	0.0095±0.0022	0.0049±0.0018

Values are mean±SEM (n=12samples from 6 rats). GR=Gastrocnemius Red, GW= Gastrocnemius White, SOL=Soleus, VL= Vastus Lateralis, EDL= Extensor Digitorum Longus.

4.5.1.3. Zucker Lean and Zucker Fat Rats

4.5.1.3.1. CB1 mRNA expression in skeletal muscle

Expression levels of CB1 in muscle tissues from VL, EDL, GR and SOL muscles were similar at 12 weeks for Zucker Fat Rat (ZFR) and Zucker Lean Rat (ZLR) (Figure 4-6). At 20 weeks ZFR had higher ($p<0.01$) expression of CB1 than ZLR. Interestingly, Wistar rat skeletal muscle tissues (GR, GW, EDL, Vl & SOL) had higher levels of CB1 expression than either ZFR and ZLR (Figure 4-6). There was no difference in CB1 expression on cultured myotubes between ZFR, ZLR and Wistar rats (Figure 4-6).

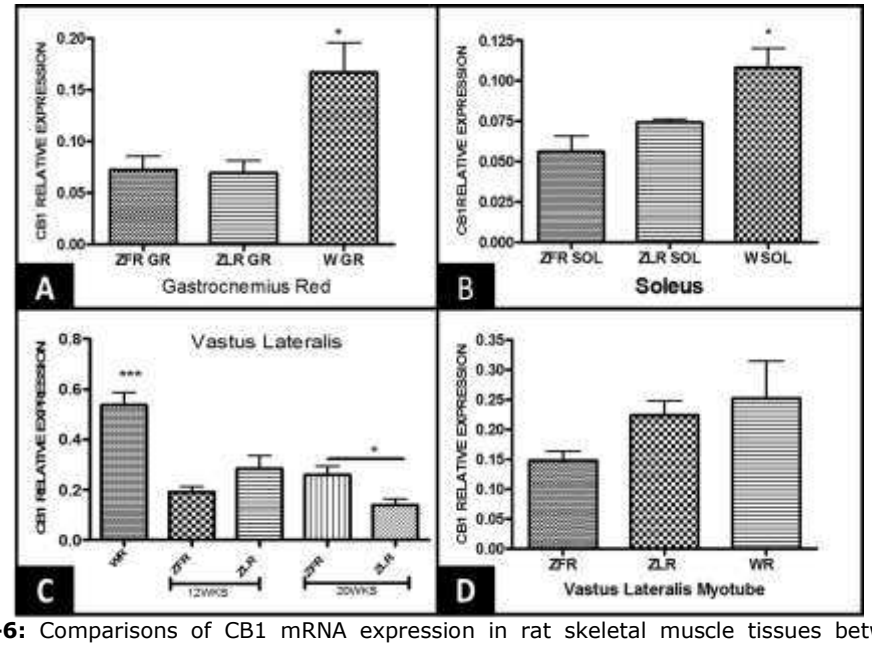

Figure 4-6: Comparisons of CB1 mRNA expression in rat skeletal muscle tissues between ZFR (Zucker Fat Rat), ZLR (Zucker Lean Rat) and WR (Wistar Rat).
A & B) *denote $P<0.05$ compared to ZLR and ZFR $P<0.01$ higher CB1 expression in WR GW than ZFR &ZLR GW. D) *** denotes $P<0.001$ compared to ZLR and ZFR, * denotes $P<0.05$ ZFR compared to ZLR (20wks). Data were normalized to TBP. Values are mean ± SEM (n=5 rats, 2 samples from each)

4.5.1.3.2. CB1 mRNA expression in other tissues

20wk old ZFR had significantly higher CB1 expression in Epididymal Adipose Tissue (EAT) ($P<0.01$) than ZLR. Similar to skeletal muscle, Wistar rat EAT had also higher CB1 expression ($P<0.001$) than ZFR and ZLR (12 & 20 wks) Figure 4-7. In liver, no differences between ZLR and ZFR CB1 expression were observed and again Wistar rats had higher expression of CB1 than ZFR and ZLR . CB1 expression in spleen and heart showed no significant differences between the different types of rats (Figure 4-7).

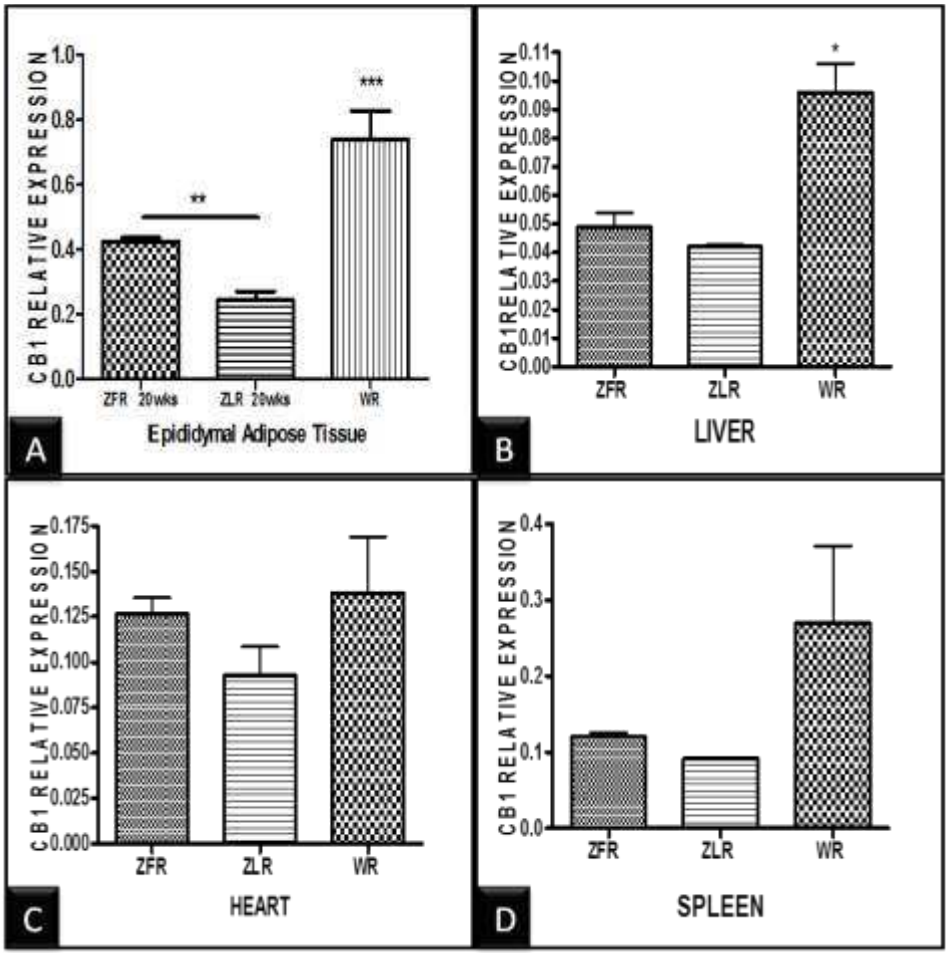

Figure 4-7: QRT-PCR analysis represents comparisons of CB1 mRNA expression in rat tissues between ZFR (Zucker Fat Rat), ZLR (Zucker Lean Rat) and WR (Wistar Rat).
A) Epididymal Adipose tissue (EAT) **denotes $P<0.01$. B) Liver * denotes $P<0.05$ compared to ZLR and ZFR higher. C) Heart. D) Spleen. Data were normalized to TBP. Values are mean ± SEM (n=3 rats).

4.5.2. CB2 mRNA expression

4.5.2.1. Human

The microarray data presented in Chapter 3 also revealed the low level expression of CB2 in skeletal muscle tissue, myoblasts and myotubes. QRT-PCR analysis confirmed the expression of CB2 in cultured cells but not in human skeletal muscle tissue. 100% myoblasts had a higher level of expression than myotubes (P<0.05). Skeletal muscle CB2 expression was very low particularly when compared with expression in spleen (P<0.001) (Table 4-4).

Table 4-4: Human CB2 mRNA expression in skeletal muscle tissue, cultured cells and spleen.

	MB 50%	MB 100%	MT	MTIS	spleen
MEAN	NED	0.004377*	0.000821	NED	0.3634***
SEM		0.001988	0.0002192		0.08643

*** denotes (P<0.001) compared to MB and MT. * denotes P<0.05 MB compared MT. Values are mean ± SEM. Data were normalized to TBP (n=3-6). NED=No Expression Detected, MB=Myoblasts, MT=Myotubes, MTIS =muscle tissue.

4.5.2.2. Wistar Rat

RT-PCR analysis demonstrated the expression of CB2 in rat skeletal muscle tissue and cultured cells. Tissue levels of CB2 expression were higher than myoblasts and myotubes in all muscle types tested (P <0.05). Skeletal muscle CB2 expression was very low when compared with the spleen CB2 expression (P<0.001) (Table 4-5).

Table 4-5: Rat skeletal muscle tissue, spleen and cultured cells CB2 mRNA expression

	GR	GW	EDL	SOL	SPLEEN
TISSUE	0.0101±0.0003*	0.0157±0.0087*	0.0454±0.0123*	0.0248±0.0148*	1.5420±0.1815***
MYOTUBE	0.0055±0.0012	0.0052±0.0007	0.0087±0.0011	0.0051±0.0017	
MYOBLAST	0.0052±0.0029	0.0039±0.0019	0.0029±0.0009	0.0018±0.0009	

* P<0.05 denotes tissues compared to myotubes and myoblasts. ***denotes P<0.001 Spleen compared to skeletal muscle tissue. Data were normalized to TBP. Values are mean ± SEM (n=3-6). GR=Gastrocnemius Red, GW= Gastrocnemius White, SOL=Soleus, VL= Vastus Lateralis, EDL= Extensor Digitorum Longus.

4.5.2.3. Zucker Fat and Lean Rat

The expression of CB2 was also investigated in fast and slow muscle tissue from ZFR and ZLR. ZFR skeletal muscle tissue had similar CB2 expression to ZLR in all types of muscle tested. CB2 expression was higher in Wistar rat skeletal muscle tissues than ZLR and ZFR skeletal muscle tissues but this reached statistical significance in GR and GW only (Figure 4-8).

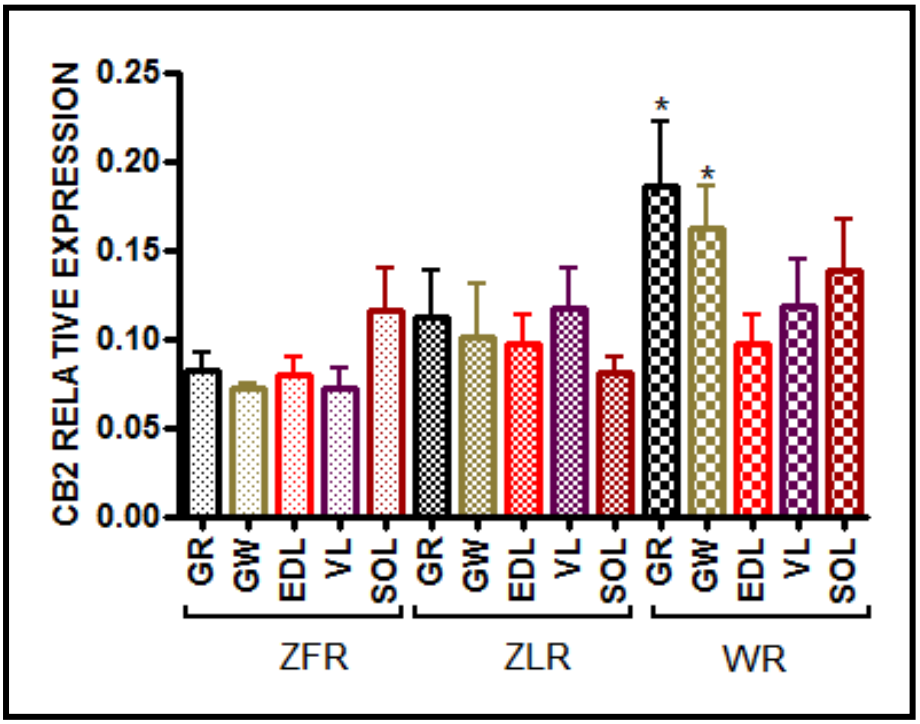

Figure 4-8: Comparisons of CB2 mRNA expression in rat skeletal muscle tissues between ZFR (Zucker Fat Rat), ZLR (Zucker Lean Rat) and WR (Wistar Rat).
* denotes ($P<0.05$) WR (GR &GW) compared to ZLR and ZFR. Data were normalized to TBP. Values are mean ± SEM (n=5-7).GR=Gastrocnemius Red, GW= Gastrocnemius White, SOL=Soleus, VL= Vastus Lateralis, EDL= Extensor Digitorum Longus.

4.5.3. GPR55 mRNA expression

The microarray analysis presented in Chapter 3 indicated the presence of GPR55 in human Skeletal muscle tissue and cultured cells (TIS=30527, MT=34893, MB=35826 ranking out 41078). However, the RT-PCR analysis revealed that neither human nor rat skeletal muscle tissues or cultured cells had

a detectable level of GPR55 expression. GPR55 expression was found in rat pancreas, spleen, and human brain (0.014± 0.001) and spleen (1.517 ± 0.3519).

4.5.4. GPR119 mRNA expression

4.5.4.1. Human

The microarray data presented in Chapter 3 revealed the expression of GPR119 in skeletal muscle tissue, myoblasts and myotubes (TIS= 22132, MB=24726, MT=24725 ranking out 41078) (Figure 4-9). The expression of GPR119 was significantly higher ($P<0.05$) in 100% MB and MT than 50% myoblasts, skeletal muscle tissue and spleen (Figure 4-10). There was no detectable level of GPR119 expression in human brain tissue (Data not shown).

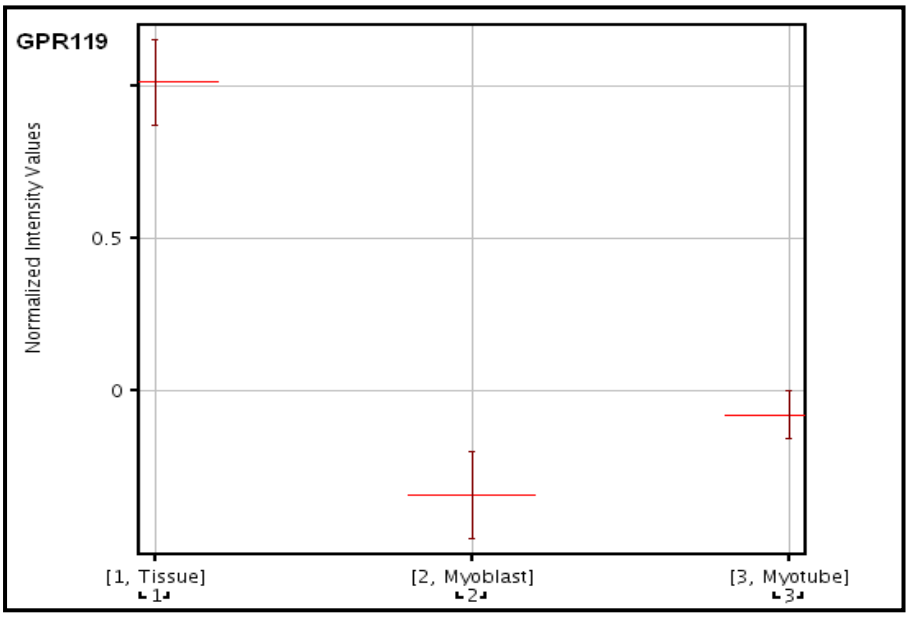

Figure 4-9: Microarray normalized intensity value (Log base 2) of GPR119 mRNA expression in human skeletal muscle Tissue, Myoblast and Myotube.

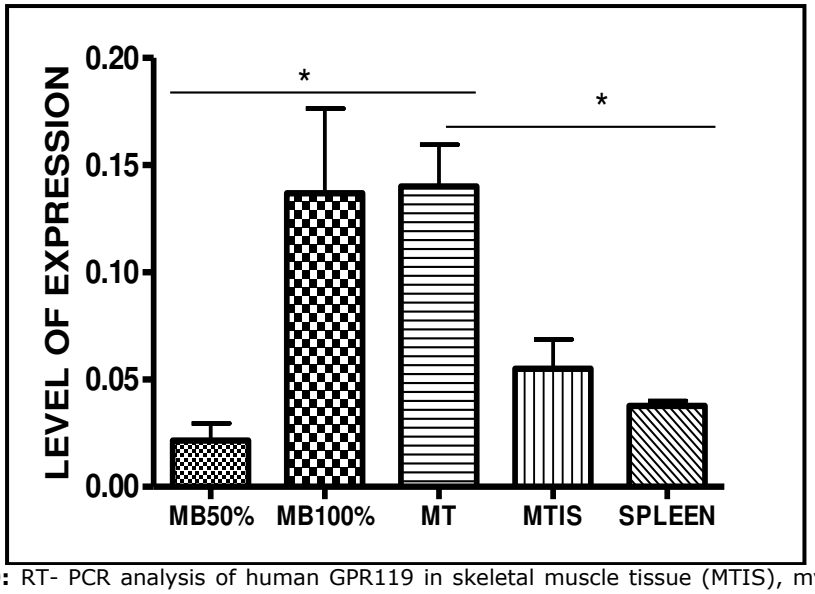

Figure 4-10: RT- PCR analysis of human GPR119 in skeletal muscle tissue (MTIS), myoblast (MB) and myotubes (MT) and spleen.
* denotes (P<0.05). Data was normalized to TBP. Values are mean ± SEM (n=6-12). MB=Myoblast, MT=Myotube, MTIS =muscle tissue.

4.5.4.2. Rat

RT-PCR analysis revealed the expression of GPR119 mRNA in all muscle types of both Wistar and Zucker rats (Figure 4-11). RT-PCR analysis also revealed that ZLR (12wks) had a trend for higher GPR119 expression than ZFR (12wks) in most of the muscles tested and this reached statistical significance in SOL muscle (P<0.05). RT-PCR also revealed the presence of GPR119 in brain, spleen and pancreas of Wistar rats (data not shown).

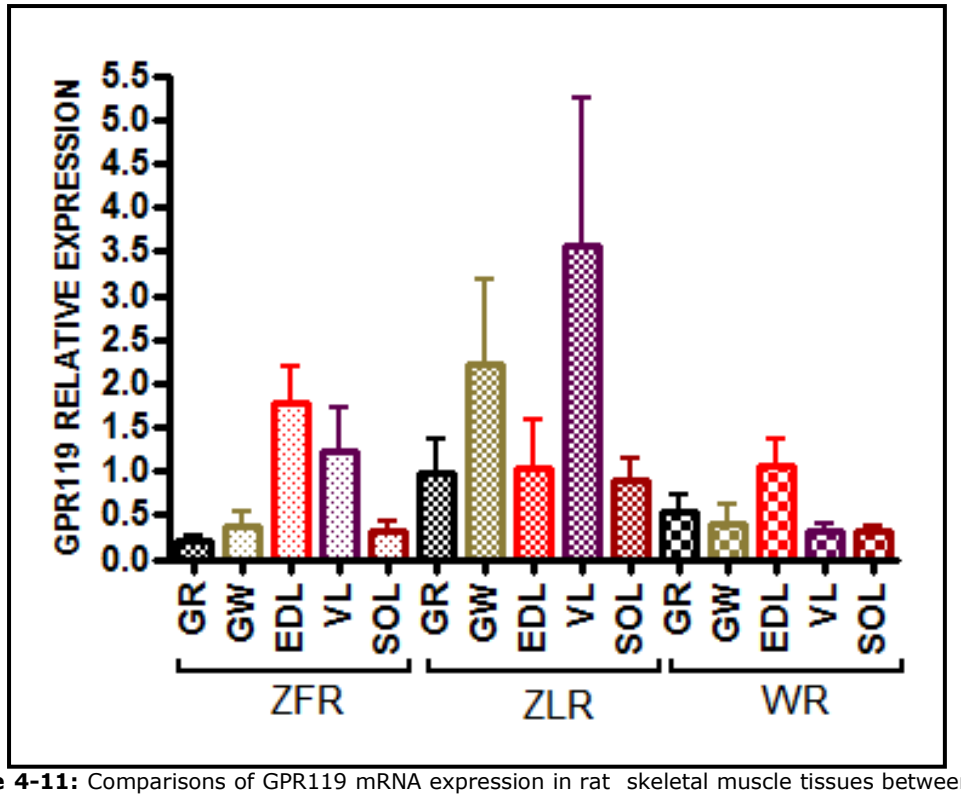

Figure 4-11: Comparisons of GPR119 mRNA expression in rat skeletal muscle tissues between ZFR (Zucker Fat Rat), ZLR (Zucker Lean Rat) and WR (Wistar Rat).
Data were normalized to TBP (n=5-7). Values are mean ± SEM. GR=Gastrocnemius Red, GW= Gastrocnemius White, SOL=Soleus, VL= Vastus Lateralis, EDL= Extensor Digitorum Longus.

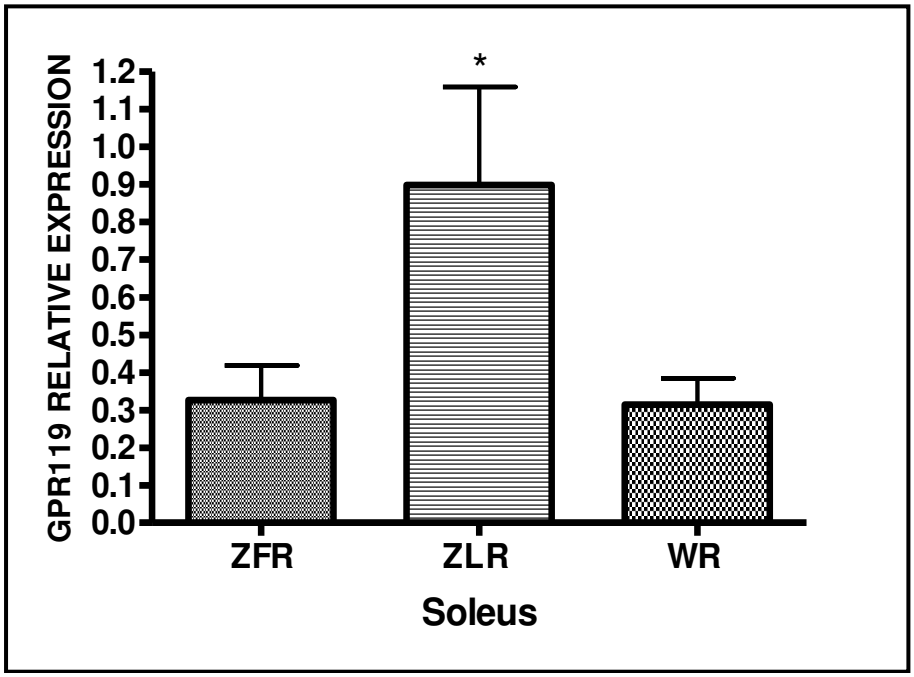

Figure 4-12: QRT-PCR analysis represent a comparisons of GPR119 mRNA expression in rat SOL tissues between ZFR (Zucker Fat Rat), ZLR (Zucker Lean Rat) and WR (Wistar Rat).
* denotes P<0.05 in ZLR than ZFR and WR. Data were normalized to TBP (n=5).Values are mean ± SEM

4.5.5. Effect of ACEA, AEA, U0126 and RIM on ERK phosphorylation

RTPCR analysis showed that human and rat (Zucker and Wistar) myotubes had detectable levels of CB1. To address the functionality of CB1, the effect of CB1 activation or inhibiton on ERK1/2 phosphorylation was investigated.

4.5.5.1. Human

Treatment of human VL myotubes with 10nM ACEA showed a time dependent increase in ERK1/2 phosphorylation (Figure 4-13). Treatment with AEA (10μM) also showed a time dependent increase in ERK1/2 phosphorylation with a significant peak ($P<0.05$) at 10min (Figure 4-14). EGF was used as a positive control for ERK phosphorylation. Pretreatment of myotubes with the MEK inhibitor U0126 (10μM) significantly inhibited ERK phosphorylation induced by EGF and ACEA (Figure 4-15).

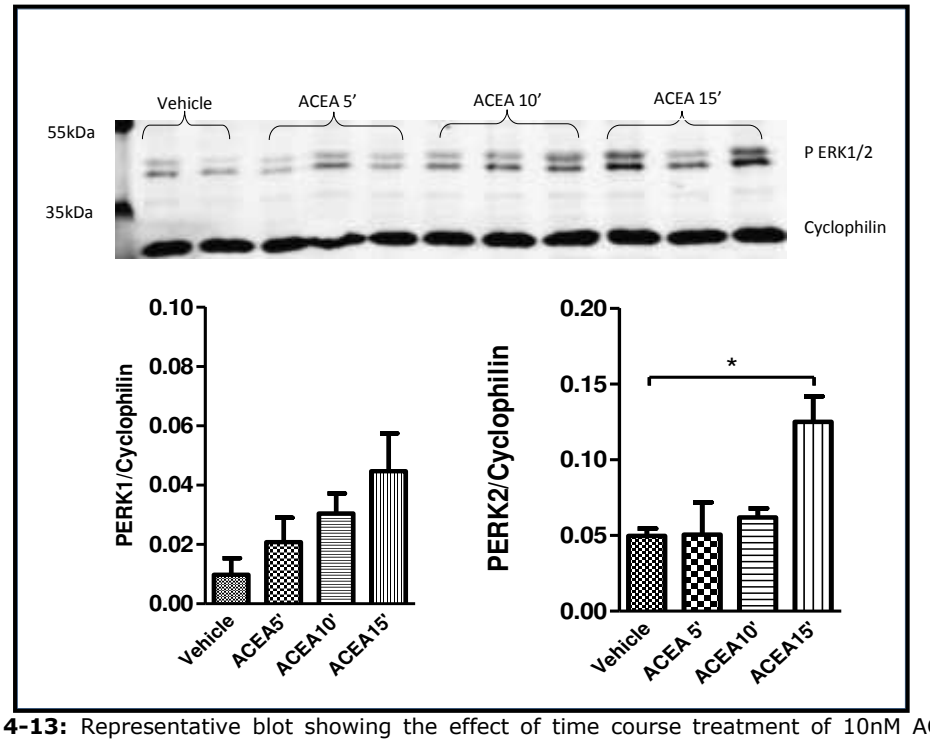

Figure 4-13: Representative blot showing the effect of time course treatment of 10nM ACEA on phosphorylation of ERK in human myotubes.
Quantified values of PERK1/CYCL, PERk2/CYCL are shown in the lower panel. Values are mean ± SEM .Data were analysed by one way ANOVA with Bonferroni post-hoc test (n=3).

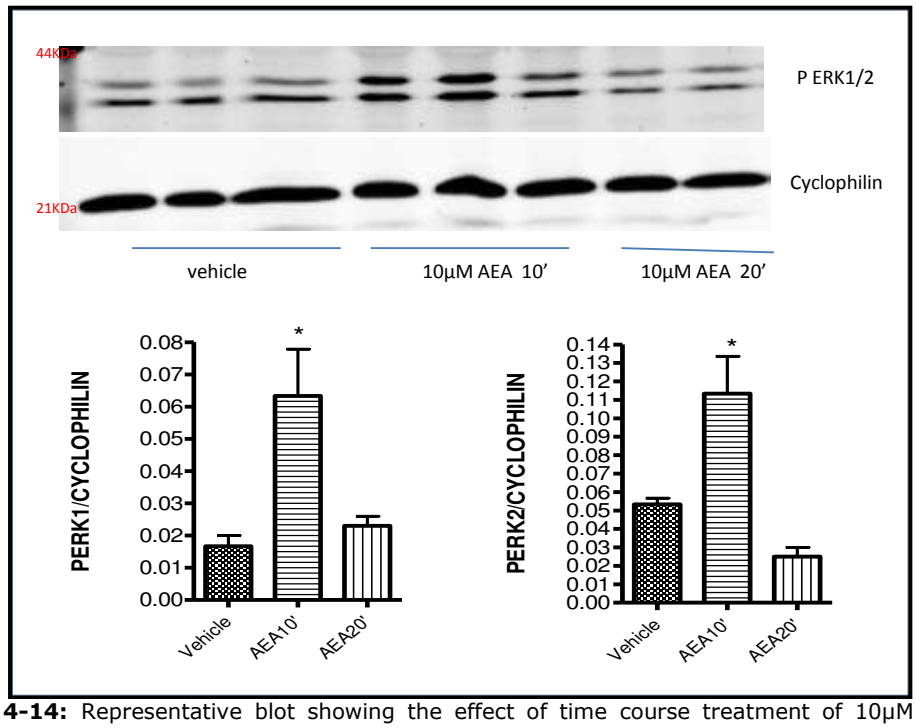

Figure 4-14: Representative blot showing the effect of time course treatment of 10µM AEA on phosphorylation of ERK in human myotubes.
Quantified values of PERK1/TERK1, PERk2/TERK2 are shown in the lower panel. * denotes P<0.05 compared to vehicle and AEA20'. Values are mean ± SEM. Data were analysed by one way ANOVA with Bonferroni post-hoc test (n=3).

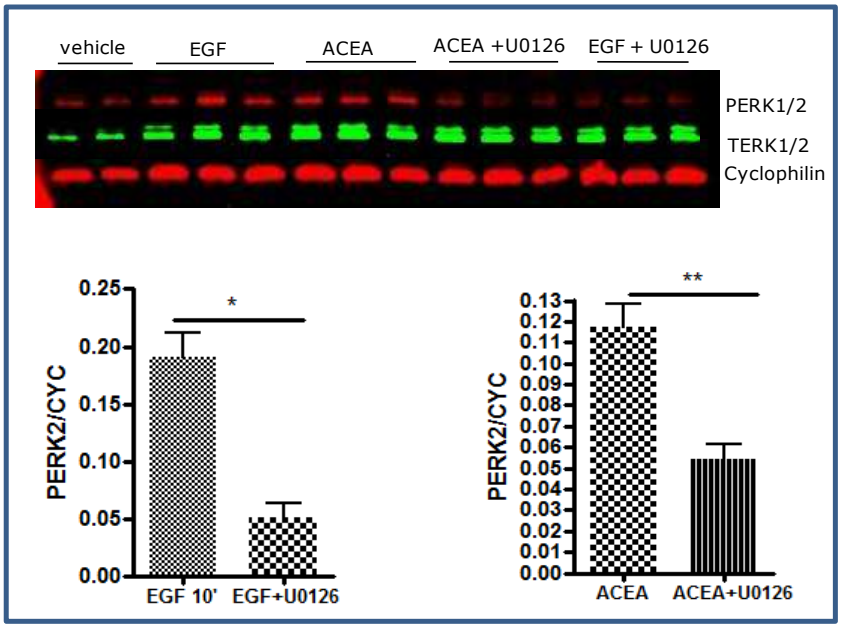

Figure 4-15: Representative blot showing the effect of 10µM U0126 on ERK phosphorylation induced by EGF (10nM) and ACEA (10nM) in human myotubes.
Quantified values of PERK2/CYC are shown in the lower panel. * denotes P<0.05 and ** denotes P<0/01. Phospho ERK1/2 (PERK) is shown in red band and total ERK1/2 (TERK) in green. Values are mean ± SEM (n=3).

4.5.5.2. Wistar Rat

Treatment of rat myotubes with 10 nM ACEA showed a rapid induction of ERK1/2 phosphorylation within 5 min and reached peak values at 10 min that was followed by a decline at 20 min (Figure 4-16). Treatment of the myotubes with 10μM AEA for 10 min led to a significant ($P<0.01$) induction of ERK1/2 phosphorylation. Pre-treatment (30 min) of the cells with 100 nM RIM or 10μM U0126 significantly inhibited ($P<0.01$) the ACEA and AEA induction of ERK1/2 phosphorylation ($P<0.01$) (Figure 4-17, Figure 4-18, Figure 4-19, respectively). It is worth mentioning that the experiments were performed in muscles consisting of different types of fibres (slow and fast) and no difference was found between the two types. The pattern of ERK1 and ERK2 phosphorylation change was also similar, thus quantification of ERK2 phosphorylation only was used as an indicator in some experiments.

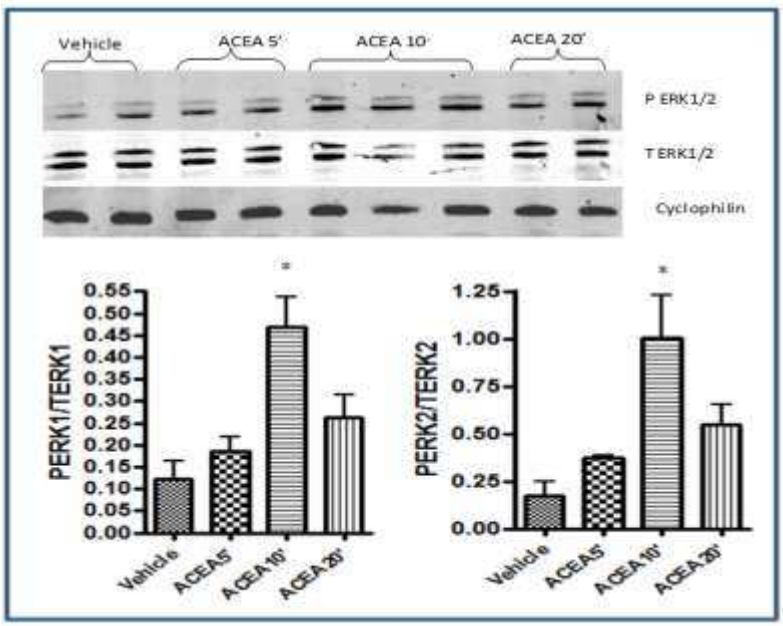

Figure 4-16: Representative blot showing the effect of time course treatment of 10nM ACEA on phosphorylation of ERK in Wistar rat myotubes.
Quantified values of PERK1/TERK1, PERk2/TERK2 are shown in the lower panel. * denotes $P<0.05$ compared to vehicle. Cyclophilin was used as a loading control. Values are mean ± SEM. Data were analysed by one way ANOVA with Bonferroni post-hoc test (n=3).

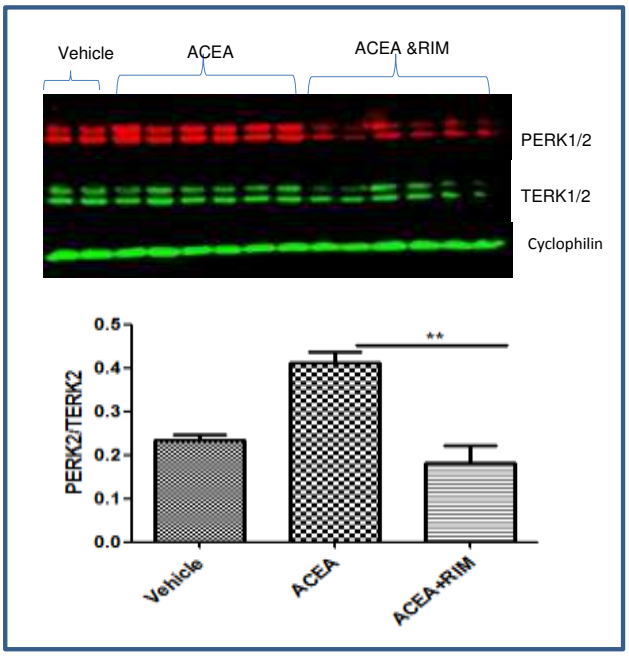

Figure 4-17: Representative blot showing the effect of 100nM RIM on ERK phosphorylation induced ACEA(10nM) in Wistar rat myotubes.
Pretretment (30min) with 100nM RIM significantly inhibited ERK1/2 phosphorylation induced by 10nM ACEA (** denotes P<0.01). Quantified values of PERK2/TERk2 are shown in the lower panel. Values are mean ± SEM. Data were analysed by one way ANOVA with Bonferroni post-hoc test. Phospho ERK1/2 (PERK) is shown in red band and total ERK1/2 (TERK) in green. Cyclophilin was used as a loading control (n=3).

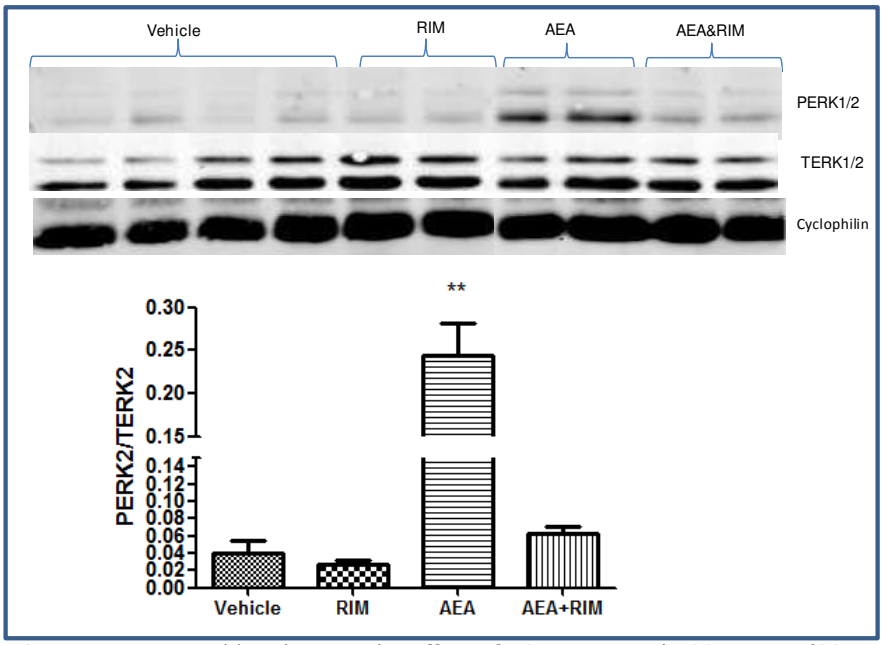

Figure 4-18: Representative blot showing the effect of 10μM AEA and 100nM RIM (30min prior) on ERK phosphorylation in Wistar rat myotubes.
Quantified values of PERK2/TERk2 are shown in the lower panel (** denotes P<0.01). Data were analysed by one way ANOVA with Bonferroni post-hoc test. Cyclophilin was used as a loading control (n=3).

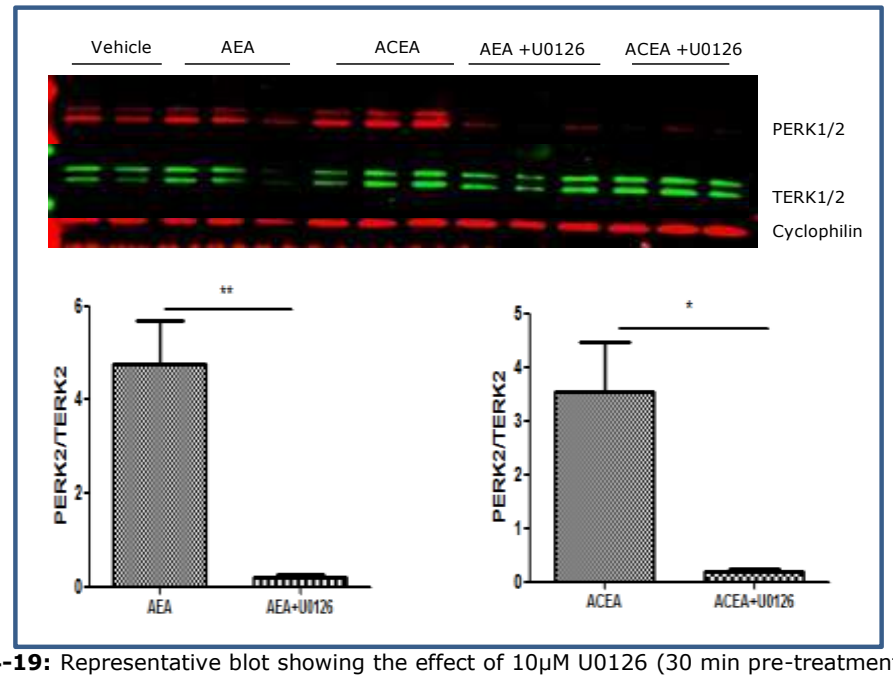

Figure 4-19: Representative blot showing the effect of 10μM U0126 (30 min pre-treatment) on ERK phosphorylation induced by AEA (10μM) and ACEA (10nM) in Wistar rat myotubes.
Quantified values of PERK2/TERk2 are shown in the lower panel. * denotes P<0.05 and ** denotes P<0/01. Data were analysed by one way ANOVA with Bonferroni post-hoc test. Phospho ERK1/2 (PERK) is shown in red band and total ERK1/2 (TERK) in green. Cyclophilin was used as a loading control (n=3).

4.5.5.3. Zucker Lean and Fat Rats

As CB1 mRNA expression was detected in both ZLR and ZFR, its functionality was investigated by studying the activation (phosphorylation) of the ERK1/2 signalling pathway. Treatment of myotubes cultured from ZLR with 10nM ACEA and 10μM AEA led to a significant induction of ERK1/2 phosphorylation at 10 and 15 min (P<0.01). Pretreatment with 100nM Rim for 30min significantly inhibited ERK1/2 phosphorylation induced by ACEA and AEA (Figure 4-20 & Figure 4-21)

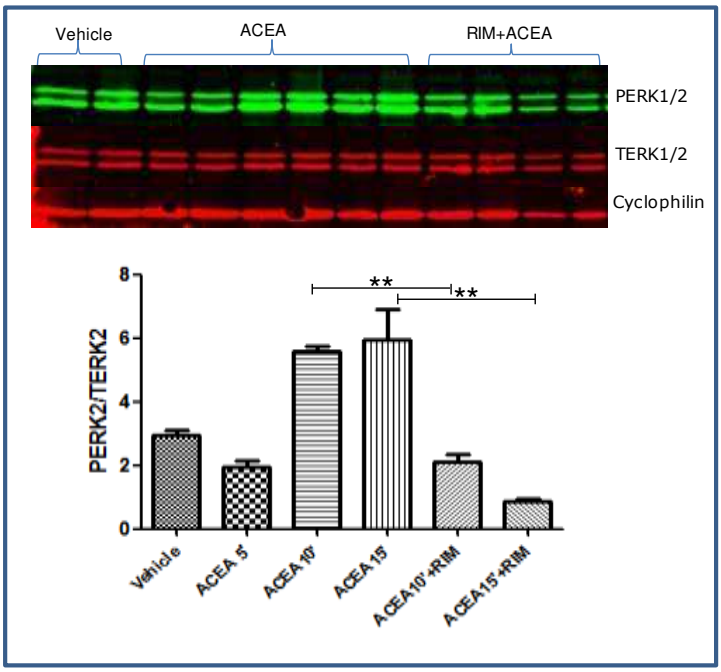

Figure 4-20: Representative blot showing the effect of 10nM ACEA and 100nM RIM (30min prior) on ERK phosphorylation in ZLR myotubes.
Quantified values of PERK2/TERk2 are shown in the lower panel (* denotes P<0.05 compared to vehicle and ** denotes P<0.01 compared to ACEA +RIM). Data were analysed by one way ANOVA with Bonferroni post-hoc test. Cyclophilin was used as a loading control.Phospho ERK1/2 (PERK) is shown in green band and total ERK1/2 (TERK) in red (n=2).

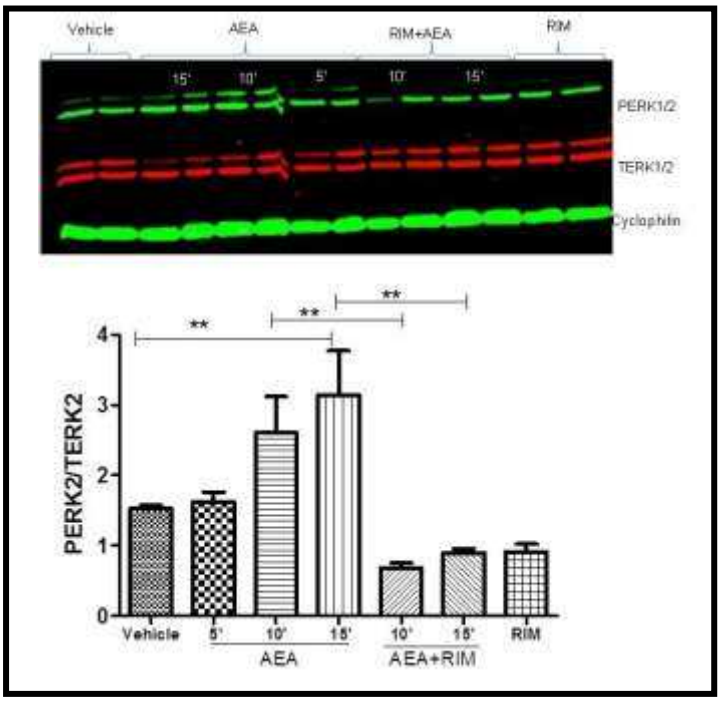

Figure 4-21: Representative blot showing the effect of 10μM ACEA and 100nM RIM (30min pre-treatment) on ERK phosphorylation in ZLR myotubes.
Quantified values of PERK2/TERK2 are shown in the lower panel (** denotes P<0.01 compared to vehicle and ACEA +RIM). Data were analysed by one way ANOVA with Bonferroni post-hoc test. Phospho ERK1/2 (PERK) is shown in green band and total ERK1/2 (TERK) in red. Cyclophilin used as a loading control (n=2)

In ZFR, the time course treatment with 10nM ACEA showed time dependent increase in ERK phosphorylation with a significant peak at 15 min ($P<0.05$) compared to vehicle (0.01% ethanol) (Figure 4-22A). Similarly, treatment of ZFR myotubes with 10 μM AEA induced a time dependent increase in ERK1/2 phosphorylation with a significant peak at 10min compared to vehicle ($P<0.05$) (Figure 4-22B). Interestingly, pre-treatment of ZFR myotubes with 100nM RIM did not inhibit ERK1/2 phosphorylation induced by ACEA (Figure 4-22C).

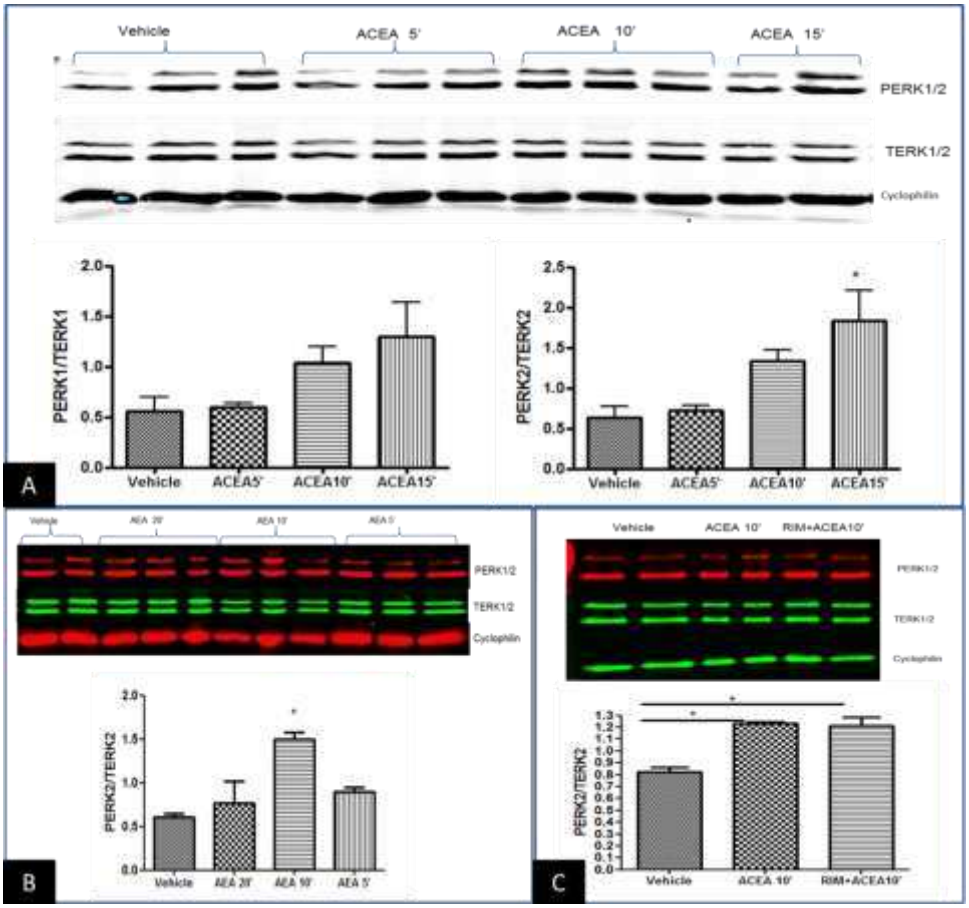

Figure 4-22: Representative blots showing the effect of 10μM ACEA, 10μM AEA and 100nM RIM (30min prior) on ERK phosphorylation in ZFR myotubes in upper panels.
Quantified values are shown in the lower panels (n=2). A) Time course treatment with 10 nM ACEA (* denotes $P<0.05$ compared to vehicle). B) Time course treatment with 10 μM AEA (* denotes $P<0.05$ compared to vehicle) C) Pre-treatment with 100nM RIM(* denotes $P<0.05$ compared to vehicle. Data were analysed by one way ANOVA with Bonferroni post-hoc test. Phospho ERK1/2 (PERK) is shown in red band and total ERK1/2 (TERK) in green. Cyclophilin was used as a loading control.

4.5.6. Effect of ACEA on MAPK38 (p38 MAPK) phosphorylation

As MAPK38 is another key signalling protein which can play a role in insulin resistance (Koistinen et al. 2003), the activation of the CB1 receptor with 10nM ACEA on MAPK38 was studied. Treatment of Wistar rat myotubes with 10nM ACEA induced MAPK38 phosphorylation at 5min ($P<0.05$) compared to vehicle (0.01%ethanol) followed by reduction at 15min (Figure 4-23). The molecular weight of Phospho and total MAPk38 were detected at 43KDa.

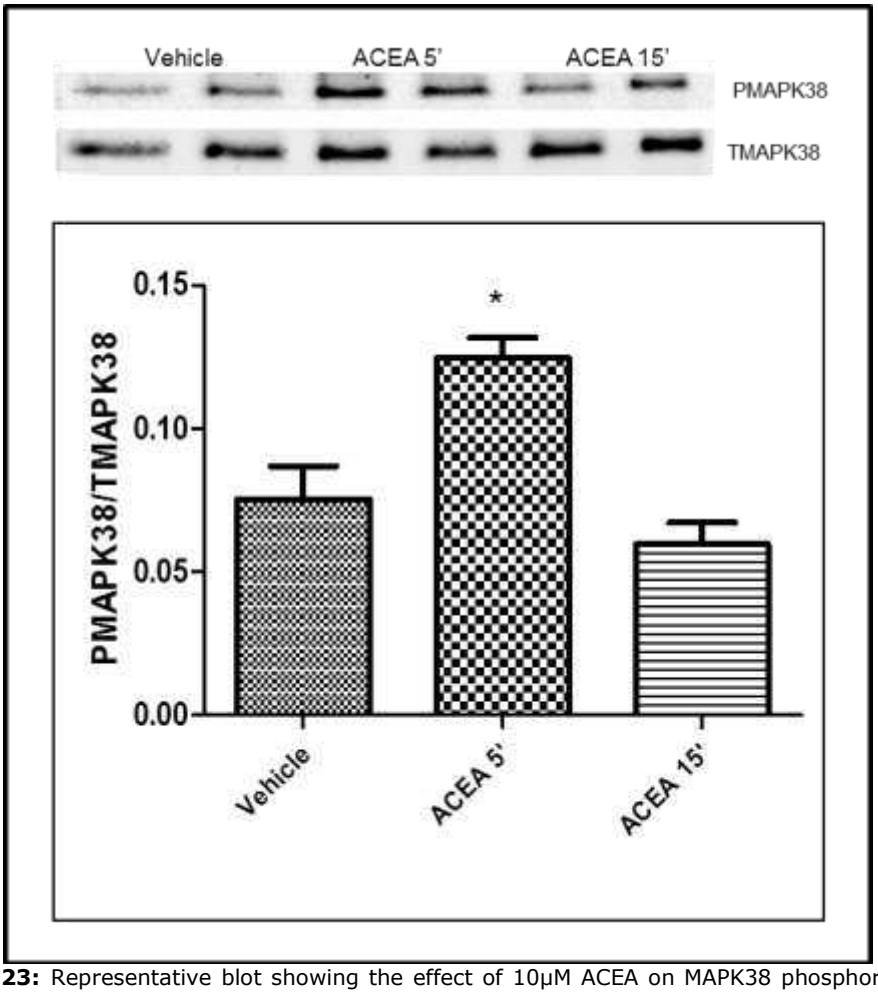

Figure 4-23: Representative blot showing the effect of 10μM ACEA on MAPK38 phosphorylation in rat myotubes.
Quantified values of PMAPK38/TMAPK38 are shown (* denotes $P<0.05$ compared to vehicle and ACEA 15'). Data were analysed by one way ANOVA with Bonferroni post-hoc test (n=2).

4.5.7. Effect of ACEA and RIM on insulin stimulated AKT phosphorylation

As AKT is a key protein in insulin signalling, AKT phosphorylation following acute insulin (100nM for 10 min) stimulation of Wistar rat myotubes which had been pre-treated with either 100nM ACEA or 100nM RIM for 24 hours was studied. Pretreatment with ACEA and RIM had no significant effect on insulin induced AKT phosphorylation (Figure 4-23). The molecular weight of the bands of Phospho AKT and Total AKT were detected at 62 KDa.

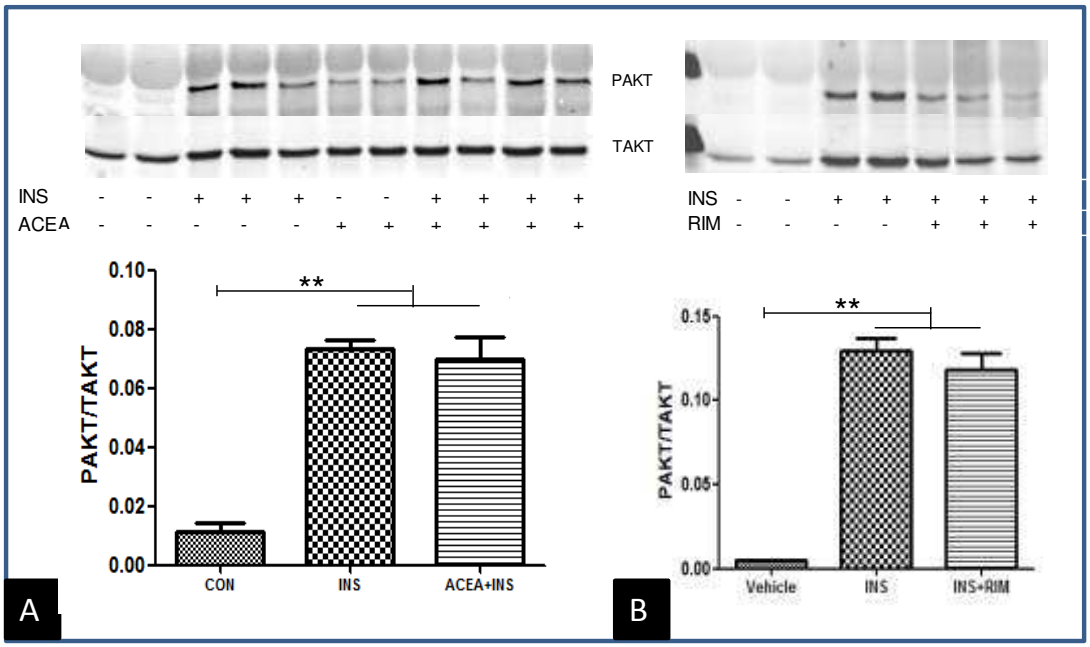

Figure 4-24: Representative blot showing the effect of 24 hours treatment with 100 nM ACEA and RIM on insulin stimulated AKT phosphorylation in Wistar rat myotubes.
Quantified values of PAKT/TAKT are shown in lower panels A) Pre-treatment (24 hours) of myotubes with 100nM ACEA ** denotes P<0.01 compared to vehicle (0.01% ethanol). B) Pre-treatment (24 hours) of myotubes with 100nM RIM *** denotes P<0.001 compared to vehicle. Data were analysed by one way ANOVA with Bonferroni post-hoc test (n=2).

4.5.8. Effect of ACEA and RIM on insulin stimulated GSK3α and GSK3β phosphorylation

As GSK is a direct target for Akt that regulates glycogen synthesis (Lindborg et al. 2010), investigation of GSK3α and GSK3β phosphorylation

under acute insulin stimulation after treatment with ACEA and Rim was carried out. Pretreatment (24hours) with 100nM ACEA and 100 nM RIM had no significant effect on insulin induced GSK3α and GSK3β phosphorylation (Figure 4-25). The molecular weight of the bands of phospho and total GSK3α and GSK3β were detected at 51 and 46 KDa, respectively.

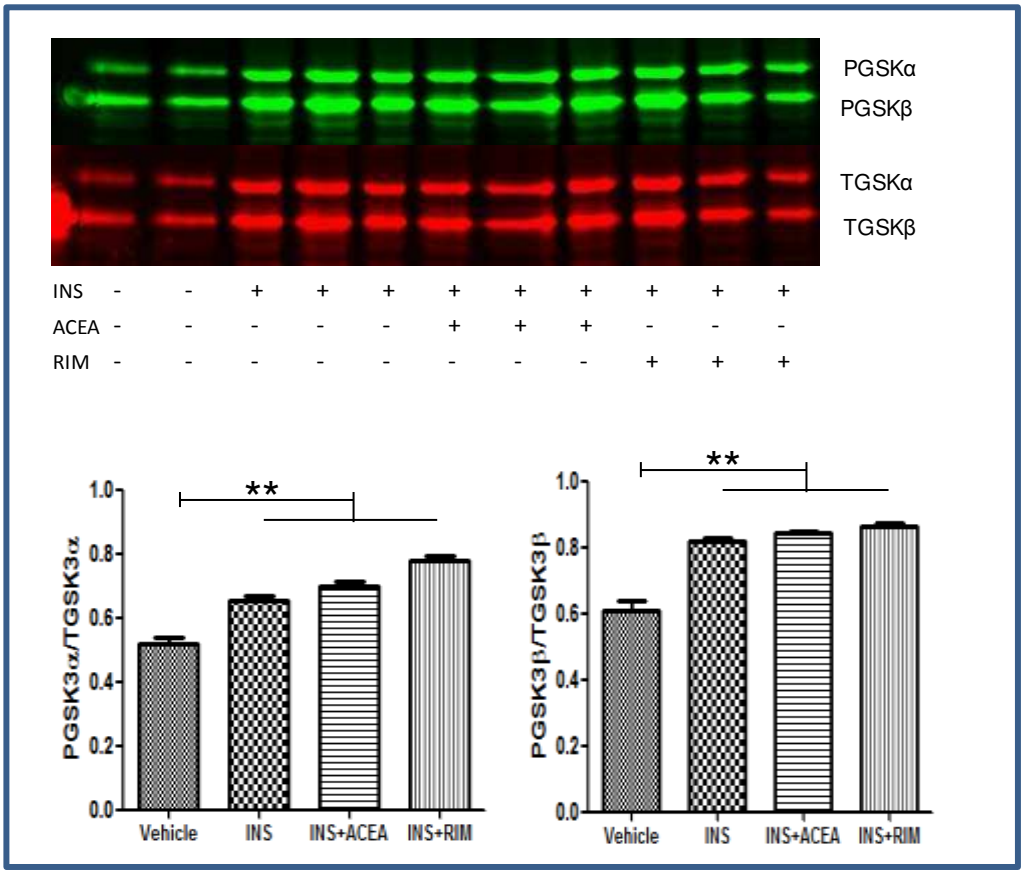

Figure 4-25: Representative blot showing the effect of 24 hours treatment with 100 nM ACEA and RIM on insulin stimulated GSK3α and GSK3β phosphorylation in Wistar rat myotubes.
Quantified values of PGSK3α/TGSK3α and PGSK3β/ TGSK3β are shown in lower panels. ** denotes $P<0.01$ compared to vehicle (0.01% ethanol). Data were analysed by one way ANOVA with Bonferroni post-hoc test (n=2).

4.5.9. Effect of ACEA and RIM on insulin stimulated ERK phosphorylation

Previous data in this Chapter showed activation and inhibition of ERK phosphorylation by CB1 receptor agonists and antagonists, respectively. A 24 hour incubation of Wistar rat myotubes with 100 nM ACEA or 100nM RIM prior to

administration of 100nM insulin for 10 min did not alter insulin induction of ERK phosphorylation (Figure 4.26).

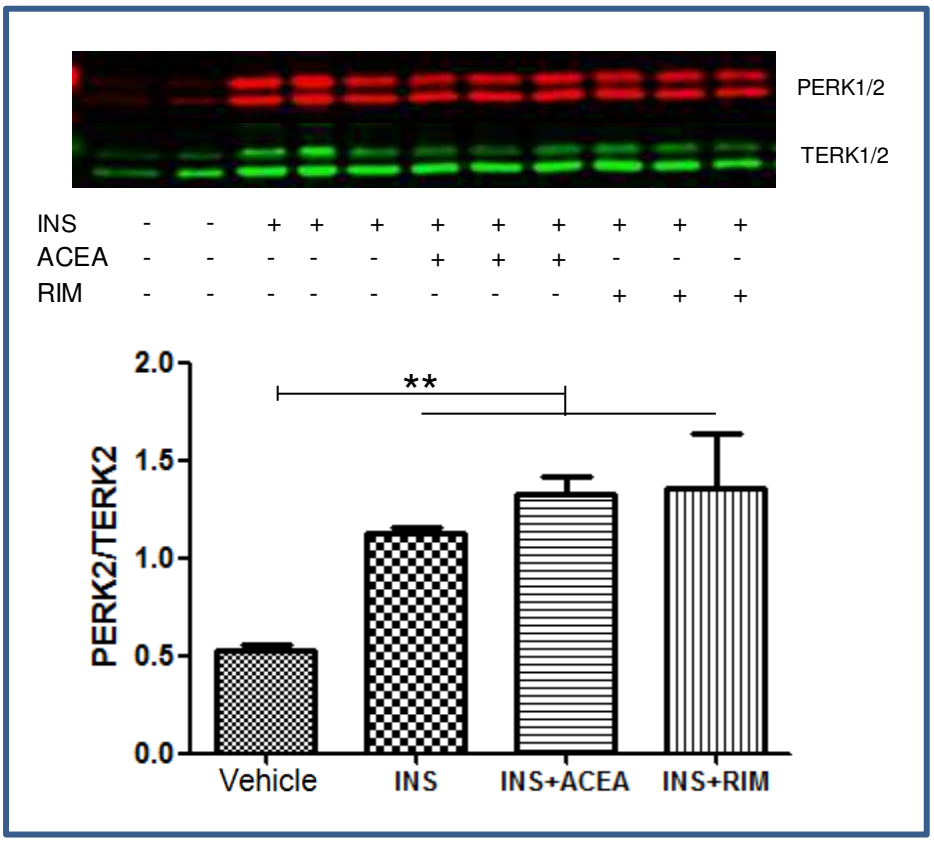

Figure 4-26: Representative blot showing the effect of 24 hours treatment with 100 nM ACEA and RIM on insulin stimulated ERK1/2 phosphorylation in Wistar rat myotubes.
Quantified values of PERK2/TERK2 are shown in lower panels. ** denotes P<0.01 compared to vehicle (0.01% ethanol). Data were analysed by one way ANOVA with Bonferroni post-hoc test (n=2).

4.5.10. Effect of ACEA and RIM on insulin stimulated MAPK 38 phosphorylation

In order to investigate the possible signalling pathways that might be involved in skeletal muscle insulin resistance, the effect of 24 hours incubation of Wistar rat myotubes with 100nM ACEA and 100nM RIM on insulin-induced MAPK38 phosphorylation was examined. 100nM ACEA in the presence or absence of insulin led to significantly higher phosphorylation of MAPK38 (P<0.01) compared to vehicle (0.01% ethanol). Insulin also induced significant

MAPK38 phosphorylation (P<0.05) compared to vehicle (0.01% ethanol) (Figure 4-27).

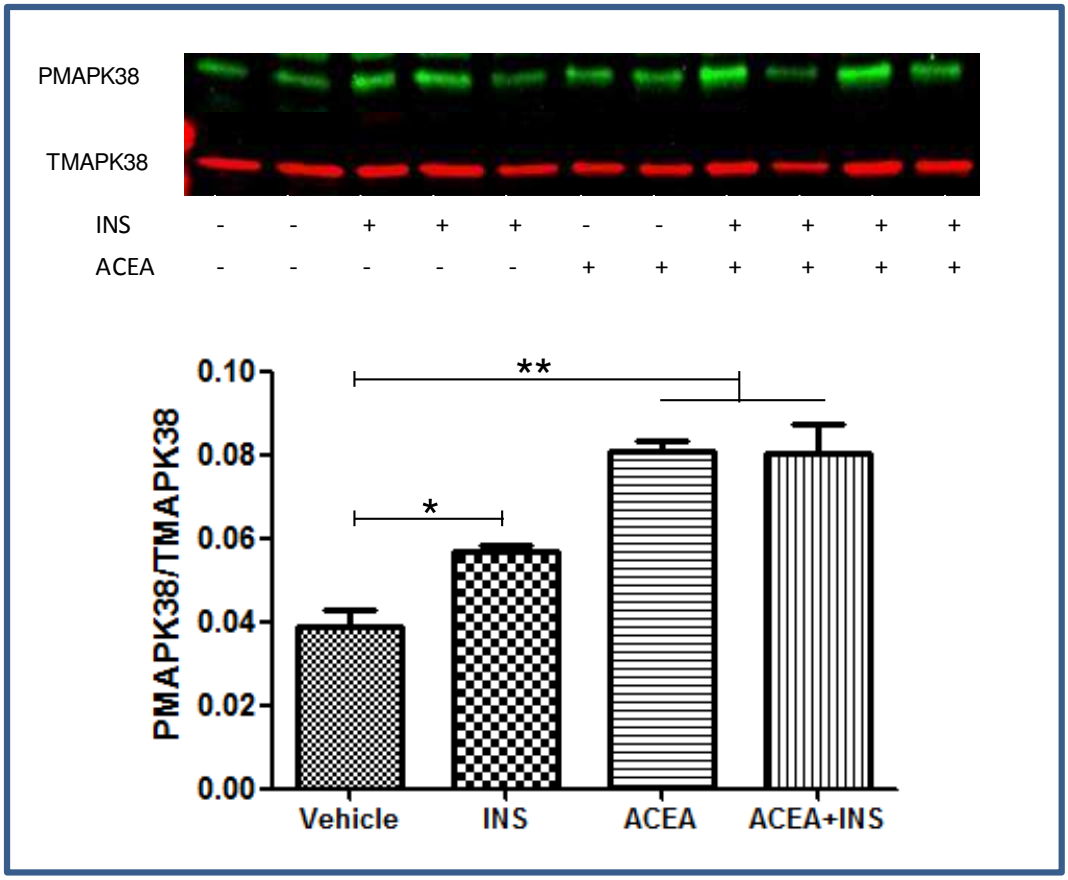

Figure 4-27: Representative blot showing the effect of 24 hours treatment with 100 nM ACEA and RIM on insulin stimulated MAPK38 phosphorylation in Wistar rat myotubes.
Quantified values of PMAPK38/TMAPK38 are shown in lower panels. * denotes P<0.05 and ** denotes P<0.01 compared to vehicle (0.01% ethanol). Data were analysed by one way ANOVA with Bonferroni post-hoc test (n=2).

4.5.11. Effect of Pertussis Toxin (PTX) on ERK phosphorylation induced by ACEA

It is well documented that the cannabinoid receptors are coupled to Gi/o protein, although recently some studies suggested the possible coupling to Gq / 11 (Dalton et al. 2009)(Matias et al. 2008). In this study, pretreatment of Wistar rat myotubes with the Gi/o inhibitor (50 nM PTX) for 30 min did not block the stimulatory effect of 10 nM ACEA on ERK phosphorylation (Figure 4-28).

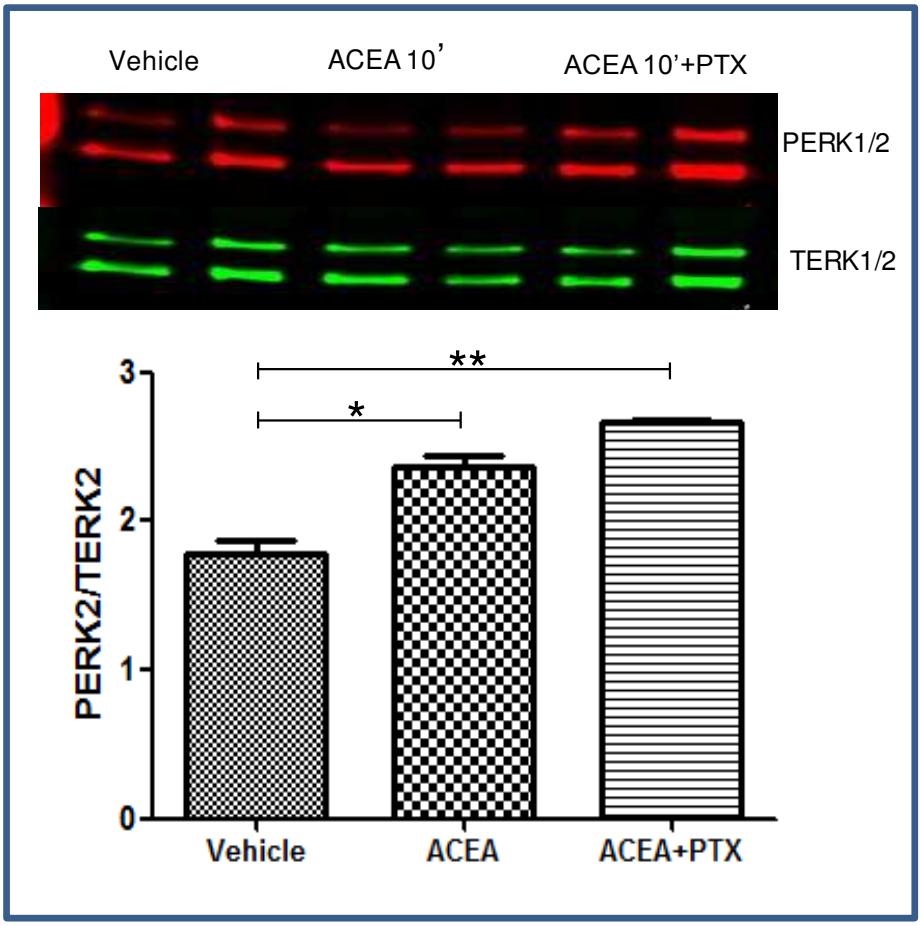

Figure 4-28: Representative blot showing the effect of 50 nM Pertusis Toxin (PTX) on ERK phosphorylation induced by 10nM ACEA in Wistar rat myotubes.
Quantified values of PERK2/TERK2 are shown in lower panels. * denotes P<0.05 and ** denotes P<0.01 compared to vehicle (0.01% ethanol). Data were analysed by one way ANOVA with Bonferroni post-hoc test (n=3).

4.5.12. Effect of CB1 receptor activation on cell proliferation

CB1 receptor activation has been reported to play an important role in cellular proliferation and differentiation (Wang et al. 2004). Incubation of 10-day myoblasts with 10nM ACEA or Vehicle (0.01% ethanol) for 24 hours showed a 2-fold increase in cell number in ACEA treated myoblasts when compared to vehicle (Fig 4.29). The percentage of Ki67 positive cells was 73.9% in ACEA treated cells and 48.3% in vehicle suggesting that ACEA increases cellular proliferation in myoblasts.

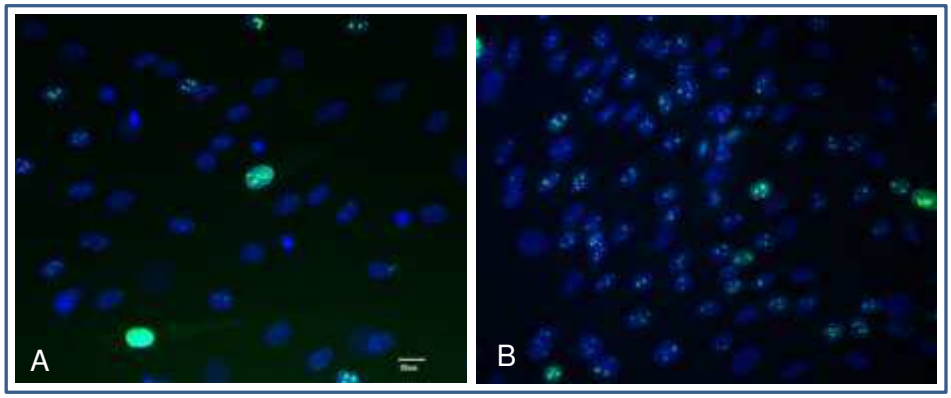

Figure 4-29: Ki67 immunofluorescence in myoblasts obtained from VL Wistar rats.
A) Cells were treated with vehicle (0.01% ethanol). B) Cells were treated with 10nM ACEA. Images were taken at 40x magnification. Scale bar 20µm. Ki67 green and DAPI blue (n=3).

4.5.13. Glucose transporters in skeletal muscle tissue and cultured cells

In this study immunofluorescence of GLUT4 in Wistar rat skeletal muscle cultured cells showed that treatment of myotubes with 100nM insulin for 10 min did not induce significant changes in GLUT4 cellular distribution between insulin and vehicle (0.01% ethanol) treated cells. Interestingly, a low level of recruitment of GLUT4 to the cell membrane was observed in some undifferentiated myoblasts (Figure 4-30C). Time course treatment (5, 10, 30 min) of rat myotubes with 100nM insulin in presence or absence of 10nM ACEA (24hours incubation prior to insulin) demonstrated no significant difference in GLUT4 cellular distribution compared to vehicle (data not shown). It is worth mentioning that the human microarray data presented in Chapter 3 showed a high level of GLUT1 (SLC2A1) expression in myoblasts and myotubes compared to muscle tissue (Table 4.6). In contrast, GLUT4 (SLC2A4) expression was much higher in tissue compared to myoblasts and myotubes (Table 4-6).

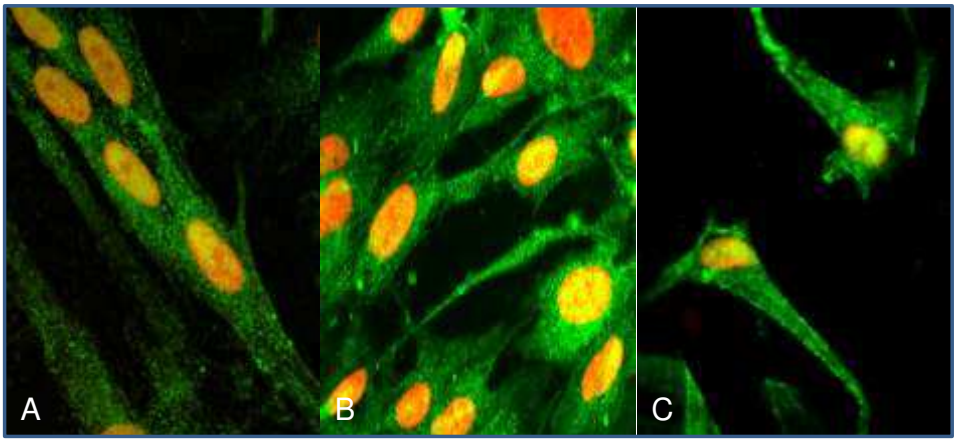

Figure 4-30: GLUT 4 immunofluorescence in Wistar rat myotubes and myoblasts.
A) Myotubes treated with vehicle (0.01% ethanol). B) Myotubes treated with 100nM insulin. C) Myoblasts treated with 100nM insulin. Images were taken at 64x magnification. Scale bar 40µm. GLUT4 green fluorescent and DAPI red fluorescence (n=3).

Table 4-6: Glucose transporters in human skeletal muscle tissue and cultured cell.

Gene Symbol	Rank			Intensity			Fold Change			Description
	MB	MT	TIS	MB	MT	TIS	MB vs MT	MT vs TIS	MB VS TIS	
SLC2A1	2709	2980	21461	3.6	3.1	-3.3	2.4	87.1	121.2	Homo sapiens solute carrier family 2 (facilitated glucose transporter), member 1 (SLC2A1), mRNA [NM_006516]
SLC2A4	35015	32232	1719	-7.8	-6.8	4.7	#N/A	-3329.2	-6342.5	Homo sapiens solute carrier family 2 (facilitated glucose transporter), member 4 (SLC2A4), mRNA [NM_001042]

MB=myoblast, MT=myotube, TIS=tissue, FC=fold change & N/A=no difference

4.6. Discussion

4.6.1. Characterisation of cannabinoid receptors.

Skeletal muscle is one of the major insulin sensitive organs and it is responsible for 80% of insulin stimulated glucose disposal. Even though high circulating levels of endocannabinoids have been reported in obese and diabetic individuals, their tissue expression levels and the link between cannabinoid receptors and insulin signalling in skeletal muscle (skeletal muscle) are still controversial (Bensaid et al. 2003; Pagotto et al. 2006; Lindborg et al. 2010). The aim of this study was to characterize the cannabinoid receptors CB1 and

CB2 and identify their role in cell signalling in human and rat skeletal muscle tissue and primary cultured skeletal muscle cells. The expression and functionality of other potential cannabinoid-related receptors, GPR 119 and GPR55 was also investigated.

The microarray analysis performed in Chapter 3 indicated the expression of CB1 and CB2 receptors as well as FAAH, MGLL, DAGLA, DAGLB and NAPE-PLD in human skeletal muscle tissue and primary cultured myoblasts and myotubes indicating that this expression is muscle specific and not the result of contaminating adipocytes or other infiltrating cell types. However, the levels of cannabinoid receptor mRNA detected by microarray was extremely low and provided no direct evidence that functional CB1 or CB2 receptors were present. This is further complicated by the fact that antibodies used to detect CB receptors in immunohistochemistry or western blots are notoriously unreliable and often give false positive results (A. Bennett, unpublished observations). QRT-PCR analysis, which is considerably more sensitive than microarray, performed in this Chapter confirmed the expression of CB1 at the mRNA level in both human and rat muscle tissues and cultured cells in agreement with Eckardt et al. (2009) and Cavuoto et al. (2007). Furthermore, human myoblasts and skeletal muscle tissue had higher CB1 expression than myotubes. In rat, a trend for a higher level of CB1 expression in fast muscles (EDL and GW) compared to slow muscles (SOL and GR) was observed which essentially agrees with results observed in a study investigating CB1 expression in different frog muscle types (Huerta et al. 2009). The QRT-PCR findings from the present study also revealed CB2 mRNA expression in rat skeletal muscle tissue and cultured cells in agreement with Cavuoto et al. (2007). Interestingly, human CB2 mRNA expression was considerable in 100% myoblasts, whereas it decreased in myotubes and was undetected in muscle tissues.

The presence of GPR119 was observed in human skeletal muscle tissue and cultured cells using both microarrays and QRT-PCR. This is an important finding as only one previous study reported the presence of GPR119 in human skeletal muscle using Northern blot (Soga et al. 2005). GPR119 mRNA expression was also detected in various rat tissues (brain, spleen, pancreas, and skeletal muscle), which is in agreement with Bonini et al. (2001) & Bonini et al. (2002). The present study is the first to investigate the presence of GPR119 in skeletal muscle cultured cells in an attempt to identify its role in cell development and signalling cascade. Even though the microarray analysis detected the expression of GPR55 in human skeletal muscle tissue and cultured cells, RT-PCR analysis failed to detect the presence of GPR55 in both human and rat skeletal muscle tissue and cultures cells. The expression of GPR55 proteins in rat skeletal muscle tissue and GPR55 mRNA in C2C12 has been reported by Simcocks et al. (2011) and Roy et al. (2010), respectively.

High levels of circulatory endocannabinoids are well documented in obese and diabetic subjects (Serrano et al. 2008). However, the presence and role of Skeletal muscle CB1 receptors in obesity and diabetes is poorly described. Pagotto et al. (2006) reported a high level of mRNA CB1 expression in soleus muscles from mice fed a high fat diet whereas Lindborg et al. (2010) observed a low CB1 protein expression in SOL from ZFR. The adipose tissue CB1 mRNA expression was upregulated in obese Zucker fat rats compared to lean littermates (Vickers et al. 2003; Pagano et al. 2007; Bensaid et al. 2003). In contrast Engeli et al. (2005) and Blüher et al. (2006) demonstrated a down regulation of CB1 mRNA in adipose tissue taken from obese subjects. High levels of CB1 mRNA and protein were observed in renal cortex of diabetic mice when compared with nondiabetic control animals (Barutta et al. 2010). In the present study, the expression levels of CB1, CB2 and GPR119 in muscle, liver, heart,

spleen and adipose tissues were similar between 12 week old Zucker Fat Rats (ZFR) and Zucker Lean Rats (ZLR), however at 20 weeks ZFR muscle and adipose tissues had a significantly higher expression of CB1 than ZLR. GPR119 is a potential cannabinoid receptor that might play a role in glucose homeostasis by two ways; firstly by stimulating insulin release from the β cells of the pancreas and secondly through the release of antihyperglycaemic agents such as glucagon like peptide (GLP) and gastric inhibitory polypeptide (GIP) from enteroendocrine cells (Drucker 2001; Meier et al. 2002; Gromada et al. 2004). In this study the expression of GPR119 in skeletal muscle tissues was higher in Zucker than Wistar rats in contrast to CB1 which has higher expression in Wistar compared to Zuckers, however the difference disappeared in myotubes cultured from the same animal, which indicates that removal of the physiological factors that differentiate the two strains of rat in cultured cells may cause the equalization of GPR119 and CB1 expressions. This hypothesis is supported by the fact that Brozinick, Roberts, & Dohm, (2003), Pender et al. (2005) and Berggren et al. (2005) did not observe a difference in insulin resistance between cultured cells from obese (insulin-resistant patients) and control subjects. Interestingly, muscle, liver and adipose tissues obtained from Wistar rats had significantly higher levels of CB1 (but not CB2) mRNA content than Zucker obese and lean rats. This finding may be due to downregulation of the CB receptors in insulin resistant states caused by elevated endogenous circulating cannabinoids. Down-regulation or reduction of receptor number, apparent shielding of the receptors from interacting ligands, and uncoupling from G-proteins in response to stimulation by cannabinoid ligands have all been previously described (Freedman and Lrfkowitz 1996 & Xiao et al. 1999). Prolonged stimulation generally leads to a significant receptor loss from the cell surface (Gainetdinov et al. 2004).

It is widely assumed that cannabinoid receptors are Gi/o protein coupled (Pertwee & Ross 2002; McAllister & Glass 2002; Matsuda et al. 1990; Dalton et al. 2009; Bellocchio et al. 2008). However Ahn et al. (2012) found that activation of ERK via a CB1 allosteric modulator was Gi independent in HEK293 and neuronal cells. Matias et al. (2008) reported that CB1 and CB2 in RIN-m5F β-cells are Gq / 11 coupled and insensitive to pertussis toxin. Stimulation of cAMP was observed in rat cultured striatal neurons and in CB1 transfected CHO cells in response to activation by the CB1 agonist HU210 suggesting that under certain circumstances, the CB1 receptors can couple to Gs proteins (Glass & Felder 1997; Turu & Hunyady 2010). The interaction of CB1 with Gs was also demonstrated in CHO cells expressing human CB1 (Demuth & Molleman 2006). In the present study PTX had no effect on ACEA stimulated MAPK phosphorylation potentially indicating that CB1 is not Gi/o coupled in skeletal muscle. However, a PTX sensitive GPCR would need to be shown to be sensitive and inhibited by PTX in myotubes in culture in order to be confident that PTX was having no effect on CB1. It is worth mentioning that unpublished data from our laboratory also demonstrated no effect of ACEA, AEA or RIM on cAMP production – if CB1 was Gi/o coupled then CB1 agonists would be expected to decrease cAMP levels. These results indicate that there is specificity between CB1 receptor coupling and tissue type.

4.6.2. Functionality of cannabinoid receptors.

The functionality of CB1 in human and rat cultured cells was assessed by studying the effect of an endogenous (AEA) and a synthetic (ACEA) agonist. As AEA is a nonspecific ligand which may act via a number of receptors including CB1, CB2 and TRPV1 (Matias et al. 2008; Cavuoto et al. 2007), ACEA was also used as it is a CB1 selective agonist (Hillard et al. 1999; Pertwee & Howlett

2010). In this study, treatment of human and rat myotubes with AEA and ACEA increased ERK1/ERK2 and p38 MAPK phosphorylation. Increased phosphorylation of MAPK by AEA and ACEA was previously reported by Eckardt et al. (2009) and Tedesco et al. (2010). Interestingly, treatment with a CB1 selective antagonist (RIM) attenuated the ERK activation induced by AEA and ACEA in cells obtained from Wistar and ZLR but not ZFR. This may indicate that CB1 agonists signalling are altered in ZFR derived cells, or that antagonists are for some reason ineffective. Previous studies indicate that CB1 antagonist AM251 was in fact more effective in high fat diet fed and/or obese rats than in lean controls, which is in potential contrast to our data (Bellocchio et al. 2008). Furthermore, rimonabant has been previously described as having a more pronounced effect upon glucose uptake in skeletal muscle myotubes obtained from obese as compared to lean individuals (Cavuoto 2010) However, the same study reported no effect of either RIM or AEA upon ERK phosphorylation. It is possible that the effects of endocannabinoid signalling upon ERK signalling are unrelated to their metabolic effects and rather, are associated with cell proliferation or differentiation (Roux & Blenis 2004). The disappearance of RIM effect on ZFR needs further investigation in terms of effects on metabolic gene expression and cell proliferation.

To further investigate the role of CB1 receptor activation in the acute modulation of insulin signalling in rat and human myotubes, the effects of CB1 agonists and antagonists on key proteins in the insulin signalling cascade were studied. Previous findings in the literature regarding the role of the cannabinoid receptor activation or inhibition on AKT are controversial. Eckardt et al. (2009) found that AEA impaired insulin-stimulated AKT (but not GSK3α/β) phosphorylation and pre-treatment with RIM completely abolished the AEA effect in human primary cultured cell. However Lindborg et al. (2010) reported that neither CB1 receptor

agonists nor antagonists altered Akt and GSK3β phosphorylation in soleus muscle from lean and obese Zucker rats. Song et al. (2011) reported that the CB1 agonist HU210 induced insulin resistance in muscle of wild-type C57BL/6 mice through inhibition of AKT phosphorylation which was prevented by pretreatment with the CB1 antagonist AM251. Esposito et al. (2008) also demonstrated that RIM increased AKT phosphorylation and glucose uptake in L6 skeletal muscle cells. Pharmacological activation or inhibition of CB1 receptor activity exerts a differential effect with regard to MAP kinase and PKB-directed signalling in L6 module (Lipina et al. 2010). In this study, neither ACEA nor RIM affected insulin-stimulated phosphorylation of Akt or GSK3α/β, indicating that modulation of CB1 receptor in skeletal muscle cultured cell does not have a role in insulin signalling. The discrepancy between this study and some earlier studies may be due to the different time point and the cell model. This can be due the difference in; concentration and duration of treatment with RIM as this study used 100nM for 30 min while Eckardt et al. (2009) used 1 μmol/l Rim for 2hrs; difference in treatment as this study used ACEA and RIM while Song et al. (2011) used HU210 and AM251; and different in cell types as Wistar skeletal muscle primary cultured cells were used in the current study while human skeletal muscle cultured cells were used in Eckardt et al. (2009) study and L6 module was used in Lipina et al. (2010b) and Esposito et al. (2008) studies. Moreover, none of the previous studies used free fatty acid free serum in culture medium prior to the treatments.

Transport instead of phosphorylation of glucose may be the rate limiting process in the uptake of glucose by cultured human muscle cells (Jacobs et al. 1990)(Perriott et al. 2001). The role of CB1 inhibition in glucose uptake was reported by Esposito et al. (2008) who found that RIM increased glucose uptake in L6 cells and Liu et al. (2005) who observed similar findings in soleus muscle

isolated from female Lep^{ob}/Lep^{ob} mice treated with RIM. It was suggested that RIM increased glucose uptake in soleus muscle through the GLUT1 glucose transporter as a low dose of insulin (10nM) was used. In the present study immunofluorescence of GLUT4 in rat skeletal muscle cultured cells showed that treatment of rat myotubes with 100nM insulin in the presence or absence of ACEA (24hours incubation prior to insulin) resulted in no difference in GLUT4 cellular distribution compared to vehicle. This result may be due to the low level of GLUT4 expression and the high level of GLUT1 expression observed in culture in Chapter 3 and previous studies in the literature (Bouché et al. 2004; Jackson et al. 2000; Al-Khalili et al. 2003). A slight recruitment of GLUT4 to cell membrane was observed in some undifferentiated myoblasts in line with a previous study by Jackson et al. (2000) who reported that the greatest stimulatory effect of insulin on glucose uptake was seen in myoblasts, and this was diminished after myoblast fusion and disappeared in fused myotubes. Photolabelling of cell surface glucose receptors is recommended for better visualization (Ijuin & Takenawa 2012; Al-Khalili et al. 2003). Insulin-dependent GLUT4 exocytosis includes several steps, including recruitment, docking and/or fusion of GLUT4-containing vesicles to the plasma membrane (Sakamoto & Holman 2008). GLUT4 exocytosis in the skeletal muscle cells is dependent on the actin cytoskeletal rearrangement occurring at the membrane ruffles (Saltiel & Kahn 2001). This indicates that not only a reduction of GLUT4 content but also a decrease in the expression of genes involved in cytoskeletal rearrangement, as observed in chapter 3, might explain the inability of insulin to affect GLUT4 cellular distribution compared to vehicle in the present study.

GPCR receptors are associated with cell lineage development and play an important role in cellular proliferation and differentiation (Wang et al. 2004). The role of CB1 in adipogenesis and neurogenesis has been reported by Matias et al.

(2008), Pagano et al. (2007) and Jin et al. (2004). Gary-bobo et al. (2006) reported that RIM can lead to a decrease in cell proliferation in mouse 3T3 cells. In this study the role of the synthetic CB1 agonist ACEA was investigated in skeletal muscle cells proliferation using the proliferation marker Ki67. This well-established proliferation marker has a distinctive distribution pattern that exclusively identifies proliferating cells (Kumai et al. 2007). Even though Ki67 is constantly present in cell cycling, its pattern of expression is variable. Depending on the stage of the cell cycle, it might appear in the small nuclei, nuclear area or disappear in resting cells as well as terminally differentiated cells (Ross & Hall 1995). The results from the present study showed that CB1 activation leads to increased expression of nuclear Ki67, indicating an increase in myoblast proliferation.

In conclusion, the expression of the CB1 cannabinoid receptor in skeletal muscle has been confirmed at the mRNA level in skeletal muscle tissue and in cultured cells. Expression of GPR119 was also confirmed in both tissue and cell cultured whereas CB2 was only found in cell culture and GPR55 expression was not detected in either tissue or cells. Subsequent studies using CB1 agonists and antagonists demonstrated that activation of CB1 robustly induced ERK and p38 MAPK phosphorylation which was inhibited by the specific antagonist rimonabant. These data demonstrate functional expression of CB1 in skeletal muscle tissue culture. The inability of rimonabant to inhibit CB1 agonist mediated ERK phosphorylation suggests altered ECS signalling in obesity however this finding requires further investigation. This study, in contrast to previous work, did not find any evidence that CB1 activation or inhibition influenced insulin signalling or glucose uptake in skeletal muscle. However the levels of proteins involved in insulin signalling and glucose uptake (in particular Glut4) are drastically reduced in cultured cells as compared to tissue and this

may account for the lack of effect of cannabinoids to influence insulin signalling and glucose uptake in this model. Further refinement of the cell culture model is needed to promote a more adult phenotype, turn on oxidative phosphorylation and increase insulin sensitive glucose uptake. A potential role for CB1 in promoting myoblast proliferation was identified – possibly involving activation of ERK signalling. Further studies looking at the effects of CB1 receptor agonists and antagonists upon markers of cell proliferation and differentiation are warranted.

CHAPTER FIVE

MOLECULAR CHARACTERISATION OF FREE FATTY ACID RECEPTOR IN SKELETAL MUSCLE

CHAPTER 5. MOLECULAR CHARACTERISATION OF FREE FATTY ACID RECEPTOR 1 (GPR40) IN SKELETAL MUSCLE

5.1. Introduction

Free fatty acids (FFAs) have been implicated in the pathogenesis of insulin resistance however the molecular mechanism by which FFAs reduce insulin sensitivity is not fully understood. Since the Randle hypothesis (excessive FFAs reduce glucose oxidation due to substrate competition) was published 40 years ago, a number of subsequent theories have been put forward to explain the role of fatty acids in the development of insulin resistance (Costanzi et al. 2008). Roden et al. (1996) suggested that inhibition of glucose transport or its phosphorylation is the main reason of insulin resistance. Tsintzas et al. (2007) and Chokkalingam et al. (2007) addressed the role of PDK4 in skeletal muscle insulin resistance induced by high FFAs. Saturated fatty acids were demonstrated to affect insulin intracellular signalling pathways in skeletal muscle and myocytes (Thompson AL et al. 2000; Yu et al. 2002). Various PKC isoforms have been shown to be involved in lipid-induced insulin resistance in skeletal muscle (Griffin et al. 1999). The role of inflammatory cytokines in insulin resistance induction have been also postulated (Sell et al. 2006; Martins et al. 2012). More recently, deorphanization of free fatty acid receptors {GPR40 (FFAR1), GPR120, GPR84, GPR42 & GPR43} provided an alternative molecular target for FFA, however the exact role of these receptors is still under investigation and little is known about their functionality in skeletal muscle. GPR40 is a promising target for diabetes treatment. It mainly binds to GPRq and weakly binds to Gi/o (Itoh et al. 2003; Kotarsky et al. 2003) and is activated by medium to long chain saturated and unsaturated fatty acids. GPR40 is expressed in a variety of tissues including β cells of the pancreas, brain, monocytes,

splenocytes, intestinal tract, skeletal muscle, liver and heart (Kotarsky et al. 2003; Swaminath 2008; Ichimura et al. 2009; Briscoe & Tadayyon 2003). The binding of FFA and esterified forms of FAs (Stewart et al. 2006) to GPR40 in β cells leads to phospholipase c activation which is followed by calcium release, activation of MAPK and increased insulin secretion (Ichimura et al. 2009; Overton et al. 2008). The activation of GPR40 receptors and the release of insulin is a glucose dependent process, GPR40 activation increases intracellular Ca^{2+} levels primarily via the coordinated enhancement of extracellular Ca^{2+} influx through LTCC and inhibition of K_{ATP} channels by glucose as well as stimulation of calcium release from endoplasmic stores through Gq-PLC signalling pathway (Feng et al. 2006; Shapiro et al. 2005). It is well documented that the acute effect of FFA in β cells is different from the chronic effect as the former leads to insulin secretion and the latter leads to impairment in β cell function and apoptosis (Swaminath 2008). As previously discussed in the general introduction chapter, the potential involvement of GPR40 in β cell glucolipotoxicity has been studied in $GPR40^{-/-}$ and GPR40 transgenic overexpression mice but the result was controversial. Steneberg et al. (2005), Brownlie et al. (2008) and Duttaroy et al. (2008) reported that GPR40 mediates both acute and chronic effects of FFA on insulin secretion. In contrast, Nagasumi et al. (2007), Latour et al. (2007), Tsujihata et al. (2011), Brownlie et al. (2008), Wu et al. (2010) and Tan et al. (2008) indicated that the lipotoxic effect of FFA is not mediated by GPR40 receptors. Authors account for these discrepancies in the GPR40−/− mouse genetic back ground, type of foods and duration of feeding. Whilst a considerable amount of work has been carried out examining the role of GPR40 in the pancreas, the mechanism of action and physiological role of GPR40 in skeletal muscle is largely unknown.

5.2. Aims

The main objectives of this study are:

- To confirm the presence of GPR40 receptors in human and rat skeletal muscle tissues and primary skeletal muscle cell culture.
- To compare the level of GPR40 receptor mRNA expression between Zucker Leans, Zucker Fat and Wistar rats in different muscle types.
- To establish the functionality of GPR40 receptor and to determine whether activation or inactivation of GPR40 receptors may have a role to play in insulin resistance.
- To compare gene expression profiles in human primary skeletal muscle cells in response to the GPR40 agonists and antagonists using DNA microarray.

5.3. Experiment design and methods

5.3.1. Sample collection and preparation

Human vastus lateralis samples were collected and divided into two parts, first part snap frozen in liquid nitrogen and the second part was used for isolation and culture of satellite cells (chapter 2 section 2.3)

Wistar, Zucker lean and fat rats skeletal muscle tissues were collected from slow (SOL & GR), fast (EDL & GW) and mixed (VL) muscle. liver, epididydmal adipose, spleen, pancreas and heart tissues were also collected and snap frozen in liquid nitrogen. Isolation and culture of satellite cells was carried out using the different muscle tissue types from both Wistar and Zucker rats.

Total RNA, mRNA, cDNA and protein preparation was performed as described in chapter 2 section 2.6.

5.3.2. QRT-PCR

Quantitative Taqman PCR was performed in the step one plus real –time PCR system (Applied Biosystems). Standard protocol as described in chapter 2 section 2.6.5 was followed. Normalization was carried out by using TATA binding protein (TBP) and RPLPO as invariant reference genes.

5.3.3. Microarray

5.3.3.1. Expirement design, procedure and data processing

Human myotubes were cultured until confluent and then incubated with 100nM AZ921 (GPR40 agonist), 5μM AZ836 (GPR40 antagonist in horse or fatty acid free serum) and AZ921+AZ836 for 24 hrs. DMSO 0.001% was used as a vehicle. Five replicates were used for each treatment condition and four replicates for the vehicle.

The cells were lysed with Trizol then total RNA was extracted and cleaned up as described in chapter 2 section 2.6. The integrity of the RNA was assessed using an Agilent Bioanalyzer. All samples subjected to microarray experiment had a RIN value greater than 8 (Appendix 5).

Whole-genome Human GeneChip HT PM Array (HG_U133+PM) was used to detect the global changes in gene expression in response to different conditions. Synthesis of labelled cRNA, hybridization and scanning of microarray were performed by Nottingham Arabidopsis Stock Centre staff according to the manufacturer's protocols (Affymetrix, Santa Clara, CA).

5.3.3.2. Data preprocessing

The RMA (Robust Multichip Averaging) was used for preprocessing. RMA corrects arrays for background using transformation, quantile normalization based on a normal distribution and then estimation of expression values on a log scale (Allison et al. 2006) .

A) Background correction on affymetrix is based on the distribution of the perfect match (PM) values among probes. The Affymetrix software computes a background-corrected intensity by subtracting the probe background signal from the estimated all probes median background intensity.
B) Quantile normalization is used to equalize the distribution of measurements on all arrays and is computed by ranking of probe intensities for each array and then taking the corresponding average value of the probe intensities.
C) Log transformation to the base 2 was taken for the normalized data after background subtraction to adjust the distribution. Then, summarization of intensities value of individual probes was carried out using Tukey's median polish.

5.3.4. Protein phosphorylation experiments

Western blots were utilized to study the effect of GPR40 agonists and antagonists, MEK inhibitor and pertussis toxin on cell signalling pathways.

5.3.4.1. ERK1/2, MAPK38, AKT and GSK3α/β

Human and rat myotubes were treated with either 10 nM GW9508, 100nM AZ921, 100 & 250 μM Oleic acid or 250 & 500 μM Palmitic acid for 5, 10,15, 20 or 30 min. GPR40 antagonists (30 nM AZ915, 100 μM AZ468 or 5 μM AZ836) , 10 μM U0126 or 50nM PTX were added 30min prior to the addition of the agonists. Human and Wistar rat myotubes were also treated with GPR40

agonists and/or antagonists for 24 hours in the absence or presence of 100 nM insulin. After treatments, cells were washed with ice-cold PBS and lysed with RIPA buffer.

5.3.5. Immunocytochemistry experiments

Wistar rat myoblasts and myotubes were cultured in fatty acid free serum for 24 hrs followed by 24h incubation with vehicle (0.001% DMSO), 100nM AZ921 or with 100nM insulin in presence or absence of 100nM AZ921 (24hrs before). Then, cells were incubated overnight with 1:100 GLUT4 or 1:500 PKC β, δ & ζ antibodies followed with an hour incubation with the secondary antibodies described in chapter 2 section 2.7.4.

5.3.6. Calcium imaging

Wistar rat myoblasts and myotubes cultured on cover slips were used to measure the intracellular calcium levels after the addition of GPR40 agonists AZ921 (1 or 3 μM) or 1 μM GW9508 for up to 30 min. 10 μM ATP for 1min was used as positive control. The cells were cultured in fatty acid free medium for 24hrs with either 6mM glucose or 25mM glucose. Calcium imaging was carried out as described in chapter 2 section 2.8.

5.4. Statistical analysis

Statistical analysis was performed with GraphPad Prism software. RT-PCR and Western blot values are expressed as mean ± S. E. M. Statistical comparisons of different groups were made by one-way analysis of variance (ANOVA) and Bonferroni's multiple comparisons post-hoc test. Unpaired two-tailed T tests were also used. A P value <0.05 was taken as the level of significance.

Microarray preprocessed data were analysed with GeneSpring GX 11

software. Transcripts with fold change of ≥1.5 and P≤0.05 (Unpaired T Test with multiple correction) were then uploaded into the Ingenuity Pathway Analysis (IPA) for further analysis. In IPA Core analysis the Fisher's Exact Test (FET) was used to calculate the P value in function and canonical analysis. FET calculates the proportion of significant molecules from the data set that map to a function similar to the proportion of the function in the reference set. Z-score and corrected bias Z-score were used in downstream effects and upstream regulator analysis. Z-score is designed to reduce the chance that random data will generate significant predictions as it identifies the biological functions that are expected to be increased or decreased given the observed gene expression change in the datasets. A significant Z-score is ≥ 2 or ≤ 2 which indicate an increase or decrease, respectively in the predicted functions.

5.5. Results

5.5.1. GPR40 mRNA expression

5.5.1.1. Human

The expression of GPR40 in human skeletal muscle tissue and cultured myoblasts and myotubes was detected by Agilent microarray with a ranking order of 32595, 29027 and 28375 out of 41078, respectively. Taqman RT-PCR confirmed the expression of GPR40 in skeletal muscle tissue and cultured cells. Higher levels of GPR40 were found in myoblasts than myotubes ($P<0.05$) Figure 5-1. Brain tissue had the highest level of GPR40 mRNA expression as compared to spleen and skeletal muscle tissue and myotubes.

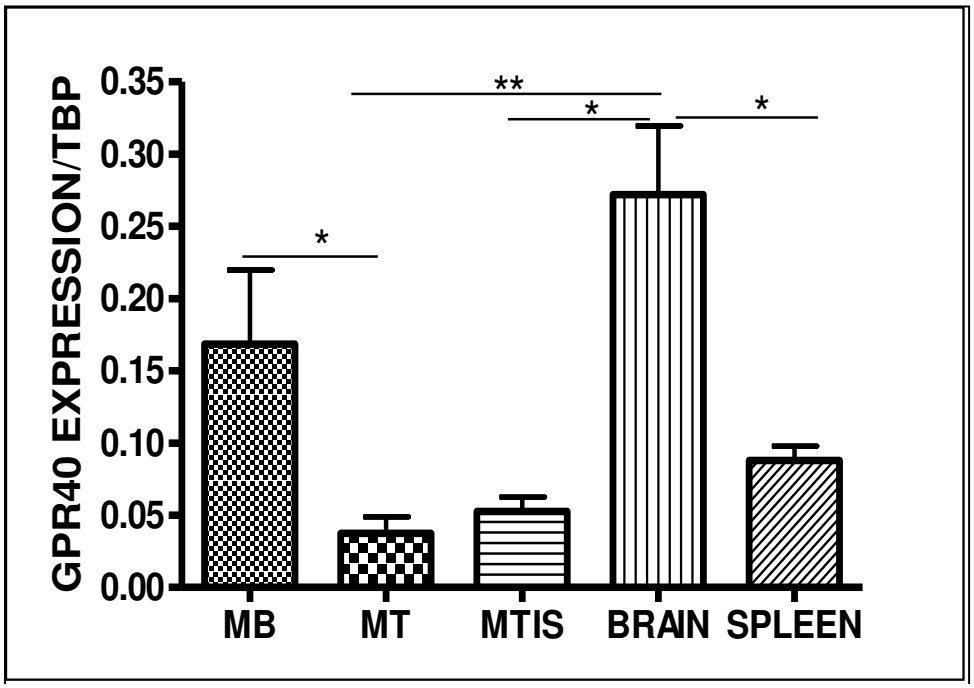

Figure 5-1: RT-PCR analysis of GPR40 relative expression in human tissues and cultured skeletal muscle cells.
TBP=TATA Binding Protein, MB=Myoblast, MT=Myotube, M=muscle, TIS=tissue. Values are mean±SEM *denotes $P<0.05$,**$P<0.01$ (N=6 samples from 3 subjects).

5.5.1.2. Wistar and Zucker rats

In Wistar, Zucker lean and Zucker fat rats in all skeletal muscle tissues and myotubes tested (Gastrocnemius, Vastus Lateralis, Soleus & Extensor digitroum longus) the expression of GPR40 mRNA was observed. Wistar rat pancreas, spleen, adipose tissue, heart and liver tissues also had detectable level of GPR40 mRNA expression. Pancreas had the highest level and was statistically significant ($P<0.05$) compared to skeletal muscle tissue, heart and liver (Figure 5-2). Zucker fat and lean spleen, adipose, heart and liver tissues also expressed GPR40 mRNA at varying levels (n=2 animals, data not shown)

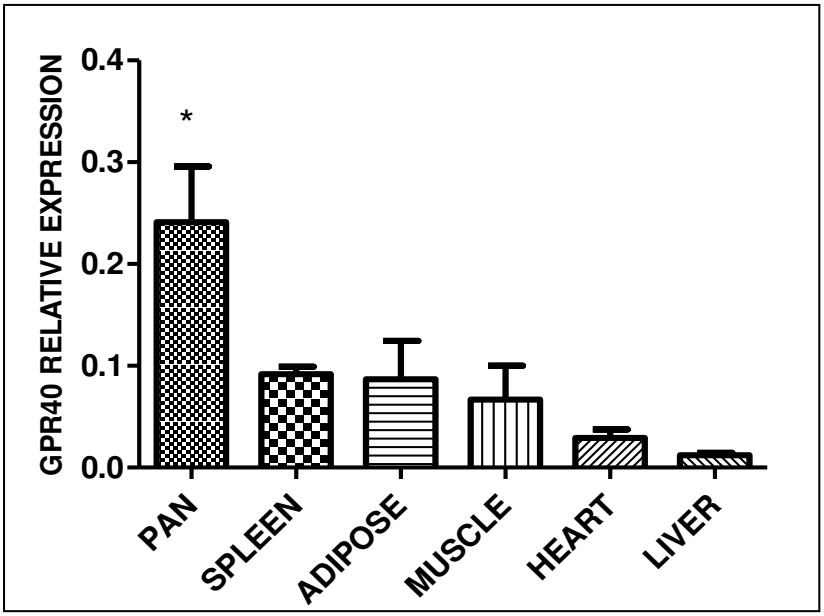

Figure 5-2: Taqman RT-PCR of GPR40 mRNA expression in rat tissues.
Data were normalized to TBP. Values are mean±SEM *denotes $P<0.05$, (n=3 rats).

GPR40 mRNA expression levels in 12 week old and 20week old Zucker fat and lean rats was also examined. There were no significant differences in GPR40 mRNA expression between ZLR and ZFR at 12 weeks. However, in 20 week old Zucker fat rats GPR40 mRNA was significantly increased in the VL ($P<0.01$) as compared to 20 week old Zucker lean rats. It is worth mentioning that Zucker rats VL and SOL had higher level of GPR40 mRNA expression than Wistar rat

(P<0.01). However, VL and SOL cultured myotubes had no significant difference in GPR40 expression between ZFR and ZLR as well as Wistar rats. The ZFR (12 and 20wks) had higher blood glucose level than ZLR (P<0.001) (table 2.1). Expecting that removal of the hyperglycemic condition in culture alters the GPR40 expression level in ZLR and ZFR, the cells were cultured in 6mM and 25mM glucose for 6 hours. Our result showed a significant higher expression level in cells cultured in 25mM compared to those cultured in 6mM glucose at 6 hours (P<0.05) however, the difference disappeared at 24hours (Figure 5-4).

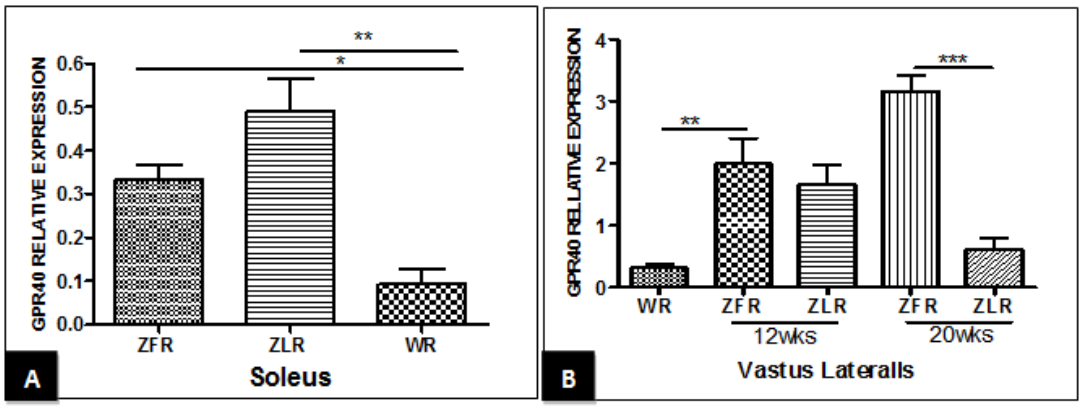

Figure 5-3: Comparative analysis of GPR40 mRNA expression in rat skeletal muscle tissues.
(A) 12 weeks Soleus * denotes P<0.05 WR compare to ZFR and ** denotes P<0,01 WR compare to ZLR. (B)12 +20 weeks Vastus lateralis ** denotes P<0,01 ZFR compare to WR and ***denotes P<0.001 ZFR compare to ZLR .. ZFR (Zucker Fat Rat), ZLR (Zucker Lean Rat) and WR (Wistar Rat). Data were normalized to TBP. Values are mean ± SEM (n=5 rats)

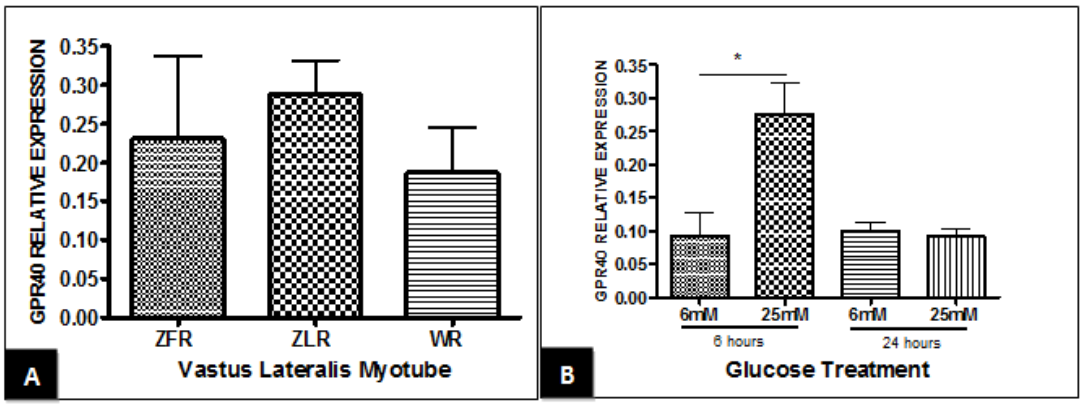

Figure 5-4: RT-PCR analysis of GPR40 mRNA expression in rat myotubes taken from ZFR (Zucker Fat Rat), ZLR (Zucker Lean Rat) and WR (Wistar Rat).
A) Cultured myotubes from different rats P>0.05. B) glucose treatment of cultured myotubes for 6 and 24 hours * denotes P<0.05 . Data were normalized to TBP. Values are mean ± SEM (n=2 independent experiments).

5.5.2. Effect GPR40 agonists and antagonists on ERK phosphorylation

Taqman QRTPCR analysis showed that human and rat myotubes had a detectable level of GPR40. To address the functionality of GPR40, we studied the effect of GPR40 activation or inhibiton on ERK1/2 phosphorylation. Cyclophilin was used as an invariant reference protein for normalization.

5.5.2.1. GW9508 and Oleic acid

Treatment of Myotubes with 10nM GW9508 cultured from both Wistar and Zucker (Fat and Lean) showed time dependent changes in ERK phosphorylation. Representative blots are shown in Figure 5-5 & Figure 5-6.

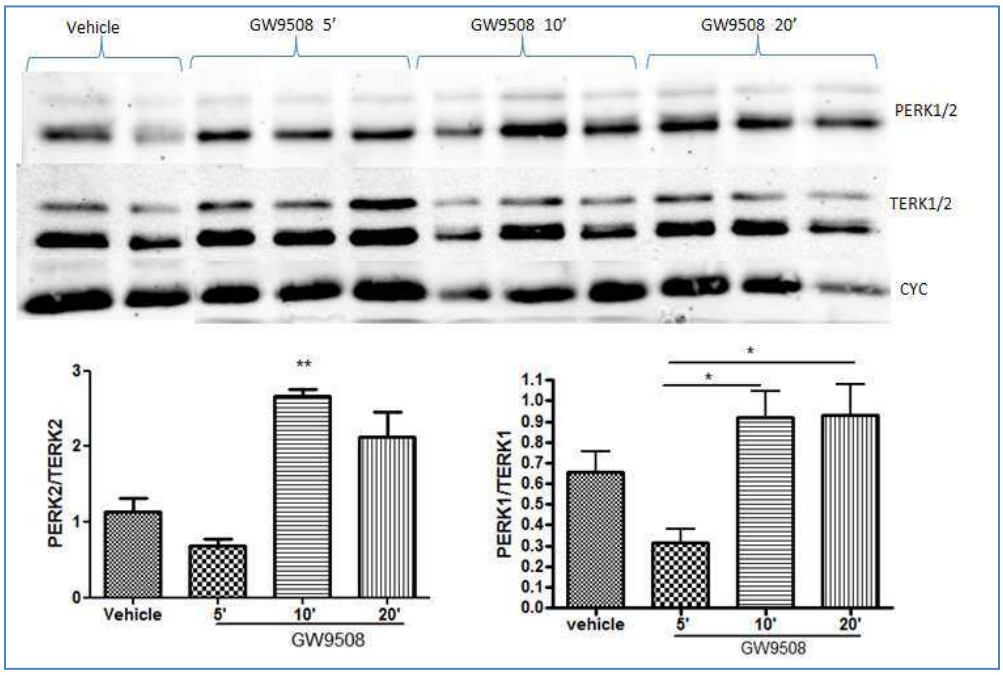

Figure 5-5: Representative blot showing the Effect of GPR40 agonist (10nM GW9508) treatment on ERK1/2 phosphorylation in Wistar rat myotubes on the upper panel.
Quantified values of PERK1/TERK1and PERK2/TERK2 on the lower panel. *denotes P<0.05 and ** denotes <0.01. Data were analysed by one way ANOVA with Bonferroni post-hoc test (N=3).

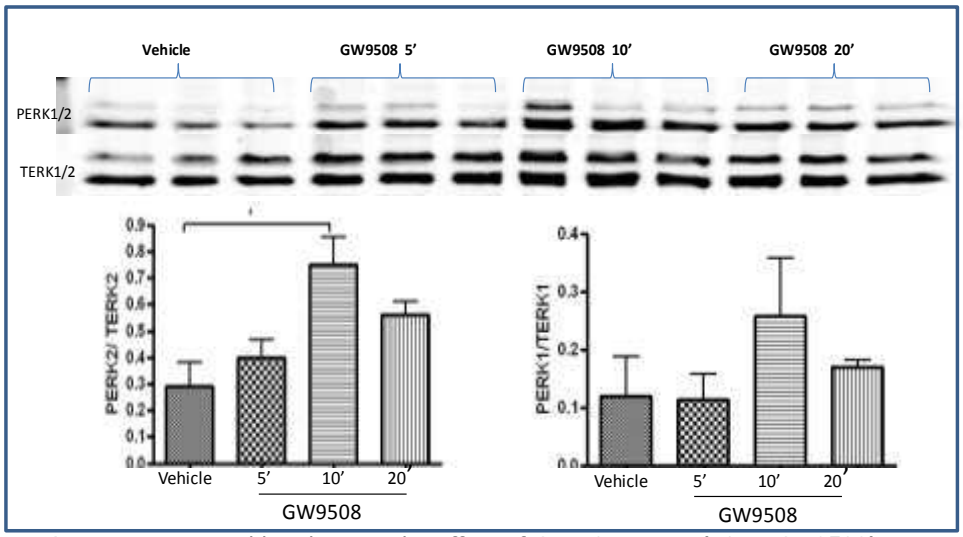

Figure 5-6: Representative blot showing the effect of GPR40 agonist (10nM GW9508) treatment on ERK1/2 phosphorylation in Zucker Fat Rat myotubes on the upper panel.
Quantified values of PERK1/TERK1 and PERK2/TERK2 on the lower panel.*denotes P<0.05 compare to vehicle. Data were analysed by one way ANOVA with Bonferroni post-hoc test (N=2).

Treatment of rat myotubes with 100 and 250 μM Oleic acid also showed a time dependent increase in ERK1/2 phosphorylation however significance ($p<0.001$) was observed with the 250μM Oleic acid concentration. Representative blots are shown in Figure 5-7 & Figure 5-8 .

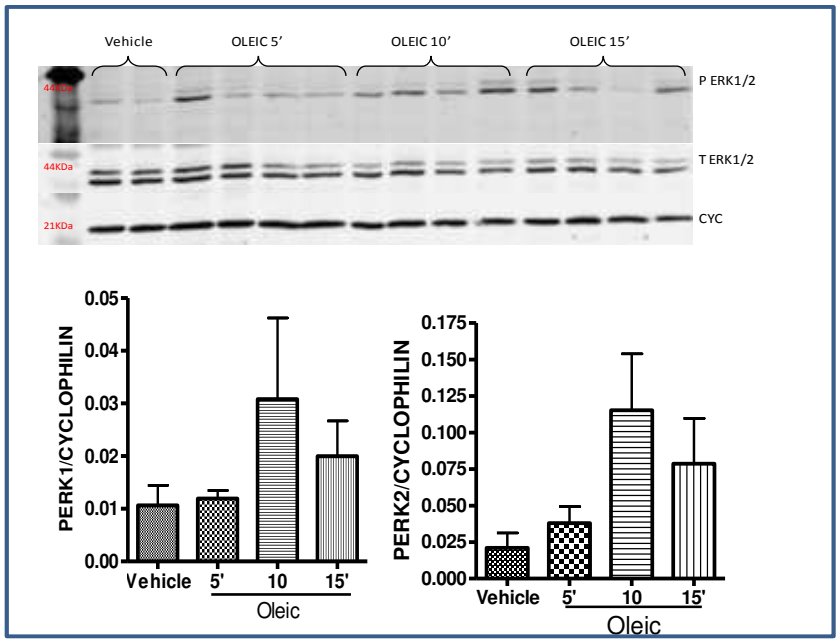

Figure 5-7: Representative blot showing the effect of 100μM Oleic acid treatment on ERK1/2 phosphorylation in rat myotubes on the upper panel.
Quantified values of PERK1/CYC and PERK2/CYC on the lower panel. Data were analysed by one way ANOVA with Bonferroni post-hoc test (N=3)

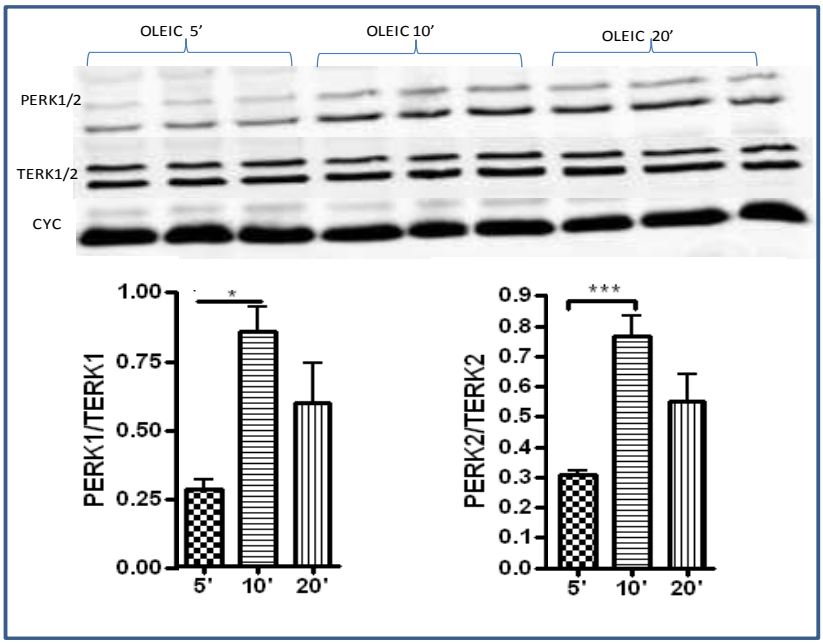

Figure 5-8: Representative blot showing the effect of 250μM Oleic acid treatment on ERK1/2 phosphorylation in Zucker Fat Rat myotubes on the upper panel.
Quantified values of PERK1/TERK1 and PERK2/TERK2 on the lower panel. *denotes P<0.05 and ***denotes <0.001. Data were analysed by one way ANOVA with Bonferroni post-hoc test (N=3)

Human myotubes treated with 10nM GW9508 and 100μM Oleic acid showed a time dependent increase in ERK1/2 phosphorylation Figure 5-9. Pre-treatment with MEK inhibitor (10μM U0126) significantly inhibited ERK phosphorylation by GW9508 Figure 5-10. Treatment of rats and human myotubes with 100, 250 and 500 μM Palmitic acid did not alter the level of ERK1/2 phosphorylation.

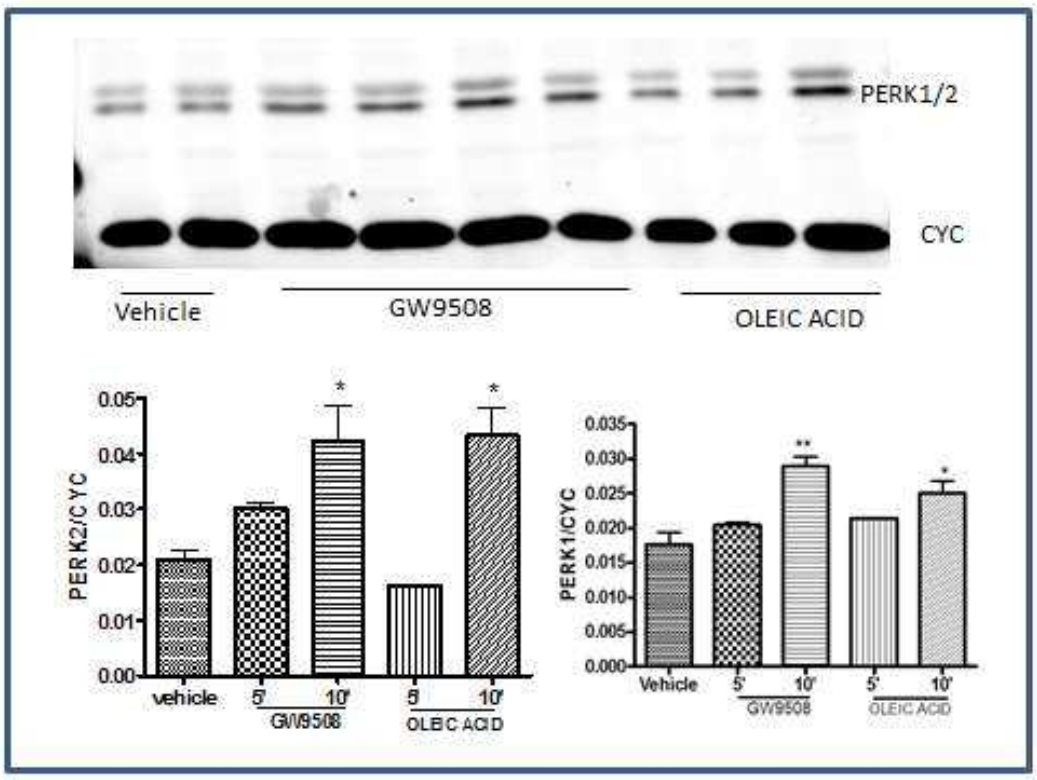

Figure 5-9: Representative blot showing the effect of 10 nM GW9508 and 100 µM Oleic acid treatment on ERK1/2 phosphorylation in human myotubes on the upper panel.
Quantified values of PERK1/CYC and PERK2/CYC on the lower panel. *denotes P<0.05 and **denotes P<0.01 compare to vehicle. Data were analysed by one way ANOVA with Bonferroni post-hoc test (N=3)

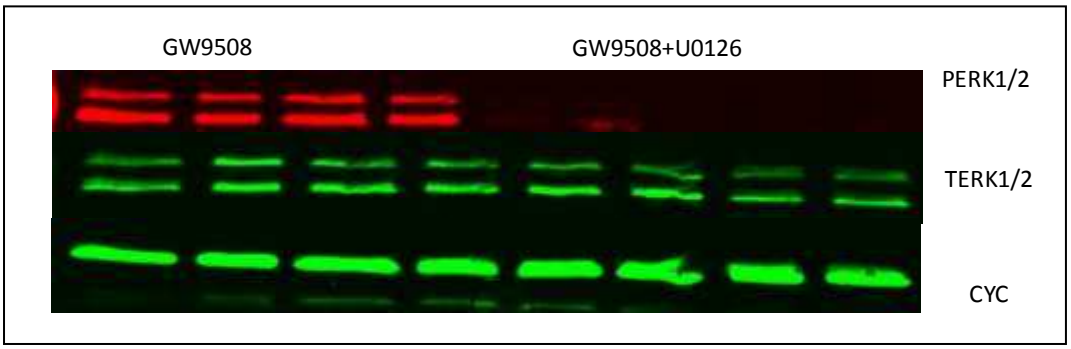

Figure 5-10: Western blot showing the effect of MEK inhibitor (10 µM U0126) on ERK1/2 phosphorylation induced by GPR40 agonist (10 nM GW9598) on human myotubes (N=3).
Phospho ERK1/2 (PERK) is shown in green band and total ERK1/2 (TERK) in red. Cyclophilin used as a loading control.

5.5.2.2. Determining the effects of GPR40 ligands AZ921 (agonist) and the antagonists (AZ915, AZ468 &AZ836) upon ERK phosphorylation

Even though GW9508 is a selective partial agonist for GPR40 with pEC_{50} values of 7.32, it also activates GPR42 and GPR43 (pEC_{50}< 4.3 and < 4.3 respectively). In this study the more potent and full GPR40 agonist (AZ921 EC_{50} 22nM) and antagonists (AZ915 IC_{50} 6nM, AZ468 IC_{50} 20μM & AZ836 IC_{50} 1μM) were used to confirm the functionality of GPR40 in skeletal muscle. Treatment of human, Wistar and Zucker rats myotubes with 100nM AZ921 induced a time dependent increase in ERK1/2 phosphorylation with a significant ($P<0.01$) peak at 15- 20min followed by a significiant ($P<0.05$) reduction at 30min (Figure 5-11 & Figure 5-12). Pre-treatment of human and rat myotubes with 100 μM AZ468 and 5 μM AZ836 significantly reduced ERK1/2 phosphorylation induced by AZ921. However the human specific antagonist AZ915 did not suppress the ERK1/2 induction by AZ921. Representative blots are shown in Figure 5-13 and Figure 5-14. Pre-treatment with MEK inhibitor (10μM U0126) significantly inhibited ERK phosphorylation by AZ921. Interestingly, the GPR40 antagonists had no effect on ERK1/2 phosphorylation induced by GW9508 and Oleic acid in both human and rats myotubes.

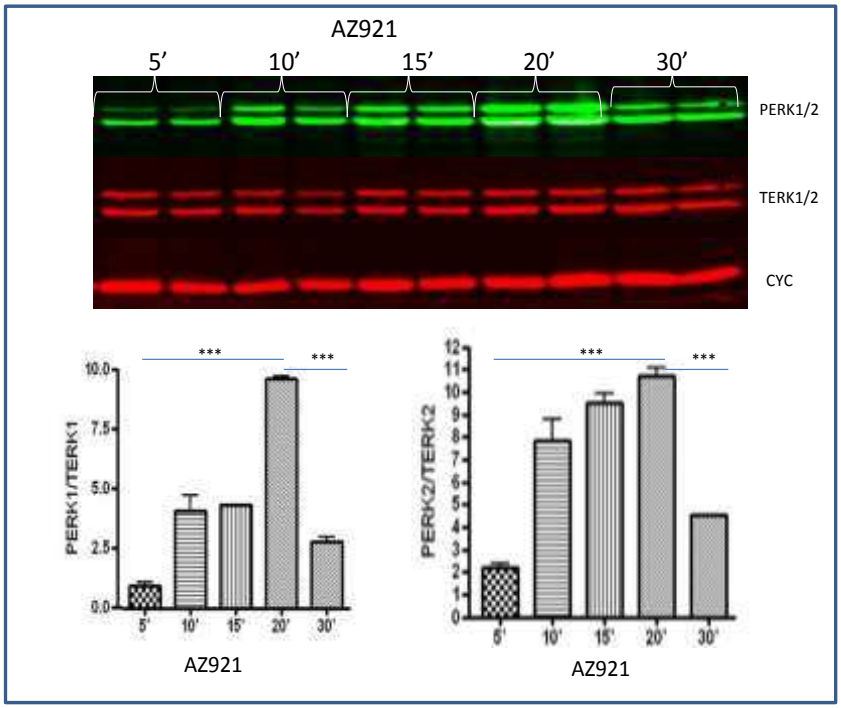

Figure 5-11: Representative blot showing the effect the GPR40 agonist (100nM AZ921) treatment on ERK1/2 phosphorylation in Wistar rat myotubes on the upper panel.
Quantified values of PERK1/TERK1 and PERK2/TERK2 on the lower panel. ***denotes P<0.001 compare to 5' and 30'.Data were analysed by one way ANOVA with Bonferroni post-hoc test (N=3). Phospho ERK1/2 (PERK) is shown in green band and total ERK1/2 (TERK) in red. Cyclophilin used as a loading control.

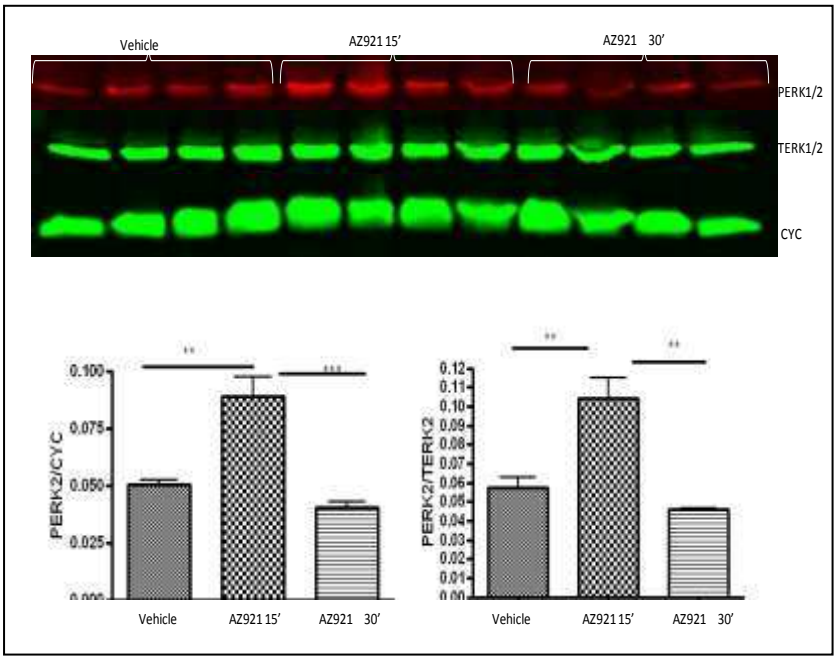

Figure 5-12: Representative blot showing the effect the GPR40 agonist (100nM AZ921) treatment on ERK1/2 phosphorylation in human myotubes on the upper panel.
Quantified values of PERK1/TERK1 and PERK2/TERK2 on the lower panel. ** denotes P<0. 01 and ***denotes P<0.001 compare to vehicle and 30'. Data were analysed by one way ANOVA with Bonferroni post-hoc test (N=3) Phospho ERK1/2 (PERK) is shown in red band and total ERK1/2 (TERK) in green. Cyclophilin used as a loading control (N=3).

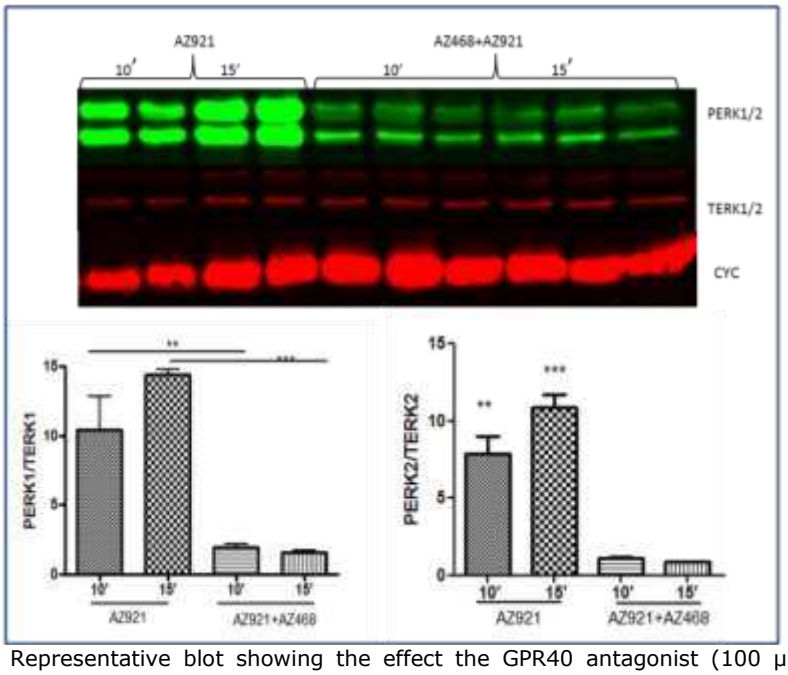

Figure 5-13: Representative blot showing the effect the GPR40 antagonist (100 μM AZ468) on ERK1/2 phosphorylation induced by GPR40 agonist (100 nM AZ921) in Wistar rat myotubes on the upper panel.
Quantified values of PERK1/TERK1 and PERK2/TERK2 on the lower panel. ** denotes P<0.01 AZ921 10' compare to AZ921+AZ46810' and ***denotes P<0.001 AZ921 15' compare to AZ921+AZ46815'. Data were analysed by one way ANOVA with Bonferroni post-hoc test (N=3). Phospho ERK1/2 (PERK) is shown in green band and total ERK1/2 (TERK) in red. Cyclophilin used as a loading control (N=3).

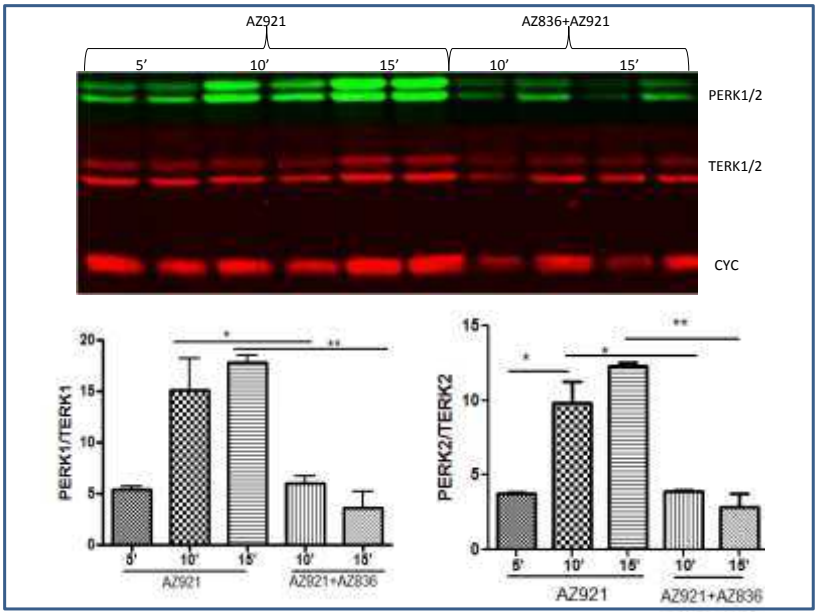

Figure 5-14: : Representative blot showing the effect the GPR40 antagonist (5μM AZ836) on ERK1/2 phosphorylation induced by GPR40 agonist (100 nM AZ921) in Zucker lean rat myotubes on the upper panel.
Quantified values of PERK1/TERK1 and PERK2/TERK2 on the lower panel. * denotes P<0.05 AZ921 10' compare to AZ921+AZ46810' and **denotes P<0.01 AZ921 15' compare to AZ921+AZ46815'. Data were analysed by one way ANOVA with Bonferroni post-hoc test (N=3). Phospho ERK1/2 (PERK) is shown in green band and total ERK1/2 (TERK) in red. Cyclophilin used as a loading control (N=3).

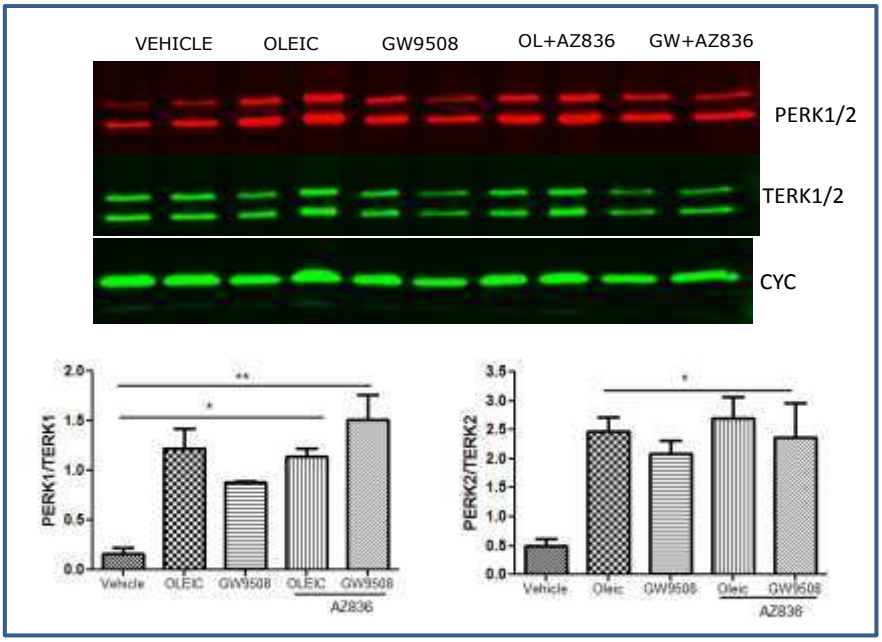

Figure 5-15: Representative blot showing the effect the GPR40 antagonist (5μM AZ836) on ERK1/2 phosphorylation induced by 250 μM OLEIC ACID (OL) and 10 nM GW9508 (GW)) in rat myotubes on the upper panel.
Quantified values of PERK1/TERK1 and PERK2/TERK2 on the lower panel. * denotes P<0.05 and **denotes compare to vehicle. Data were analysed by one way ANOVA with Bonferroni post-hoc test (N=3). Phospho ERK1/2 (PERK) is shown in red band and total ERK1/2 (TERK) in green. Cyclophilin used as a loading control (N=3).

5.5.3. Effect of GPR40 agonists and antagonists on insulin stimulated AKT phosphorylation

AKT is a key signalling protein in insulin signalling (Lindborg et al. 2010). It has been found that insulin has a diverse role in its action along metabolic and mitogenic signalling pathways (Koistinen et al. 2003). AKT phosphorylation under acute insulin (100nM for 10 min) stimulation of Wistar rat and human myotubes pre-treated with 100nM AZ921,10nM GW9508, 250 μM Oleic acid for 24 hours with or without 5 μM AZ836 (antagonist) was studied. Pretreatment with 100nM AZ921 significantly (P<0.01) decreased insulin induced AKT phosphorylation in human myotubes (Figure 5-16) but the difference did not reach significance (P=0.07) in rat myotubes (Figure 5-17). Interestingly, 10nM GW9508 had no effect on insulin stimulated AKT phosphorylation while 250 μM

Oleic acid increased it (P<0.05) Figure 5-18.The GPR40 antagonist AZ836 abolished the effect of the agonist (AZ921) and had no effect on Oleic acid induction of AKT phosphorylation. The molecular weight of the bands of Phospho AKT and Total AKT were detected at 62 KDa.

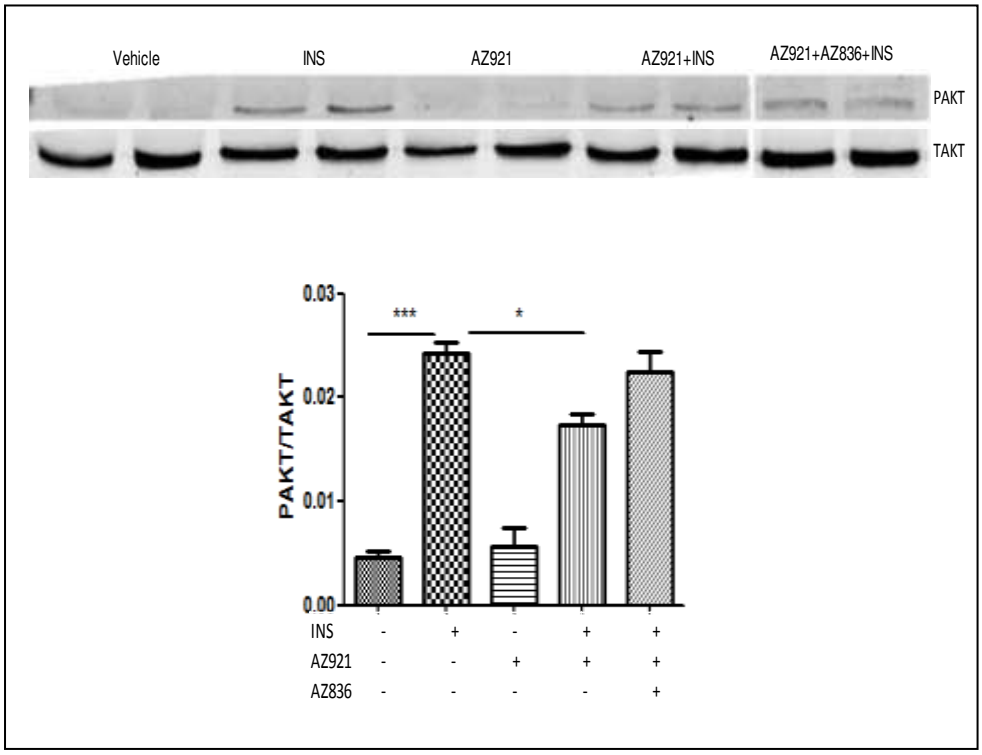

Figure 5-16: Representative blot showing the effect of GPR40 agonist (100nM AZ921) and antagonist (5 μM AZ836) on insulin stimulated AKT phosphorylation in human myotubes.
Pre-treatment (24 hours) of myotubes with 100nM AZ921 significantly reduce the acute (10min) stimulatory effect of 100 nM INS (insulin) on AKT phosphorylation. *** denotes P<0.001 compare to vehicle and * denotes P<0.05 compare to insulin. Data were analysed by one way ANOVA with Bonferroni post-hoc test (n=4 samples /2 subjects).

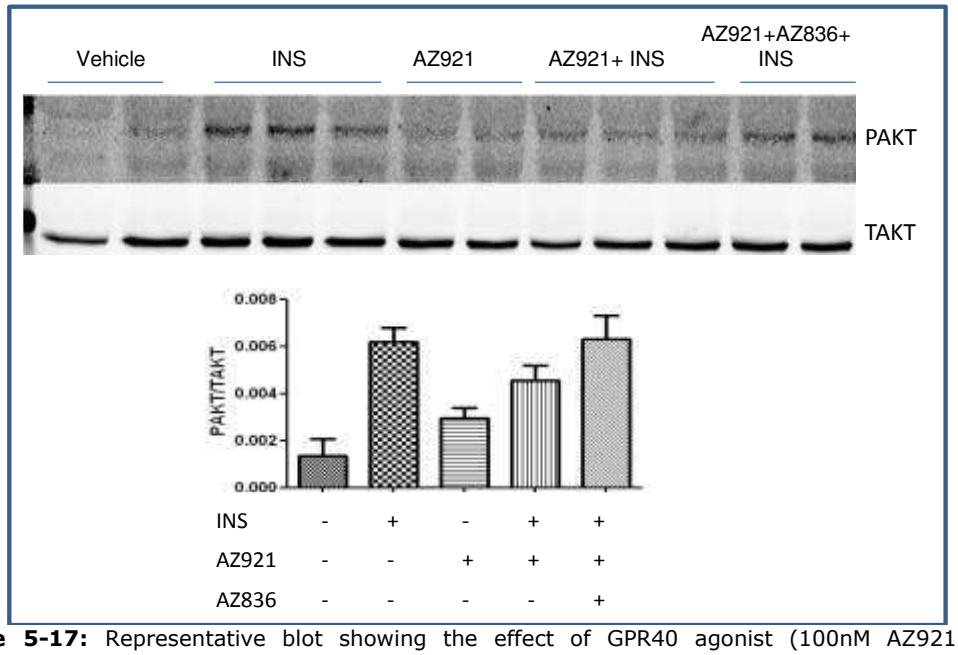

Figure 5-17: Representative blot showing the effect of GPR40 agonist (100nM AZ921) and antagonist (5 μM AZ836) on insulin stimulated AKT in Wistar rat myotubes.
Pre-treatment (24 hours) of myotubes with AZ921 and AZ836 had a trend of reduction on the acute (10min) stimulatory effect of 100 nM INS (insulin) on AKT phosphorylation. Data were analysed by one way ANOVA with Bonferroni post-hoc test (n=4 samples/2rats).

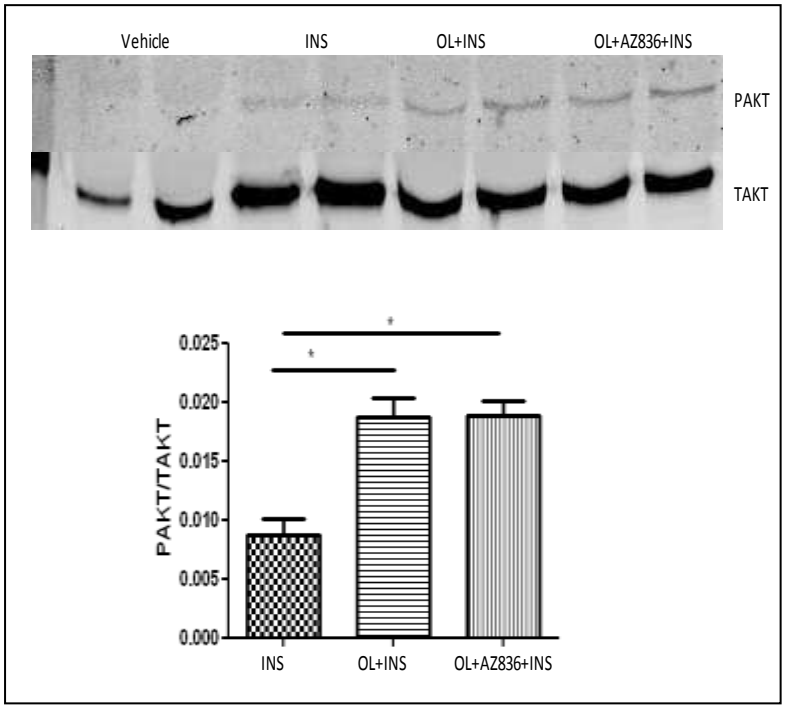

Figure 5-18: Representative blot showing the effect of GPR40 agonist (250 μM Oleic acid) and antagonist (5 μM AZ836) on insulin stimulated AKT phosphorylation in Wistar rat myotubes (n= 4 samples/2rats).
Pre-treatment (24 hours) of myotubes with 100 μM Oleic acid increase the acute (10min) stimulatory effect of 100 nM INS (insulin) on AKT phosphorylation. * denotes $P<0.05$ compare to insulin. Data were analysed by one way ANOVA with Bonferroni post-hoc test.

5.5.4. Effect of AZ921 and AZ836 on insulin stimulated GSK3β phosphorylation

GSK is another key signalling protein in insulin signalling that regulates glycogen synthesis (Lindborg et al. 2010). We examined GSK3β phosphorylation under acute insulin stimulation after treatment with 100nM AZ921 and 5 μM AZ836. Pretreatment (24 hours) with 100nM AZ921 had no significant effect on insulin induced GSK3β phosphorylation however, the addition of the antagonist AZ836 30 mins before the agonist increased insulin induction of GSK phosphorylation ($P<0.01$) (Figure 5-19). The molecular weight of the bands of Phospho and Total GSK3β were detected at 46 KDa.

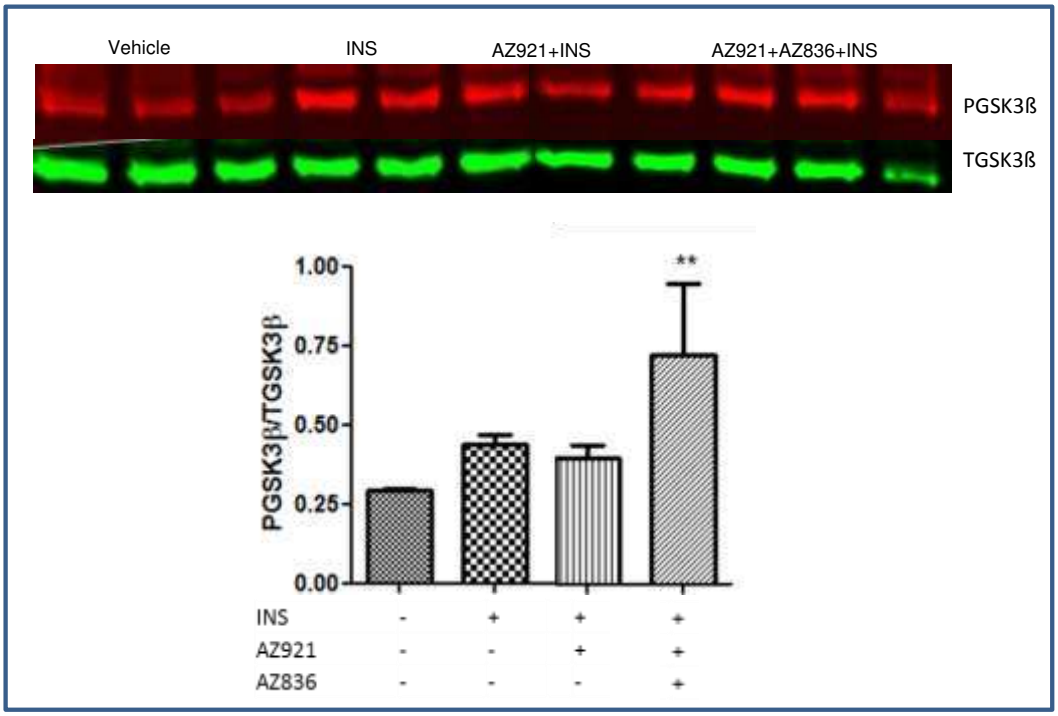

Figure 5-19: Effect of GPR40 agonist (100nM AZ921) and antagonist (5 μM AZ836) on insulin stimulated GSK3β phosphorylation in human myotubes.
Pre-treatment (24 hours) of myotubes with 100nM AZ921 had no effect on the acute (10min) stimulatory effect of 100 nM INS (insulin) on GSK3β phosphorylation while the antagonist (AZ836) significantly increase it. ** denotes $P<0.01$ compare to insulin. Phospho GSK3β is shown in red band and total GSK3β in red. Data were analysed by one way ANOVA with Bonferroni post-hoc test (n=4samples/2 subjects).

5.5.5. Effect of AZ921, GW9508, Oleic acid and Palmitic acid on MAPK38 phosphorylation

MAPK38 is another key signalling protein which might play a role in insulin resistance (Koistinen et al. 2003). incubation of Wistar rat and human myotubes with 100 nM AZ921, 250 µM Oleic acid and 250 µM Palmitic acid had no effect on insulin induction of MAPK38 phosphorylation however, 10nM GW9508 significantly induced it (P<0.01) (Figure 5-20).

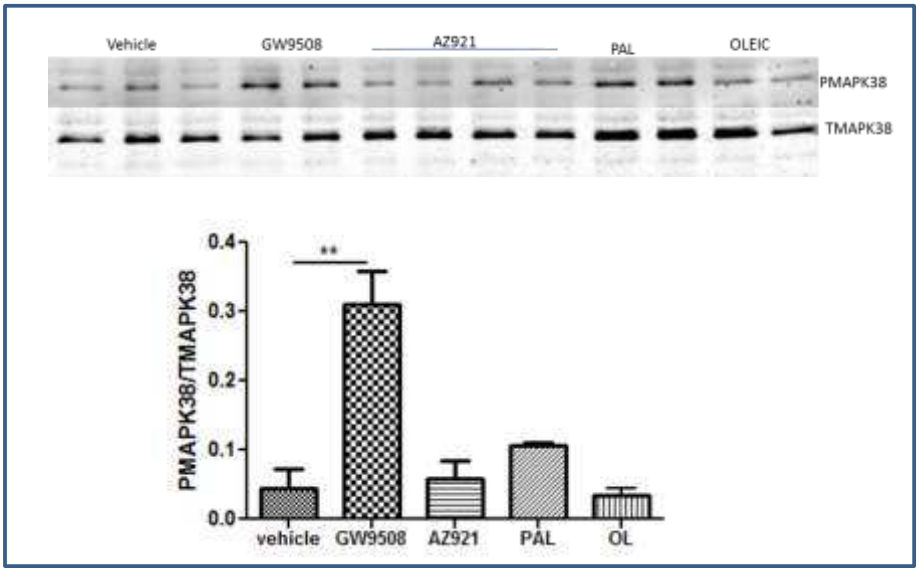

Figure 5-20: Representative blot showing the effect 10 min treatment of 10 nM GW9508, AZ921 (100nM),Palmitic acid (250µM PAL) or 250 µM OLEIC ACID (OL) on MAPK38 phosphorylation on human myotubes.
** P<0.01 compared to vehicle. Data were analysed by one way ANOVA with Bonferroni post-hoc test (n=3.

5.5.6. Effect of Pertussis Toxin (PTX) on ERK and MAPK38 phosphorylation induced by GPR40 agonists

GPR40 has previously been described as being mainly linked to Gq although it can be weakly coupled to Gi/o (Itoh et al. 2003; Kotarsky et al. 2003). In this study, pretreatment of Wistar rat myotubes with Gi/o specific inhibitor PTX (50 nM) for 30 min (P<0.05) reduced the effect of 250 µM Oleic acid, 10nM GW9508 (P<0.05) and 100nM AZ921 on ERK1/2 phosphorylation, however, the latter did not reach statistical significance (Figure 5-21). PTX also

reduced the effect of 10nM GW9508 (P<0.05) on MAPK38 phosphorylation (Figure 5-22).

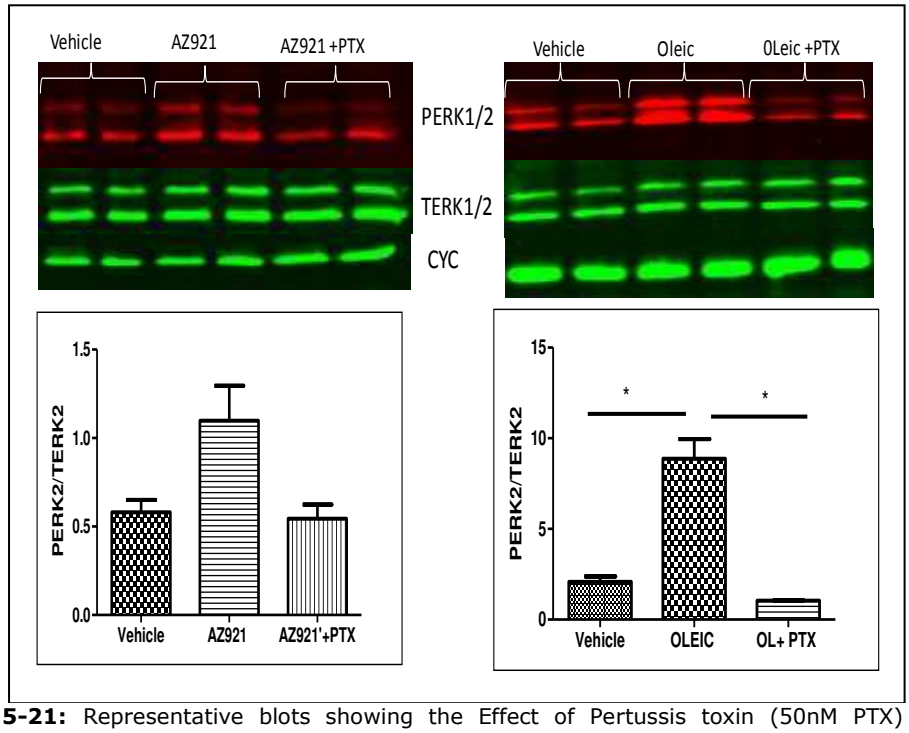

Figure 5-21: Representative blots showing the Effect of Pertussis toxin (50nM PTX) on ERK phosphorylation induced by 100 nM AZ921 & 250 µM Oleic acid on Wistar rat myotubes.
* denotes P<0.05. Phospho ERK1/2 (PERK) is shown in red band and total ERK1/2 (TERK) in green. Cyclophilin was used as a loading control. Data were analysed by one way ANOVA with Bonferroni post-hoc test (n=3).

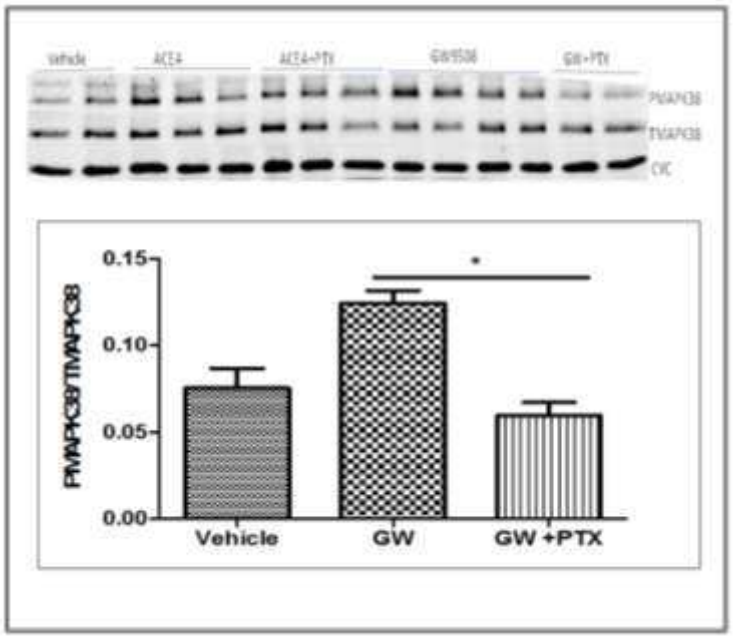

Figure 5-22: Representative blots showing the Effect of Pertussis toxin (50nM PTX) on MAPK38 phosphorylation induced by 10 nM GW9508 Wistar rat myotubes.
* denotes P<0.05. Cyclophilin was used as a loading control. Data were analysed by one way ANOVA with Bonferroni post-hoc test (n=3).

5.5.7. Effect of GPR40 agonists (AZ921 and GW9508) on intracellular calcium ion release

As GPR40 is predominantly a Gαq coupled receptor anticipated to increase intracellular calcium, calcium mobilization is used a functional read out in the majority of publications. The addition of AZ921 (1 & 3 μM) or GW9508 (1 μM) for 5, 10 and 30 min to cells cultured (myoblasts and myotubes) in 6mM or 25mM glucose for 6hrs did not produce any change in calcium ion levels (Figure 5-23). However, the addition of 10 μM ATP produced a rapid elevation of calcium in almost 96% of the cells. The experiment was done 3 times using cells from different animals.

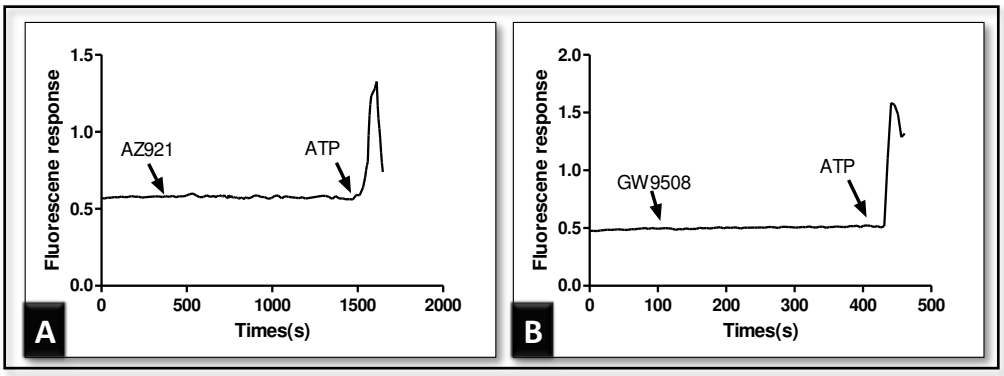

Figure 5-23: A representative trace showing the effect of GPR40 agonist.
A) 1 μM of AZ921, B) 10nM GW9805 and 10 μM ATP in the 340/380 nm excitation length wave ratios in Wistar rat myotubes (n=3 independent experiments).

5.5.8. Effect of GPR40 agonist (AZ921), MEK inhibitor (U0126) and Palmitic acid on Cytokine (TNFα and IL6) mRNA expression

There is now a strong appreciation that the secretory products of muscle, also referred to as myokines, are part of a muscle-to-fat signalling possibly modulating insulin sensitivity in skeletal muscle (Eckardt et al. 2008). Treatment of human myotubes with 100nM AZ921 alone for 24hrs did not have any significant changes in IL6 and TNFα mRNA expression ($P>0.05$) however pretreatment with U0126 (30 min) before the addition of AZ921 had a

significant effect on IL6 mRNA expression only (Figure 5-24). However, 250μM Palmitic acid had a significant (P<0.05) effect on both IL6 and TNFα mRNA expression. Interestingly, the MEK inhibitor and GPR40 antagonist did not block the effect of Palmitic acid on IL6 and TNFα mRNA expression. In fact, the MEK inhibitor had a synergistic effect on TNFα mRNA expression Figure 5-25.

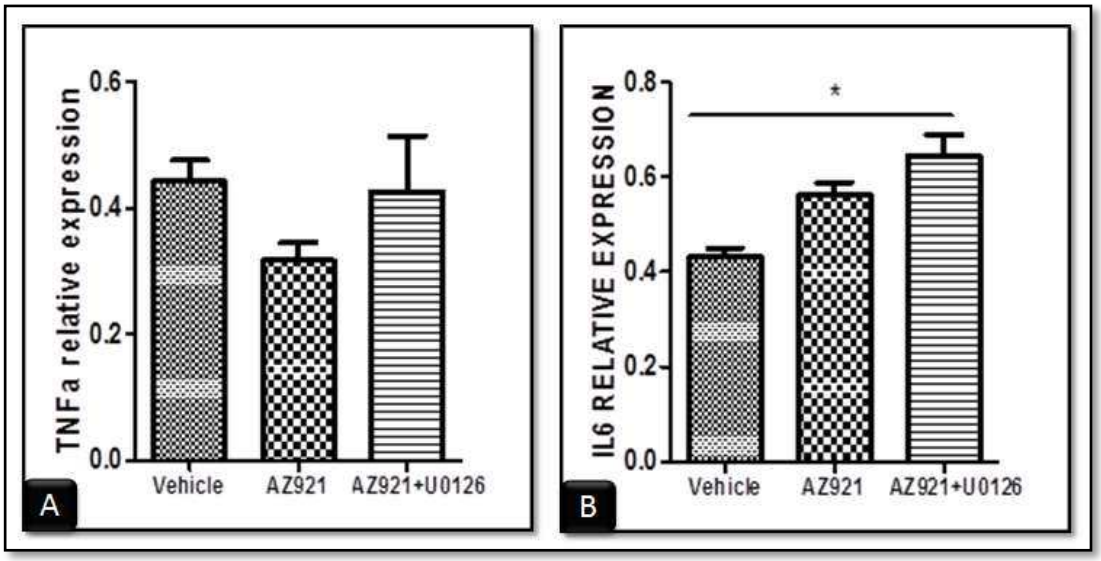

Figure 5-24: Quantitative analysis RT-PCR of TNFα (A) or IL6 (B) mRNA expression in human myotubes.
Cells were treated with GPR40 agonist (100 nM AZ921) with or without 10 μM MEK inhibitor (U0126) for 24 hrs. * denotes P<0.05. Data were normalized by TBP and RPLPO. Values are mean±SEM Bonferroni's Multiple Comparison Test (n=3 independent experiments)

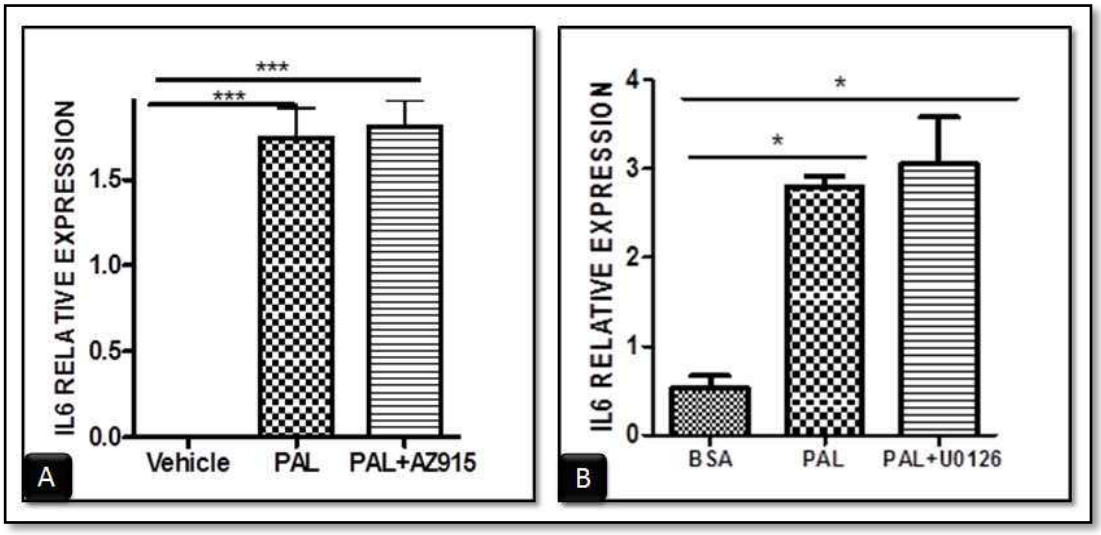

Figure 5-25: Quantitative analysis RT-PCR of IL6 mRNA expression in human myotubes.
(A) Cells were treated with 250 μM Palmitic acid with or without 30 nM GPR40 antagonist (AZ915) for 24 hrs. (B) Cells were treated with 250 μM Palmitic acid with or without 10 μM MEK inhibitor (U0126) for 24 hrs. * denotes P<0.05 & *** denote P<0.001. Data were normalized by TBP and RPLPO. Values are mean±SEM Bonferroni's Multiple Comparison Test (n=3 independent experiments)

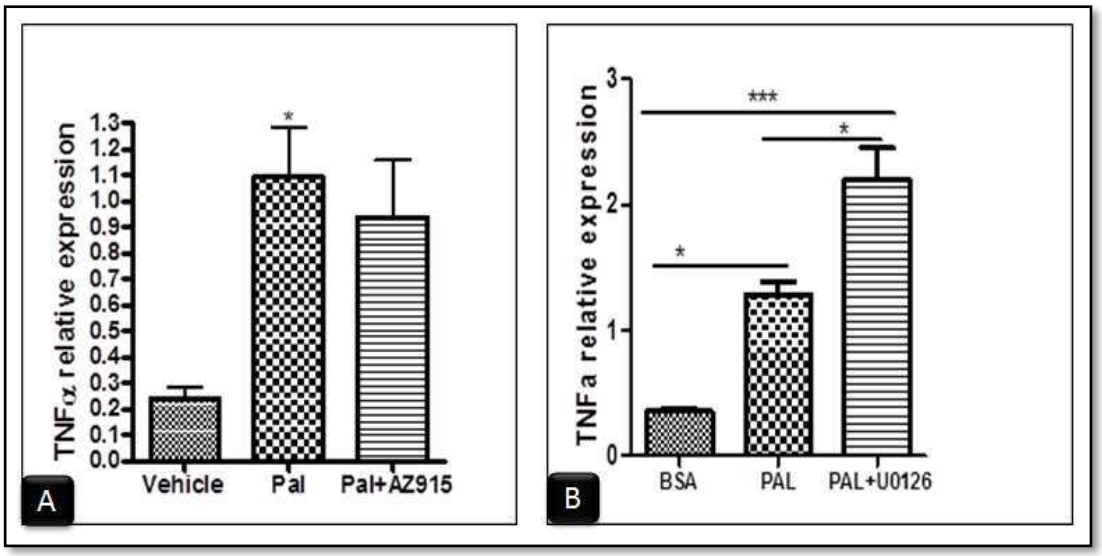

Figure 5-26: Quantitative analysis RT-PCR of TNFα mRNA expression in human myotubes. (A) Cells were treated with 250 μM Palmitic acid with or without 30 nM GPR40 antagonist (AZ915) for 24 hrs. (B) Cells were treated with 250 μM Palmitic acid with or without 10 μM MEK inhibitor (U0126) for 24 hrs. * denotes P<0.05 & *** denote P<0.001. Data were normalized by TBP and RPLPO. Values are mean±SEM Bonferroni's Multiple Comparison Test (n=3 independent experiments)

5.5.9. Effect of GPR40 agonist (AZ921), antagonist (AZ915), MEK inhibitor (U0126), Oleic and Palmitic acids on PKD4 mRNA expression

Substrate competition between fatty acids and glucose occurs at the level of the pyruvate dehydrogenase complex which is regulated by pyruvate de-hydrogenase kinase (PDK), which plays an important role in the development of insulin resistance (Sugden 2003). Treatment of human and Wistar rat myotubes with 100nM AZ921, 250 μM Oleic acid and 30nM AZ915 for 24hrs did not have any significant (P>0.05) effect on PDK4 mRNA expression Figure 5-27. However, 250μM Palmitic acid and 10 μM U0126 caused a significant (P<0.01) change in PDK4 mRNA expression. Interestingly, the MEK inhibitor and the GPR40 antagonist did not block the effect of Palmitic acid but Oleic acid did block it.

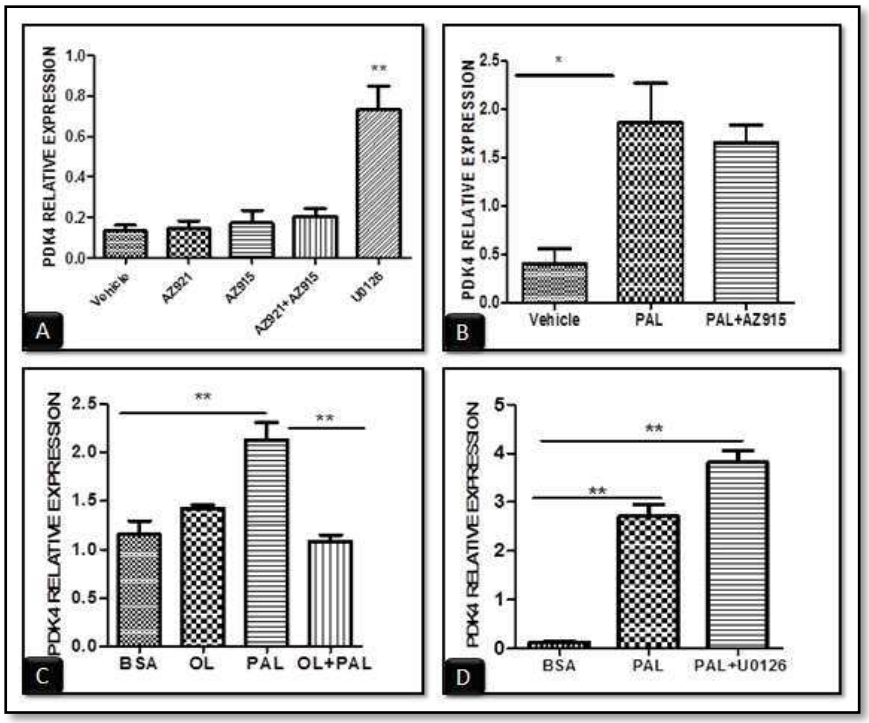

Figure 5-27: Quantitative analysis RT-PCR of PDK4 mRNA expression in human myotubes. A) Cells were treated with 100 nM AZ921, 30nM AZ915, AZ921+AZ915 or 10μM MEK inhibitor (U0126) for 24 hrs. B) Cells were treated with 250 μM Palmitic acid with or without or GPR40 antagonist (AZ915 30nM) for 24 hrs. C) Cell were 24 hrs treated with 250 μM Palmitic acid, 250 μM Oleic acid or Oleic (OL)+ Palmitic acids (PAL). Cells were treated with 250 μM Palmitic acid with or without 10 μM MEK inhibitor (U0126) for 24 hrs. * denotes $P<0.05$ & ** denote $P<0.01$. Data were normalized by TBP and RPLPO. Values are mean±SEM Bonferroni's Multiple Comparison Test (n=3 independent experiments)

5.5.10. Microarray result

Previous findings in this chapter indicate that GPR40 is expressed and functional in rat and human skeletal muscle cultured myotubes. However the exact role of GPR40 in metabolism could not be clearly stated. As this is the first study carried out in skeletal muscle, the influence of GPR40 agonists and antagonists on global gene expression was investigated using Affymetrix microarray.

Human myotubes were cultured in 25cm^2 flasks and incubated with vehicle (0.01% DMSO), GPR40 agonist (AZ921 100nM), GPR40 antagonist (AZ836 5μM) or the agonist with antagonist for 24 hours. The antagonist was used 30 min prior to the addition of the agonist. The cells were cultured in fatty

acid free serum or horse serum (for the antagonist only) containing media before performing the treatments.

5.5.10.1. Initial characterisation of microarray gene expression data

Principal component analysis (PCA) of global gene expression profiles revealed two distinct populations where the control, agonist and agonist with antagonist form a group and the antagonist (horse and free fatty acid) form another group (Figure 5-28). Two ways hierarchal clustering based on conditions and entities showed similar result to the PCA analysis. Hierarchal clustering showed that control and agonist with antagonist are the closest groups Figure 5-29. The reproducibility of the data was assessed by the correlation coefficients of the normalized data. The correlation coefficient between the replicates in each treatment condition was 0.99 across all the samples.

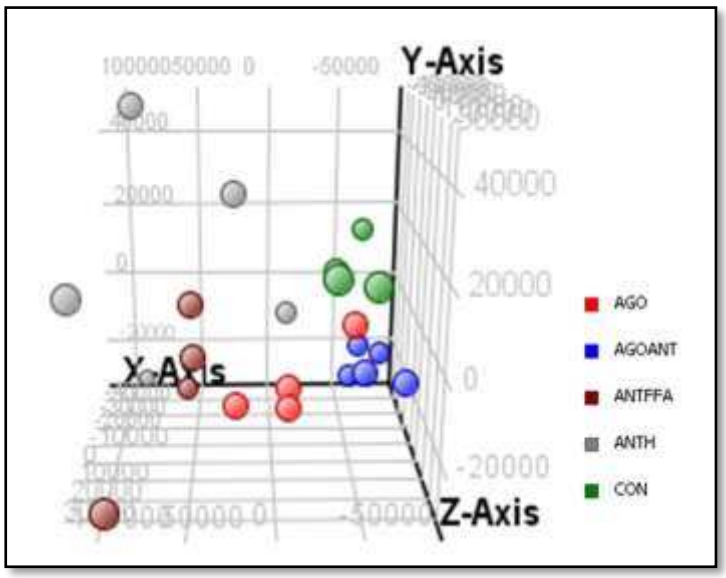

Figure 5-28: Principal component analysis (PCA) plot showing the distribution of subjects along 3 eigenvectors.
The plot showing two distinct groups, the first group formed from Vehicle (CON) 0 .001 DMSO, GPR40 agonist (AGO) 100nM AZ921, GPR40 antagonist 5μM AZ836 with the agonist (AGOANT)and the second group includes the antagonist groups (cells cultured in 5% fatty acid free medium (ANTFFA) or 6%horse (ANTH) serum medium). Samples were displayed in respect to the first components and coloured by the treatment parameter. (4-5 flasks from 1 subject)

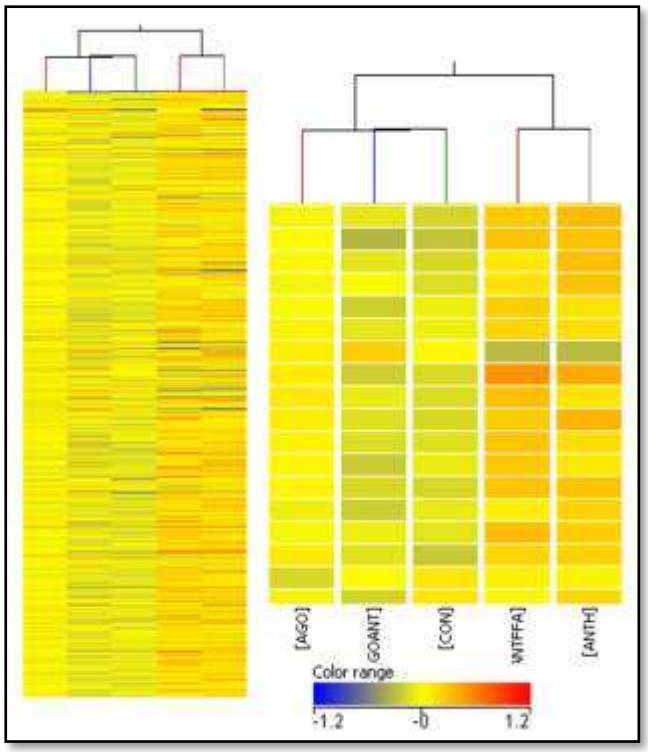

Figure 5-29: Dendrogram showing the hierarchical cluster analysis of gene expression profile. The agonist, the agonist with the antagonist and the vehicle clustering in one group and the antagonist form another group. Each row corresponds to a single gene, and each column corresponds to a single condition. The branch lengths indicate the correlation with which genes or samples were joined, with longer branches indicating a lower correlation. Color represents different transcript expression levels.

5.5.10.2. The effect of GPR40 agonists and antagonists on gene expression profiles

Treatment of human myotubes with 100nM AZ921 for 24 hours did not appear to produce significant differences in gene expression. When applying a two fold cut off change (agonist vs vehicle), $p<0.05$ and the Benjamini-Hochberg multiple testing comparison, only 4 transcripts appeared to be significantly up regulated; MALAT1 (metastasis associated lung adenocarcinoma transcript 1), CENPF (centromere protein F), AHSA2 (activator of heat shock protein ATPase homolog 2) and NEAT (nuclear paraspeckle assembly transcript Applying 1.5 fold change cut off (agonist vs vehicle), 154 transcripts were found to be statistically significantly altered (appendix 6). These transcripts were then

uploaded into the Ingenuity pathway (IPA) software in order to identify metabolic processes and signalling pathways that may be influenced by the activation of GPR40. The IPA network function analysis revealed that most genes in this data set are associated with cell cycle and cellular assembly and organization network. However, there were no significant canonical pathways. As the z score was insignificant, no prediction states could be addressed in downstream and upstream regulators. Almost similar results were found when the gene differences between the effects of the agonist/antagonist in the human myotubes were compared to vehicle. The 64 transcripts with a fold change of 1.5 showed no significant pathways or prediction states as the Z-score was insignificant. The PCA blot and the hierarchical clustering showed the similarities between the agonist, antagonist with agonist and vehicle.

A confirmation of GPR40 agonist effect on the metabolic genes was done by using Taqman® Low-Density Custom Array using Micro Fluidic cards (ABI Applied Bio systems, UK) where a quantification of expression of 45 key metabolic genes in human skeletal muscle genes including; transcriptional activators, cells signalling proteins, substrate transporters, lipogenic enzymes, and proteins catalysing glucose and fat oxidation. As listed in Table 5-1 most genes had a fold change of <1.5 except PDK4 (pyruvate dehydrogenase kinase, isozyme 4) and PYGM (phosphorylase glycogen, muscle) which had a fold change of 1.6 and -1.5, respectively. It is worth mentioning that the RT-PCR showed no significant difference on PDK4 expression between the GPR40 agonist and the vehicle Figure 5-27.

Table 5-1: Gene card analysis for the effect of the GPR40 agonist on the metabolic genes

ID	Fold Change	Entrez Gene Name	Location	Type(s)
PDK4	1.615	pyruvate dehydrogenase kinase, isozyme 4	Cytoplasm	kinase
MLXIPL	1.239	MLX interacting protein-like	Nucleus	transcription regulator
SURF1	1.155	surfeit 1	Cytoplasm	enzyme
NR1H3	1.132	nuclear receptor subfamily 1, group H, member 3	Nucleus	ligand-dependent nuclear receptor
IRS1	1.124	insulin receptor substrate 1	Cytoplasm	enzyme
TALDO1	1.118	transaldolase 1	Cytoplasm	enzyme
ACADL	1.092	acyl-CoA dehydrogenase, long chain	Cytoplasm	enzyme
HMBS	1.092	hydroxymethylbilane synthase	Cytoplasm	enzyme
PPP1CC	1.056	protein phosphatase 1, catalytic subunit, gamma isozyme	Cytoplasm	phosphatase
PIK3R1	1.044	phosphoinositide-3-kinase, regulatory subunit 1 (alpha)	Cytoplasm	kinase
HK2	1.041	hexokinase 2	Cytoplasm	kinase
DGAT1	1.014	diacylglycerol O-acyltransferase 1	Cytoplasm	enzyme
NDUFS4	-1.015	NADH dehydrogenase (ubiquinone) Fe-S protein 4, 18kDa	Cytoplasm	enzyme
GYG1	-1.038	glycogenin 1	Cytoplasm	enzyme
LDHB	-1.044	lactate dehydrogenase B	Cytoplasm	enzyme
SCD	-1.055	stearoyl-CoA desaturase (delta-9-desaturase)	Cytoplasm	enzyme
FOXO3	-1.067	forkhead box O3	Nucleus	transcription regulator
DGKA	-1.073	diacylglycerol kinase, alpha 80kDa	Cytoplasm	kinase
APOE	-1.076	apolipoprotein E	Extracellular Space	transporter
SDHB	-1.081	succinate dehydrogenase complex, subunit B, iron sulfur (Ip)	Cytoplasm	enzyme
SREBF1	-1.086	sterol regulatory element binding transcription factor 1	Nucleus	transcription regulator
DGKD	-1.098	diacylglycerol kinase, delta 130kDa	Cytoplasm	kinase
COX7A2	-1.099	cytochrome c oxidase subunit VIIa polypeptide 2 (liver)	Cytoplasm	enzyme
TKT	-1.099	transketolase	Cytoplasm	enzyme
FOXO1	-1.108	forkhead box O1	Nucleus	transcription regulator
NR1H2	-1.110	nuclear receptor subfamily 1, group H, member 2	Nucleus	ligand-dependent nuclear receptor
PDK2	-1.112	pyruvate dehydrogenase kinase, isozyme 2	Cytoplasm	kinase
IRS2	-1.121	insulin receptor substrate 2	Cytoplasm	enzyme
PDP2	-1.139	pyruvate dehyrogenase phosphatase catalytic subunit 2	Cytoplasm	phosphatase
ALDOA	-1.141	aldolase A, fructose-bisphosphate	Cytoplasm	enzyme
G6PD	-1.145	glucose-6-phosphate dehydrogenase	Cytoplasm	enzyme
ABCA1	-1.152	ATP-binding cassette, sub-family A (ABC1), member 1	Plasma Membrane	transporter
CPT1B	-1.156	carnitine palmitoyltransferase 1B (muscle)	Cytoplasm	enzyme
AKT2	-1.180	v-akt murine thymoma viral oncogene homolog 2	Cytoplasm	kinase
SLC2A4	-1.183	solute carrier family 2 (facilitated glucose transporter), member 4	Plasma Membrane	transporter
SLC27A1	-1.189	solute carrier family 27 (fatty acid transporter), member 1	Plasma Membrane	transporter
PFKM	-1.193	phosphofructokinase, muscle	Cytoplasm	kinase
PPM2C	-1.209	pyruvate dehyrogenase phosphatase catalytic subunit 1	Cytoplasm	phosphatase
ADFP	-1.222	perilipin 2	Plasma Membrane	other
ACACB	-1.277	acetyl-CoA carboxylase beta	Cytoplasm	enzyme
ACLY	-1.294	ATP citrate lyase	Cytoplasm	enzyme
CD36	-1.300	CD36 molecule (thrombospondin receptor)	Plasma Membrane	transmembrane receptor
FASN	-1.301	fatty acid synthase	Cytoplasm	enzyme
PPARGC1	-1.381	peroxisome proliferator-activated receptor gamma, coactivator 1 alpha	Nucleus	transcription regulator
PKM2	-1.387	pyruvate kinase, muscle	Cytoplasm	kinase
PYGM	-1.508	phosphorylase, glycogen, muscle	Cytoplasm	enzyme

GPR40 Antagonist effects, Human myotubes were treated with GPR40 antagonist AZ836 for 24 hours in Ham-F 10 media containing 5% free fatty acid serum or 6% horse serum to study global gene change in the presence and absence of fatty acids. There was no significant difference in the transcripts between the two conditions (FFA serum and Horse serum). Applying a 2 fold change (antagonist vs vehicle) with unpaired TTEST with correction (Benjamin-Hochberg) showed 178 regulated transcripts. The transcripts were then loaded into the IPA where all species, molecules and/or relationships were considered. IPA analysis showed that most genes are associated with development and cell death and survival in the downstream functions however the Z-score was insignificant. The upstream regulators and canonical pathways were also with insignificant z score or with bias.

Further analysis of transcripts (2538) with a fold change of 1.5 and multiple correction test (FDR) were carried out. In the biological functions (Table 5-2), large numbers of genes were associated with cell cycle, cell death and survival, cell assembly and organization and development disorder. Prediction of activation with Z-score ≥2 were found in cell survival, proliferation of cells, organization of cytoplasm and cytoskeletal, cell growth, differentiation of cells and cell movement. Predictions of inhibition were associated with the following functions annotation: apoptosis, organismal death, congenital anomalies, developmental disorders and growth failure (Table 5-4). The number of genes associated with metabolism was low and their functions were not predictable. The function networks and the canonical pathways had insignificant Z score or with bias. Interesting findings were found when the upstream regulators with significant bias corrected Z- score were correlated with functions which also have significant Z score. The analysis was carried out as follows:

1. The genes which are responsible for functions with significant Z scores were identified.

2. The upstream regulators with significant bias corrected Z score were identified (Table 5-3).
3. Correlation of downstream genes for the upstream regulators with the significant functions (Table 5-4).
4. Ranking of the genes with significant functions involved in the upstream.
5. Further analysis of some upstream regulators from different types with high bias corrected Z scores was carried (Table 5-5).

The upstream regulators ERBB2, PPARD, MAPK8 (JUNC1) and IL3 were further analysed. In all these regulators the highest number of downstream transcripts was associated with cell proliferation (70%, 57%, 82% and 80%). Other significant functions such as organization of cytoskeletal, cell survival, cell movement and cell differentiation also have a considerable numbers of downstream transcripts (Table 5-4). A closer look for genes regulated by ERBB2 revealed that most genes which have a role of cell proliferation and survival were upregulated such as (BCL2, HES1, HES2, LTBP3, NOTCH1, TNC, ERBB3, ESR1, ESR2, ETV6 and MAPKBP3) while genes arrest cell cycle and inhibit proliferation were down regulated (RECK, PDCD4, ITGA2, CUL3, CDKNIB, CAPZA2, DPT & JAG1) (Table 5-5). The transcription factor PPARD (peroxisome proliferator-activated receptor delta) was predicted to be activated as most downstream transcripts in the data set which are regulated by PPARD were activated. Most of PPARD downstream transcripts were associated with fatty acid metabolism however BCL2 (antiapoptotic factor) were among them. BCL2 and CDKNIB (cyclin-dependent kinase inhibitor) were downstream transcripts of MAPK8 (JUNC1). The up regulated cytokines IL3 is a potent growth promoting cytokines which has a role in cell proliferation and cell death and survival. The anti-apoptotic factors BCL2, ATF (activation transcription factor) as well as CDKNIB were among downstream transcripts of IL3 (Table 5-5).

Table 5-2: The biological functions ascribed to genes that were altered by treatment with GPR40 antagonist.

	Category	Functions Annotation	Activation z-score	p-Value	Predicted Activation State	# Molecules
1	Cellular Movement	cell movement	4.685	1.40E-07	Increased	359
2	Cell Death and Survival	cell survival	4.64	1.02E-07	Increased	250
3	Gene Expression	transactivation	4.289	4.16E-05	Increased	119
4	Cellular Development	differentiation of cells	4.149	3.15E-05	Increased	339
5	Cellular Growth and Proliferation	proliferation of cells	3.718	1.34E-11	Increased	630
6	Inflammatory Response	phagocytosis	3.599	3.70E-03	Increased	50
7	Cellular Function and Maintenance	organization of cytoplasm	3.22	1.03E-09	Increased	263
8	Cellular Function and Maintenance	organization of cytoskeleton	3.16	9.42E-09	Increased	240
9	Post-Translational Modification	phosphorylation of protein	3.091	2.00E-03	Increased	129
10	Immune Cell Trafficking	adhesion of lymphocytes	3.084	1.21E-03	Increased	25
11	Cellular Movement	cell movement of tumor cell lines	2.921	6.16E-03	Increased	121
12	Cell Morphology	formation of cellular protrusions	2.742	2.85E-07	Increased	151
13	Cellular Function and Maintenance	microtubule dynamics	2.729	3.70E-09	Increased	211
14	Cellular Movement	invasion of cells	2.67	3.86E-03	Increased	124
15	Cardiovascular System Development and Function	development of vascular system	2.665	5.71E-09	Increased	208
16	Behavior	behavior	2.577	3.67E-06	Increased	179
17	Hematological System Development and Function	differentiation of blood cells	2.49	2.66E-03	Increased	133
18	Cellular Function and Maintenance	endocytosis	2.421	2.68E-05	Increased	57
19	Cellular Development	differentiation of endothelial cells	2.326	3.84E-03	Increased	24
20	Connective Tissue Development and Function	proliferation of fibroblast cell lines	2.288	3.51E-04	Increased	81
21	Cellular Function and Maintenance	cellular homeostasis	2.287	5.59E-04	Increased	237
22	Small Molecule Biochemistry	quantity of cyclic nucleotides	2.28	5.75E-03	Increased	37
23	Tissue Development	skin development	2.198	2.03E-03	Increased	49
24	Cell Death and Survival	cell viability of tumor cell lines	2.161	2.37E-05	Increased	134
25	Gene Expression	expression of RNA	2.074	9.31E-08	Increased	384
26	Cell-To-Cell Signaling and Interaction	interaction of lymphocytes	2.034	2.46E-03	Increased	22
27	Cellular Growth and Proliferation	proliferation of epithelial cells	2.001	4.31E-03	Increased	70
28	Organismal Injury and Abnormalities	injury of lung	-2.067	5.04E-03	Decreased	23
29	Cardiovascular Disease	Cardiac Fibrosis	-2.139	8.00E-04	Decreased	26
30	Cell Death and Survival	apoptosis of hematopoietic cell lines	-2.622	1.51E-03	Decreased	42
31	Cardiovascular Disease	Hypertension	-2.784	1.85E-03	Decreased	59
32	Cardiovascular Disease	Heart Disease	-2.973	4.84E-04	Decreased	167

Table 5-3: The upstream regulators

Symbol	z scor	Entrez Gene Name	Type(s)
ERBB2	4.168	v-erb-b2 erythroblastic leukemia viral oncogene homolog 2	kinase
BDNF	3.505	brain-derived neurotrophic factor	growth factor
IL3	3.489	interleukin 3 (colony-stimulating factor, multiple)	cytokine
Ins1	3.372	insulin I	other
PPARD	3.326	peroxisome proliferator-activated receptor delta	ligand-dependent nuclear receptor
CEBPB	3.256	CCAAT/enhancer binding protein (C/EBP), beta	transcription regulator
MAPK8	3.124	mitogen-activated protein kinase 8	kinase
TCF3	3.067	transcription factor 3	transcription regulator
STAT5B	2.809	signal transducer and activator of transcription 5B	transcription regulator
RUNX2	2.7	runt-related transcription factor 2	transcription regulator
FGF7	2.671	fibroblast growth factor 7	growth factor
MAPK1	2.582	mitogen-activated protein kinase 1	kinase
AKT1	2.577	v-akt murine thymoma viral oncogene homolog 1	kinase
STAT5A	2.561	signal transducer and activator of transcription 5A	transcription regulator
IL12A	2.548	interleukin 12A (natural killer cell stimulatory factor 1)	cytokine
NR1H3	2.42	nuclear receptor subfamily 1, group H, member 3	ligand-dependent nuclear receptor
ADORA2A	2.228	adenosine A2a receptor	G-protein coupled receptor
HMOX1	2.142	heme oxygenase (decycling) 1	enzyme
FABP4	-2	fatty acid binding protein 4, adipocyte	transporter
KIAA1524	-2.121	KIAA1524	other
ACACB	-2.213	acetyl-CoA carboxylase beta	enzyme
IFNB1	-2.227	interferon, beta 1, fibroblast	cytokine
IRF4	-2.383	interferon regulatory factor 4	transcription regulator
FGF19	-2.401	fibroblast growth factor 19	growth factor

Table 5-4: The biological function releated to the upstream regulators

Upstream Regulator (# downstream transcripts)	Rank (out of 42413)	Cellular Growth and Proliferation	Cellular Function and Maintenance	Cell Death and Survival	Cellular Movement	Cellular Development
		proliferation of cells	organization of cytoskeleton	cell survival	cell movement	differentiation of cells
ERBB2 (69)	11117	48	16	28	37	35
		70%	23%	41%	54%	51%
PPARD (23)	3793	13	6	6	8	9
		57%	26%	26%	35%	39%
MAPK8 (17)	1162	14	6	10	14	8
		82%	35%	59%	82%	47%
IL3 (45)	26439	36	15	17	22	25
		80%	33%	38%	49%	56%

Table 5-5: list of downstream transcripts of the activated upstream regulators ERBB2, PPARD, MAPK8 and Il3

Sympol	Rank (out of 42413)	fold change	Entrez Gene Name
ERBB2			
ABHD5	2541	-1.700	abhydrolase domain containing 5
ACAA2	14630	2.279	acetyl-CoA acyltransferase 2
ADAM8	32890	1.944	ADAM metallopeptidase domain 8
AHNAK	3176	1.780	AHNAK nucleoprotein
ANGPTL4	39127	1.885	angiopoietin-like 4
BACE1	18802	1.643	beta-site APP-cleaving enzyme 1
BARD1	6884	-1.521	BRCA1 associated RING domain 1
BCL2	21143	1.767	B-cell CLL/lymphoma 2
BMP7	30496	1.545	bone morphogenetic protein 7
CAPZA2	1626	-1.516	capping protein (actin filament) muscle Z-line, alpha 2
CDC42SE1	9613	1.578	CDC42 small effector 1
CDKN1B	74	-1.751	cyclin-dependent kinase inhibitor 1B (p27, Kip1)
CDKN2B	934	1.599	cyclin-dependent kinase inhibitor 2B (p15, inhibits CDK4)
COL1A1	12590	1.965	collagen, type I, alpha 1
CSF2	6181	1.520	colony stimulating factor 2 (granulocyte-macrophage)
CUL3	385	-2.206	cullin 3
CYB561	862	1.569	cytochrome b561
DPT	40	-2.054	dermatopontin
DZIP3	2688	-1.632	DAZ interacting protein 3, zinc finger
EDN1	259	-1.708	endothelin 1
ERBB3	1604	1.539	v-erb-b2 erythroblastic leukemia viral oncogene homolog 3 (avian)
ESR1	9062	1.729	estrogen receptor 1
ESR2	19888	1.724	estrogen receptor 2 (ER beta)
ETV6	546	1.691	ets variant 6
FASN	13229	1.575	fatty acid synthase
FOLR1	39796	1.730	folate receptor 1 (adult)
GNAI1	971	-1.727	guanine nucleotide binding protein (G protein), alpha inhibiting activity polypeptide 1
GPC1	31733	1.566	glypican 1
HBB	31701	1.546	hemoglobin, beta
HES1	28725	2.367	hairy and enhancer of split 1, (Drosophila)
HES2	31636	1.657	hairy and enhancer of split 2 (Drosophila)
HMGB2	12249	1.603	high mobility group box 2
IGF2R	8473	1.525	insulin-like growth factor 2 receptor
IGFBP5	2098	1.604	insulin-like growth factor binding protein 5
ITGA2	2297	-1.587	integrin, alpha 2 (CD49B, alpha 2 subunit of VLA-2 receptor)
ITGB1	4594	1.540	integrin, beta 1 (fibronectin receptor, beta polypeptide, antigen CD29 includes MDF2, MSK12)
JAG1	50	-1.519	jagged 1
KIFC3	10791	1.694	kinesin family member C3
KLK3	22064	1.512	kallikrein-related peptidase 3
LTBP3	3266	1.759	latent transforming growth factor beta binding protein 3
MAP1B	38828	1.939	microtubule-associated protein 1B
MAPK8IP3	17850	1.546	mitogen-activated protein kinase 8 interacting protein 3
MARCKS	8273	1.622	myristoylated alanine-rich protein kinase C substrate
MMP11	23175	1.577	matrix metallopeptidase 11 (stromelysin 3)
MMP13	28630	1.554	matrix metallopeptidase 13 (collagenase 3)
MYBL2	40936	1.619	v-myb myeloblastosis viral oncogene homolog (avian)-like 2

Table 5-5: (Continued)

Sympol	Rank (out of 42413)	fold change	Entrez Gene Name
MYCN	8252	1.658	v-myc myelocytomatosis viral related oncogene, neuroblastoma derived (avian)
NDUFV1	19232	1.632	NADH dehydrogenase (ubiquinone) flavoprotein 1, 51kDa
NEDD9	58	-1.599	neural precursor cell expressed, developmentally down-regulated 9
NFKB2	26777	1.577	nuclear factor of kappa light polypeptide gene enhancer in B-cells 2 (p49/p100)
NOTCH1	6928	1.553	notch 1
NRBP1	27326	1.553	nuclear receptor binding protein 1
PDCD4	413	-1.538	programmed cell death 4 (neoplastic transformation inhibitor)
PDLIM4	4760	1.717	PDZ and LIM domain 4
PHLDB1	20337	1.501	pleckstrin homology-like domain, family B, member 1
PTPRB	532	1.551	protein tyrosine phosphatase, receptor type, B
RAD51AP1	4159	-1.585	RAD51 associated protein 1
RECK	398	-1.504	reversion-inducing-cysteine-rich protein with kazal motifs
SMAD2	805	-1.506	SMAD family member 2
SOX4	18098	1.766	SRY (sex determining region Y)-box 4
SPDEF	32544	1.838	SAM pointed domain containing ets transcription factor
SQLE	4228	1.841	squalene epoxidase
TAPBP	5601	1.531	TAP binding protein (tapasin)
TGM1	36781	1.504	transglutaminase 1 (K polypeptide epidermal type I, protein-glutamine-gamma-glutamyltransferase)
TNC	8987	1.619	tenascin C
TSC22D1	6000	-1.515	TSC22 domain family, member 1
VWF	33081	1.550	von Willebrand factor
ZEB1	4497	-1.512	zinc finger E-box binding homeobox 1
ZFP36L2	12914	1.568	ZFP36 ring finger protein-like 2
PPARD			
ACSL6	14686	1.522	acyl-CoA synthetase long-chain family member 6
ADORA1	21524	1.751	adenosine A1 receptor
ANGPTL4	39127	1.885	angiopoietin-like 4
APOE	15270	1.588	apolipoprotein E
BCL2	21143	1.767	B-cell CLL/lymphoma 2
C10orf35	40329	1.536	chromosome 10 open reading frame 35
DNASE1L2	39735	1.596	deoxyribonuclease I-like 2
FAM131C	35062	1.524	family with sequence similarity 131, member C
FASN	13229	1.575	fatty acid synthase
LGALS4	34618	1.588	lectin, galactoside-binding, soluble, 4
LIPE	14721	1.503	lipase, hormone-sensitive
MDFI	38204	1.577	MyoD family inhibitor
MERTK	15837	1.539	c-mer proto-oncogene tyrosine kinase
MFGE8	27161	1.552	milk fat globule-EGF factor 8 protein
PDE4C	25508	1.749	phosphodiesterase 4C, cAMP-specific
PKLR	37387	1.729	pyruvate kinase, liver and RBC
PNPLA2	22659	1.897	patatin-like phospholipase domain containing 2
PPARD	3793	1.650	peroxisome proliferator-activated receptor delta
SCD	2975	1.680	stearoyl-CoA desaturase (delta-9-desaturase)
SFI1	3393	1.534	Sfi1 homolog, spindle assembly associated (yeast)
SIRT5	9246	1.592	sirtuin 5

Table 5-5: (Continued)

Sympol	Rank (out of 42413)	fold change	Entrez Gene Name
MAPK8			
ABCA1	16186	1.531	ATP-binding cassette, sub-family A (ABC1), member 1
ADARB1	4234	1.690	adenosine deaminase, RNA-specific, B1
APOE	15270	1.588	apolipoprotein E
B4GALT1	8289	1.634	UDP-Gal:betaGlcNAc beta 1,4- galactosyltransferase, polypeptide 1
BCL2	21143	1.767	B-cell CLL/lymphoma 2
CDKN1B	74	-1.751	cyclin-dependent kinase inhibitor 1B (p27, Kip1)
COL1A1	12590	1.965	collagen, type I, alpha 1
FASLG	27081	1.746	Fas ligand (TNF superfamily, member 6)
FUS	25083	1.663	fused in sarcoma
HDAC6	21612	1.643	histone deacetylase 6
HMOX1	41664	1.503	heme oxygenase (decycling) 1
LHB	41626	1.550	luteinizing hormone beta polypeptide
MMP13	28630	1.554	matrix metallopeptidase 13 (collagenase 3)
MTHFR	18698	1.687	methylenetetrahydrofolate reductase (NAD(P)H)
NPPB	36493	1.628	natriuretic peptide B
PPARD	3793	1.650	peroxisome proliferator-activated receptor delta
IL3			
ATF5	14193	2.008	activating transcription factor 5
BCL2	21143	1.767	B-cell CLL/lymphoma 2
BRD4	9200	1.695	bromodomain containing 4
CALR	7641	1.647	calreticulin
CD86	18463	1.502	CD86 molecule
CDKN1B	74	-1.751	cyclin-dependent kinase inhibitor 1B (p27, Kip1)
CITED2	20	-1.698	Cbp/p300-interacting transactivator, with Glu/Asp-rich carboxy-terminal domain, 2
CREM	545	-1.860	cAMP responsive element modulator
CSF2	6181	1.520	colony stimulating factor 2 (granulocyte-macrophage)
CTLA4	21903	1.658	cytotoxic T-lymphocyte-associated protein 4
DOK2	41089	1.554	docking protein 2, 56kDa
EIF1AY	238	-1.511	eukaryotic translation initiation factor 1A, Y-linked
ELAVL3	21278	1.792	ELAV (embryonic lethal, abnormal vision, Drosophila)-like 3 (Hu antigen C)
ELK4	12144	1.520	ELK4, ETS-domain protein (SRF accessory protein 1)
FASN	13229	1.575	fatty acid synthase
FUS	25083	1.663	fused in sarcoma
GADD45B	8746	1.540	growth arrest and DNA-damage-inducible, beta
GNA13	4528	-1.552	guanine nucleotide binding protein (G protein), alpha 13
GPRIN1	35608	1.691	G protein regulated inducer of neurite outgrowth 1
HNF1A	25673	1.551	HNF1 homeobox A
HNF4A	17649	1.657	hepatocyte nuclear factor 4, alpha
HNRNPA2B1	28705	1.658	heterogeneous nuclear ribonucleoprotein A2/B1
HSP90B1	8246	1.525	heat shock protein 90kDa beta (Grp94), member 1
IL3RA	26750	1.561	interleukin 3 receptor, alpha (low affinity)
ITGB7	38078	1.691	integrin, beta 7
KLF9	2909	-1.516	Kruppel-like factor 9
MID1	857	-1.766	midline 1 (Opitz/BBB syndrome)
NEDD9	58	-1.599	neural precursor cell expressed, developmentally down-regulated 9
NOTCH1	6928	1.553	notch 1
OSM	14303	1.551	oncostatin M
PAPPA2	903	1.709	pappalysin 2
PFKL	31867	1.517	phosphofructokinase, liver
PIWIL1	38444	1.524	piwi-like RNA-mediated gene silencing 1
PROX1	27589	1.795	prospero homeobox 1
RB1	688	-1.640	retinoblastoma 1
RPL7	10007	1.845	ribosomal protein L7
RPS12	19618	1.767	ribosomal protein S12
SH3BP1	27923	1.531	SH3-domain binding protein 1
SMAD5	4356	1.642	SMAD family member 5
SOCS3	11892	1.621	suppressor of cytokine signaling 3
SOX4	18098	1.766	SRY (sex determining region Y)-box 4
SPI1	34675	1.720	spleen focus forming virus (SFFV) proviral integration oncogene spi1
TAX1BP1	446	-1.860	Tax1 (human T-cell leukemia virus type I) binding protein 1
VAV2	12604	1.839	vav 2 guanine nucleotide exchange factor
WNK1	25979	1.674	WNK lysine deficient protein kinase 1

5.6. Discussion

There is a gathering body of evidence linking elevated FFA and the development of insulin resistance. The pathology of insulin resistance is complex and it must be multifactorial. The possibility that the activation or the inhibition of the GPR40 receptor may play a part in the role of FFAs in insulin resistance has sparked considerable interest in the experimentation on this receptor, from basic research to potential drug discovery efforts. The roles of GPR40 in the pancreas have been extensively studied (Wu et al. 2010; Tsujihata et al. 2011;Doshi et al. 2009) however, the relationship between the well-documented detrimental chronic effects of fatty acids on pancreatic islets and GPR40 is under debate. Steneberg et al. (2005) suggests that GPR40 mediates both the acute and chronic effects of FFAs in pancreatic islet and that antagonist rather than agonist might be useful in diabetes treatment while Tan et al. (2008) and Costanzi et al. (2008) suggest that an agonist could be useful in treatment of diabetes. Hence, GPR40 antagonists or agonists may represent a useful therapeutic strategy for the prevention and treatment of obesity-associated type 2 diabetes. Given the number of fatty acids that are agonists for GPR40 it is conceivable that the physiologically relevant FFAs for GPR40 may vary in a tissue dependent fashion. As skeletal muscle plays a core role in glucose disposal and insulin resistance, the goal of this study was to characterise the mechanisms of action and the functionality of GPR40 receptor in human and rat skeletal muscle at the molecular level.

5.6.1. Characterization of GPR40 in human and rat skeletal muscle tissue and cultured cells

The expression of GPR40 is well documented in pancreas however its expression in other tissues is controversial. In this study, microarray and RT-PCR

data revealed the expression of GPR40 in human skeletal muscle tissue and primary cultured cells. This is in agreement with Kotarsky et al. (2003) and Briscoe et al. (2003) who reported the expression of GPR40 in human skeletal muscle by using Northern blot and RT-PCR, respectively. The RT-PCR data showed a higher level of GPR40 mRNA expression in myoblasts in comparison to myotubes and tissue. Human brain and spleen tissues also expressed GPR40 in agreement with Swaminath (2008), Brownlie et al. (2008) and Hirasawa et al. (2008).

The expression of GPR40 is not only tissue specific but may also be species specific. Rat RT-PCR data showed the expression of GPR40 mRNA in Wistar rat fast and slow muscle fibres without any significant difference between the two types. In contrast, Steneberg et al. (2005) and Itoh et al. (2003) could not find GPR40 mRNA expression in either mouse or rat skeletal muscle tissue. GPR40 expression was also found in rat pancreas, spleen, adipose, heart and liver but not in rat brain in agreement with Itoh et al. (2003) and Brownlie et al. (2008). Decrease in GPR40 expression in high fat diet fed mice (11 weeks) was observed by Kebede et al. (2012) while Briscoe et al. (2003) detected a significant increase in expression of GPR40 mRNA in whole pancreas of ob/ob mice compared with control lean mice. In the current study, expression levels of GPR40 were similar at 12 weeks for Zucker fat Rat (ZFR) and Zucker Lean Rat (ZLR), however at 20 weeks ZFR had a significantly ($p<0.01$) higher expression of GPR40 than ZLR. Interstingly, ZFR and ZLR slow (SOL) and mixed (VL) muscle fibres but not the fast (GR and EDL) had higher expression of GPR40 compared to Wistar rats muscle fibres. This may indicate strain specific differences and a relationship between GPR40 expression and insulin sensitivity as slow fibres are more sensitive to insulin. Cultured myotubes from ZFR, ZLR and Wistar rats had no significant difference in GPR40 expression. Insulin

resistance has previously been shown to disappear in cultured myotubes from obese and diabetic patients (Sell et al. 2008; Pender et al. 2005; Brozinick et al. 2003) indicating that removal from the obese environment restores normal insulin signalling to cultured cells. Hence, the cells were cultured in high (25mM) glucose for 6 and 24 hours. Interestingly, cells cultured in 25mM glucose had a significantly higher level of GPR40 expression. Kebede et al. (2012) also observed a higher GPR40 mRNA expression in human and rat pancreatic islets cultured in high glucose and they concluded that the main effect of glucose on GPR40 expression does not lie at the level of mRNA stability but, rather, at the transcriptional level. Moreover, the addition GPR40 ligand for 6 hours, led to a significant down-regulation of cell surface expressed GPR40, presumably via receptor-specific internalization (Kaplamadzhiev et al. 2010; Hu et al. 2009). Expression of the GPR40 has also been shown to be reduced under glucolipotoxic conditions in rats (Fontés et al. 2010) and in islets from T2D patients (Del Guerra et al. 2010). Therefore, further investigation is needed to determine the mechanisms involved in the effects of high glucose as well as GPR40 ligands on GPR40 mRNA expression in skeletal muscle.

5.6.2. Effector mechanisms

A gathering body of evidence suggests that the GPR40 receptor couples to the Gαq/11 subunit of G protein (Shapiro et al. 2005; Tan et al. 2008). MAPK activation can occur downstream of signaling pathways initiated by receptors coupled to either Gi or Gq (Itoh et al. 2003; Kotarsky et al. 2003). Studying the signalling mechanisms downstream of GPR40, we found that PTX (Gi inhibitor) significantly decreased MAPK phosphorylation induced by GW9508 and oleic acid suggesting that GPR40 is a Gi coupled receptor in skeletal muscle. In support of this finding are the studies conducted by Fujita et al. (2011), Hidalgo et al.

(2011) and Yonezawa et al. (2008) who found that activation of GPR40 was PTX sensitive in skin, PTX decreased calcium release in bovine neutrophils and decreased cAMP production in bovine mammary epithelial cell, respectively. In this study PTX only partially decreased the ERK1/2 phosphorylation induced by AZ921 suggesting that GPR40 may not only be Gi coupled in skeletal muscle. Itoh et al. (2003) found that GPR40 activation in CHO cells transfected with human GPR40 decreased cAMP production with no effect of PTX, a finding which was not detected in CHO cells transfected with mouse GPR40 suggesting that human GPR40 couples mainly with Gq and partially with Gi However, mouse GPR40 couples with Gq only in CHO cells indicating species difference in the coupling of GPR40 with G proteins. Furthermore, research by 2012 Nobel Laureate in Chemistry Robert J. Lefkowitz and his colleagues has clearly demonstrated that 7TMRs can couple to multiple heterotrimeric G proteins as well as to G protein-independent and/or dependent pathways to promote the activation of numerous signaling cascades in a ligand and context dependent manner (Mancini & Poitout 2013).

Stimulation of calcium release via receptor coupling to Gq with subsequent activation of phospholipase C and release of IP3 is frequently use as a functional read out. However, stimulation of calcium release via coupling to Gi in an IP3-independent manner has been reported by Dorn et al, (1997). In this study 1μM GW9508 and 3 μM AZ921 were used to evaluate the role of GPR40 in calcium release in Wistar rat myotubes and myoblasts cultured in 6mM or 25mM glucose. Neither GW9508 nor AZ921 had any effect on intracellular calcium release. As a reduction of expression in cultured cells of genes involved in calcium signalling was detected by our microarray data (chapter 3) we used 10 μM ATP as a positive control. ATP produced a rapid response even though microarray data showed a low expression of the ryanodine receptors in cultured myotube and

myoblast compare to skeletal muscle tissue. The increase in calcium release upon GPR40 activation in β cells is well documented. The elevation of intracellular calcium in β cells occurs not only through a PLC pathway but also through L-type calcium channels and β cell secretagogues which have little or no effect in the presence of low concentrations of glucose (Fujiwara et al. 2005; Yonezawa et al. 2004; Yonezawa et al. 2008). Induction of calcium release from other cell types has also been reported, e.g. oleic acid (500μM) and GW9508 (50μM) induced calcium release in bovine neutrophil and HEK-GPR40 cells (Hidalgo et al. 2011). In this study GW9508 was used as the potency of GW9508 (pE_{C50} 7.32±0.03) was greater than that observed for the long chain fatty acid linoleic acid (pE_{C50} 5.65±0.06) (Briscoe et al. 2006). The discrepancy between our results and certain previous reports might be explained by the complexity of the role of the FFAs on calcium release in skeletal muscle (Gamberucci et al. 2003), the dependence on high glucose levels in other tissue types (Berchtold et al. 2000), the very high concentrations of GPR40 agonists used by some researchers (Hidalgo et al. 2011) and/or the type of cell used. Moreover, increased calcium release by oleic and linoleic acids in primary mouse β cells and INS1 cells was reported by (Schnell et al. 2007) however Briscoe et al. (2006) were able to observe increases in calcium release in GPR40-expressing HEK-293 cells but not in isolated rat or mouse islets following incubation with GW9508. Collectively, this indicates that physiological differences between the cell lines and primary cells could be contributory factors.

5.6.3. Functionality of skeletal muscle GPR40

The functionality of GPR40 was investigated by assessing the direct effect of the endogenous GPR40 agonists (oleic and palmitic acids), synthetic agonists (GW9508 and AZ921) and synthetic antagonists (AZ915, AZ836 and AZ468) on

the activation of key proteins involved in insulin signalling cascades in human and rat (Wistar and Zucker) myotubes. The main findings from these experiments showed that time course treatment with 10nM GW9508 and 250μM oleic but not palmitic acid induced ERK1/2 phosphorylation in human, Wistar rat, ZLR and ZFR myotubes. Time course treatment with 100nM AZ921 also induced ERK1/2 phosphorylation in both human and rat myotubes. The MEK inhibitor (10 μM U0126) abolished the effects of all agonists while the GPR40 antagonist (AZ836 and AZ468) decreased the induction produced by AZ921 only. This may indicate that the agonists work through different sites. Even though this study is the first study to investigate the role of GPR40 in skeletal muscle, the results are in line with previous reports in other cell types. Zhang et al. (2007) indicated that oleate but not palmitate could activate ERK1/2 via GPR40 in mouse β-cell line NIT-1. Itoh et al. (2003) found that oleic acid increased ERK1/2 phosphorylation in Chinese hamster ovary (CHO) transfected with human GPR40. The effect of the AZ antagonists on AZ921 suggests that the specificity of the Astra Zeneca compounds is limited to activation by certain ligands only. This is in general agreement with previous studies, Briscoe et al. (2006) reported that the GPR40 antagonist GW1100 prevented the effects of GW9508 but not linoleic acid on GPR40. Hu et al. (2009) reported that the antagonist DC26126 decreased ERK phosphorylation induced by oleic and linolelic acid in GPR40 expressing CHO cells. The effect of GPR40 agonists on MAPK38 was different to those observed with ERK as GW9508 only induced MAPK38 phosphorylation in agreement with Zhang et al. (2007) and Yonezawa et al. (2008) who reported that oleate had no effect on phosphorylation of Jun and MAPK38. This apparent discrepancy between effects of different FFAs is most likely attributable to activation of distinct allosteric sites on the receptor by different molecules. Interestingly, Lin et al. (2012) described three novel GPR40

allosteric agonists that bind to separate sites and display complex binding and functional cooperativity with one another and with the endogenous GPR40 ligands docosahexaenoic acid and linoleic acid. Positive allosteric modulation of GPR40 activity presents an attractive therapeutic avenue that would offer additional advantages over orthosteric GPR40 agonists (Mancini & Poitout 2013).

One of the most important downstream targets of insulin action is Akt, a serine/threonine kinase which plays a major role in insulin signalling pathway. In this study the effect of GPR40 agonists on the insulin stimulation of AKT phosphorylation in human and Wistar rat myotubes was inconsistent; GW9508 had no effect, oleic acid increased, and AZ921 decreased the effect of insulin stimulation upon AKT phosphorylation and the GPR40 antagonists abolished the effect of AZ921 only. Furthermore, the GPR40 agonists had no effect on insulin stimulation of GSK3β phosphorylation while the GPR40 antagonist significantly increased it. In support of our results, an increase in Akt phosphorylation levels in liver of obese Zucker rats treated with the GPR40 antagonist DC260126 was reported by Zhang et al. (2010) and increased Akt phosphorylation by oleate in bovine mammary epithelial cells (bMEC) was observed by Yonezawa et al. (2008). In contrast, Briscoe et al. (2006) did not observe any effect of oleate on Akt phosphorylation. Collectively this observation indicates that the GPR40 antagonist not the agonist might play a role in insulin signalling. In fact, the use of GPR40 antagonist rather than agonist in treatment of diabetes was suggested by Steneberg et al. (2005), Zhang et al. (2010), Brownlie et al. (2008) and (Duttaroy et al.2008.). In contrast, Nagasumi et al. (2007), Latour et al. (2007) and Tsujihata et al. (2011) suggested the use of GPR40 agonists in treatment of diabetes. GPR40 agonists are insulinotropic agents because they stimulate insulin secretion and counter the adverse effects on β-cell survival (Wagner et al. 2013). In addition, the GPR40 agonist TAK-875 significantly augmented

plasma insulin levels and reduced fasting hyperglycaemia in male Zucker diabetic fatty rats without any risk of hypoglycaemia (Tsujihata et al. 2011). In fact, in May 2013, the Takeda Pharmaceutical Company Limited ("Takeda") announced the results of a Phase III clinical trial 24 weeks treatment with fasiglifam (TAK-875) which showed a statistically significant and clinically relevant reduction in HbA1c levels in type 2 diabetes patients. Interestingly, Nagasumi et al. (2013) observed that the lack of GPR40 does not exacerbate glucose intolerance and insulin resistance induced by high-fat diet. The role of the GPR40 receptor in insulin signalling effects upon glucose metabolism in skeletal muscle cell culture cannot be accurately studied as GLUT4 translocation and glucose uptake experiments could not be performed on our cell model. As previously mentioned in Chapters 3 and 4, cultured cells have very low GLUT4 and high GLUT1. Thus, other possible roles through which FFA induce insulin resistance were studied.

5.6.4. GPR40 activation and Cytokines

Obesity induced inflammation which is characterized by infiltration of macrophages and the secretion of inflammatory cytokines in metabolically active tissues is critical for the development of insulin resistance. In this study, a GPR40 agonist (100nM AZ921 for 24 hours) had no effect on TNF-α and IL6 mRNA expression in cultured myotubes, however, 250μM palmitic acid caused a significant ($P<0.05$) increase in both IL-6 and TNFα mRNA expression. The effect of palmitic acid was not altered by a MEK inhibitor (U0126) or a GPR40 antagonist in either human or Wistar rat myotubes. This indicates that GPR40 receptor activation does not affect skeletal muscle expression of TNFα and IL6 and that the effects of palmitic acid are also unlikely to be mediated by GPR40. Indeed, Wu et al. (2010) have previously reported that the palmitate mediated

increase in IL-6 does not occur as a result of GPR40 activation. In addition, Fujita et al. (2011) found that stimulation of GPR40 by GW9508 actually attenuates the induction of inflammatory cytokines and chemokines in keratinocytes and suppresses allergic inflammation in the skin. The result of this study and some previous reports indicate that GPR40 has no role in the elevation of cytokine production observed in obesity where circulating FFA levels are elevated.

5.6.5. GPR40 activation and PDK4

Pyruvate dehydrogenase kinases (PDK) phosphorylate and inactivate pyruvate dehydrogenase complex (PDH) which catalyzes the conversion of pyruvate to acetyl CoA. PDK4 expression can be induced by starvation, high-fat diet and diabetes (Wu et al. 1999). Regulation of the activity of the pyruvate dehydrogenase complex in skeletal muscle plays an important role in fuel selection and glucose homeostasis. Insulin resistance is associated with increased skeletal muscle PDK expression (Kim et al. 2006). In this study treatment of human and Wistar rat myotubes with AZ921, Oleic acid and AZ915 for 24hrs did not have any significant effect upon PDK4 mRNA expression. However, Palmitic acid and U0126 caused a significant ($P<0.01$) change in PDK4 mRNA expression. Grassian et al. (2011) and Johnson & Denton (2003) reported that the MEK inhibitors (UO126 and PD98059) increased PDK4 mRNA and protein levels and decreased relative PDH flux. Interestingly, the MEK inhibitor and the GPR40 antagonist did not block the effect of Palmitic acid but Oleic acid was effective in blocking palmitate induced increases in PDK4 expression. The protective effect of oleic acid on palmitic acid induced inflammation, apoptosis and insulin resistance in skeletal muscle has been observed by many researchers (Coll et al. 2008; Chavez et al. 2003; Peng et al. 2011; Hardy et al.

2005). Overall the presented data suggest that palmitic acid does not exert its effects via GPR40, and the role of oleate in reducing the detrimental effects of palmitate are also unlikely to involve GPR40 signalling

5.6.6. Effects of modulating GPR40 activity upon transcriptional networks

This study is the first study to explore the functionality of GPR40 receptor in skeletal muscle. Global expression profiling with oligonucleotide microarray and Taqman® Low-Density Array were used to systematically characterize gene expression profiles in myotubes treated with GPR40 agonists and antagonists. The effects of GPR40 activation or inhibition on gene expression were studied to further understanding and provide new insight of GPR40 mechanisms in skeletal muscle.

Treatment of human myotubes with the GPR40 agonist (AZ921) alone or in combination with the GPR40 antagonist (AZ836) did not produce any significant alteration in biological functions or canonical pathways when data with a fold change >1.5 and analysed using IPA. However, the GPR40 antagonist (AZ836) produced significant changes in a number of gene regulatory pathways. Interestingly, the effects of the antagonist in cells cultured in lipid-free medium were similar to those cultured in horse serum which may contain lipid species that are capable of binding to and activating GPR40. This may indicate that GPR40 is at least constitutively active, or that myotubes produce GPR40 ligands which then act in an autocrine manner. It is now accepted that constitutive activity is a feature associated with many G protein-coupled receptors, the majority of GPCRs show some level of spontaneous activity in the absence of agonists (Milligan 2003) and that the majority of antagonists are actually inverse agonists which can reduce the basal activity a receptor (Kenakin 2001). A high-

level of constitutive activity of GPR40 was indicated by experiments employing cell membrane preparations and the binding of [35S]guanosine 5'-O-[γ-thio] triphosphate (Stoddart & Milligan 2010).

Analysis of the effects of the GPR40 antagonist by IPA revealed that most genes were associated with cell proliferation, differentiation, cytoskeleton organization, movement and survival. IPA analysis indicated that the increased expression of several upstream regulators of transcription. Among the upstream regulators ERBB2, PPARD, MAPK8 and IL3 were chosen for further analysis to highlight their role in cell proliferation as they have a high predicted Z-score.

ERBB2 is a member of the EGF receptor (EGFR) family of receptor tyrosine kinases (RTK), composed of 4 closely related type 1 RTKs including the EGFR (ERBB1/HER1), ERBB2 (Neu/HER2), ERBB3 (HER3), and ERBB4 (HER4) (Lahlou et al. 2012; Olayioye et al. 2000). In different cell types, EGFR transactivation can mediate GPCR-induced Ras/Raf/MEK/ERK and PI3-kinase/Akt activation and thereby contributes to the coupling between GPCRs and cell cycle progression (Rozengurt 2007). Moreover, ERBB RTKs integrate signalling events emanating from other receptor classes, such as G-protein-coupled receptors and cytokine receptors (Olayioye et al. 2000). In this study, the expression of ERBB2 in cultured myotubes was revealed by microarray with a rank of 11117 out of 42413. The role of ERBB2 receptors in skeletal muscle was studied by Leu (2003) who reported that ERBB2 signalling is an essential regulator for the formation of both neuromuscular synapses and muscle spindles in mice. A similar findings were reported by Andrechek et al. (2002) who found ERBB2 receptors in skeletal muscle tissue and cultured myoblasts and highlighted the importance of ERBB2 signalling in regeneration of muscle fibres.

The microarray data showed that treatment with a GPR40 antagonist led to

increased expression of ERBB2 in cultured skeletal muscle cells. Ingenuity pathway analysis demonstrated that the expression of 46 genes known to be transcriptionally regulated by ERBB2 was altered by GPR40 antagonist treatment. The majority of these downstream transcripts were found to be associated with cell proliferation and development. Under normal conditions, ErbB receptors are expressed at very low levels in a variety of tissues and cells of epithelial, mesothelium, endothelial, and neuronal origin where they elicit broad biological functions, including organ development, maintenance of cell proliferative and differentiation states, and the regulation of tissue homeostasis (Alaoui-Jamali et al. 2003). Overexpression of ERBB2 increases cell proliferation and survival (Kurokawa & Arteaga 2001). Overexpression of ERBB2 has also been reported in numerous cancers, including breast, lung, gastric, oral and ovarian tumors (Olayioye et al. 2000). Overexpression of the human ERBB2 gene correlates with a lower survival rate in breast cancer patients (Yang et al. 2000). Besides their role cancer pathology, ERBB2 and ERBB3 are also required for normal development as ablation of ERBB2 or ERBB3 causes embryonic lethality (Ponomareva et al. 2006; Lahlou et al. 2012).

Unlike other members of the family, ERBB2 is not directly ligand activated, it does however interact with other ligand-bound EGF receptor family members to form a heterodimer, stabilizing ligand binding and enhancing kinase-mediated activation of downstream signalling pathways. ErbB2 is the preferred heterodimerization partner for all other ERBB family members and plays a role in the potentiation of ERBB receptor signalling (Graus-Porta et al. 1997). In fact, the ErbB2-ErbB3 heterodimer is the most potent ErbB signalling complex in terms of cell growth and transformation (Olayioye et al. 2000). It is worth mentioning that homodimers are weakly active or are devoid of kinase activity (Benlimame et al. 2005). Inactivation of ERBB2 by blocking antibodies decreases

ERBB3 tyrosine phosphorylation and inhibits cell proliferation whereas transcriptional repression of ERBB3 expression blocks ERBB2-induced proliferation in mouse mammary epithelial cell culture (Lahlou et al. 2012). ERBB3 was found to be elevated following GPR40 antagonist treatment which indicates that ErbB2/ErbB3 heterodimer activity may be increased.

If the increased expression of ErbB2 and ErbB3 observed in GPR40 antagonist treated cells leads to physiologically significant changes in cell behaviour, then the expression of genes downstream of the ErbB heterodimer would be expected to alter accordingly. The section that follows describes changes in expression of genes regulated by ErbB2:ErbB3 and discusses how the pattern of gene expression changes may lead to increased cell proliferation and reduced apoptosis.

The estrogen receptor (ER) belongs to a nuclear receptor superfamily of ligand-activated transcription factors that play a central role in cell proliferation (Stoica, Franke, Wellstein, et al. 2003). The estrogen-mediated signalling plays a central role in ERBB2/PI-3K/Akt signalling in hormone-dependent breast cancer (Stoica, Franke, Moroni, et al. 2003). ERBB2 activation by heregulin leads to cell growth and ER regulation in breast cancer cells (Pietras et al. 1995). Interestingly, the ER (ESR1 & ESR2) were among the upregulated downstream transcripts of ERBB2 in the current study which indicates that they also might play a role in skeletal muscle proliferation induced by GPR40 antagonist treatment. The apoptotic resistance factor BCL2 (B-cell CLL/lymphoma 2) (Zhou et al. 2002) was also one of the upregulated downstream transcripts of ERBB2. Studies using MCF-7 cells with or without ErbB2 expression, Guo et al. (2004) showed an enhancement in Bcl-2 levels in ErbB2-overexpressing cells.

ETS factors are known to act as positive or negative regulators of cell

proliferation, differentiation and apoptosis (Watson et al. 2010). One ETS family member, ETV6, was another upregulated transcript in the current study. Galang et al. (2004) reported an elevated expression of ETV6 in mammary tumours compared to normal mammary tissue.

Transforming growth factor beta (TGF-β) is a cytokine which potently inhibits the growth of normal epithelial cells as well as some breast cancer cell lines in culture (Wilson et al. 2005). Latent TGF-beta binding protein (LTBP) attaches to TGF-β and prevents binding to TGF-β receptors leading to increased cell proliferation. LTBP3 expression was found to be elevated in the GPR40 antagonist treated cells. LTBP-3 knockdown via siRNA mediated silencing resulted in reduced cell proliferation and reduced osteogenic differentiation (Koil et al. 2008). Furthermore, ERBB2/HER-2 overexpression promotes the growth and malignancy of mammary epithelial cells, in part, by conferring resistance to the growth inhibitory effects of TGF-β (Wilson et al. 2005).

The Notch family includes four conserved transmembrane receptors (Notch1 - Notch4) and five surface localized ligands (Jagged1, Jagged2, Delta-like1, Delta-like2 and Delta-like3), which play fundamental roles in self-renewal, proliferation, adhesion and migration (Le Friec et al. 2012). Notch1 and JAG1 expression were altered by GPR40 antagonist treatment (Notch1 increased and JAG decreased). JAG1 has been reported to significantly reduce endothelial cell proliferation by Liebler et al. (2012) and an increase in Notch1 coupled with reduced JAG1 expression may contribute to increased myoblast proliferation.

The cell cycle is regulated by both the positive (cyclin-dependent kinase CDK1) and negative (cyclin-dependent dependent kinase inhibitors CDKN1B) regulators (Aleem et al. 2005). CDKN1B is one of the transcripts that is downregulated by ERBB2. Down-regulation of CDKN1B (p27) has been described

in cells in which ERBB2 was overexpressed (Yang et al. 2000). It was by this group that the HER-2/Grb2/Ras/MAPK pathway was demonstrated to be involved in the down-regulation of p27.

The E3 ligase (Cul3) and the adhesive protein Dermatopontin (DPT) were also among the downregulated transcripts that have been previously been described as being under the regulation of ERBB2. CUL3 is a crucial regulator of cell proliferation, and has been reported to be responsible for the degradation of Cyclin E (McEvoy & Kossatz 2007). When Cul3 levels are reduced, CyclinE activity increases, driving cells into S phase and promoting cell proliferation. DPT is an extracellular matrix protein and is assumed to play important roles in cell-matrix interactions and matrix assembly (Kuroda et al. 1999). DPT has been shown to interact with, and enhance the activity of TGF-β (OKAMOTO et al. 1999) Thus the decrease in DPT may further decrease the anti-proliferative effects of TGF-β.

The adhesion molecule α2-integrin (ITGA2) was also a downregulated downstream transcript of ERBB2 in this study, in agreement with Ye et al. (1996) who reported that overexpression of the ERBB2 gene in a non-tumorigenic human mammary epithelial cell line, MTSV1-7, induced a downregulation of transcription of the genes coding for adhesion molecules E-cadherin and α2-integrin. The activation of α2β1 integrin has been demonstrated previously to inhibit ERBB2-mediated cell proliferation in mammary epithelial cells (Baeckstro et al. 2000).

Matrix metalloproteinases (MMPs) play a major role in cell proliferation, migration ,differentiation and apoptosis and are negatively regulated by MMP inhibitory proteins such as RECK (reversion-inducing-cysteine-rich protein with kazal motifs) (Noda et al. 2003). Hsu et al. (2006)

demonstrated that the over expression of ERBB2 inhibits the expression of the RECK in B104-1-1 cells, NIH/3T3 (cells expressing constitutively active HER-2/neu) and human HaCaT keratinocytes cells via the ERK signalling pathway. RECK can inhibit cell proliferation by downregulation of a ubiquitin ligase component, S-phase kinase-associated protein 2 (SKP2), and upregulation of its substrate, p27 (KIP1). p27 acts by inhibiting Cdk2 and instigates a blockade at G1 (Yoshida et al. 2011). As ERBB2 also directly decreases p27/Cdk2 interaction (Lane et al. 2000) this should lead to a decrease in Cdk2 activity and subsequent increase in cellular proliferation.

PDCD4 (programmed cell death 4) is a tumour suppressor gene and the expression of PDCD4 in rat skeletal muscle tissue and myoblasts was reported by Zargar et al. (2011). Our data indicate that PDCD4 is downregulated by GPR40 antagonist treatment. Huang et al. (2009) found that PDCD4 is down-regulated by miR-21 in breast cancer cells expressing ERBB2 and as PDCD4 is positively regulated by the TGF-β pathway (Baeckstro et al. 2000) it is possible that ERBB2 suppression of TGF-β signalling may be responsible for the reduction of PCDC4 mRNA in this study.

The capping protein (CPAZA2) which tightly binds to the fast growing ends of actin filaments in skeletal muscle and regulates its growth (Eckert et al. 2012) was found to be inhibited by the GPR40 antagonist in this study and it is one of the downstreams of ERBB2. The expression of CPAZA2 and many of the genes mentioned above were found to be altered in a similar manner by a microarray study in which ERBB receptors were stably overexpressed in a polyclonal cell population as single or paired combinations using murine and human breast cell models (Alaoui-Jamali et al. 2003).

It worth mentioning that another microarray study was carried out by

Mackay et al. (2003) to evaluate the role of ERBB2 overexpression in the ERBB2-transfected breast luminal epithelial cell line C5.2, the ERBB2-amplicon-containing breast cancer cell line BT474, and ERBB2-overexpressing invasive ductal breast carcinomas. The results of our microarray regarding the downstream transcripts of ERBB2 were in agreement with the Mackay study for both downregulation (RECK, PDCD4, ITGA2, CUL3, CDKNIB, CAPZA2, DPT, JAG1))or upregulation (BCL2, HES1, HES2, LTBP3, NOTCH1, TNC, ERBB3, ESR1, ESR2, ETV6 and MAPKBP3) of genes by increased ERBB2 expression induced by the GPR40 antagonist in human myotubes. The following figure shows a suggested pathway through which elevated ERBB2 expression caused by GPR40 antagonist treatment may lead to increased cell proliferation. The figure illustrates that the GPR40 proliferative and anti-apoptotic effects are through the activation of ERBB2. The ERBB3/ERBB2 heterodimer generate a spectrum of signalling pathway through, 1) AKT pathway to activate BCL2, ESR1 and ESR2. 2) Notch pathway, to activate HES1 and HES2 as well as to inhibit JAG1. 3) MAPK pathways to inhibit TGFβ, CDKNIB, RECK, POCD4 and ITGA2 as well as to activate ETV6. 4) Direct or indirect pathways to inhibit CUL3, CAPZA2 and DPT as well as to activate LTBP3. These pathways modulate cell proliferation and apoptosis by;

1. Inhibition of TGFβ which subsequently leads to an increase in cell proliferation via the downregulation of CUL3 and DPT as well as through the upregulation of LTBP.
2. Activation of CDK which leads to increase in cell proliferation via the upregulation of JUN1, HES1, HES2, Notch1, ESR1 and ESR2 as well as through the downregulation of CDKNIB (p27) and RECK.
3. Upregulation of BCL2 which is a powerful anti-apoptotic factor.

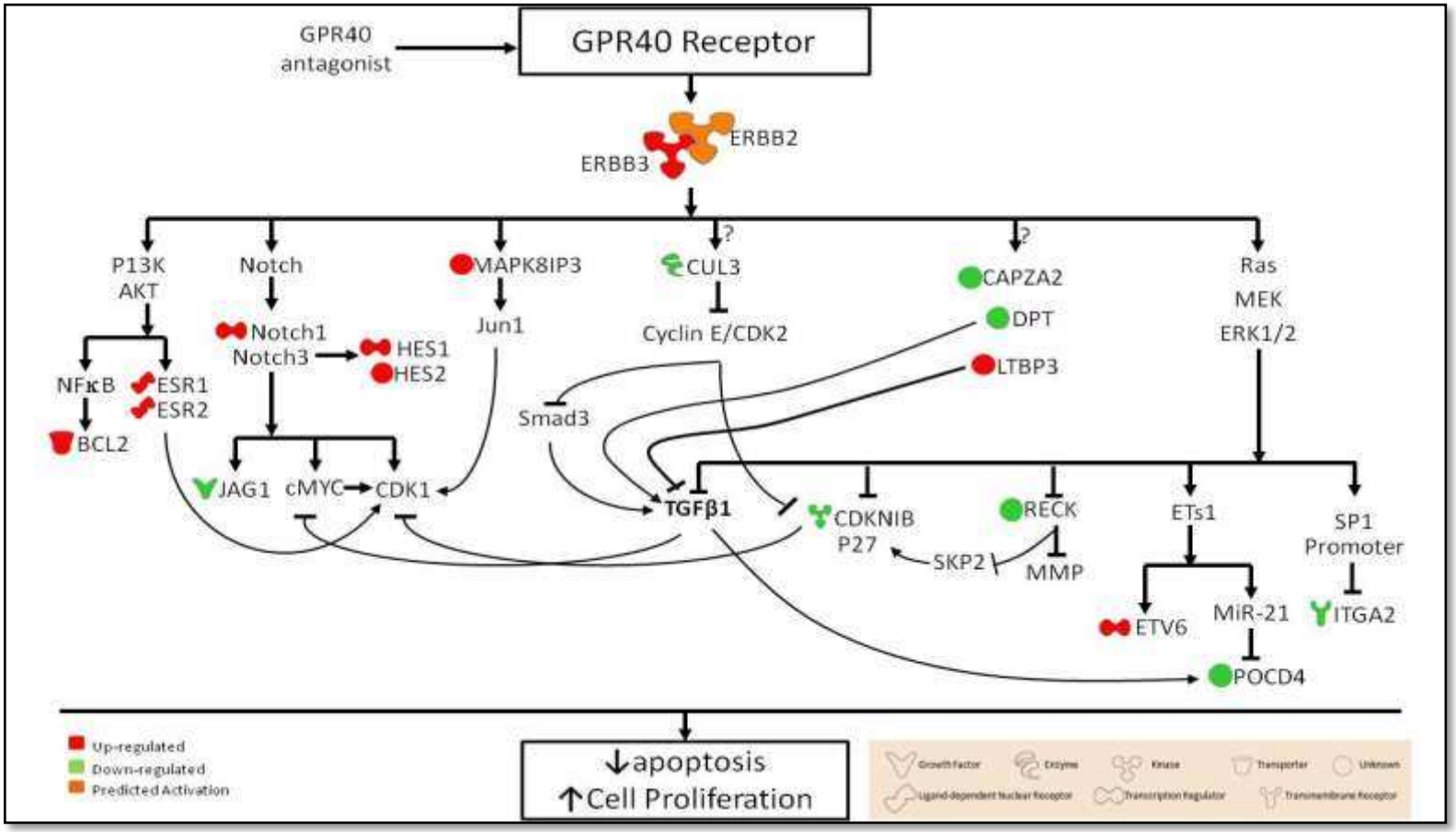

Figure 5-30: A proposed molecular mechanism through which the activated ERBB2 upstream leads to cell proliferation.
ERBB2 associated with ERBB3 to form a functional heterodimer which generated a diverse spectrum of signaling pathways such as 1) PI3K/AKT pathway to activate BCL2, ESR1 and ESR2. 2) Notch pathway, to activate HES1 and HES2 as well as to inhibit JAG1. 3) RAS/MEK/ERK pathways to inhibit TGFβ, CDKNIB, RECK, POCD4 and ITGA2 as well as to activate ETV6. 4) Direct or indirect pathways to inhibit CUL3, CAPZA2 and DPT as well as to activate LTBP3. The ERBB2/ERBB3 seems to modulate apoptosis and cell proliferation in a direct or indirect ways by the activation of BCL2 and CDK as well as by inhibition of TGFβ .The human myotubes were treat with 5μM AZ836 (GPR40 antagonist) for 24 hours. All transcripts shown had a fold-change of >1.5, and P<0.05.

ID	Entrez Gene Name	Reference
BCL2	B-cell CLL/lymphoma 2	(Zhou et al. 2002)(Guo et al. 2004) (Lobenhofer et al. 2000)
CAPZA2	capping protein (actin filament) muscle Z-line, alpha 2	(Alaoui-jamali et al. 2003)(Eckert et al. 2012)
CDK1	cyclin-dependent kinase 1	(Le Friec et al. 2012)(Aleem et al. 2005)
CDKN1B	cyclin-dependent kinase inhibitor 1B (p27, Kip1)	(Yang et al. 2000)(Lane et al. 2000)
cMYC	avian myelocytomatosis viral	(Le Friec et al. 2012)(Frederick et al. 2004)
CUL3	cullin 3	(Sumara et al. 2007)(Mcevoy et al. 2007)
DPT	dermatopontin	(Kuroda et al. 1999)(Okamoto et al. 1999)
ERBB2	v-erb-b2 erythroblastic leukemia viral oncogene homolog 2 (HER2/NEU)	(Rozengurt 2007)(Olayioye et al. 2000)(Alaoui-jamali et al. 2003) (Riese et al. 1995)
ERBB3	v-erb-b2 erythroblastic leukemia viral oncogene homolog 3	(Olayioye et al. 2000)(Graus-Porta et al. 1997)(Graus-Porta et al. 1997)(Mackay et al. 2003)
ESR1	estrogen receptor 1	(Stoica, Franke, Wellstein, et al. 2003)(Pietras et al. 1995)
ESR2	estrogen receptor 2 (ER beta)	(Stoica, Franke, Moroni, et al. 2003).
ETV6	ets variant 6	(Watson et al. 2010)(Watson et al. 2010)
HES1	hairy and enhancer of split 1	(Pradeep et al. 2012)
HES2	hairy and enhancer of split 2	(Pradeep et al. 2012)
ITGA2	integrin, alpha 2 (CD49B, alpha 2 subunit of VLA-2 receptor)	(Ye et al. 1996)(Baekstrom et al 2000).
JAG1	jagged 1	(Liebler et al. 2012)
LTBP3	latent transforming growth factor beta binding protein 3	(KOIL et al. 2008)
MAPK8IP3	mitogen-activated protein kinase 8 interacting protein 3 (JIP)	(Mackay et al. 2003)(Jiao et al. 2010) (Meixner et al. 2010)
MMP	matrix metallopeptidase	(Hsu et al. 2006)
NOTCH	notch	(Le Friec et al. 2012).
PDCD4	programmed cell death 4 (neoplastic transformation inhibitor)	(Zargar et al. 2011)(Baeckstro et al. 2000)(Huang et al. 2009)
RECK	reversion-inducing-cysteine-rich protein with kazal motifs	(Hsu et al. 2006) (Noda et al. 2003)(Yoshida et al. 2011)
SKP2	S-phase kinase-associated protein 2 (SKP2)	(Yoshida et al. 2011)
TGFB1	Transforming growth factor beta	(Wilson et al. 2005)(Frederick et al. 2004)

PPARD is implicated in developmental and metabolic regulation in several tissues and gene disruption is often lethal due to a placental defect (Luquet et al. 2005). In adipocytes, PPARδ initiates the adipogenic action of long-chain fatty acids by stimulating preadipocyte proliferation (JEHL-PIETRI et al. 2000) and the induction of PPARγ promotes expression of adipogenesis program (Bastie et al. 1999). In keratinocytes, PPARδ up-regulation results in increased resistance to TNFα-induced apoptosis and increases the rate of keratinocyte differentiation (Michalik et al. 2003). Luquet et al. (2005) demonstrated that PPARδ is involved in the control of cellular proliferation in intestinal crypts. In skeletal muscle, overexpression of PPARδ in skeletal muscles greatly influenced both development and metabolic capability of mouse muscles by promoting a net increase of fibres with an oxidative metabolic capability (Luquet et al. 2003). PPARδ expression in skeletal muscle is greater than other PPARs and higher expression is observed in oxidative type I muscle fibres compared with glycolytic type II muscle fibres (Ehrenborg & Krook 2009). The role of PPARδ on the regulation of lipid metabolism in skeletal muscle is documented (Krämer et al. 2007; Jucker et al. 2007; Ehrenborg & Krook 2009). In this study a number of downstream targets of PPARδ were associated with lipid metabolism however the most significant pathway in terms of Z score that was predicted to be regulated by PPARδ activation was associated with cell proliferation. In support of this result, Angione et al. (2011) demonstrated that PPARδ has a critical role in satellite cell proliferation and postnatal regeneration of skeletal muscles through reduction of Forkhead box class O transcription factor 1 (FoxO1) gene expression. The role of phosphatidylinositol 3-kinase and AKT pathways in mediation of cell proliferation of endothelial and skeletal muscle progenitor cells was reported by Han et al. (2008) and Chakravarthy et al. (2000), respectively. In addition, Bonala et al. (2012) reported that activation of PPARδ led to

inhibition of myostatin activity and thus increased myogenesis. Myostatin is a secreted growth and differentiation factor that is a member of the TGF beta protein family which inhibits muscle differentiation and growth. Interestingly, ERBB2 overexpression inhibits TGF beta and BCL2 is also a downstream transcript of PPARδ indicates that upstream regulators may a have a synergistic effect on cell proliferation.

MAPK8 (JNK1) is another upstream regulator the expression of which is associated with cell proliferation, cell death and survival. MAPK kinase is involved in cell proliferation and transformation. Several studies have shown that overexpression of MEK1 alone can lead to up-regulation of cyclin D1 and down-regulation of p27 (Yang et al. 2000). Interestingly, some genes which influenced by ERBB2 are also targets of MAPK8 such as CDK1, CDKN1B, BCL2. Upregulation of MMP by stress-activated MAPK signaling pathways was demonstrated by (Oh et al. 2001; Nielsen et al. 2008). Moreover, CDKN1B, NOTCH1 and BCL2 are also regulated by IL-3 as well as ERBB2.

IL-3 is a cytokine which has a key role in cell proliferation and survival (Ebner et al. 2002). It is worth mentioning that ATF (activating transcription factor 5) is another downstream transcript of the upstream regulator IL-3. ATF is a member of the ATF/CREB family of transcription factors which have important roles in differentiation and regulation of the cell cycle (Gho et al. 2008). Persengiev et al. (2002) demonstrated that ATF suppresses apoptosis resulting from cytokine deprivation in an interleukin 3 (IL-3)-dependent cell line, which indicates that ATF is an anti-apoptotic factor.

Collectively, treatment of human skeletal muscle cultured cells with the GPR40 antagonist induced activation of cell proliferation through different upstream regulators which seem to have different pathways although certain downstream transcripts were found to be common to several upstream factors.

CHAPTER SIX

GENERAL DISCUCSION AND FUTURE ASPECTS

CHAPTER 6. General Discussion and Future Aspects

The mechanisms behind the development of insulin resistance in skeletal muscle are very complex and have not being completely understood. The association between lipid over supply and insulin resistance is well established. The insulin resistance in skeletal muscle is of particular importance because muscle is the major site of insulin stimulated glucose uptake. Interference with insulin signal transduction by lipid activated signalling pathways is likely to play an important role in the initiation of insulin resistance which usually develops decades before overt diabetes (Dipl-Pharm & Zierath 2005). Isolated skeletal muscle preparations are short lived for experimental manipulation, and they are invasive for human studies. Several muscle cell lines of animal origin are currently available (rat L6 and mouse C2C12 of skeletal muscle origin and mouse BC3H1 of brain tumour origin). There are no muscle cell lines of human origin that have been equally characterized. Primary skeletal muscle cell cultures have been shown to retain the metabolic characteristics of the tissue donor and thus reflect alterations in metabolism as seen in specific disease states such as obesity and type 2 diabetes mellitus (Gaster et al. 2004)(Steinberg et al. 2006). The human muscle cells were shown to have a saturable glucose uptake system and to be more sensitive to insulin than the rat cell line (Sarabia et al. 1992). However contamination by fibroblasts and the potential for spontanous differentiation of myoblasts to myotube are the main problems of primary culture (Gaster et al. 2001). Human muscle cells in culture as well as rat L6 muscle cell lines express higher ratios of GLUT1/GLUT4 transporters than do adult rat or human muscles while other cell lines (BC3H1, C2C12, and G8) have been reported to express detectable levels of only GLUT1 (Sarabia et al. 1992). Hence, it appears that human primary muscle cell cultures are the most suitable model for studying muscle mechanisms in vitro. In an attempt to define defects in insulin signalling in skeletal muscle,

characterized and to better understand the effects of GPRC ligands (in particular CB1 and GPR40 agonists/antagonist) in human muscle, we have used human and rat (Wistar and Zuckers) primary muscle cell cultures.

In the present thesis, high-density oligonucleotide arrays were used mainly to characterize changes in global mRNA expression patterns during human myogenesis as well as to investigate potential differences in the expression of metabolic genes and GPRCRs between skeletal muscle tissue and primary cultured cells in a genome-wide perspective. Studying the difference between myoblast and myotubes as well as myotubes and skeletal muscle tissue shows that human cultured cell is a suitable model for studying myogenesis. This thesis showed that the myogenic markers (PAX7 and PAX3) and transcriptional regulator of myogenesis such as MYOD1, MYF5, CDK6 and Myogenin were higher in culture cells than tissue. Moreover, MYOD1 and MYF5, which are responsible for myogenin formation and CDK, were higher in myoblasts than myotubes. It is well known that the CDk level increases in the late stage of myoblasts proliferation to arrest cell cycle and starts the differentiation stage (Tomczak et al., 2004). Genes encoding cell adhesion molecules were expressed higher in myotubes compared to myoblasts and whole muscle tissue providing a clearer indication of how the plasma membrane and extracellular matrix may be modified prior to cell fusion and suggesting their potential role during the steps of myogenic differentiation.

Human skeletal muscle culture has been used for the investigation of the biochemical and genetic basis of peripheral insulin resistance. Insulin enhancement of the rate of 2-deoxyglucose uptake in these cells is 2 fold less than insulin responsiveness typically observed in human forearm muscle balance studies (Perriott et al. 2001). This low degree of insulin responsiveness makes these cells questionable for assessing insulin effects on glucose utilization and for establishing the mechanism of impaired insulin sensitivity. In the present thesis,

the MAPKs pathway was not affected in cultured cells compared to tissue whereas the PI3K/AKT pathway and the GLUT4 translocation were affected. Interestingly, most of the negative regulators of insulin transduction pathway had higher expression in myotubes compared to skeletal muscle tissue such as PTEN, SHIP2, SOSC3 and LAR. It is worth mentioning that not only the expression of GLUT4 (SLC2A4) but also genes responsible for GLUT4 trafficking such as VAM2 and TC10 had lower expression in myotubes than skeletal muscle tissue. In addition, genes associated with carbohydrate, protein and lipid metabolisms as well as energy production were expressed at lower levels in myotubes compared to skeletal muscle tissue. In fact, genes encoding key regulators of glycogenolysis and glycolysis as well as most genes in TCA Cycle, β oxidation, and oxidative phosphorylation were expressed at lower levels in myotubes when compared to skeletal muscle tissue. Interestingly, the expression of genes that are involved in the transcriptional control of fatty acid oxidation and glucose homeostasis such as PPARA, PPARG, PPARGCIA & PPARGC1B (Semple 2006; Wahli & Michalik 2012; Lefebvre & Chinetti 2006) was also lower in myotubes when compared to tissue. Collectively, this implies that cultured cells are in a non-functional stage that does not demand more energy for metabolism. The metabolic requirements of skeletal muscle are highly variable, the working contracting muscle is a high consumer of ATP, and is also under hormonal control. In the basal (fasting and resting) state, approximately 80% of blood glucose is metabolized in an insulin-independent manner by the brain, gut, and red blood cells, whereas insulin-sensitive tissues (skeletal muscle and fat) require only small quantities. However, after insulin stimulation, skeletal muscle accounts for 75% of glucose utilization (Ehrenborg & Krook 2009). Not surprisingly, the expression of genes responsible for muscle structure subunit and phenotypes (Desmin, Tropomyosin, Troponin, Tropomodulin and myosin light and heavy chain) was higher in tissue than

cultured cells suggesting that cultured cells are relatively immature and specific transcriptional programs generating mature muscle phenotype are activated in vivo but not in cultured muscle cells. The ability of skeletal muscle to increase muscle size together with an ability to alter protein isoform expression, gives muscle the ability to adapt to the different challenges that may be placed up on it (use hypertrophy and disuse atrophy) (Harridge 2007). In fact, the decrease in metabolic genes and genes involved in muscle contraction demonstrated in cultured cells in this thesis, indicated a phenotype associated with disuse atrophy. Interestingly, a higher level of expression of metabolic genes in myotubes compared to myoblasts was also observed indicating an essential modification change (i.e cells are differentiated and gaining muscle phenotype) prior to fusion occurring. Collectively, the use of skeletal muscle culture cannot be used as a reliable model for a complete study of the insulin signalling pathway. In this work, the use of 100nM insulin in cultured cells induced ERK1/2, MAPK38, AKT and GSKα/β phosphorylation (activation) although no GLUT4 recruitment to the membrane was observed. This may be due to the fact that GLUT4 transport is a complex process as discussed in previous chapters. The decreased expression of GLUT4, the increase of GLUT1, the decrease in actin remodelling genes and the decrease in genes involved in calcium signalling and consequently muscle contraction altogether lead to the suggestion that insulin stimulated GLUT4 transport may also be impaired in those cells. The qualitative differences between cultured human muscle cells and adult human skeletal muscle may be related to the less mature state of the cells in culture, to the lack of innervation in culture, or to other conditions typical of the culture procedure. Therefore, better visualization method (GLUT4 photolabelling), intravital measurement of GLUT4-GFP chimeras, antibody-based determinations, exofacial tagged GLUT4, and affinity photolabeling techniques should be used to assess the regulation of

GLUT4 traffic. Optimizations of culture methods (electrical stimulation and introduction of continuous flow) as well as co-culture with other cells such as adipose tissue to study the cross talk between tissues are required.

The expression of cannabinoid and potential cannabinoid receptors as well as GPR40 was detected at the mRNA level by microarray, but their level of expression was low. The microarray technology, whilst effective as a tool for analysis of global gene expression changes, can lack the sensitivity to detect transcripts expressed at low but functional levels. Therefore, the expression levels of GPCRs were further investigated using QRT-PCR, which is a more sensitive technique for the detection of mRNA.

As illustrated in chapter 4, QRT-PCR analysis revealed the expression of CB1 in human and rat (Wistar and Zucker) skeletal muscle at different stage of differentiation and in different muscle phenotypes. In addition, CB1 mRNA expression was observed in rat heart, spleen, brain and adipose tissue. To the best of our knowledge, this is the first study that characterized the CB1 expression in this wide range of tissues by extracting mRNA from total RNA prior to cDNA synthesis as CB1 receptor is a single axon gene. The QRT-PCR findings from the present study also revealed the presence of CB2 mRNA expression in rat skeletal muscle tissue and cultured cells in agreement with Cavuoto et al. (2007). However, human CB2 mRNA expression was detected in cultured cells only in contrast to Cavuoto et al. (2007) who used 10 times over the standard loading amount for RT-PCR. The low level of CB2 in skeletal muscle tissue might be the reason for the underestimation of the role of CB2 in skeletal muscle. It is worth mentioning that (Bermudez-Silva et al. 2007) reported activation of cannabinoid CB2 receptors by CB2 agonist (JWH133) improved glucose tolerance after a glucose load, whereas blockade of cannabinoid CB2 receptors by AM630 counteracted this effect, leading to glucose intolerance in rats. Moreover,

(Rajesh et al. 2008) observed that CB2 agonists decrease vascular smooth muscle proliferation and migration induced by TNFα and as a result clinically CB2 agonists are under trial in post balloon implantation. The expression of the potential cannabinoid receptor GPR119 was also observed in human and rat skeletal muscle tissue and cultured cells. To the best of our knowledge, this is the first study revealing the presence of GPR119 in skeletal muscle using QRT-PCR.

High levels of circulatory endocannabinoids are well documented in obese and diabetic subjects (Serrano et al. 2008). However, the presence and role of skeletal muscle CB1 receptors in obesity and diabetes is poorly described. Pagotto et al. (2006) reported a high level of mRNA CB1 expression in soleus muscles from mice fed a high fat diet whereas Lindborg et al. (2010) observed a low CB1 protein expression in soleus muscles from ZFR. In the present study, the expression levels of CB1, CB2 and GPR119 in muscle, liver, heart, spleen and adipose tissues were similar between 12week old Zucker Fat Rats (ZFR) and Zucker Lean Rats (ZLR), however at 20 weeks ZFR muscle and adipose tissues had a significantly higher expression of CB1 than ZLR. The expression of GPR119 in skeletal muscle tissue was higher in Zucker than Wistar rats in contrast to CB1 which has higher expression in Wistar compared to Zuckers. However, the difference disappeared in myotubes cultured from the same animal, which indicates that removal of the physiological factors that differentiate the two strains of rat in cultured cells may cause the equalization of GPR119 and CB1 expressions. This hypothesis is supported by the fact that Brozinick, Roberts, & Dohm, (2003), Pender et al. (2005) and Berggren et al. (2005) did not observe a difference in insulin resistance between cultured cells from obese (insulin-resistant patients) and control subjects.

The functionality of CB1 receptor in skeletal muscle was assessed by studying the effects of selective CB1 agonists and antagonists on ERK1/2 phoshorylation. CB1 activation of members of the MAP family such as ERK1/2 and MAPK38 is well documented and has been reviewed by (Demuth & Molleman 2006) and (Pertwee & Ross 2002). As described in chapter 4, ACEA and AEA lead to time dependent increase in ERK1/2 phosphorylation with a peak at 10 min in human and rat (Wistar and Zuckers) myotubes. Treatment with a CB1 selective antagonist (Rimonabant, RIM) alone attenuated ERK activation in cells obtained from Wistar and ZLR but not ZFR. The inability of rimonabant to inhibit CB1 agonist mediated ERK phosphorylation suggests altered ECS signalling in obesity and diabetes, however further investigation in terms of effects on metabolic gene expression and cell proliferation is needed. It is possible that the effects of endocannabinoids upon ERK signalling are unrelated to their metabolic effects and rather, are associated with cell proliferation or differentiation. The immunocytochemistry study using the proliferative marker Ki67 showed that ACEA induce cell proliferation in Wistar rat however, proliferation and differentiation assays are needed to confirm the role of CB1 activation in proliferation.

To further investigate the role of CB1 receptor activation in the acute modulation of insulin signalling in rat and human myotubes, the effects of CB1 agonists and antagonists on key proteins in the insulin signalling cascade were studied. The results from this thesis indicated that neither ACEA nor RIM affect insulin-stimulated phosphorylation of ERK1/2, MAPK38, PKB/Akt or GSK3α/β indicating that modulation of CB1 receptor in skeletal muscle cultured cell does not have a role in insulin signalling. Previous findings in the literature regarding the role of the cannabinoid receptor activation or inhibition on AKT are controversial. Eckardt et al. (2009) found that AEA impaired insulin-stimulated

AKT (but not GSK3α/β) phosphorylation and pre-treatment with RIM completely abolished the AEA effect in human primary skeletal muscle cultured cells. In contrast, Lindborg et al. (2010) reported that neither CB1 receptor agonists nor antagonists altered Akt and GSK3β phosphorylation in soleus muscle from lean and obese Zucker rats. (Song et al. 2011) reported that the CB1 agonist HU210 induced insulin resistance in muscle of wild-type C57BL/6 mice through inhibition of AKT phosphorylation which was prevented by pretreatment with the CB1 antagonist AM251. (Esposito et al. 2008) also demonstrated that RIM increased AKT phosphorylation and glucose uptake in L6 skeletal muscle cells. (Lipina et al. 2010) showed that pharmacological activation or inhibition of CB1 receptor activity exerts a differential effect with regard to MAP kinase and PKB/Akt-directed signalling in L6 cells. The discrepancy between this study and some earlier studies may be due to the different time points studied and the cell model used as previously discussed in chapter 4. It is interesting to note that even though the mRNA expression of CB1 and insulin signalling cascade genes were found to be low in cultured myotubes by micrroarray, the CB1 is functional (as indicated by the ACEA and AEA induced increase in ERK1/2 phosphorylation) and treatment with insulin can induce phosphorylation of ERK1/2, MAPK38, AKT and GSKα/β. The inability of insulin to induce GLUT4 transport may be due to the complexity of this transport process as discussed earlier. The findings of this thesis suggest that CB1 activation or inhibition has no role in modulating the activity of key proteins involved in insulin signalling.

There is a growing body of evidence linking elevated FFA and the development of insulin resistance. The role of GPR40 in glucose homeostasis in pancreas has been extensively studied; however its role in skeletal muscle has not been reported. To the best of our knowledge, this is the first study to characterize the GPR40 receptors in human and rats (Wistar and Zuckers) in

different stage of muscle development and in different muscle phenotypes. Even though the microarray data showed very low level of expression of GPR40 mRNA, the QRT-PCR confirmed the expression of GPR40 in human and rat skeletal muscle tissue and cultured cells. The higher level of GPR40 mRNA expression in myoblasts in comparison to myotubes and tissue suggested a possible role of GPR40 in cell proliferation. Human brain and spleen tissues also expressed GPR40 in agreement with Swaminath (2008) and Hirasawa et al. (2008). The GPR40 expression was also found in rat pancreas, spleen, adipose, heart and liver but not in rat brain in agreement with Itoh et al. (2003) and Brownlie et al. (2008). Interestingly, Ma et al. (2007) detected GPR40 expression in monkey brain. This indicates that the expression of GPR40 is not only tissue specific but also species specific.

Decrease in GPR40 expression in response to a high fat diet in mice was observed by Kebede et al. (2012), whereas Briscoe et al. (2003) detected a significant increase in expression of GPR40 mRNA in whole pancreas of ob/ob mice compared with control lean mice. In the present thesis, expression levels of GPR40 were similar at 12weeks for Zucker fat Rat (ZFR) and Zucker Lean Rat (ZLR), however at 20 weeks ZFR had higher expression of GPR40 than ZLR. Not surprisingly, cultured myotubes from ZFR, ZLR and Wistar rats had no significant difference in GPR40 expression, however cells cultured in 25mM glucose had a high level of GPR40 expression. Kebede et al. (2012) also observed a higher GPR40 mRNA expression in human and rat islets cultured in high glucose and they concluded that the main effect of glucose on GPR40 expression does not lie at the level of mRNA stability but, rather, at the transcriptional level. In contrast, Fontés et al. (2010) found low expression of the GPR40 gene under glucolipotoxic conditions in rat β cells and Del_Guerra et al. (2010) in islets from T2D patients. Interestingly, the addition GPR40 ligand for 6 hours, led to a

significant down-regulation of GPR40, i.e., G protein-coupled receptor-specific internalization (Kaplamadzhiev et al. 2010; Hu et al. 2009). Therefore, further confirmation and investigation is needed to see the effect of high glucose as well as GPR40 ligands on GPR40 mRNA expression in skeletal muscle.

As discussed in chapter 5, even though a growing body of evidence suggested that the GPR40 receptor couples to the Gαq/11 subunit of G protein (Shapiro et al. 2005)(Carina P 2008), other studies suggested that GPR40 is coupled to Gi/o (Fujita et al. 2011), (Hidalgo et al. 2011) and (Yonezawa et al. 2008). Studying the signalling mechanisms downstream of GPR40, we found that PTX (a Gi inhibitor) attenuates MAPK phosphorylation induced by GPR40 agonists suggesting that GPR40 is a Gi coupled receptor in skeletal muscle. Moreover, GPR40 agonists had no effect on intracellular calcium release in Wistar rat myotubes and myoblasts while ATP produced a quick response. This indicates that even though cultured muscle cells are relatively immature and a decrease in the expression of calcium signalling and ryanodine receptor genes was observed by microarray analysis, the cells still responding to stimulation of calcium release. Calcium imaging assays might be unreliable methods to study the functional read out of GPR40 because it has a high constitutive activity (Stoddart & Milligan 2010). Thus, these results should be verified through the use of PLC inhibitors (such as U73122), Gαq inhibitors (such as YM-254890) as well as measurements of cAMP production in skeletal muscle in response to treatment with GPR40 agonists and antagonits.

Even though the role of GPR40 in the regulation of insulin secretion is well documented, it is still a matter of debate whether activation or inhibition of GPR40 would be beneficial for the treatment of type 2 diabetes (Ou et al. 2013). In humans, clinical trials with the GPR40 agonist TAK-875 improved glucose tolerance and glycaemic control significantly without causing hypoglycaemia. Ito

et al. (2013) observed a significant improvement of postprandial and fasting hyperglycaemia, as well as a decrease in glycosylated Hb, with the use of TAK-875 in Zucker obese rats and additive improvements were also observed in combination with metformin. Lin et al. (2011) demonstrated that acute administration of AMG837 (a potent GPR40 partial agonist) lowered glucose excursions and increased glucose stimulated insulin secretion during glucose tolerance tests in both normal and Zucker obese rats. These finding support the potential use of GPR40 agonists for the treatment of type 2 diabetes. However, Zhang et al. (2010) showed that the GPR40 antagonist DC260126 improves insulin tolerance and increase insulin signalling in diabetic Zucker rats. Collectively, these finding raise a question about the use of GPR40 in the treatment of diabetes, thus it is necessary to further investigate the role of GPR40 agonists and antagonists in other species and tissues. The current thesis is the first study to evaluate the role of GPR40 in skeletal muscle insulin resistance and cell proliferation. The main findings showed (1) Activation of ERK1/2 by GW9508, AZ921, and Oleic acid but not Palmitic acid, (2) Activation of MAPK38 by GW9508 only, (3) inhibition of ERK/2 phosphorylation induced by AZ921 only by the antagonists (AZ836 and AZ468) in human and rat (Wistar and Zuckers) myotubes. These findings were in agreement with previous reports as discussed in Chapter 5. The apparent difference between effects of the various GPR40 agonists is most likely attributable to activation of distinct allosteric sites on the receptor by different molecule structure. Interestingly, Lin et al. (2012) described three novel GPR40 allosteric agonists that bind to separate sites and display complex binding and function cooperatively with one another and with the endogenous GPR40 ligands docosahexaenoic acid and linoleic acid. Positive allosteric modulation of GPR40 activity presents an attractive therapeutic avenue that would offer additional advantages over

orthosteric GPR40 agonists (Mancini & Poitout 2013). The selective inhibitory effect of the 2 antagonists on AZ921 indicates the specificity of the Astra Zeneca compounds used in this thesis.

Activation of ERK1/2 also plays a major role in cell proliferation, differentiation and transformation (Fredriksson R 2003). Thus, this thesis also investigated the effect of GPR40 agonists and antagonists on key regulatory proteins in insulin signalling namely AKT and GSKα/β. The effect of GPR40 agonists on the insulin stimulation of AKT in human and Wistar rat myotubes was inconsistent; GW9508 had no effect, AZ921 decreased the effect of insulin stimulation of AKT phosphorylation, and the GPR40 antagonist (AZ836) abolished the effect of AZ921 only. Furthermore, the GPR40 agonists had no effect on insulin stimulation of GSK3β phosphorylation while the GPR40 antagonist significantly increased it. This indicates the modulation of GPR40 receptors by the antagonist may have a stimulatory effect on insulin signalling. Other possible targets involved in the development of lipid-induced insulin resistance in skeletal muscle such as PDK4 (a molecular inhibitor of glucose oxidation) and the proinflammatory cytokines IL6 and TNFα were also investigated. The main finding was that the GPR40 agonist AZ921had no effect on IL6, TNFα or PDK4 mRNA expression in human and rat myotubes. This finding indicates that GPR40 receptor may not mediate skeletal muscle insulin resistance through induction of TNFα, IL6 or PDK4 in skeletal muscle.

The role of GPR40 agonists and antagonists in skeletal muscle were further investigated using Affymetrix microarrays. Interestingly, no relationship was found between GPR40 activation or inhibition with alterations in the expression of metabolic genes suggesting that GPR40 may have other, as yet unidentified, roles in skeletal muscle. In fact, the GPR40 antagonist had a strong relationship with genes involved in cell proliferation particularly with ERBB2, an epidermal

growth factor receptor (EGFR). Cross-talk between G protein-coupled receptors (GPCRs) and EGFR signalling systems is widely established in a variety of normal and transformed cell types. As discussed earlier in chapter 5, the GPR40 agonist AZ921had no significant affect which might due to the high constitutive activity of GPR40. In summary, treatment of human skeletal muscle cultured cells with a GPR40 antagonist induced activation of cell proliferation through different upstream regulators which seem to have different pathways as 2 to 4 downstream transcripts were found to be in common. This study concluded that it is the GPR40 antagonist and not the agonist that leads to cell proliferation and suggested the potential use of GPR40 antagonist in treatment of human muscle disease. The role of the GPR40 agonists in human breast cancer cell line (MCF-7), mammary epithelial and human bronchial epithelial cells proliferation was previously demonstrated (Yonezawa et al. 2004) (Yonezawa et al. 2008) (Hardy et al. 2005) (Gras et al. 2009b). One important aspect of any GPR40 agonist or antagonist that may be used to treat a chronic condition such as type 2 diabetes or muscle disease is the potential for GPR40 modulation to exert carcinogenic effects. This warrants further investigation as it might hold the key to the use of GPR40 agonists and antagonist in near future. Prolonged clinical studies will ultimately establish the long-term use of GPR40 agonists or antagonists by delineating the biological functions of GPR40 and whether these can be modulated to treat human disease.

REFERENCES

References

Abdul-Ghani, M. a et al., 2008. Deleterious action of FA metabolites on ATP synthesis: possible link between lipotoxicity, mitochondrial dysfunction, and insulin resistance. American journal of physiology. Endocrinology and metabolism, 295(3), pp.E678–85. Available at: http://www.ncbi.nlm.nih.gov/pubmed/18593850 [Accessed May 28, 2013].

Ahlgren, U. et al., 1998. beta -Cell-specific inactivation of the mouse Ipf1/Pdx1 gene results in loss of the beta -cell phenotype and maturity onset diabetes. Genes & Development, 12(12), pp.1763–1768. Available at: http://www.genesdev.org/cgi/doi/10.1101/gad.12.12.1763 [Accessed May 25, 2013].

Ahn, K.H., Mahmoud, M.M. & Kendall, D.A., 2012. Allosteric modulator ORG27569 induces CB1 cannabinoid receptor high affinity agonist binding state, receptor internalization, and Gi protein-independent ERK1/2 kinase activation. The Journal of Biological Chemistry, 287(15), pp.12070–82. Available at: http://www.ncbi.nlm.nih.gov/pubmed/22343625.

AJ, W. et al., 2009. Fatty acid incubation of myotubes from humans with type 2 diabetes leads to enhanced release of β-oxidation products because of impaired fatty acid oxidation effects. Diabetes, 58(3), pp.527–535. Available at: http://diabetes.diabetesjournals.org/content/58/3/527.short [Accessed January 20, 2014].

Alaoui-Jamali, M., Song, D. & Benlimame, N., 2003. Regulation of multiple tumor microenvironment markers by overexpression of single or paired combinations of ErbB receptors. Cancer research, 63(13), pp.3764–3774. Available at: http://cancerres.aacrjournals.org/content/63/13/3764.short [Accessed January 21, 2014].

Aleem, E., Kiyokawa, H. & Kaldis, P., 2005. Cdc2-cyclin E complexes regulate the G1/S phase transition. Nature cell biology, 7(8), pp.831–6. Available at: http://www.ncbi.nlm.nih.gov/pubmed/16007079 [Accessed August 10, 2013].

Al-Khalili, L. et al., 2003. Insulin action in cultured human skeletal muscle cells during differentiation: assessment of cell surface GLUT4 and GLUT1 content. Cellular and molecular life sciences : CMLS, 60(5), pp.991–8. Available at: http://www.ncbi.nlm.nih.gov/pubmed/12827286.

Allison, D.B. et al., 2006. Microarray data analysis: from disarray to consolidation and consensus. Nature reviews. Genetics, 7(1), pp.55–65. Available at: http://www.ncbi.nlm.nih.gov/pubmed/16369572 [Accessed March 1, 2012].

Alquier, T., Peyot, M. & Latour, M., 2009. Deletion of GPR40 impairs glucose-induced insulin secretion in vivo in mice without affecting intracellular fuel metabolism in islets. Diabetes, 58(11), pp.2607–2615. Available at: http://diabetes.diabetesjournals.org/content/58/11/2607.short [Accessed January 21, 2014].

Andrechek, E., 2002. ErbB2 is required for muscle spindle and myoblast cell survival. Molecular and cellular biology, 22(13), pp.4714–4722. Available at: http://mcb.asm.org/content/22/13/4714.short [Accessed January 21, 2014].

Angione, A.R. et al., 2011. PPARδ regulates satellite cell proliferation and skeletal muscle regeneration. Skeletal muscle, 1(1), p.33. Available at: http://www.pubmedcentral.nih.gov/articlerender.fcgi?artid=3223495&tool=pmcentrez&rendertype=abstract [Accessed August 12, 2013].

Arner, P., 2002. Insulin resistance in type 2 diabetes: role of fatty acids. Diabetes/metabolism research and reviews, 18 Suppl 2, pp.S5–9. Available at: http://www.ncbi.nlm.nih.gov/pubmed/11921432.

Artmann, A. et al., 2008. Influence of dietary fatty acids on endocannabinoid and N-acylethanolamine levels in rat brain, liver and small intestine. Biochimica et

biophysica acta, 1781(4), pp.200–12. Available at: http://www.ncbi.nlm.nih.gov/pubmed/18316044 [Accessed March 19, 2012].

B, U. et al., 2005. Dynamic changes in fat oxidation in human primary myocytes mirror metabolic characteristics of the donor. Journal of Clinical Investigation, 115(7), pp.1934–1941. Available at: http://www.jci.org/cgi/content/abstract/115/7/1934 [Accessed January 20, 2014].

Baeckstro, D., Lu, P. & Taylor-papadimitriou, J., 2000. Activation of the alpha2beta1 integrin prevents c-erbB2-induced scattering and apoptosis of human mammary epithelial cells in collagen. Oncogene, 19(40), pp.4592–4603.

Baker, P.E. et al., 2006. Analysis of gene expression differences between utrophin/dystrophin-deficient vs mdx skeletal muscles reveals a specific upregulation of slow muscle genes in limb muscles. Neurogenetics, 7(2), pp.81–91. Available at: http://www.ncbi.nlm.nih.gov/pubmed/16525850 [Accessed March 21, 2012].

Bartoov-Shifman, R. et al., 2007. Regulation of the gene encoding GPR40, a fatty acid receptor expressed selectively in pancreatic beta cells. The Journal of biological chemistry, 282(32), pp.23561–71. Available at: http://www.ncbi.nlm.nih.gov/pubmed/17525159 [Accessed May 25, 2013].

Barutta, F., Corbelli, A. & Mastrocola, R., 2010. Cannabinoid receptor 1 blockade ameliorates albuminuria in experimental diabetic nephropathy. Diabetes, 59(4), pp.1046–1054. Available at: http://diabetes.diabetesjournals.org/content/59/4/1046.short [Accessed January 21, 2014].

Bastie, C. et al., 1999. Expression of Peroxisome Proliferator-activated Receptor PPARdelta Promotes Induction of PPARgamma and Adipocyte Differentiation in 3T3C2 Fibroblasts. Journal of Biological Chemistry, 274(31), pp.21920–21925. Available at: http://www.jbc.org/cgi/doi/10.1074/jbc.274.31.21920 [Accessed August 21, 2013].

Beauchamp, J.R. et al., 1999. Dynamics of myoblast transplantation reveal a discrete minority of precursors with stem cell-like properties as the myogenic source. The Journal of cell biology, 144(6), pp.1113–22. Available at: http://www.pubmedcentral.nih.gov/articlerender.fcgi?artid=2150577&tool=pmcentrez&rendertype=abstract.

Bellocchio, L. et al., 2008. The endocannabinoid system and energy metabolism. Journal of neuroendocrinology, 20(6), pp.850–7. Available at: http://www.ncbi.nlm.nih.gov/pubmed/18601709 [Accessed March 16, 2012].

Benlimame, N. et al., 2005. FAK signaling is critical for ErbB-2/ErbB-3 receptor cooperation for oncogenic transformation and invasion. The Journal of cell biology, 171(3), pp.505–16. Available at: http://www.pubmedcentral.nih.gov/articlerender.fcgi?artid=2171271&tool=pmcentrez&rendertype=abstract [Accessed August 12, 2013].

Bensaid, M. et al., 2003. The cannabinoid CB1 receptor antagonist SR141716 increases Acrp30 mRNA expression in adipose tissue of obese fa/fa rats and in cultured adipocyte cells. Molecular pharmacology, 63(4), pp.908–14. Available at: http://www.ncbi.nlm.nih.gov/pubmed/12644592.

Berchtold, M.W., Brinkmeier, H. & Müntener, M., 2000. Calcium ion in skeletal muscle: its crucial role for muscle function, plasticity, and disease. Physiological reviews, 80(3), pp.1215–65. Available at: http://www.ncbi.nlm.nih.gov/pubmed/10893434.

Berggren, J.R. et al., 2005. Glucose Uptake in Muscle Cell Cultures from Endurance-Trained Men. Medicine & Science in Sports & Exercise, 37(4), pp.579–584. Available at: http://content.wkhealth.com/linkback/openurl?sid=WKPTLP:landingpage&an=00005768-200504000-00008 [Accessed June 8, 2013].

Bermudez-Silva, F.J. et al., 2007. Role of cannabinoid CB2 receptors in glucose homeostasis in rats. European Journal of Pharmacology, 565(1-3), pp.207–211.

Available at: http://linkinghub.elsevier.com/retrieve/pii/S001429990700249X [Accessed June 19, 2013].

Bhasker, C.R. & Friedmann, T., 2008. Insulin-like growth factor-1 coordinately induces the expression of fatty acid and cholesterol biosynthetic genes in murine C2C12 myoblasts. BMC genomics, 9, p.535. Available at: http://www.pubmedcentral.nih.gov/articlerender.fcgi?artid=2628395&tool=pmcentrez&rendertype=abstract [Accessed December 9, 2012].

Biressi, S., Molinaro, M. & Cossu, G., 2007. Cellular heterogeneity during vertebrate skeletal muscle development. Developmental biology, 308(2), pp.281–93. Available at: http://www.ncbi.nlm.nih.gov/pubmed/17612520 [Accessed August 12, 2013].

Blau, H.M. & Webster, C., 1981. Isolation and characterization of human muscle cells. Proceedings of the National Academy of Sciences of the United States of America, 78(9), pp.5623–7. Available at: http://www.pubmedcentral.nih.gov/articlerender.fcgi?artid=348807&tool=pmcentrez&rendertype=abstract.

Blüher, M. et al., 2006. Dysregulation of the peripheral and adipose tissue endocannabinoid system in human abdominal obesity. Diabetes, 55(11), pp.3053–60. Available at: http://www.pubmedcentral.nih.gov/articlerender.fcgi?artid=2228260&tool=pmcentrez&rendertype=abstract [Accessed June 15, 2013].

Boden, G. & Shulman, G.I., 2002. Free fatty acids in obesity and type 2 diabetes: defining their role in the development of insulin resistance and beta-cell dysfunction. European journal of clinical investigation, 32 Suppl 3, pp.14–23. Available at: http://www.ncbi.nlm.nih.gov/pubmed/12028371.

Bonala, S. et al., 2012. Peroxisome proliferator-activated receptor β/δ induces myogenesis by modulating myostatin activity. The Journal of biological chemistry, 287(16), pp.12935–51. Available at: http://www.pubmedcentral.nih.gov/articlerender.fcgi?artid=3339972&tool=pmcentrez&rendertype=abstract [Accessed August 20, 2013].

Bonini, J., Borowsky, B. & Adham, N., 2001. DNA encoding SNORF25 receptor. US Patent …, 1(12). Available at: http://www.google.com/patents?hl=en&lr=&vid=USPAT6221660&id=SCEGAAAAEBAJ&oi=fnd&dq=DNA+Encoding+SNORF25+Receptor&printsec=abstract [Accessed September 1, 2013].

Bonini, J., Borowsky, B. & Adham, N., 2002. Methods of identifying compounds that bind to SNORF25 receptors. US Patent, 1(12). Available at: http://www.google.com/patents?hl=en&lr=&vid=USPAT6468756&id=AawKAAAAEBAJ&oi=fnd&dq=METHODS+OF+IDENTIFYING+COMPOUNDS+THAT+BIND+TO+SNORF25+RECEPTORS&printsec=abstract [Accessed September 1, 2013].

Bouché, C. et al., 2004. The cellular fate of glucose and its relevance in type 2 diabetes. Endocrine reviews, 25(5), pp.807–30. Available at: http://www.ncbi.nlm.nih.gov/pubmed/15466941 [Accessed November 3, 2012].

Braiman, L. et al., 2001. Activation of Protein Kinase Cζ Induces Serine Phosphorylation of VAMP2 in the GLUT4 Compartment and Increases Glucose Transport in Skeletal Muscle. Molecular and cellular biology, 21(22), pp.7852–7861. Available at: http://mcb.asm.org/content/21/22/7852.short.

Briscoe, C. & Tadayyon, M., 2003. The orphan G protein-coupled receptor GPR40 is activated by medium and long chain fatty acids. Journal of Biological …, 278(13), pp.11303–11311. Available at: http://www.jbc.org/content/278/13/11303.short [Accessed January 21, 2014].

Briscoe, C.P. et al., 2006. Pharmacological regulation of insulin secretion in MIN6 cells through the fatty acid receptor GPR40: identification of agonist and antagonist small molecules. British journal of pharmacology, 148(5), pp.619–28. Available at: http://www.pubmedcentral.nih.gov/articlerender.fcgi?artid=1751878&tool=pmcentrez&rendertype=abstract [Accessed March 12, 2012].

Brownlie, R. et al., 2008. The long-chain fatty acid receptor, GPR40, and glucolipotoxicity: investigations using GPR40-knockout mice. Biochemical Society transactions, 36(Pt 5), pp.950–4. Available at: http://www.ncbi.nlm.nih.gov/pubmed/18793167 [Accessed March 12, 2012].

Brozinick, J.T., Roberts, B.R. & Dohm, G.L., 2003. Defective signaling through Akt-2 and -3 but not Akt-1 in insulin-resistant human skeletal muscle: potential role in insulin resistance. Diabetes, 52(4), pp.935–941. Available at: http://www.ncbi.nlm.nih.gov/pubmed/12663464.

Burant, C.F. et al., 2012. TAK-875 versus placebo or glimepiride in type 2 diabetes mellitus: a phase 2, randomised, double-blind, placebo-controlled trial. Lancet, 379(9824), pp.1403–11. Available at: http://www.ncbi.nlm.nih.gov/pubmed/22374408 [Accessed January 10, 2014].

Burstein, S., 2005. PPAR-gamma: a nuclear receptor with affinity for cannabinoids. Life sciences, 77(14), pp.1674–84. Available at: http://www.ncbi.nlm.nih.gov/pubmed/16005906 [Accessed March 22, 2012].

Cartoni, C. et al., 2010. Taste preference for fatty acids is mediated by GPR40 and GPR120. The Journal of neuroscience : the official journal of the Society for Neuroscience, 30(25), pp.8376–82. Available at: http://www.ncbi.nlm.nih.gov/pubmed/20573884 [Accessed May 24, 2013].

Cavuoto, P et al., 2007. Effects of cannabinoid receptors on skeletal muscle oxidative pathways. Molecular and cellular endocrinology, 267(1-2), pp.63–9. Available at: http://www.ncbi.nlm.nih.gov/pubmed/17270342 [Accessed March 21, 2012].

Cavuoto, P., 2010. Endocannabinoids and skeletal muscle glucose uptake. University of Adelaide, Thesis(December). Available at: http://ebooks.adelaide.edu.au/dspace/handle/2440/65871 [Accessed January 11, 2014].

Cavuoto, Paul et al., 2007. The expression of receptors for endocannabinoids in human and rodent skeletal muscle. Biochemical and biophysical research communications, 364(1), pp.105–10. Available at: http://www.ncbi.nlm.nih.gov/pubmed/17935697 [Accessed March 21, 2012].

Chakravarthy, M. V et al., 2000. Insulin-like growth factor-I extends in vitro replicative life span of skeletal muscle satellite cells by enhancing G1/S cell cycle progression via the activation of phosphatidylinositol 3'-kinase/Akt signaling pathway. The Journal of biological chemistry, 275(46), pp.35942–52. Available at: http://www.ncbi.nlm.nih.gov/pubmed/10962000 [Accessed August 21, 2013].

Chang, L., Chiang, S.-H. & Saltiel, A.R., 2005. Insulin signaling and the regulation of glucose transport. Molecular medicine (Cambridge, Mass.), 10(7-12), pp.65–71. Available at: http://www.pubmedcentral.nih.gov/articlerender.fcgi?artid=1431367&tool=pmcentrez&rendertype=abstract [Accessed August 29, 2013].

Chavez, J.A. et al., 2003. A role for ceramide, but not diacylglycerol, in the antagonism of insulin signal transduction by saturated fatty acids. The Journal of biological chemistry, 278(12), pp.10297–303. Available at: http://www.ncbi.nlm.nih.gov/pubmed/12525490 [Accessed March 21, 2012].

Chavez, J.A. et al., 2005. Acid ceramidase overexpression prevents the inhibitory effects of saturated fatty acids on insulin signaling. The Journal of biological chemistry, 280(20), pp.20148–53. Available at: http://www.ncbi.nlm.nih.gov/pubmed/15774472 [Accessed May 28, 2013].

Chemello, F. et al., 2011. Microgenomic analysis in skeletal muscle: expression signatures of individual fast and slow myofibers. PloS one, 6(2), p.e16807. Available at: http://www.pubmedcentral.nih.gov/articlerender.fcgi?artid=3043066&tool=pmcentrez&rendertype=abstract [Accessed June 3, 2013].

Chen, Y.-W. et al., 2007. Transcriptional pathways associated with skeletal muscle disuse atrophy in humans. Physiological genomics, 31(3), pp.510–20. Available at: http://www.ncbi.nlm.nih.gov/pubmed/17804603 [Accessed September 2, 2013].

Chiang, S.-H., Chang, L. & Saltiel, A.R., 2006. TC10 and insulin-stimulated glucose transport. Methods in enzymology, 406, pp.701–14. Available at: http://www.ncbi.nlm.nih.gov/pubmed/16472699.

Chokkalingam, K. et al., 2007. High-fat/low-carbohydrate diet reduces insulin-stimulated carbohydrate oxidation but stimulates nonoxidative glucose disposal in humans: An important role for skeletal muscle pyruvate dehydrogenase kinase 4. The Journal of clinical endocrinology and metabolism, 92(1), pp.284–92. Available at: http://www.ncbi.nlm.nih.gov/pubmed/17062764 [Accessed June 17, 2013].

Chu, Z.-L. et al., 2007. A role for beta-cell-expressed G protein-coupled receptor 119 in glycemic control by enhancing glucose-dependent insulin release. Endocrinology, 148(6), pp.2601–9. Available at: http://www.ncbi.nlm.nih.gov/pubmed/17289847 [Accessed August 27, 2013].

Coll, T. et al., 2008. Oleate reverses palmitate-induced insulin resistance and inflammation in skeletal muscle cells. The Journal of biological chemistry, 283(17), pp.11107–16. Available at: http://www.ncbi.nlm.nih.gov/pubmed/18281277 [Accessed March 12, 2012].

Cornish, J. et al., 2008. Modulation of osteoclastogenesis by fatty acids. Endocrinology, 149(11), pp.5688–95. Available at: http://www.ncbi.nlm.nih.gov/pubmed/18617622 [Accessed May 24, 2013].

Costanzi, S., Neumann, S. & Gershengorn, M.C., 2008. Seven transmembrane-spanning receptors for free fatty acids as therapeutic targets for diabetes mellitus: pharmacological, phylogenetic, and drug discovery aspects. The Journal of biological chemistry, 283(24), pp.16269–73. Available at: http://www.pubmedcentral.nih.gov/articlerender.fcgi?artid=2423253&tool=pmcentrez&rendertype=abstract [Accessed March 5, 2012].

Cota, D. & Marsicano, G., 2003. The endogenous cannabinoid system affects energy balance via central orexigenic drive and peripheral lipogenesis. Journal of clinical investigation, 112(3), pp.423–431. Available at: http://www.jci.org/cgi/content/abstract/112/3/423 [Accessed January 21, 2014].

Dalton, G.D. et al., 2009. Signal transduction via cannabinoid receptors. CNS & neurological disorders drug targets, 8(6), pp.422–31. Available at: http://www.ncbi.nlm.nih.gov/pubmed/19839935.

Demuth, D.G. & Molleman, A., 2006. Cannabinoid signalling. Life sciences, 78(6), pp.549–63. Available at: http://www.ncbi.nlm.nih.gov/pubmed/16109430 [Accessed June 16, 2013].

Dietze, D. et al., 2002. Impairment of insulin signaling in human skeletal muscle cells by co-culture with human adipocytes. Diabetes, 51(8), pp.2369–76. Available at: http://www.ncbi.nlm.nih.gov/pubmed/12145147.

Di-Marzo, V. & Matias, I., 2005. Endocannabinoid control of food intake and energy balance. Nature neuroscience, 8(5), pp.585–9. Available at: http://www.ncbi.nlm.nih.gov/pubmed/15856067 [Accessed February 29, 2012].

Dipl-Pharm, S. & Zierath, J., 2005. Tackling the insulin-signalling cascade. Canadian Journal of Diabetes, 29(3), pp.239–245. Available at: http://www.diabetes.ca/Files/Zierath-Tackling_pages_239-245.pdf [Accessed January 19, 2014].

Dorn, G. et al., 1997. Alpha 2A-adrenergic receptor stimulated calcium release is transduced by Gi-associated G(beta gamma)-mediated activation of phospholipase C. Biochemistry, 36(21), pp.6415–1423. Available at: http://www.ncbi.nlm.nih.gov/pubmed/9174358.

Doshi, L., Brahma, M. & Sayyed, S., 2009. Acute administration of GPR40 receptor agonist potentiates glucose-stimulated insulin secretion in vivo in the rat.

Metabolism. Available at: http://www.sciencedirect.com/science/article/pii/S0026049508003946 [Accessed September 2, 2013].

Doshi, L.S. et al., 2009. Acute administration of GPR40 receptor agonist potentiates glucose-stimulated insulin secretion in vivo in the rat. Metabolism, 58(3), pp.333–343. Available at: http://dx.doi.org/10.1016/j.metabol.2008.10.005.

Drucker, D.J., 2001. Development of glucagon-like peptide-1-based pharmaceuticals as therapeutic agents for the treatment of diabetes. Current pharmaceutical design, 7(14), pp.1399–412. Available at: http://www.ncbi.nlm.nih.gov/pubmed/11472275.

Duguez, S. et al., 2003. Myogenic and nonmyogenic cells differentially express proteinases, Hsc/Hsp70, and BAG-1 during skeletal muscle regeneration. American journal of physiology. Endocrinology and metabolism, 285(1), pp.E206–15. Available at: http://www.ncbi.nlm.nih.gov/pubmed/12791605 [Accessed September 3, 2013].

Duttaroy, A. & Albuquerque, B., 2008. An improved metabolic phenotype in mice deficient in free fatty acid receptor GPR40 in response to a high fat diet. NOVARTIS, p.40. Available at: http://professional.diabetes.org/Content/Posters/2008/p1121-P.pdf [Accessed January 21, 2014].

Ebner, S. et al., 2002. 3: human monocytes cultured in the presence of IL-3 and IL-4 differentiate into dendritic cells that produce less IL-12 and shift Th cell responses toward a Th2 cytokine. J Immunol., 168(12), pp.6199–6207. Available at: http://www.jimmunol.org/content/168/12/6199.short [Accessed January 21, 2014].

Eckardt, K. et al., 2009. Cannabinoid type 1 receptors in human skeletal muscle cells participate in the negative crosstalk between fat and muscle. Diabetologia, 52(4), pp.664–74. Available at: http://www.ncbi.nlm.nih.gov/pubmed/19089403 [Accessed March 16, 2012].

Eckardt, K., Sell, H. & Eckel, J., 2008. Novel aspects of adipocyte-induced skeletal muscle insulin resistance. Archives of physiology and biochemistry, 114(4), pp.287–98. Available at: http://www.ncbi.nlm.nih.gov/pubmed/18946789 [Accessed March 5, 2012].

Eckert, C. et al., 2012. Conservation and divergence between cytoplasmic and muscle-specific actin capping proteins: insights from the crystal structure of cytoplasmic Cap32/34 from Dictyostelium discoideum. BMC structural …, 12(12). Available at: http://www.biomedcentral.com/1472-6807/12/12/ [Accessed January 21, 2014].

Edfalk, S., Steneberg, P. & Edlund, H., 2008. Gpr40 is expressed in enteroendocrine cells and mediates free fatty acid stimulation of incretin secretion. Diabetes, 57(September). Available at: http://diabetes.diabetesjournals.org/content/57/9/2280.short [Accessed May 25, 2013].

Ehrenborg, E. & Krook, A., 2009. Regulation of skeletal muscle physiology and metabolism by peroxisome proliferator-activated receptor δ. Pharmacological reviews, 61(3), pp.373–393. Available at: http://intl.pharmrev.org/content/61/3/373.short [Accessed January 21, 2014].

Eisenberg, E. & Levanon, E.Y., 2003. Human housekeeping genes are compact. Trends in genetics : TIG, 19(7), pp.362–5. Available at: http://www.ncbi.nlm.nih.gov/pubmed/12850439.

Engeli, S., 2008a. Peripheral metabolic effects of endocannabinoids and cannabinoid receptor blockade. Obesity facts, 1(1), pp.8–15. Available at: http://www.ncbi.nlm.nih.gov/pubmed/20054157 [Accessed March 21, 2012].

Engeli, S., 2008b. The Endocannabinoid System, Obesity, and Insulin Resistance Stefan Engeli, MD Corresponding. Clinical Research, 2(1), pp.72–78. Available at: http://link.springer.com/article/10.1007/s12170-008-0014-3.

Engeli, S., Böhnke, J. & Feldpausch, M., 2005. Activation of the peripheral endocannabinoid system in human obesity. Diabetes, 54(10), pp.2838–2843.

Available at: http://diabetes.diabetesjournals.org/content/54/10/2838.short [Accessed January 21, 2014].

Esposito, I. et al., 2008. The Cannabinoid CB1 Receptor Antagonist Rimonabant Stimulates 2-Deoxyglucose Uptake in Skeletal Muscle Cells by Regulating the Expression of Phosphatidylinositol-3-kinase. Molecular Pharmacology, 74(6), pp.1678–1686.

Feng, D.D. et al., 2006. Reduction in voltage-gated K+ currents in primary cultured rat pancreatic beta-cells by linoleic acids. Endocrinology, 147(2), pp.674–82. Available at: http://www.ncbi.nlm.nih.gov/pubmed/16254037 [Accessed May 23, 2013].

Ferdaoussi, M. et al., 2012. G protein-coupled receptor (GPR)40-dependent potentiation of insulin secretion in mouse islets is mediated by protein kinase D1. Diabetologia, 55(10), pp.2682–92. Available at: http://www.ncbi.nlm.nih.gov/pubmed/22820510 [Accessed May 23, 2013].

Fischer, Y. et al., 1995. 5-Hydroxytryptamine Stimulates Glucose Transport in Cardiomyocytes Via a Monoamine Oxidase-Dependent Reaction. The Biochemical journal, 311 (Pt 2, pp.575–83. Available at: http://www.pubmedcentral.nih.gov/articlerender.fcgi?artid=1136038&tool=pmcentrez&rendertype=abstract.

Flodgren, E. et al., 2007. GPR40 is expressed in glucagon producing cells and affects glucagon secretion. Biochemical and biophysical research communications, 354(1), pp.240–5. Available at: http://www.ncbi.nlm.nih.gov/pubmed/17214971 [Accessed June 16, 2013].

Le Foll, C. et al., 2009. Characteristics and mechanisms of hypothalamic neuronal fatty acid sensing. American journal of physiology. Regulatory, integrative and comparative physiology, 297(3), pp.R655–64. Available at: http://www.pubmedcentral.nih.gov/articlerender.fcgi?artid=2739790&tool=pmcentrez&rendertype=abstract.

Fontés, G. et al., 2010. Glucolipotoxicity age-dependently impairs beta cell function in rats despite a marked increase in beta cell mass. Diabetologia, 53(11), pp.2369–79. Available at: http://www.pubmedcentral.nih.gov/articlerender.fcgi?artid=2947580&tool=pmcentrez&rendertype=abstract [Accessed May 23, 2013].

Fredriksson, R. et al., 2003. The G-protein-coupled receptors in the human genome form five main families. Phylogenetic analysis, paralogon groups, and fingerprints. Molecular pharmacology, 63(6), pp.1256–72. Available at: http://www.ncbi.nlm.nih.gov/pubmed/12761335.

Le Friec, G. et al., 2012. The CD46-Jagged1 interaction is critical for human TH1 immunity. Nature immunology, 13(12), pp.1213–21. Available at: http://www.pubmedcentral.nih.gov/articlerender.fcgi?artid=3505834&tool=pmcentrez&rendertype=abstract [Accessed August 12, 2013].

Fujita, T. et al., 2011. A GPR40 Agonist GW9508 Suppresses CCL5 , CCL17 , and CXCL10 Induction in Keratinocytes and Attenuates Cutaneous Immune Inflammation. Journal of Investigative Dermatology, 131(8), pp.1660–1667. Available at: http://dx.doi.org/10.1038/jid.2011.123.

Fujiwara, K., Maekawa, F. & Yada, T., 2005. Oleic acid interacts with GPR40 to induce Ca2+ signaling in rat islet beta-cells: mediation by PLC and L-type Ca2+ channel and link to insulin release. American journal of physiology. Endocrinology and metabolism, 289(4), pp.E670–7. Available at: http://www.ncbi.nlm.nih.gov/pubmed/15914509 [Accessed March 12, 2012].

Gainetdinov, R.R. et al., 2004. Desensitization of G protein-coupled receptors and neuronal functions. Annual review of neuroscience, 27, pp.107–44. Available at: http://www.ncbi.nlm.nih.gov/pubmed/15217328 [Accessed May 27, 2013].

Galang, C.K. et al., 2004. Changes in the expression of many Ets family transcription factors and of potential target genes in normal mammary tissue and tumors. The

Journal of biological chemistry, 279(12), pp.11281–92. Available at: http://www.ncbi.nlm.nih.gov/pubmed/14662758 [Accessed August 12, 2013].

Galgani, J.E. et al., 2013. Enhanced Skeletal Muscle Lipid Oxidative Efficiency in Insulin-Resistant Vs Insulin-Sensitive Nondiabetic, Nonobese Humans. The Journal of clinical endocrinology and metabolism, 98(4), pp.E646–53. Available at: http://www.ncbi.nlm.nih.gov/pubmed/23393182 [Accessed May 27, 2013].

Gamberucci , Alessandra, Fulceri, Rosella, Benedetti, A., 2003. inhibiton of store-dependent capacitative Ca influx by unsaturated fatty acids. Chaos, Solitons & Fractals, 15(5), p.II. Available at: http://linkinghub.elsevier.com/retrieve/pii/S0960077902004344.

Gary-Bobo, M., Elachouri, G. & Scatton, B., 2006. CB1 receptor antagonist rimonabant (SR141716) inhibits cell proliferation and increases markers of adipocyte maturation in cultured mouse 3T3 F442A preadipocytes. Mol Pharmacol., 69(2), pp.471–478. Available at: http://molpharm.aspetjournals.org/content/69/2/471.short [Accessed January 21, 2014].

Gaster, M. et al., 2004. Reduced lipid oxidation in skeletal muscle from type 2 diabetic subjects may be of genetic origin: evidence from cultured myotubes. Diabetes, 53(3), pp.542–8. Available at: http://www.ncbi.nlm.nih.gov/pubmed/14988236.

Gaster, M., Beck-Nielsen, H. & Schrøder, H.D., 2001. Proliferation conditions for human satellite cells. The fractional content of satellite cells. APMIS : acta pathologica, microbiologica, et immunologica Scandinavica, 109(11), pp.726–34. Available at: http://www.ncbi.nlm.nih.gov/pubmed/11900051.

Gho, J.W.-M. et al., 2008. Re-expression of transcription factor ATF5 in hepatocellular carcinoma induces G2-M arrest. Cancer research, 68(16), pp.6743–51. Available at: http://www.ncbi.nlm.nih.gov/pubmed/18701499 [Accessed August 21, 2013].

Glass, M. & Felder, C.C., 1997. Concurrent stimulation of cannabinoid CB1 and dopamine D2 receptors augments cAMP accumulation in striatal neurons: evidence for a Gs linkage to the CB1 receptor. The Journal of neuroscience : the official journal of the Society for Neuroscience, 17(14), pp.5327–33. Available at: http://www.ncbi.nlm.nih.gov/pubmed/9204917.

Gonthier, M. et al., 2007. Identification of endocannabinoids and related compounds in human fat cells. Obesity (Silver Spring)., 15(4), pp.837–845. Available at: http://onlinelibrary.wiley.com/doi/10.1038/oby.2007.581/full [Accessed January 21, 2014].

Gonzalez de Aguilar, J.-L. et al., 2008. Gene profiling of skeletal muscle in an amyotrophic lateral sclerosis mouse model. Physiological genomics, 32(2), pp.207–18. Available at: http://www.ncbi.nlm.nih.gov/pubmed/18000159 [Accessed March 10, 2012].

Goodwin, B. et al., 2000. A regulatory cascade of the nuclear receptors FXR, SHP-1, and LRH-1 represses bile acid biosynthesis. Molecular cell, 6(3), pp.517–26. Available at: http://www.ncbi.nlm.nih.gov/pubmed/11030332.

Gras, D. et al., 2009a. Thiazolidinediones induce proliferation of human bronchial epithelial cells through the GPR40 receptor. American journal of physiology. Lung cellular and molecular physiology, 296(6), pp.L970–8. Available at: http://www.ncbi.nlm.nih.gov/pubmed/19346435 [Accessed October 7, 2012].

Gras, D. et al., 2009b. Thiazolidinediones induce proliferation of human bronchial epithelial cells through the GPR40 receptor. American journal of physiology. Lung cellular and molecular physiology, 296(6), pp.L970–8. Available at: http://www.ncbi.nlm.nih.gov/pubmed/19346435 [Accessed August 21, 2013].

Grassian, A.R. et al., 2011. Erk regulation of pyruvate dehydrogenase flux through PDK4 modulates cell proliferation. Genes & development, 25(16), pp.1716–33. Available at: http://www.pubmedcentral.nih.gov/articlerender.fcgi?artid=3165936&tool=pmcentrez&rendertype=abstract [Accessed March 21, 2012].

Graus-Porta, D. et al., 1997. ErbB-2, the preferred heterodimerization partner of all ErbB receptors, is a mediator of lateral signaling. The EMBO journal, 16(7), pp.1647–55. Available at: http://www.pubmedcentral.nih.gov/articlerender.fcgi?artid=1169769&tool=pmcentrez&rendertype=abstract.

Griffin, M.E. et al., 1999. Free fatty acid-induced insulin resistance is associated with activation of protein kinase C theta and alterations in the insulin signaling cascade. Diabetes, 48(6), pp.1270–4. Available at: http://www.ncbi.nlm.nih.gov/pubmed/10342815.

Gromada, J. et al., 2004. Glucagon-like peptide-1: regulation of insulin secretion and therapeutic potential. Basic & clinical pharmacology & toxicology, 95(6), pp.252–62. Available at: http://www.ncbi.nlm.nih.gov/pubmed/15569269.

Del Guerra, S. et al., 2010. G-protein-coupled receptor 40 (GPR40) expression and its regulation in human pancreatic islets: the role of type 2 diabetes and fatty acids. Nutrition, metabolism, and cardiovascular diseases : NMCD, 20(1), pp.22–5. Available at: http://www.ncbi.nlm.nih.gov/pubmed/19758793.

Guigal, N. et al., 2002. Uncoupling protein-3 (UCP3) mRNA expression in reconstituted human muscle after myoblast transplantation in RAG2-/-/gamma c/C5(-) immunodeficient mice. The Journal of biological chemistry, 277(49), pp.47407–11. Available at: http://www.ncbi.nlm.nih.gov/pubmed/12351640 [Accessed March 12, 2012].

Guillet-Deniau, I., 1997. Identification and Localization of a Skeletal Muscle Secrotonin 5-HT2A Receptor Coupled to the Jak/STAT Pathway. Journal of Biological Chemistry, 272(23), pp.14825–14829. Available at: http://www.jbc.org/cgi/doi/10.1074/jbc.272.23.14825 [Accessed August 29, 2013].

Guo, G. et al., 2004. Expression of ErbB2 enhances radiation-induced NF-kappaB activation. Oncogene, 23(2), pp.535–45. Available at: http://www.ncbi.nlm.nih.gov/pubmed/14724581 [Accessed August 12, 2013].

Gyorffy, B. et al., 2009. Evaluation of microarray preprocessing algorithms based on concordance with RT-PCR in clinical samples. PloS one, 4(5), p.e5645. Available at: http://www.pubmedcentral.nih.gov/articlerender.fcgi?artid=2680989&tool=pmcentrez&rendertype=abstract [Accessed November 2, 2012].

Habets, P.E.M.H. et al., 1999. RNA Content Differs in Slow and Fast Muscle Fibers: Implications for Interpretation of Changes in Muscle Gene Expression. Journal of Histochemistry & Cytochemistry, 47(8), pp.995–1004. Available at: http://jhc.sagepub.com/lookup/doi/10.1177/002215549904700803 [Accessed September 1, 2013].

Hajduch, E., 1999. Serotonin (5-Hydroxytryptamine), a Novel Regulator of Glucose Transport in Rat Skeletal Muscle. Journal of Biological Chemistry, 274(19), pp.13563–13568. Available at: http://www.jbc.org/cgi/doi/10.1074/jbc.274.19.13563 [Accessed June 10, 2013].

Halse, R. & Bonavaud, S., 2001. Control of glycogen synthesis by glucose, glycogen, and insulin in cultured human muscle cells. Diabetes, 50(April). Available at: http://diabetes.diabetesjournals.org/content/50/4/720.short [Accessed January 19, 2014].

Han, G.-M. et al., 2003. Analysis of gene expression profiles in human systemic lupus erythematosus using oligonucleotide microarray. Genes and immunity, 4(3), pp.177–86. Available at: http://www.ncbi.nlm.nih.gov/pubmed/12700592 [Accessed March 12, 2012].

Han, J.-K. et al., 2008. Peroxisome proliferator-activated receptor-delta agonist enhances vasculogenesis by regulating endothelial progenitor cells through genomic and nongenomic activations of the phosphatidylinositol 3-kinase/Akt pathway. Circulation, 118(10), pp.1021–33. Available at: http://www.ncbi.nlm.nih.gov/pubmed/18711014 [Accessed August 21, 2013].

Han, M.S. et al., 2011. Lysophosphatidylcholine as an effector of fatty acid-induced insulin resistance. Journal of lipid research, 52(6), pp.1234–46. Available at: http://www.pubmedcentral.nih.gov/articlerender.fcgi?artid=3090244&tool=pmcentrez&rendertype=abstract [Accessed May 21, 2013].

Hannah, V.C. et al., 2001. Unsaturated fatty acids down-regulate srebp isoforms 1a and 1c by two mechanisms in HEK-293 cells. The Journal of biological chemistry, 276(6), pp.4365–72. Available at: http://www.ncbi.nlm.nih.gov/pubmed/11085986 [Accessed March 21, 2012].

Hardy, S. et al., 2005. Oleate promotes the proliferation of breast cancer cells via the G protein-coupled receptor GPR40. The Journal of biological chemistry, 280(14), pp.13285–91. Available at: http://www.ncbi.nlm.nih.gov/pubmed/15695516 [Accessed March 12, 2012].

Harridge, S.D.R., 2007. Plasticity of human skeletal muscle: gene expression to in vivo function. Experimental physiology, 92(5), pp.783–97. Available at: http://www.ncbi.nlm.nih.gov/pubmed/17631518 [Accessed September 2, 2013].

Haslett, J.N. & Kunkel, L.M., 2002. Microarray analysis of normal and dystrophic skeletal muscle. International journal of developmental neuroscience : the official journal of the International Society for Developmental Neuroscience, 20(3-5), pp.359–65. Available at: http://www.ncbi.nlm.nih.gov/pubmed/12175874.

Henry, R. & Ciaraldi, T., 1996. Glycogen synthase activity is reduced in cultured skeletal muscle cells of non-insulin-dependent diabetes mellitus subjects. Journal of Clinical Investigation, 98(5), pp.1231–1236. Available at: http://www.ncbi.nlm.nih.gov/pmc/articles/PMC507545/ [Accessed January 19, 2014].

Hidalgo, M.A. et al., 2011. Biochemical and Biophysical Research Communications Oleic acid induces intracellular calcium mobilization , MAPK phosphorylation , superoxide production and granule release in bovine neutrophils. Biochemical and Biophysical Research Communications, 409(2), pp.280–286. Available at: http://dx.doi.org/10.1016/j.bbrc.2011.04.144.

Higginson, J., Wackerhage, H. & Woods, N., 2002. Blockades of mitogen-activated protein kinase and calcineurin both change fibre-type markers in skeletal muscle culture. Pflügers Archiv. Available at: http://link.springer.com/article/10.1007/s00424-002-0939-1 [Accessed August 12, 2013].

Hillard, C.J. et al., 1999. Synthesis and characterization of potent and selective agonists of the neuronal cannabinoid receptor (CB1). The Journal of pharmacology and experimental therapeutics, 289(3), pp.1427–33. Available at: http://www.ncbi.nlm.nih.gov/pubmed/10336536.

Hirabara, S.M., Curi, R. & Maechler, P., 2010. Saturated fatty acid-induced insulin resistance is associated with mitochondrial dysfunction in skeletal muscle cells. Journal of cellular physiology, 222(1), pp.187–94. Available at: http://www.ncbi.nlm.nih.gov/pubmed/19780047 [Accessed May 28, 2013].

Hirasawa, A. et al., 2008. Production and characterization of a monoclonal antibody against GPR40 (FFAR1; free fatty acid receptor 1). Biochemical and biophysical research communications, 365(1), pp.22–8. Available at: http://www.ncbi.nlm.nih.gov/pubmed/17980148 [Accessed September 2, 2013].

Hollander, P., 2007. Endocannabinoid blockade for improving glycemic control and lipids in patients with type 2 diabetes mellitus. The American journal of medicine, 120(2 Suppl 1), pp.S18–28; discussion S29–32. Available at: http://www.ncbi.nlm.nih.gov/pubmed/17296341 [Accessed March 21, 2012].

Holloway, G.P. et al., 2007. Skeletal muscle mitochondrial FAT/CD36 content and palmitate oxidation are not decreased in obese women. American journal of physiology. Endocrinology and metabolism, 292(6), pp.E1782–9. Available at: http://www.ncbi.nlm.nih.gov/pubmed/17311893 [Accessed May 28, 2013].

Howlett, A.C., 2005. Cannabinoid Receptor Signaling. Handb Exp Pharmacol, 168, pp.53–79. Available at: http://www.ncbi.nlm.nih.gov/pubmed/16596771.

Hsu, M.-C., Chang, H.-C. & Hung, W.-C., 2006. HER-2/neu represses the metastasis suppressor RECK via ERK and Sp transcription factors to promote cell invasion. The Journal of biological chemistry, 281(8), pp.4718–25. Available at: http://www.ncbi.nlm.nih.gov/pubmed/16377629 [Accessed August 12, 2013].

Hu, H. et al., 2009. Biochemical and Biophysical Research Communications A novel class of antagonists for the FFAs receptor GPR40. Biochemical and Biophysical Research Communications, 390(3), pp.557–563. Available at: http://dx.doi.org/10.1016/j.bbrc.2009.10.004.

Huang, T.-H. et al., 2009. Up-regulation of miR-21 by HER2/neu signaling promotes cell invasion. The Journal of biological chemistry, 284(27), pp.18515–24. Available at: http://www.pubmedcentral.nih.gov/articlerender.fcgi?artid=2709372&tool=pmcentrez&rendertype=abstract [Accessed August 12, 2013].

Huerta, M. et al., 2009. Effects of cannabinoids on caffeine contractures in slow and fast skeletal muscle fibers of the frog. The Journal of membrane biology, 229(2), pp.91–9. Available at: http://www.pubmedcentral.nih.gov/articlerender.fcgi?artid=2697372&tool=pmcentrez&rendertype=abstract [Accessed March 21, 2012].

Ichimura, A. et al., 2009. Free fatty acid receptors act as nutrient sensors to regulate energy homeostasis. Prostaglandins & other lipid mediators, 89(3-4), pp.82–8. Available at: http://www.ncbi.nlm.nih.gov/pubmed/19460454 [Accessed March 21, 2012].

Ijuin, T. & Takenawa, T., 2012. Regulation of Insulin Signaling and Glucose Transporter 4 (GLUT4) Exocytosis by Phosphatidylinositol 3,4,5-Trisphosphate (PIP3) Phosphatase, Skeletal Muscle, and Kidney Enriched Inositol Polyphosphate Phosphatase (SKIP). The Journal of biological chemistry, 287(10), pp.6991–9. Available at: http://www.pubmedcentral.nih.gov/articlerender.fcgi?artid=3293580&tool=pmcentrez&rendertype=abstract [Accessed March 12, 2012].

Ito, R. et al., 2013. TAK-875, a GPR40/FFAR1 agonist, in combination with metformin prevents progression of diabetes and β-cell dysfunction in Zucker diabetic fatty rats. British journal of pharmacology, 170(3), pp.568–80. Available at: http://www.ncbi.nlm.nih.gov/pubmed/23848179 [Accessed December 12, 2013].

Itoh, Y. et al., 2003. Free fatty acids regulate insulin secretion from pancreatic beta cells through GPR40. Nature, 422(6928), pp.173–6. Available at: http://www.ncbi.nlm.nih.gov/pubmed/12629551.

Jackson, S. et al., 2000. Decreased insulin responsiveness of glucose uptake in cultured human skeletal muscle cells from insulin-resistant nondiabetic relatives of type 2 diabetic families. Diabetes, 49(7), pp.1169–77. Available at: http://www.ncbi.nlm.nih.gov/pubmed/10909975.

Jacobs, A.E., Oosterhof, A. & Veerkamp, J.H., 1990. 2-Deoxy-D-glucose uptake in cultured human muscle cells. Biochimica et Biophysica Acta, 1051(3), pp.230–236. Available at: http://www.ncbi.nlm.nih.gov/pubmed/2310773.

Janot, M. et al., 2009. Glycogenome expression dynamics during mouse C2C12 myoblast differentiation suggests a sequential reorganization of membrane glycoconjugates. BMC genomics, 10, p.483. Available at: http://www.pubmedcentral.nih.gov/articlerender.fcgi?artid=2772862&tool=pmcentrez&rendertype=abstract [Accessed November 25, 2012].

Jean-Baptiste, G. et al., 2005. Peptide and non-peptide G-protein coupled receptors (GPCRs) in skeletal muscle. Peptides, 26(8), pp.1528–36. Available at: http://www.ncbi.nlm.nih.gov/pubmed/16042993 [Accessed August 9, 2013].

JeBailey, L. et al., 2004. Skeletal muscle cells and adipocytes differ in their reliance on TC10 and Rac for insulin-induced actin remodeling. Molecular endocrinology (Baltimore, Md.), 18(2), pp.359–72. Available at: http://www.ncbi.nlm.nih.gov/pubmed/14615606 [Accessed August 19, 2013].

JEHL-PIETRI, C., BASTIE, C. & GILLOT, I., 2000. Peroxisome-proliferator-activated receptor δ mediates the effects of long-chain fatty acids on post-confluent cell

proliferation. Biochem. J, 98, pp.93–98. Available at: http://www.biochemj.org/bj/350/bj3500093.htm [Accessed January 19, 2014].

Jin, K. et al., 2004. Defective adult neurogenesis in CB1 cannabinoid receptor knockout mice. Molecular pharmacology, 66(2), pp.204–8. Available at: http://www.ncbi.nlm.nih.gov/pubmed/15266010.

Johnson, S. & Denton, R., 2003. Insulin stimulation of pyruvate dehydrogenase in adipocytes involves two distinct signalling pathways. Biochemical Journal, 356, pp.351–356. Available at: http://www.ncbi.nlm.nih.gov/pmc/articles/PMC1223089/ [Accessed June 5, 2013].

Jucker, B.M. et al., 2007. Selective PPARdelta agonist treatment increases skeletal muscle lipid metabolism without altering mitochondrial energy coupling: an in vivo magnetic resonance spectroscopy study. American journal of physiology. Endocrinology and metabolism, 293(5), pp.E1256–64. Available at: http://www.ncbi.nlm.nih.gov/pubmed/17726146 [Accessed August 12, 2013].

K. Matsuda-Nagasumi1,*, R. Takami-Esaki2, K. Iwachidow2, Y. Yasuhara1, H. Tanaka2, K. Ogi3, M. Nakata2, T. Yano2, S. Hinuma4, S. Taketomi4, H. Odaka4, Y.K., Lack of GPR40 FFAR1 does not induce diabetes even under insulin resistance condition - Matsuda-Nagasumi - 2013 - Diabetes, Obesity and Metabolism - Wiley Online Library.

Kaplamadzhiev, D., Hisha, H. & Adachi, Y., 2010. Bone marrow-derived stromal cells can express neuronal markers by DHA/GPR40 signaling. Biosci Trends, 4(3), pp.119–29. Available at: http://www.irdrjournal.com/examples/Figure_Sample_BST.pdf [Accessed January 20, 2014].

Kebede, M. et al., 2012. Glucose activates free fatty acid receptor 1 gene transcription via phosphatidylinositol-3-kinase-dependent O-GlcNAcylation of pancreas-duodenum homeobox-1. Proceedings of the National Academy of Sciences of the United States of America, 109(7), pp.2376–81. Available at: http://www.pubmedcentral.nih.gov/articlerender.fcgi?artid=3289358&tool=pmcentrez&rendertype=abstract [Accessed May 24, 2013].

Kebede, M., Alquier, T. & Latour, M., 2008. The fatty acid receptor GPR40 plays a role in insulin secretion in vivo after high-fat feeding. Diabetes, 57(9), pp.2432–2437. Available at: http://diabetes.diabetesjournals.org/content/57/9/2432.short [Accessed January 21, 2014].

Kenakin, T., 2001. Inverse, protean, and ligand-selective agonism: matters of receptor conformation. The FASEB journal, 15(3), pp.598–611. Available at: http://www.fasebj.org/content/15/3/598.short [Accessed January 20, 2014].

Kim, Y.I. et al., 2006. Insulin regulation of skeletal muscle PDK4 mRNA expression is impaired in acute insulin-resistant states. Diabetes, 55(8), pp.2311–7. Available at: http://www.ncbi.nlm.nih.gov/pubmed/16873695 [Accessed March 21, 2012].

Kislinger, T. et al., 2005. Proteome dynamics during C2C12 myoblast differentiation. Molecular & cellular proteomics : MCP, 4(7), pp.887–901. Available at: http://www.ncbi.nlm.nih.gov/pubmed/15824125 [Accessed June 2, 2013].

Kobilka, B., 2007. G protein coupled receptor structure and activation. Biochimica et Biophysica Acta (BBA)-Biomembranes, 1768(4), pp.794–807. Available at: http://www.sciencedirect.com/science/article/pii/S0005273606003981 [Accessed January 20, 2014].

Koistinen, H. a, Chibalin, a V & Zierath, J.R., 2003. Aberrant p38 mitogen-activated protein kinase signalling in skeletal muscle from Type 2 diabetic patients. Diabetologia, 46(10), pp.1324–8. Available at: http://www.ncbi.nlm.nih.gov/pubmed/12937895 [Accessed October 30, 2012].

Koli, K., Ryynänen, M. & Keski-Oja, J., 2008. Latent TGF-beta binding proteins (LTBPs)-1 and -3 coordinate proliferation and osteogenic differentiation of human mesenchymal stem cells. Bone, 43(4), pp.679–688. Available at: http://www.ncbi.nlm.nih.gov/pubmed/18672106.

Kotarsky, K., Nilsson, N. & Flodgren, E., 2003. A human cell surface receptor activated by free fatty acids and thiazolidinedione drugs. Biochem Biophys Res Commun., 301(2), pp.406–410. Available at: http://www.sciencedirect.com/science/article/pii/S0006291X02030644 [Accessed January 21, 2014].

Koves, T.R. et al., 2008. Mitochondrial overload and incomplete fatty acid oxidation contribute to skeletal muscle insulin resistance. Cell metabolism, 7(1), pp.45–56. Available at: http://www.ncbi.nlm.nih.gov/pubmed/18177724 [Accessed May 21, 2013].

Krämer, D.K. et al., 2007. Role of AMP kinase and PPARdelta in the regulation of lipid and glucose metabolism in human skeletal muscle. The Journal of biological chemistry, 282(27), pp.19313–20. Available at: http://www.ncbi.nlm.nih.gov/pubmed/17500064 [Accessed August 9, 2013].

Kroeze, W.K., Sheffler, D.J. & Roth, B.L., 2003. G-protein-coupled receptors at a glance. Journal of cell science, 116(Pt 24), pp.4867–9. Available at: http://www.ncbi.nlm.nih.gov/pubmed/14625380 [Accessed August 7, 2013].

Kubis, H.-P. et al., 2003. Ca2+ transients activate calcineurin/NFATc1 and initiate fast-to-slow transformation in a primary skeletal muscle culture. American journal of physiology. Cell physiology, 285(1), pp.C56–63. Available at: http://www.ncbi.nlm.nih.gov/pubmed/12606309 [Accessed March 12, 2012].

Kudla, a J. et al., 1998. The FGF receptor-1 tyrosine kinase domain regulates myogenesis but is not sufficient to stimulate proliferation. The Journal of cell biology, 142(1), pp.241–50. Available at: http://www.pubmedcentral.nih.gov/articlerender.fcgi?artid=2133035&tool=pmcentrez&rendertype=abstract.

Kumai, Y. et al., 2007. Modulation of MyoD- and Ki- 67- Positive Satellite Cells in the Short- Term Denervated Rat Thyroarytenoid Muscle. The Laryngoscope, 117(11), pp.2063–7. Available at: http://onlinelibrary.wiley.com/doi/10.1097/MLG.0b013e318133a13c/full [Accessed January 20, 2014].

Kuninger, D., Kuzmickas, R. & Peng, B., 2004. Gene discovery by microarray: identification of novel genes induced during growth factor-mediated muscle cell survival and differentiation. Genomics. Available at: http://www.sciencedirect.com/science/article/pii/S0888754304002162 [Accessed August 12, 2013].

Kunos, G., 2007. Understanding metabolic homeostasis and imbalance: what is the role of the endocannabinoid system? The American journal of medicine, 120(9 Suppl 1), pp.S18–24; discussion S24. Available at: http://www.ncbi.nlm.nih.gov/pubmed/17720356 [Accessed March 21, 2012].

Kuroda, K., Okamoto, O. & Shinkai, H., 1999. Dermatopontin expression is decreased in hypertrophic scar and systemic sclerosis skin fibroblasts and is regulated by transforming growth factor-β1, interleukin-4,. Journal of investigative dermatology, pp.706–710. Available at: http://www.nature.com/jid/journal/v112/n5/abs/5600454a.html [Accessed August 13, 2013].

Kurokawa, H. & Arteaga, C., 2001. Inhibition of erbB receptor (HER) tyrosine kinases as a strategy to abrogate antiestrogen resistance in human breast cancer. Clinical cancer research. Available at: http://clincancerres.aacrjournals.org/content/7/12/4436s.short [Accessed August 13, 2013].

Lahlou, H. et al., 2012. Uncoupling of PI3K from ErbB3 impairs mammary gland development but does not impact on ErbB2-induced mammary tumorigenesis. Cancer research, 72(12), pp.3080–90. Available at: http://www.ncbi.nlm.nih.gov/pubmed/22665265 [Accessed August 12, 2013].

Lambert, G. et al., 2003. The farnesoid X-receptor is an essential regulator of cholesterol homeostasis. The Journal of biological chemistry, 278(4), pp.2563–70. Available at: http://www.ncbi.nlm.nih.gov/pubmed/12421815 [Accessed August 29, 2013].

Lan, H. et al., 2008. Lack of FFAR1/GPR40 Does Not Protect Mice From High-Fat Diet–Induced Metabolic Disease. Diabetes, 57(November), pp.2999–3006. Available at: http://diabetes.diabetesjournals.org/content/57/11/2999.short [Accessed January 21, 2014].

Lander, E.S. et al., 2001. Initial sequencing and analysis of the human genome. Nature, 409(6822), pp.860–921. Available at: http://www.ncbi.nlm.nih.gov/pubmed/11237011.

Lane, H.A. et al., 2000. ErbB2 Potentiates Breast Tumor Proliferation through Modulation of p27 Kip1 -Cdk2 Complex Formation: Receptor Overexpression Does Not Determine Growth Dependency. Mol Cell Biol., 20(9), pp.3210–3223. Available at: http://www.thebonejournal.com/article/S8756-3282(08)00324-4/abstract.

Latour, M.G. et al., 2007. GPR40 is necessary but not sufficient for fatty acid stimulation of insulin secretion in vivo. Diabetes, 56(4), pp.1087–94. Available at: http://www.pubmedcentral.nih.gov/articlerender.fcgi?artid=1853382&tool=pmcentrez&rendertype=abstract [Accessed March 11, 2012].

Lauckner, J.E. et al., 2008. GPR55 is a cannabinoid receptor that increases intracellular calcium and inhibits M current. Proceedings of the National Academy of Sciences of the United States of America, 105(7), pp.2699–704. Available at: http://www.pubmedcentral.nih.gov/articlerender.fcgi?artid=2268199&tool=pmcentrez&rendertype=abstract.

Layne, A.S. et al., 2011. Impaired muscle AMPK activation in the metabolic syndrome may attenuate improved insulin action after exercise training. The Journal of clinical endocrinology and metabolism, 96(6), pp.1815–26. Available at: http://www.pubmedcentral.nih.gov/articlerender.fcgi?artid=3100747&tool=pmcentrez&rendertype=abstract [Accessed May 28, 2013].

Lefebvre, P. & Chinetti, G., 2006. Sorting out the roles of PPARα in energy metabolism and vascular homeostasis. Journal of Clinical Investigation, 116(3), pp.571–580. Available at: http://www.ncbi.nlm.nih.gov/pmc/articles/PMC1386122/ [Accessed January 20, 2014].

Leu, M., 2003. Erbb2 regulates neuromuscular synapse formation and is essential for muscle spindle development. Development, 130(11), pp.2291–2301. Available at: http://dev.biologists.org/cgi/doi/10.1242/dev.00447 [Accessed August 12, 2013].

Liebler, S.S. et al., 2012. No evidence for a functional role of bi-directional Notch signaling during angiogenesis. PloS one, 7(12), p.e53074. Available at: http://www.pubmedcentral.nih.gov/articlerender.fcgi?artid=3532505&tool=pmcentrez&rendertype=abstract [Accessed August 12, 2013].

Lillioja, S. et al., 1987. Skeletal muscle capillary density and fiber type are possible determinants of in vivo insulin resistance in man. The Journal of clinical investigation, 80(2), pp.415–24. Available at: http://www.pubmedcentral.nih.gov/articlerender.fcgi?artid=442253&tool=pmcentrez&rendertype=abstract.

Lin, D. et al., 2012. Identification and pharmacological characterization of multiple allosteric binding sites on the free fatty acid 1 receptor. … pharmacology. Available at: http://molpharm.aspetjournals.org/content/82/5/843.short [Accessed August 19, 2013].

Lin, D.C.-H. et al., 2011. AMG 837: a novel GPR40/FFA1 agonist that enhances insulin secretion and lowers glucose levels in rodents. PloS one, 6(11), p.e27270. Available at: http://www.pubmedcentral.nih.gov/articlerender.fcgi?artid=3210765&tool=pmcentrez&rendertype=abstract [Accessed May 23, 2013].

Lindborg, K. a et al., 2010. Effects of in vitro antagonism of endocannabinoid-1 receptors on the glucose transport system in normal and insulin-resistant rat skeletal muscle.

Diabetes, obesity & metabolism, 12(8), pp.722–30. Available at: http://www.ncbi.nlm.nih.gov/pubmed/20590750 [Accessed March 21, 2012].

Lipina, C., Stretton, C. & Hastings, S., 2010. Regulation of MAP Kinase–Directed Mitogenic and Protein Kinase B–Mediated Signaling by Cannabinoid Receptor Type 1 in Skeletal Muscle Cells. Diabetes, 59(February), pp.375–385. Available at: http://diabetes.diabetesjournals.org/content/59/2/375.short [Accessed January 21, 2014].

Liu, Y.L. et al., 2005. Effects of the cannabinoid CB1 receptor antagonist SR141716 on oxygen consumption and soleus muscle glucose uptake in Lep(ob)/Lep(ob) mice. International journal of obesity (2005), 29(2), pp.183–7. Available at: http://www.ncbi.nlm.nih.gov/pubmed/15558076 [Accessed February 29, 2012].

Luo, J. et al., 2012. A Potent class of GPR40 full agonists engages the enteroinsular axis to promote glucose control in rodents. PloS one, 7(10), p.e46300. Available at: http://www.pubmedcentral.nih.gov/articlerender.fcgi?artid=3467217&tool=pmcentrez&rendertype=abstract [Accessed May 24, 2013].

Luquet, S. et al., 2005. Roles of PPAR delta in lipid absorption and metabolism: a new target for the treatment of type 2 diabetes. Biochimica et biophysica acta, 1740(2), pp.313–7. Available at: http://www.ncbi.nlm.nih.gov/pubmed/15949697 [Accessed August 12, 2013].

Luquet, S., Lopez-Soriano, J. & Holst, D., 2003. Peroxisome proliferator-activated receptor δ controls muscle development and oxidative capability. The FASEB Journal, 17(15), p.2299:2301. Available at: http://www.fasebj.org/content/17/15/2299.short [Accessed January 20, 2014].

Luttrell, L.M. & Lefkowitz, R.J., 2002. The role of beta-arrestins in the termination and transduction of G-protein-coupled receptor signals. Journal of cell science, 115(Pt 3), pp.455–65. Available at: http://www.ncbi.nlm.nih.gov/pubmed/11861753.

Ma, D. et al., 2007. Expression of free fatty acid receptor GPR40 in the central nervous system of adult monkeys. Neuroscience research, 58(4), pp.394–401. Available at: http://www.ncbi.nlm.nih.gov/pubmed/17583366 [Accessed March 12, 2012].

Ma, K. & Saha, P., 2006. Farnesoid X receptor is essential for normal glucose homeostasis. Journal of Clinical …, 116(4), p.1102:1109. Available at: http://www.jci.org/cgi/content/abstract/116/4/1102 [Accessed January 20, 2014].

Mackay, A. et al., 2003. cDNA microarray analysis of genes associated with ERBB2 (HER2/neu) overexpression in human mammary luminal epithelial cells. Oncogene, 22(17), pp.2680–8. Available at: http://www.ncbi.nlm.nih.gov/pubmed/12730682 [Accessed August 12, 2013].

Mancini, A.D. & Poitout, V., 2013. The fatty acid receptor FFA1/GPR40 a decade later: how much do we know? Trends in endocrinology and metabolism: TEM, pp.1–10. Available at: http://www.ncbi.nlm.nih.gov/pubmed/23631851 [Accessed May 2, 2013].

Martin, S. et al., 1996. The glucose transporter (GLUT-4) and vesicle-associated membrane protein-2 (VAMP-2) are segregated from recycling endosomes in insulin-sensitive cells. The Journal of cell biology, 134(3), pp.625–35. Available at: http://www.pubmedcentral.nih.gov/articlerender.fcgi?artid=2120947&tool=pmcentrez&rendertype=abstract.

Martins, A.R. et al., 2012. Mechanisms underlying skeletal muscle insulin resistance induced by fatty acids: importance of the mitochondrial function. Lipids in health and disease, 11(1), p.30. Available at: http://www.pubmedcentral.nih.gov/articlerender.fcgi?artid=3312873&tool=pmcentrez&rendertype=abstract [Accessed May 23, 2013].

Matias, I. et al., 2006. Regulation, function, and dysregulation of endocannabinoids in models of adipose and beta-pancreatic cells and in obesity and hyperglycemia. The Journal of clinical endocrinology and metabolism, 91(8), pp.3171–80. Available at: http://www.ncbi.nlm.nih.gov/pubmed/16684820 [Accessed June 18, 2013].

Matias, I., Cristino, L. & Di Marzo, V., 2008. Endocannabinoids: some like it fat (and sweet too). Journal of neuroendocrinology, 20 Suppl 1, pp.100–9. Available at: http://www.ncbi.nlm.nih.gov/pubmed/18426508 [Accessed March 21, 2012].

Matsuda, L., Lolait, S. & Brownstein, M., 1990. Structure of a cannabinoid receptor and functional expression of the cloned cDNA. NATURE. Available at: http://proxychi.baremetal.com/druglibrary.net/crl/receptors/receptors/Matsuda_et.al_90_Structure_Nature.pdf [Accessed January 19, 2014].

Matsuda-Nagasumi1, K. et al., 2013. Lack of GPR40 FFAR1 does not induce diabetes even under insulin resistance condition - Matsuda-Nagasumi - 2013 - Diabetes, Obesity and Metabolism - Wiley Online Library. Diabetes, obesity & metabolism, 15(6), pp.538–45. Available at: http://www.ncbi.nlm.nih.gov/pubmed/23331570.

McAllister, S.D. & Glass, M., 2002. CB(1) and CB(2) receptor-mediated signalling: a focus on endocannabinoids. Prostaglandins, leukotrienes, and essential fatty acids, 66(2-3), pp.161–71. Available at: http://www.ncbi.nlm.nih.gov/pubmed/12052033 [Accessed June 16, 2013].

McEvoy, J. & Kossatz, U., 2007. Constitutive turnover of cyclin E by Cul3 maintains quiescence. Molecular and cellular biology, 27(10), pp.3651–3666. Available at: http://mcb.asm.org/content/27/10/3651.short [Accessed January 20, 2014].

Meier, J.J. et al., 2002. Gastric inhibitory polypeptide: the neglected incretin revisited. Regulatory peptides, 107(1-3), pp.1–13. Available at: http://www.ncbi.nlm.nih.gov/pubmed/12137960.

Michael, L.F. et al., 2001. Restoration of insulin-sensitive glucose transporter (GLUT4) gene expression in muscle cells by the transcriptional coactivator PGC-1. Proceedings of the National Academy of Sciences of the United States of America, 98(7), pp.3820–5. Available at: http://www.pubmedcentral.nih.gov/articlerender.fcgi?artid=31136&tool=pmcentrez&rendertype=abstract.

Michalik, L., Desvergne, B. & Wahli, W., 2003. Peroxisome proliferator-activated receptors beta/delta: emerging roles for a previously neglected third family member. Current Opinion in Lipidology, 14(2), pp.129–135.

Mieczkowska, A. et al., 2012. Thiazolidinediones induce osteocyte apoptosis by a G protein-coupled receptor 40-dependent mechanism. Journal of Biological …, 287(28), pp.23517–13526. Available at: http://www.jbc.org/content/287/28/23517.short [Accessed January 21, 2014].

Milligan, G., 2003. Constitutive activity and inverse agonists of G protein-coupled receptors: a current perspective. Molecular pharmacology, 64(6), pp.1271–6. Available at: http://www.ncbi.nlm.nih.gov/pubmed/14645655.

Milligan, G. & Kostenis, E., 2006. Heterotrimeric G-proteins: a short history. British journal of pharmacology, 147 Suppl , pp.S46–55. Available at: http://www.pubmedcentral.nih.gov/articlerender.fcgi?artid=1760735&tool=pmcentrez&rendertype=abstract [Accessed August 23, 2013].

Milligan, G., Stoddart, L. & Brown, A., 2006. G protein-coupled receptors for free fatty acids. Cellular signalling, 18(9), pp.1360–1365. Available at: http://www.sciencedirect.com/science/article/pii/S089865680600074X [Accessed January 20, 2014].

Moran, J.L. et al., 2002. Gene expression changes during mouse skeletal myoblast differentiation revealed by transcriptional profiling. Physiological genomics, 10(2), pp.103–11. Available at: http://www.ncbi.nlm.nih.gov/pubmed/12181367 [Accessed November 25, 2012].

Murgia, M., Serrano, A. & Calabria, E., 2000. Ras is involved in nerve-activity-dependent regulation of muscle genes. Nature cell …. Available at: http://www.nature.com/ncb/journal/v2/n3/abs/ncb0300_142.html [Accessed August 12, 2013].

Nagasumi, K. et al., 2009. Overexpression of GPR40 in pancreatic beta-cells augments glucose-stimulated insulin secretion and improves glucose tolerance in normal and diabetic mice. Diabetes, 48(5), pp.1067–1076. Available at: http://www.ncbi.nlm.nih.gov/pubmed/19401434.

New, D.C. & Wong, Y.H., 2007. Molecular mechanisms mediating the G protein-coupled receptor regulation of cell cycle progression. Journal of molecular signaling, 2, p.2. Available at: http://www.pubmedcentral.nih.gov/articlerender.fcgi?artid=1808056&tool=pmcentrez&rendertype=abstract [Accessed August 23, 2013].

Nielsen, B.S. et al., 2008. Matrix metalloproteinase 13 is induced in fibroblasts in polyomavirus middle T antigen-driven mammary carcinoma without influencing tumor progression. PloS one, 3(8), p.e2959. Available at: http://www.pubmedcentral.nih.gov/articlerender.fcgi?artid=2493034&tool=pmcentrez&rendertype=abstract [Accessed August 12, 2013].

Noda, M., Oh, J. & Takahashi, R., 2003. RECK: a novel suppressor of malignancy linking oncogenic signaling to extracellular matrix remodeling. Cancer and Metastasis Rev, 22(2-3), pp.167–175. Available at: http://link.springer.com/article/10.1023/A:1023043315031 [Accessed January 20, 2014].

Noguchi, S. et al., 2003. cDNA microarray analysis of individual Duchenne muscular dystrophy patients. Human Molecular Genetics, 12(6), pp.595–600. Available at: http://www.hmg.oxfordjournals.org/cgi/doi/10.1093/hmg/ddg065 [Accessed June 3, 2013].

O'Sullivan, S.E., 2007. Cannabinoids go nuclear: evidence for activation of peroxisome proliferator-activated receptors. British journal of pharmacology, 152(5), pp.576–82. Available at: http://www.pubmedcentral.nih.gov/articlerender.fcgi?artid=2190029&tool=pmcentrez&rendertype=abstract [Accessed March 22, 2012].

Odilo Mueller, Lightfoot, S. & Schroeder, A., 2004. RNA integrity number (RIN)–Standardization of RNA Quality Control. Agilent Application Note, …. Available at: http://gene-quantification.net/RIN.pdf [Accessed January 20, 2014].

Oh, S.M. et al., 2001. Human neutrophil lactoferrin trans-activates the matrix metalloproteinase 1 gene through stress-activated MAPK signaling modules. The Journal of biological chemistry, 276(45), pp.42575–9. Available at: http://www.ncbi.nlm.nih.gov/pubmed/11535608 [Accessed August 12, 2013].

OKAMOTO, O. et al., 1999. Dermatopontin interacts with transforming growth factor β and enhances its biological activity. Biochem. J, 337(3), pp.537–541. Available at: http://www.biochemj.org/bj/337/bj3370537.htm [Accessed January 20, 2014].

Olayioye, M. et al., 2000. NEW EMBO MEMBERS'REVIEW: The ErbB signaling network: receptor heterodimerization in development and cancer. The EMBO journal, 19(13), pp.3159–3167. Available at: http://www.ncbi.nlm.nih.gov/pmc/articles/PMC313958/ [Accessed January 20, 2014].

Osei-Hyiaman, D., 2005. Endocannabinoid activation at hepatic CB1 receptors stimulates fatty acid synthesis and contributes to diet-induced obesity. Journal of Clinical …, 115(5), pp.1298–1305. Available at: http://www.jci.org/cgi/content/abstract/115/5/1298 [Accessed January 20, 2014].

Ou, H. et al., 2013. Multiple mechanisms of GW-9508, a selective G protein-coupled receptor 40 agonist, in the regulation of glucose homeostasis and insulin sensitivity. American Journal of …. Available at: http://ajpendo.physiology.org/content/304/6/E668.short [Accessed August 19, 2013].

Overton, H. a, Fyfe, M.C.T. & Reynet, C., 2008. GPR119, a novel G protein-coupled receptor target for the treatment of type 2 diabetes and obesity. British journal of pharmacology, 153 Suppl (October 2007), pp.S76–81. Available at:

http://www.pubmedcentral.nih.gov/articlerender.fcgi?artid=2268073&tool=pmcentrez&rendertype=abstract [Accessed March 11, 2012].

Pagano, C. et al., 2007. The endogenous cannabinoid system stimulates glucose uptake in human fat cells via phosphatidylinositol 3-kinase and calcium-dependent mechanisms. The Journal of clinical endocrinology and metabolism, 92(12), pp.4810–9. Available at: http://www.ncbi.nlm.nih.gov/pubmed/17785353 [Accessed March 21, 2012].

Pagotto, U. et al., 2006. The emerging role of the endocannabinoid system in endocrine regulation and energy balance. Endocrine reviews, 27(1), pp.73–100. Available at: http://www.ncbi.nlm.nih.gov/pubmed/16306385 [Accessed October 21, 2012].

Parker, M.H., Seale, P. & Rudnicki, M. a, 2003. Looking back to the embryo: defining transcriptional networks in adult myogenesis. Nature reviews. Genetics, 4(7), pp.497–507. Available at: http://www.ncbi.nlm.nih.gov/pubmed/12838342 [Accessed March 12, 2012].

Pedersen, B.K. et al., 2007. Role of myokines in exercise and metabolism. Journal of applied physiology (Bethesda, Md. : 1985), 103(3), pp.1093–8. Available at: http://www.ncbi.nlm.nih.gov/pubmed/17347387 [Accessed May 21, 2013].

Pender, C. et al., 2005. Analysis of insulin-stimulated insulin receptor activation and glucose transport in cultured skeletal muscle cells from obese subjects. Metabolism: clinical and experimental, 54(5), pp.598–603. Available at: http://www.ncbi.nlm.nih.gov/pubmed/15877289.

Peng, G. et al., 2011. Oleate blocks palmitate-induced abnormal lipid distribution, endoplasmic reticulum expansion and stress, and insulin resistance in skeletal muscle. Endocrinology, 152(6), pp.2206–18. Available at: http://www.ncbi.nlm.nih.gov/pubmed/21505048 [Accessed May 21, 2013].

Perriott, Laureta M, Kono, T., Whitesell, R.R., Knobel, S.M., David, W., et al., 2001. Glucose uptake and metabolism by cultured human skeletal muscle cells : rate-limiting steps Glucose uptake and metabolism by cultured human skeletal muscle cells : rate-limiting steps.

Perriott, Laureta M, Kono, T., Whitesell, R.R., Knobel, S.M., Piston, W., et al., 2001. Glucose uptake and metabolism by cultured human skeletal muscle cells : rate-limiting steps Glucose uptake and metabolism by cultured human skeletal muscle cells : rate-limiting steps.

Perriott, L M et al., 2001. Glucose uptake and metabolism by cultured human skeletal muscle cells: rate-limiting steps. American journal of physiology. Endocrinology and metabolism, 281(1), pp.E72–80. Available at: http://www.ncbi.nlm.nih.gov/pubmed/11404224.

Persengiev, S.P., Devireddy, L.R. & Green, M.R., 2002. Inhibition of apoptosis by ATFx: a novel role for a member of the ATF/CREB family of mammalian bZIP transcription factors. Genes & development, 16(14), pp.1806–14. Available at: http://www.pubmedcentral.nih.gov/articlerender.fcgi?artid=186387&tool=pmcentrez&rendertype=abstract [Accessed August 12, 2013].

Pertwee, R. & Howlett, A., 2010. International Union of Basic and Clinical Pharmacology. LXXIX. Cannabinoid receptors and their ligands: beyond CB1 and CB2. Pharmacological …, 62(4), pp.588–631. Available at: http://pharmrev.aspetjournals.org/content/62/4/588.short [Accessed January 21, 2014].

Pertwee, R.G. & Ross, R. a, 2002. Cannabinoid receptors and their ligands. Prostaglandins, leukotrienes, and essential fatty acids, 66(2-3), pp.101–21. Available at: http://www.ncbi.nlm.nih.gov/pubmed/12052030 [Accessed May 22, 2013].

Petersen, K.F. et al., 2007. The role of skeletal muscle insulin resistance in the pathogenesis of the metabolic syndrome. Proceedings of the National Academy of Sciences of the United States of America, 104(31), pp.12587–94. Available at:

http://www.pubmedcentral.nih.gov/articlerender.fcgi?artid=1924794&tool=pmcentrez&rendertype=abstract.

Petersen, K.F. & Shulman, G.I., 2002. Pathogenesis of skeletal muscle insulin resistance in type 2 diabetes mellitus. The American journal of cardiology, 90(5A), p.11G–18G. Available at: http://www.ncbi.nlm.nih.gov/pubmed/12231074.

Pette, D. & Staron, R.S., 2001. Transitions of muscle fiber phenotypic profiles. Histochemistry and cell biology, 115(5), pp.359–72. Available at: http://www.ncbi.nlm.nih.gov/pubmed/11449884.

Pietras, R., Arboleda, J. & Reese, D., 1995. HER-2 tyrosine kinase pathway targets estrogen receptor and promotes hormone-independent growth in human breast cancer cells. Oncogene. Available at: http://www.ncbi.nlm.nih.gov/pubmed/7784095 [Accessed August 13, 2013].

Piomelli, D., 2003. The molecular logic of endocannabinoid signalling. Nature Reviews Neuroscience. Available at: http://www.nature.com/nrn/journal/v4/n11/abs/nrn1247.html [Accessed September 1, 2013].

Pirgon, Ö., Bilgin, H. & Çekmez, F., 2013. Association Between Insulin Resistance and Oxidative Stress Parameters in Obese Adolescents with Non-Alcoholic Fatty Liver Disease. J Clin Res Pediatr Endocrinol., 5(1), pp.33–39. Available at: http://www.ncbi.nlm.nih.gov/pmc/articles/PMC3628390/ [Accessed January 21, 2014].

Ponomareva, O., Ma, H. & Vock, V., 2006. Defective neuromuscular synaptogenesis in mice expressing constitutively active ErbB2 in skeletal muscle fibers. Molecular and Cellular Neuroscience, 31(2), pp.334–345. Available at: http://www.sciencedirect.com/science/article/pii/S1044743105002496 [Accessed January 20, 2014].

Pu, J. & Liu, P., 2012. Fatty Acids Stimulate Glucose Uptake by the PI3K/AMPK/Akt and PI3K/ERK1/2 Pathways. Available at: http://cdn.intechopen.com/pdfs/38814/InTech-Fatty_acids_stimulate_glucose_uptake_by_the_pi3k_ampk_akt_and_pi3k_erk1_2_pathways.pdf [Accessed January 20, 2014].

Radonić, A. et al., 2004. Guideline to reference gene selection for quantitative real-time PCR. Biochemical and Biophysical Research Communications, 313(4), pp.856–862. Available at: http://linkinghub.elsevier.com/retrieve/pii/S0006291X03025646 [Accessed March 10, 2012].

Rajesh, M. et al., 2008. CB2 cannabinoid receptor agonists attenuate TNF-alpha-induced human vascular smooth muscle cell proliferation and migration. British journal of pharmacology, 153(2), pp.347–57. Available at: http://www.pubmedcentral.nih.gov/articlerender.fcgi?artid=2219520&tool=pmcentrez&rendertype=abstract [Accessed March 22, 2012].

Randle, P., 1998. Regulatory interactions between lipids and carbohydrates: the glucose fatty acid cycle after 35 years. Diabetes/metabolism reviews, 14(4), pp.263–283. Available at: http://onlinelibrary.wiley.com/doi/10.1002/(SICI)1099-0895(199812)14:4%3C263::AID-DMR233%3E3.0.CO;2-C/full [Accessed January 20, 2014].

Raymond, F. et al., 2010. Comparative gene expression profiling between human cultured myotubes and skeletal muscle tissue. BMC genomics, 11, p.125. Available at: http://www.pubmedcentral.nih.gov/articlerender.fcgi?artid=2838843&tool=pmcentrez&rendertype=abstract.

Roche, R. et al., 2006. Presence of the cannabinoid receptors, CB1 and CB2, in human omental and subcutaneous adipocytes. Histochemistry and cell biology, 126(2), pp.177–87. Available at: http://www.ncbi.nlm.nih.gov/pubmed/16395612 [Accessed September 1, 2013].

Roden, M. & Price, T., 1996. Mechanism of free fatty acid-induced insulin resistance in humans. Journal of Clinical Investigation, 97(12), pp.2859–2865. Available at:

http://www.ncbi.nlm.nih.gov/pmc/articles/PMC507380/ [Accessed January 20, 2014].

Rodríguez de Fonseca, F. et al., 2005. The endocannabinoid system: physiology and pharmacology. Alcohol and alcoholism (Oxford, Oxfordshire), 40(1), pp.2–14. Available at: http://www.ncbi.nlm.nih.gov/pubmed/15550444 [Accessed May 24, 2013].

Rose, D.P., 1997. Effects of dietary fatty acids on breast and prostate cancers: evidence from in vitro experiments and animal studies. The American journal of clinical nutrition, 66(6 Suppl), p.1513S–1522S. Available at: http://www.ncbi.nlm.nih.gov/pubmed/9394709.

Rosenblatt, J. & Lunt, A., 1995. Culturing satellite cells from living single muscle fiber explants. In Vitro Cell Dev Biol Anim, 31(10), pp.773–779. Available at: http://link.springer.com/article/10.1007/BF02634119 [Accessed January 20, 2014].

Ross, W. & Hall, P. a, 1995. Ki67: from antibody to molecule to understanding? Clinical molecular pathology, 48(3), pp.M113–7. Available at: http://www.pubmedcentral.nih.gov/articlerender.fcgi?artid=407942&tool=pmcentrez&rendertype=abstract.

Roux, P. & Blenis, J., 2004. ERK and p38 MAPK-activated protein kinases: a family of protein kinases with diverse biological functions. Microbiology and molecular biology reviews, 68(2), pp.320–344. Available at: http://mmbr.asm.org/content/68/2/320.short [Accessed January 20, 2014].

Roy, A.C. et al., 2010. Blocking GPR55 up-regulates mRNA expression of transcription factors and enzymes involved in enhancing oxidative capacity in skeletal muscle. Obesity Research & Clinical Practice, 4, pp.S7–S8. Available at: http://linkinghub.elsevier.com/retrieve/pii/S1871403X10000372 [Accessed September 1, 2013].

Rozengurt, E., 2007. Mitogenic signaling pathways induced by G protein- coupled receptors. Journal of cellular physiology, (July), pp.589–602. Available at: http://onlinelibrary.wiley.com/doi/10.1002/jcp.21246/full [Accessed January 21, 2014].

Ruiz-Alcaraz, A.J. et al., 2013. Obesity-induced insulin resistance in human skeletal muscle is characterised by defective activation of p42/p44 MAP kinase. PloS one, 8(2), p.e56928. Available at: http://www.pubmedcentral.nih.gov/articlerender.fcgi?artid=3585240&tool=pmcentrez&rendertype=abstract [Accessed May 27, 2013].

Ryberg, E. et al., 2007. The orphan receptor GPR55 is a novel cannabinoid receptor. British journal of pharmacology, 152(7), pp.1092–101. Available at: http://www.pubmedcentral.nih.gov/articlerender.fcgi?artid=2095107&tool=pmcentrez&rendertype=abstract [Accessed March 16, 2012].

Saghizadeh, M. & Ong, J., 1996. The expression of TNF alpha by human muscle. Relationship to insulin resistance. Journal of Clinical Investigation, 15; 97(4), pp.1111–1116. Available at: http://www.ncbi.nlm.nih.gov/pmc/articles/PMC507159/ [Accessed January 20, 2014].

Sakamoto, K. & Holman, G.D., 2008. Emerging role for AS160/TBC1D4 and TBC1D1 in the regulation of GLUT4 traffic. American journal of physiology. Endocrinology and metabolism, 295(1), pp.E29–37. Available at: http://www.pubmedcentral.nih.gov/articlerender.fcgi?artid=2493596&tool=pmcentrez&rendertype=abstract [Accessed May 30, 2013].

Salehi, a et al., 2005. Free fatty acid receptor 1 (FFA(1)R/GPR40) and its involvement in fatty-acid-stimulated insulin secretion. Cell and tissue research, 322(2), pp.207–15. Available at: http://www.ncbi.nlm.nih.gov/pubmed/16044321 [Accessed May 23, 2013].

Saltiel, A. & Kahn, C., 2001. Insulin signalling and the regulation of glucose and lipid metabolism. Nature. Available at: http://www.ncbi.nlm.nih.gov/pmc/articles/PMC1431367/ [Accessed June 16, 2013].

Samocha-Bonet, D. et al., 2012. Overfeeding reduces insulin sensitivity and increases oxidative stress, without altering markers of mitochondrial content and function in humans. PloS one, 7(5), p.e36320. Available at: http://www.pubmedcentral.nih.gov/articlerender.fcgi?artid=3346759&tool=pmcentrez&rendertype=abstract [Accessed June 23, 2013].

Samuel, V., Petersen, K. & Shulman, G., 2010. Lipid-induced insulin resistance: unravelling the mechanism. The Lancet, 375(9733), pp.2267–2277. Available at: http://www.sciencedirect.com/science/article/pii/S0140673610604084 [Accessed June 19, 2013].

Sarabia, V. et al., 1992. Glucose transport in human skeletal muscle cells in culture. Stimulation by insulin and metformin. The Journal of clinical investigation, 90(4), pp.1386–95. Available at: http://www.pubmedcentral.nih.gov/articlerender.fcgi?artid=443184&tool=pmcentrez&rendertype=abstract.

Sawzdargo, M. et al., 1997. A cluster of four novel human G protein-coupled receptor genes occurring in close proximity to CD22 gene on chromosome 19q13.1. Biochemical and biophysical research communications, 239(2), pp.543–7. Available at: http://www.ncbi.nlm.nih.gov/pubmed/9344866.

Schäfer, B. et al., 2004. Distinct ADAM metalloproteinases regulate G protein-coupled receptor-induced cell proliferation and survival. The Journal of biological chemistry, 279(46), pp.47929–38. Available at: http://www.ncbi.nlm.nih.gov/pubmed/15337756 [Accessed August 23, 2013].

Scheen, A., Finer, N. & Hollander, P., 2006. Efficacy and tolerability of rimonabant in overweight or obese patients with type 2 diabetes: a randomised controlled study. The lancet, 368(9548), pp.1660–1672. Available at: http://www.sciencedirect.com/science/article/pii/S0140673606695718 [Accessed January 20, 2014].

Schmitz-Peiffer, C. et al., 1997. Alterations in the expression and cellular localization of protein kinase C isozymes ε and θ are associated with insulin resistance in skeletal muscle of the high-fat–fed. Diabetes, 46(2), pp.169–178. Available at: http://diabetes.diabetesjournals.org/content/46/2/169.short [Accessed January 20, 2014].

Schmitz-Peiffer, C., 2000. Signalling aspects of insulin resistance in skeletal muscle: mechanisms induced by lipid oversupply. Cellular signalling. Available at: http://www.sciencedirect.com/science/article/pii/S0898656800001108 [Accessed June 18, 2013].

Schnell, S., Schaefer, M. & Schöfl, C., 2007. Free fatty acids increase cytosolic free calcium and stimulate insulin secretion from beta-cells through activation of GPR40. Molecular and cellular endocrinology, 263(1-2), pp.173–80. Available at: http://www.ncbi.nlm.nih.gov/pubmed/17101212 [Accessed August 28, 2013].

Seale, P. et al., 2000. Pax7 is required for the specification of myogenic satellite cells. Cell, 102(6), pp.777–86. Available at: http://www.ncbi.nlm.nih.gov/pubmed/11030621.

Sell, H. et al., 2008. Skeletal muscle insulin resistance induced by adipocyte-conditioned medium: underlying mechanisms and reversibility. American journal of physiology. Endocrinology and metabolism, 294(6), pp.E1070–7. Available at: http://www.ncbi.nlm.nih.gov/pubmed/18364460 [Accessed March 21, 2012].

Sell, H., Dietze-Schroeder, D. & Eckel, J., 2006. The adipocyte-myocyte axis in insulin resistance. Trends in endocrinology and metabolism: TEM, 17(10), pp.416–22. Available at: http://www.ncbi.nlm.nih.gov/pubmed/17084639 [Accessed March 5, 2012].

Semple, R., 2006. PPARγ and human metabolic disease. Journal of Clinical Investigation, 116(3), pp.581–589. Available at: http://www.jci.org/cgi/content/abstract/116/3/581 [Accessed January 20, 2014].

Serrano, A. et al., 2008. The cannabinoid CB1 receptor antagonist SR141716A (Rimonabant) enhances the metabolic benefits of long-term treatment with oleoylethanolamide in Zucker rats. Neuropharmacology, 54(1), pp.226–34. Available at: http://www.ncbi.nlm.nih.gov/pubmed/17467748 [Accessed March 22, 2012].

Shapiro, H. et al., 2005. Role of GPR40 in fatty acid action on the. Biochemical and Biophysical Research Communications, 335(1), pp.97–104. Available at: http://www.ncbi.nlm.nih.gov/pubmed/16081037.

Shefer, G., Wleklinski-Lee, M. & Yablonka-Reuveni, Z., 2004. Skeletal muscle satellite cells can spontaneously enter an alternative mesenchymal pathway. Journal of cell science, 117(Pt 22), pp.5393–404. Available at: http://www.ncbi.nlm.nih.gov/pubmed/15466890 [Accessed March 16, 2012].

Shen, X. et al., 2003. Genome-wide examination of myoblast cell cycle withdrawal during differentiation. Developmental dynamics : an official publication of the American Association of Anatomists, 226(1), pp.128–38. Available at: http://www.ncbi.nlm.nih.gov/pubmed/12508234 [Accessed November 10, 2012].

Shi, H. et al., 2007. Extracellular signal-regulated kinase pathway is differentially involved in beta-agonist-induced hypertrophy in slow and fast muscles. American journal of physiology. Cell physiology, 292(5), pp.C1681–9. Available at: http://www.ncbi.nlm.nih.gov/pubmed/17151143 [Accessed March 22, 2012].

Shi, H. et al., 2008. Modulation of skeletal muscle fiber type by mitogen-activated protein kinase signaling. FASEB journal : official publication of the Federation of American Societies for Experimental Biology, 22(8), pp.2990–3000. Available at: http://www.ncbi.nlm.nih.gov/pubmed/18417546 [Accessed March 22, 2012].

Shi, X. & Garry, D.J., 2010. Myogenic regulatory factors transactivate the Tceal7 gene and modulate muscle differentiation. The Biochemical journal, 428(2), pp.213–21. Available at: http://www.ncbi.nlm.nih.gov/pubmed/20307260 [Accessed March 21, 2012].

Siegel, A.L., Kuhlmann, P.K. & Cornelison, D.D.W., 2011. Muscle satellite cell proliferation and association: new insights from myofiber time-lapse imaging. Skeletal muscle, 1(1), p.7. Available at: http://www.pubmedcentral.nih.gov/articlerender.fcgi?artid=3157006&tool=pmcentrez&rendertype=abstract [Accessed March 22, 2012].

Simcocks, A.C. et al., 2011. Putative endocannabinoid receptor GPR55 is expressed in skeletal muscle. Obesity Research & Clinical Practice, 5, pp.63–64. Available at: http://linkinghub.elsevier.com/retrieve/pii/S1871403X11000688.

Smyth, G.K., Yang, Y.H. & Speed, T., 2003. Statistical issues in cDNA microarray data analysis. Methods in molecular biology (Clifton, N.J.), 224, pp.111–36. Available at: http://www.ncbi.nlm.nih.gov/pubmed/12710670.

Soga, T. et al., 2005. Lysophosphatidylcholine enhances glucose-dependent insulin secretion via an orphan G-protein-coupled receptor. Biochemical and biophysical research communications, 326(4), pp.744–51. Available at: http://www.ncbi.nlm.nih.gov/pubmed/15607732 [Accessed March 16, 2012].

Solinas, G. et al., 2006. Saturated fatty acids inhibit induction of insulin gene transcription by JNK-mediated phosphorylation of insulin-receptor substrates. Proc Natl Acad Sci U S A, 103(44), pp.16454–16459. Available at: http://www.pnas.org/content/103/44/16454.short [Accessed January 20, 2014].

Song, D. et al., 2011. Acute cannabinoid receptor type 1 (CB1R) modulation influences insulin sensitivity by an effect outside the central nervous system in mice. Diabetologia, 54(5), pp.1181–9. Available at: http://www.ncbi.nlm.nih.gov/pubmed/21340622 [Accessed June 15, 2013].

Soranzo, N. et al., 2009. Meta-analysis of genome-wide scans for human adult stature identifies novel Loci and associations with measures of skeletal frame size. PLoS genetics, 5(4), p.e1000445. Available at: http://www.pubmedcentral.nih.gov/articlerender.fcgi?artid=2661236&tool=pmcentrez&rendertype=abstract [Accessed August 14, 2013].

Steinberg, G.R. et al., 2006. The suppressor of cytokine signaling 3 inhibits leptin activation of AMP-kinase in cultured skeletal muscle of obese humans. The Journal of clinical endocrinology and metabolism, 91(9), pp.3592–7. Available at: http://www.ncbi.nlm.nih.gov/pubmed/16822822 [Accessed January 13, 2014].

Steneberg, P., Rubins, N. & Bartoov-Shifman, R., 2005. The FFA receptor GPR40 links hyperinsulinemia, hepatic steatosis, and impaired glucose homeostasis in mouse. Cell metabolism, 1(April), pp.245–258. Available at: http://www.sciencedirect.com/science/article/pii/S1550413105000860 [Accessed January 21, 2014].

Stern-Straeter, J. et al., 2009. Identification of valid reference genes during the differentiation of human myoblasts. BMC molecular biology, 10, p.66. Available at: http://www.pubmedcentral.nih.gov/articlerender.fcgi?artid=2714309&tool=pmcentrez&rendertype=abstract [Accessed March 22, 2012].

Stewart, G. et al., 2006. Mouse GPR40 heterologously expressed in Xenopus oocytes is activated by short-, medium-, and long-chain fatty acids. American journal of physiology. Cell physiology, 290(3), pp.C785–92. Available at: http://www.ncbi.nlm.nih.gov/pubmed/16267104 [Accessed September 6, 2013].

Stoddart, L. a & Milligan, G., 2010. Constitutive activity of GPR40/FFA1 intrinsic or assay dependent? Methods in enzymology, 484(10), pp.569–90. Available at: http://www.ncbi.nlm.nih.gov/pubmed/21036251 [Accessed August 20, 2013].

Stoddart, L.A., Smith, N.J. & Milligan, G., 2008. International Union of Pharmacology . LXXI . Free Fatty Acid Receptors FFA1 , -2 , and -3 : Pharmacology and Pathophysiological Functions. Pharmacology, 60(4), pp.405–417.

Stoica, G.E., Franke, T.F., Moroni, M., et al., 2003. Effect of estradiol on estrogen receptor-alpha gene expression and activity can be modulated by the ErbB2/PI 3-K/Akt pathway. Oncogene, 22(39), pp.7998–8011. Available at: http://www.ncbi.nlm.nih.gov/pubmed/12970748 [Accessed August 12, 2013].

Stoica, G.E., Franke, T.F., Wellstein, A., et al., 2003. Estradiol rapidly activates Akt via the ErbB2 signaling pathway. Molecular endocrinology (Baltimore, Md.), 17(5), pp.818–30. Available at: http://www.ncbi.nlm.nih.gov/pubmed/12554767 [Accessed August 13, 2013].

Storz, P. et al., 1999. Cross-talk mechanisms in the development of insulin resistance of skeletal muscle cells palmitate rather than tumour necrosis factor inhibits insulin-dependent protein kinase B (PKB)/Akt stimulation and glucose uptake. European journal of biochemistry / FEBS, 266(1), pp.17–25. Available at: http://www.ncbi.nlm.nih.gov/pubmed/10542046.

Stuart, C. a et al., 2013. Slow-twitch fiber proportion in skeletal muscle correlates with insulin responsiveness. The Journal of clinical endocrinology and metabolism, 98(5), pp.2027–36. Available at: http://www.ncbi.nlm.nih.gov/pubmed/23515448 [Accessed May 28, 2013].

Sugden, M., 2003. PDK4: A factor in fatness? Obesity research, 11(2), pp.167–169. Available at: http://onlinelibrary.wiley.com/doi/10.1038/oby.2003.26/full [Accessed January 21, 2014].

Suh, H.N. et al., 2008. Linoleic acid stimulates gluconeogenesis via Ca2+/PLC, cPLA2, and PPAR pathways through GPR40 in primary cultured chicken hepatocytes. American journal of physiology. Cell physiology, 295(6), pp.C1518–27. Available at: http://www.ncbi.nlm.nih.gov/pubmed/18842827 [Accessed March 12, 2012].

Swaminath, G., 2008. Fatty acid binding receptors and their physiological role in type 2 diabetes. Archiv der Pharmazie, 341(12), pp.753–61. Available at: http://www.ncbi.nlm.nih.gov/pubmed/19009545 [Accessed March 20, 2012].

Tam, C. et al., 2010. Short-term overfeeding may induce peripheral insulin resistance without altering subcutaneous adipose tissue macrophages in humans. Diabetes, 59(9), pp.2164–2170. Available at: http://diabetes.diabetesjournals.org/content/59/9/2164.short [Accessed January 20, 2014].

Tan, C.P. et al., 2008. Selective small-molecule agonists of G protein–coupled receptor 40 promote glucose-dependent insulin secretion and reduce blood glucose in mice. Diabetes, 57(8), pp.2211–2219. Available at: http://diabetes.diabetesjournals.org/content/57/8/2211.short [Accessed January 21, 2014].

Tedesco, L., Valerio, A. & Dossena, M., 2010. Cannabinoid Receptor Stimulation Impairs Mitochondrial Biogenesis in Mouse White Adipose Tissue, Muscle, and Liver The Role of eNOS, p38 MAPK, and AMPK. Diabetes, 59(11), pp.2826–2836. Available at: http://diabetes.diabetesjournals.org/content/59/11/2826.short [Accessed January 21, 2014].

Thompson AL et al., 2000. Effects of individual fatty acids on glucose uptake and glycogen synthesis in soleus muscle in vitro. Am J Physiol Endocrinol Metab, 279(3), pp.E577–E584. Available at: http://ajpendo.physiology.org/content/279/3/E577.short [Accessed January 20, 2014].

Tomczak, K.K. et al., 2004. Expression profiling and identification of novel genes involved in myogenic differentiation. FASEB journal : official publication of the Federation of American Societies for Experimental Biology, 18(2), pp.403–5. Available at: http://www.ncbi.nlm.nih.gov/pubmed/14688207.

Tsintzas, K., 2006. Differential regulation of metabolic genes in skeletal muscle during starvation and refeeding in humans. The Journal of Physiology, 575(1), pp.291–303. Available at: http://www.jphysiol.org/cgi/doi/10.1113/jphysiol.2006.109892 [Accessed June 17, 2013].

Tsintzas, K. et al., 2007. Elevated free fatty acids attenuate the insulin-induced suppression of PDK4 gene expression in human skeletal muscle: potential role of intramuscular long-chain acyl-coenzyme A. The Journal of clinical endocrinology and metabolism, 92(10), pp.3967–72. Available at: http://www.ncbi.nlm.nih.gov/pubmed/17652214 [Accessed June 15, 2013].

Tsujihata, Y. et al., 2011. TAK-875 , an Orally Available G Protein-Coupled Receptor 40 / Free Fatty Acid Receptor 1 Agonist , Enhances Glucose- Dependent Insulin Secretion and Improves Both Postprandial and Fasting Hyperglycemia in Type 2 Diabetic Rats □. Pharmacology, pp.228–237.

Turu, G. & Hunyady, L., 2010. Signal transduction of the CB1 cannabinoid receptor. Journal of molecular endocrinology, 44(2), pp.75–85. Available at: http://www.ncbi.nlm.nih.gov/pubmed/19620237 [Accessed October 30, 2012].

Van-Harken, D.R., Dixon, C.W. & Heimberg, M., 1969. Hepatic Lipid Metabolism in Experimental Diabetes. The Journal of biological chemistry, 224(9), pp.2278–2285. Available at: http://www.ncbi.nlm.nih.gov/pubmed/5783834.

Van-Sickle, M.D. et al., 2005. Identification and functional characterization of brainstem cannabinoid CB2 receptors. Science (New York, N.Y.), 310(5746), pp.329–32. Available at: http://www.ncbi.nlm.nih.gov/pubmed/16224028 [Accessed January 10, 2014].

Vettor, R. et al., 2008. Loss-of-function mutation of the GPR40 gene associates with abnormal stimulated insulin secretion by acting on intracellular calcium mobilization. The Journal of clinical endocrinology and metabolism, 93(9), pp.3541–50. Available at: http://www.ncbi.nlm.nih.gov/pubmed/18583466 [Accessed May 23, 2013].

Vickers, S.P. et al., 2003. Preferential effects of the cannabinoid CB1 receptor antagonist, SR 141716, on food intake and body weight gain of obese (fa/fa) compared to lean Zucker rats. Psychopharmacology, 167(1), pp.103–11. Available at: http://www.ncbi.nlm.nih.gov/pubmed/12632249 [Accessed February 29, 2012].

Wagner, R. et al., 2013. Reevaluation of Fatty acid receptor 1 (FFAR1/GPR40) as drug target for the stimulation of insulin secretion in humans. Diabetes, 62(June), pp.2106–2111. Available at: http://www.ncbi.nlm.nih.gov/pubmed/23378609 [Accessed May 24, 2013].

Wahli, W. & Michalik, L., 2012. PPARs at the crossroads of lipid signaling and inflammation. Trends in Endocrinology & Metabolism. Available at: http://www.sciencedirect.com/science/article/pii/S1043276012000707 [Accessed September 7, 2013].

Waller-Evans, H. et al., 2010. The orphan adhesion-GPCR GPR126 is required for embryonic development in the mouse. PloS one, 5(11), p.e14047. Available at: http://www.pubmedcentral.nih.gov/articlerender.fcgi?artid=2987804&tool=pmcentrez&rendertype=abstract [Accessed June 10, 2013].

Wang, D. et al., 2007. Bcl10 plays a critical role in NF- B activation induced by G protein-coupled receptors. Proc Natl Acad Sci U S A, 104(1), pp.145–150. Available at: http://www.ncbi.nlm.nih.gov/pubmed/17179215.

Wang, H. et al., 2009. Skeletal muscle–specific deletion of lipoprotein lipase enhances insulin signaling in skeletal muscle but causes insulin resistance in liver and other tissues. Diabetes, 58(January). Available at: http://diabetes.diabetesjournals.org/content/58/1/116.short [Accessed June 9, 2013].

Wang, K. et al., 2008. JAK2/STAT2/STAT3 are required for myogenic differentiation. The Journal of biological chemistry, 283(49), pp.34029–36. Available at: http://www.pubmedcentral.nih.gov/articlerender.fcgi?artid=2662224&tool=pmcentrez&rendertype=abstract [Accessed March 15, 2012].

Wang, L. et al., 2011. Acute stimulation of glucagon secretion by linoleic acid results from GPR40 activation and [Ca2+]i increase in pancreatic islet {alpha}-cells. The Journal of endocrinology, 210(2), pp.173–9. Available at: http://www.ncbi.nlm.nih.gov/pubmed/21565851 [Accessed August 29, 2013].

Wang, Y.-X. et al., 2004. Regulation of muscle fiber type and running endurance by PPARdelta. PLoS biology, 2(10), p.e294. Available at: http://www.pubmedcentral.nih.gov/articlerender.fcgi?artid=509410&tool=pmcentrez&rendertype=abstract [Accessed March 12, 2012].

Wappler, F., Fiege, M. & Schulte am Esch, J., 2001. Pathophysiological role of the serotonin system in malignant hyperthermia. British journal of anaesthesia, 87(5), pp.794–8. Available at: http://www.ncbi.nlm.nih.gov/pubmed/11878537.

Warrington, J. a et al., 2000. Comparison of human adult and fetal expression and identification of 535 housekeeping/maintenance genes. Physiological genomics, 2(3), pp.143–7. Available at: http://www.ncbi.nlm.nih.gov/pubmed/11015593.

Watson, D.K. et al., 2010. ETS transcription factor expression and conversion during prostate and breast cancer progression. The Open Cancer Journal, (3), pp.24–39. Available at: http://benthamscience.com/open/tocj/articles/V003/SI0022TOCJ/24TOCJ.pdf [Accessed January 20, 2014].

Wauquier, F., Philippe, C. & Léotoing, L., 2013. The Free Fatty Acid Receptor G Protein-coupled Receptor 40 (GPR40) Protects from Bone Loss through Inhibition of Osteoclast Differentiation. Journal of Biological …. Available at: http://www.jbc.org/content/288/9/6542.short [Accessed August 12, 2013].

Wei, Y. et al., 2008. Skeletal muscle insulin resistance: role of inflammatory cytokines and reactive oxygen species. American journal of physiology. Regulatory, integrative and comparative physiology, 294(3), pp.R673–80. Available at: http://www.ncbi.nlm.nih.gov/pubmed/18094066 [Accessed March 5, 2012].

Weigert, C. et al., 2005. Interleukin-6 acts as insulin sensitizer on glycogen synthesis in human skeletal muscle cells by phosphorylation of Ser473 of Akt. American journal of physiology. Endocrinology and metabolism, 289(2), pp.E251–7. Available at: http://www.ncbi.nlm.nih.gov/pubmed/15755769 [Accessed March 12, 2012].

Weiss, N. et al., 2010. In vivo expression of G-protein beta1gamma2 dimer in adult mouse skeletal muscle alters L-type calcium current and excitation-contraction coupling. The Journal of physiology, 588(Pt 15), pp.2945–60. Available at:

http://www.pubmedcentral.nih.gov/articlerender.fcgi?artid=2956909&tool=pmcentrez&rendertype=abstract [Accessed August 23, 2013].

Wilson, C. a et al., 2005. HER-2 overexpression differentially alters transforming growth factor-beta responses in luminal versus mesenchymal human breast cancer cells. Breast cancer research : BCR, 7(6), pp.R1058–79. Available at: http://www.pubmedcentral.nih.gov/articlerender.fcgi?artid=1410754&tool=pmcentrez&rendertype=abstract [Accessed August 12, 2013].

Wilson, R.I. & Nicoll, R. a, 2002. Endocannabinoid signaling in the brain. Science (New York, N.Y.), 296(5568), pp.678–82. Available at: http://www.ncbi.nlm.nih.gov/pubmed/11976437 [Accessed June 14, 2013].

Wu, P. et al., 1999. Mechanism responsible for inactivation of skeletal muscle pyruvate dehydrogenase complex in starvation and diabetes. Diabetes, 48(8), pp.1593–9. Available at: http://www.ncbi.nlm.nih.gov/pubmed/10426378.

Wu, P., Yang, L. & Shen, X., 2010. Biochemical and Biophysical Research Communications The relationship between GPR40 and lipotoxicity of the pancreatic b-cells as well as the effect of pioglitazone. Biochemical and Biophysical Research Communications, 403(1), pp.36–39. Available at: http://dx.doi.org/10.1016/j.bbrc.2010.10.105.

Xiao, Z. et al., 1999. of G-protein-coupled Receptors AGONIST-INDUCED PHOSPHORYLATION OF THE CHEMOATTRACTANT RECEPTORcAR1 LOWERS ITS INTRINSIC AFFINITY. Journal of Biological Chemistry, 274(3), pp.1440–1448. Available at: http://europepmc.org/abstract/MED/8701085 [Accessed January 20, 2014].

Yablonka-Reuveni, Z. et al., 2008. Defining the transcriptional signature of skeletal muscle stem cells. Journal of animal science, 86(14 Suppl), pp.E207–16. Available at: http://www.ncbi.nlm.nih.gov/pubmed/17878281 [Accessed March 1, 2012].

Yablonka-Reuveni, Z., 1988. Discrimination of myogenic and nonmyogenic cells from embryonic skeletal muscle by 90 degrees light scattering. Cytometry, 9(2), pp.121–5. Available at: http://www.ncbi.nlm.nih.gov/pubmed/3359891.

Yablonka-Reuveni, Z. & Nameroff, M., 1987. Skeletal muscle cell populations. Separation and partial characterization of fibroblast-like cells from embryonic tissue using density centrifugation. Histochemistry, 87(1), pp.27–38. Available at: http://link.springer.com/10.1007/BF00518721.

Yang, H.Y. et al., 2000. Oncogenic signals of HER-2/neu in regulating the stability of the cyclin-dependent kinase inhibitor p27. The Journal of biological chemistry, 275(32), pp.24735–9. Available at: http://www.ncbi.nlm.nih.gov/pubmed/10859299 [Accessed August 12, 2013].

Ye, J. et al., 1996. Sp1 binding plays a critical role in Erb-B2- and v-ras-mediated downregulation of alpha2-integrin expression in human mammary epithelial cells. Molecular and cellular biology, 16(11), pp.6178–89. Available at: http://www.pubmedcentral.nih.gov/articlerender.fcgi?artid=231621&tool=pmcentrez&rendertype=abstract.

Yonezawa, T. et al., 2008. Unsaturated fatty acids promote proliferation via ERK1 / 2 and Akt pathway in bovine mammary epithelial cells q. Biochem Biophys Res Commun, 367(4), pp.729–735. Available at: http://www.ncbi.nlm.nih.gov/pubmed/18191634.

Yonezawa, T., Katoh, K. & Obara, Y., 2004. Existence of GPR40 functioning in a human breast cancer cell line, MCF-7. Biochem Biophys Res Commun, 314(3), pp.805–809. Available at: http://www.sciencedirect.com/science/article/pii/S0006291X03028031 [Accessed January 20, 2014].

Yoshida, Y. et al., 2011. Involvement of the SKP2–p27KIP1 pathway in suppression of cancer cell proliferation by RECK. Oncogene. Available at: http://www.nature.com/onc/journal/vaop/ncurrent/full/onc2011570a.html [Accessed September 5, 2013].

Yu, C. et al., 2002. Mechanism by which fatty acids inhibit insulin activation of insulin receptor substrate-1 (IRS-1)-associated phosphatidylinositol 3-kinase activity in muscle. The Journal of biological chemistry, 277(52), pp.50230–6. Available at: http://www.ncbi.nlm.nih.gov/pubmed/12006582 [Accessed May 21, 2013].

Zammit, P.S. et al., 2006. Pax7 and myogenic progression in skeletal muscle satellite cells. Journal of cell science, 119(Pt 9), pp.1824–32. Available at: http://www.ncbi.nlm.nih.gov/pubmed/16608873 [Accessed March 19, 2012].

Zargar, S. et al., 2011. Skeletal muscle protein synthesis and the abundance of the mRNA translation initiation repressor PDCD4 are inversely regulated by fasting and refeeding in rats. American journal of physiology. Endocrinology and metabolism, 300(6), pp.E986–92. Available at: http://www.ncbi.nlm.nih.gov/pubmed/21406616 [Accessed August 12, 2013].

Zebedin, E. et al., 2004. Fiber type conversion alters inactivation of voltage-dependent sodium currents in murine C2C12 skeletal muscle cells. American journal of physiology. Cell physiology, 287(2), pp.C270–80. Available at: http://www.ncbi.nlm.nih.gov/pubmed/15044148 [Accessed May 28, 2013].

Zhang, X. et al., 2010. DC260126 , a small-molecule antagonist of GPR40 , improves insulin tolerance but not glucose tolerance in obese Zucker rats. Biomedicine et Pharmacotherapy, 64(9), pp.647–651. Available at: http://dx.doi.org/10.1016/j.biopha.2010.06.008.

Zhang, Y. et al., 2007. The role of G protein-coupled receptor 40 in lipoapoptosis in mouse beta-cell line NIT-1. Journal of molecular endocrinology, 38(6), pp.651–61. Available at: http://www.ncbi.nlm.nih.gov/pubmed/17556534 [Accessed March 12, 2012].

Zhao, Y.-F., Pei, J. & Chen, C., 2008. Activation of ATP-sensitive potassium channels in rat pancreatic beta-cells by linoleic acid through both intracellular metabolites and membrane receptor signalling pathway. The Journal of endocrinology, 198(3), pp.533–40. Available at: http://www.ncbi.nlm.nih.gov/pubmed/18550787 [Accessed March 12, 2012].

Zhou, R., Heiden, M. Vander & Rudin, C., 2002. Genotoxic exposure is associated with alterations in glucose uptake and metabolism. Cancer research, 62(12), pp.3515–3520. Available at: http://cancerres.aacrjournals.org/content/62/12/3515.short [Accessed January 21, 2014].

APPENDICES

Appendices

Appendix 1: RNA Electrophoresis File Run Summary

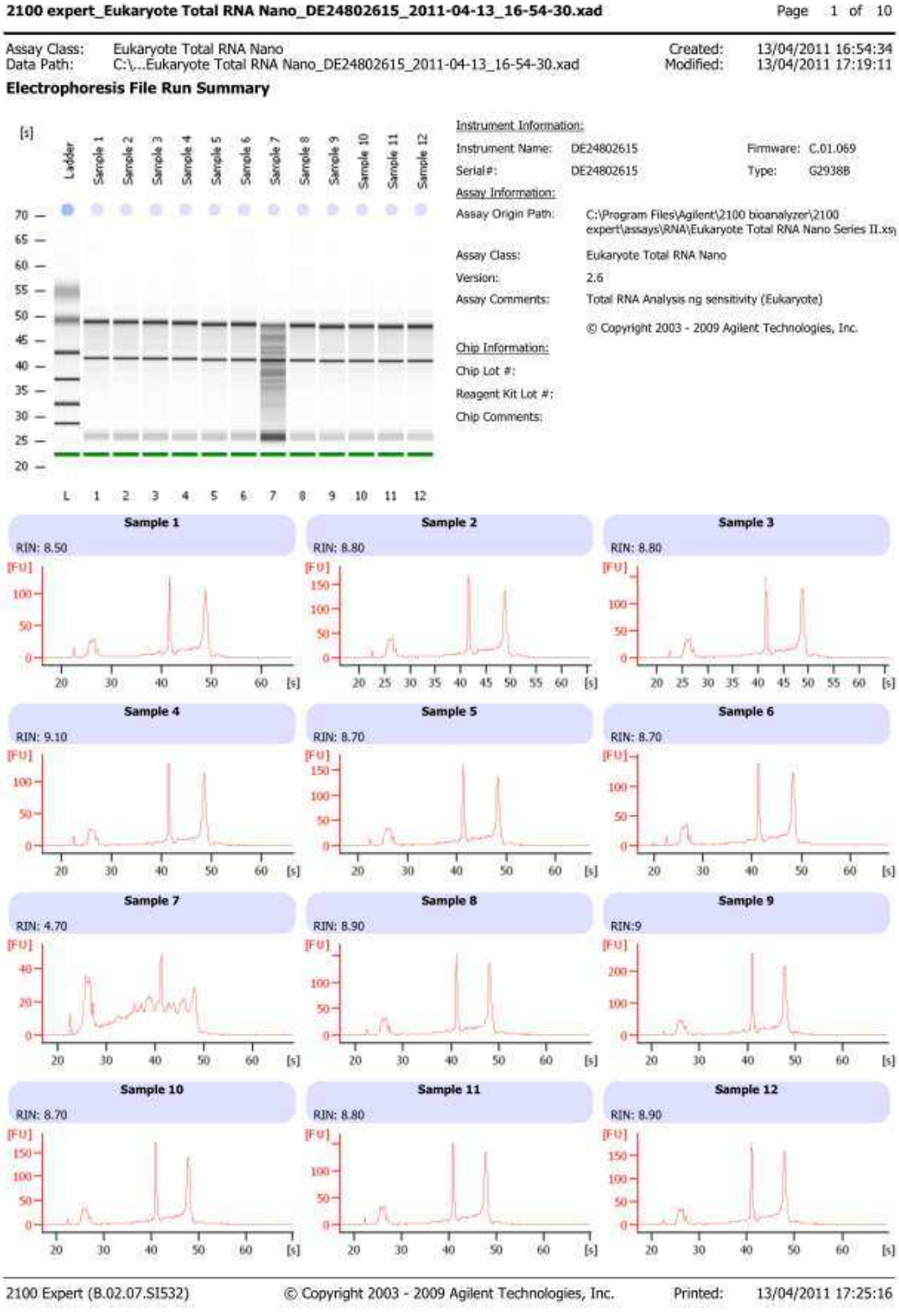

Appendix 2: Quality Control Report – Agilent Technologies.

QC Report - Agilent Technologies : 1 Color Gene Expression

Date	Friday, May 14, 2010 - 16:52	Grid	014850_D_F_20100430
Image	US83103526_251485050012_S01_H [1_2]	BG Method	No Background
Protocol	GE1_105_Jan09 (Read Only)	Background Detrend	On(FeatNCRange, LoPass)
User Name	Administrator	Multiplicative Detrend	True
FE Version	10.7.1.1	Additive Error	1(Green)
Sample(red/green)		Saturation Value	657231 (g)

Spot Finding of the Four Corners of the Array

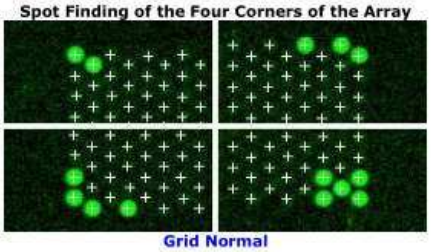

Grid Normal

	Feature	Local Background
	Green	Green
Non Uniform	40	6
Population	118	647

Spatial Distribution of All Outliers on the Array

532 rows x 85 columns

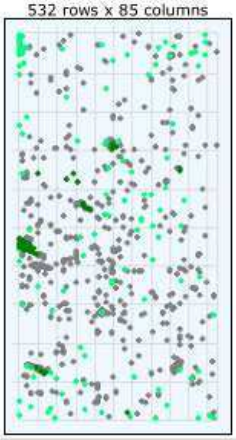

FeatureNonUnif (Green) = 40(0.09%)

GeneNonUnif (Green) = 39 (0.095 %)

BG NonUniform BG Population

Green FeaturePopulation Green Feature NonUniform

Net Signal Statistics

Agilent SpikeIns:

	Green
# Saturated Features	0
99% of Sig. Distrib.	48860
50% of Sig. Distrib.	195
1% of Sig. Distrib.	23

Non-Control probes:

	Green
# Saturated Features	0
99% of Sig. Distrib.	35339
50% of Sig. Distrib.	86
1% of Sig. Distrib.	23

Histogram of Signals Plot

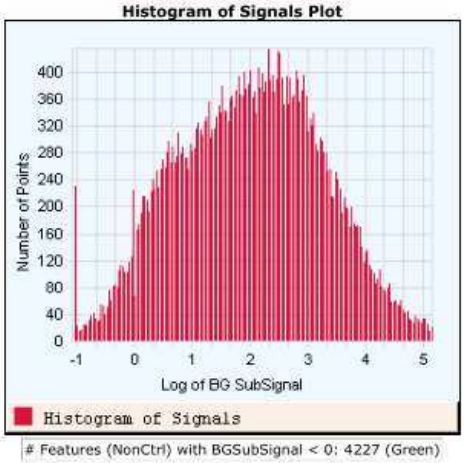

Features (NonCtrl) with BGSubSignal < 0: 4227 (Green)

Negative Control Stats

	Green
Average Net Signals	23.87
StdDev Net Signals	1.40
Average BG Sub Signal	-1.93
StdDev BG Sub Signal	1.30

Local Bkg (inliers)

	Green
Number	44368
Avg	25.90
SD	1.35

Foreground Surface Fit

	Green
RMS_Fit	0.68
RMS_Resid	1.45
Avg_Fit	33.78

Multiplicative Surface Fit

	Green
RMS_Fit	0.13

Reproducibility: %CV for Replicated Probes

	Median %CV Signal (inliers)	
	Non-Control probes Green	Agilent SpikeIns Green
BGSubSignal	15.21	14.04
ProcessedSignal	4.99	4.81

Agilent SpikeIns Signal Statistics

Probe Name	Log (Relative Conc.)	Median (Log Proc. Sig.)	% CV	StdDev
(+)E1A_r60_3	0.30	0.18	218.38	0.29
(+)E1A_r60_a104	1.30	0.29	84.94	0.19
(+)E1A_r60_a107	2.30	0.88	35.74	0.13
(+)E1A_r60_a135	3.30	1.74	13.02	0.05
(+)E1A_r60_a20	3.83	2.16	4.81	0.02
(+)E1A_r60_a22	4.30	2.59	5.05	0.02
(+)E1A_r60_a97	4.82	3.21	6.73	0.03
(+)E1A_r60_n11	5.30	3.81	4.71	0.02
(+)E1A_r60_n9	5.82	4.05	4.60	0.02
(+)E1A_r60_1	6.30	4.63	2.92	0.01

Spatial Distribution of Median Signals for each Row

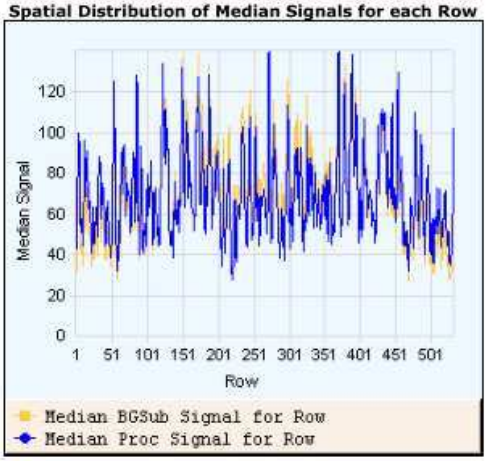

Spatial Distribution of Median Signals for each Column

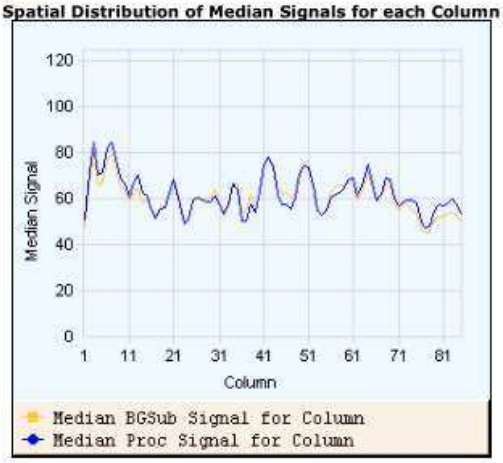

Agilent SpikeIns: %CV of Avg. Processed Signal Plot

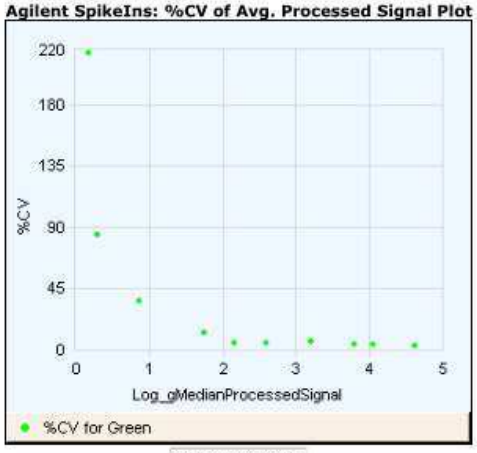

Median %CV:4.81

Evaluation Metrics for GE1_QCMT_Jan09 : Good (9)

Metric Name	Value	Excellent	Good	Evaluate
AnyColorPrcntFeatNonUn...	0.09		<1	>1
gNegCtrlAveBGSubSig	-1.93		-10 to 5	<-10 or >5
gNegCtrlSDevBGSubSig	1.30		<10	>10
absGE1E1aSlope	0.95		0.90 to 1.20	<0.90 or >1.20
gNonCntrlMedCVProcSign...	4.99		<8	>8
gE1aMedCVProcSignal	4.81		<8	>8
gSpatialDetrendRMSFilt...	1.45		<15	>15
DetectionLimit	0.89		0.01 to 2	<0.01 or >2
gNegCtrlAveNetSig	23.87		<40	>40

♦ Excellent ♦ Good ♦ Evaluate

Agilent SpikeIns: Log(Signal) vs. Log(Relative concentration) Plot

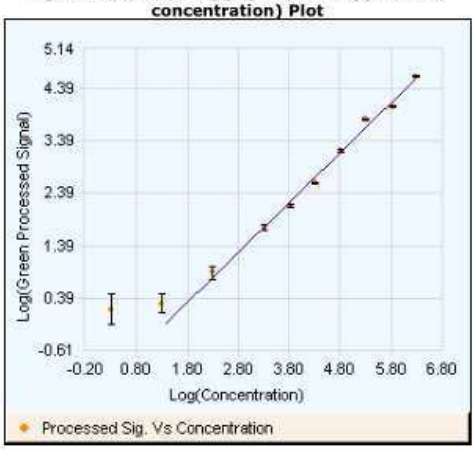

Agilent Spike-In Concentration-Response Statistics

Linear Range Statistics:

Low Signal	-0.07
High Signal	5.88
Low Relative Concentration	1.38
High Relative Concentration	7.66
Slope	0.95
R^2 Value	0.99

Signal Detection Limit Statistics

Saturation Point	5.82
Low Threshold	-0.18
Low Threshold Error	0.37
Spike-In Detection Limit	0.89

Appendix 3: List of low expressed genes in myotube compared to skeletal muscle tissue

Table 1: List of low expressed genes in myotube compared to skeletal muscle tissue related to Carbohydrate metabolism.

Symbol	Entrez Gene Name	Fold Change
FBP2	fructose-1,6-bisphosphatase 2	-6480.477
PYGM	phosphorylase, glycogen, muscle	-4373.799
SLC2A4	solute carrier family 2 (facilitated glucose transporter), member 4	-3329.179
LPL	lipoprotein lipase	-2198.27
GPD1	glycerol-3-phosphate dehydrogenase 1 (soluble)	-1028.407
PGAM2	phosphoglycerate mutase 2 (muscle)	-779.711
mir-133	microRNA 133b	-715.926
CXCL14	chemokine (C-X-C motif) ligand 14	-709.304
DLK1	delta-like 1 homolog (Drosophila)	-511.989
PLCD4	phospholipase C, delta 4	-289.439
NOS1	nitric oxide synthase 1 (neuronal)	-245.532
CD38	CD38 molecule	-227.534
HRASLS	HRAS-like suppressor	-217.855
PRKCQ	protein kinase C, theta	-206.128
P2RY2	purinergic receptor P2Y, G-protein coupled, 2	-201.032
PDK4	pyruvate dehydrogenase kinase, isozyme 4	-176.367
PHKG1	phosphorylase kinase, gamma 1 (muscle)	-173.694
CD36	CD36 molecule (thrombospondin receptor)	-165.23
KLF15	Kruppel-like factor 15	-158.555
UCP3	uncoupling protein 3 (mitochondrial, proton carrier)	-156.344
PHKA1	phosphorylase kinase, alpha 1 (muscle)	-146.376
MLXIPL	MLX interacting protein-like	-113.783
PFKFB1	6-phosphofructo-2-kinase/fructose-2,6-biphosphatase 1	-112.554
ESRRG	estrogen-related receptor gamma	-91.59
HYAL1	hyaluronoglucosaminidase 1	-89.867
SLC25A12	solute carrier family 25 (aspartate/glutamate carrier), member 12	-88.9
CAMK2A	calcium/calmodulin-dependent protein kinase II alpha	-62.127
ATP2A2	ATPase, Ca++ transporting, cardiac muscle, slow twitch 2	-61.947
BMP5	bone morphogenetic protein 5	-60.751
EEF1A2	eukaryotic translation elongation factor 1 alpha 2	-54.824
PPARGC1A	peroxisome proliferator-activated receptor gamma, coactivator 1 alpha	-51.108
CKM	creatine kinase, muscle	-50.899
AQP1	aquaporin 1 (Colton blood group)	-50.721
PPARGC1B	peroxisome proliferator-activated receptor gamma, coactivator 1 beta	-49.366
ESR1	estrogen receptor 1	-48.794
AGL	amylo-alpha-1, 6-glucosidase, 4-alpha-glucanotransferase	-47.748
EPM2A	epilepsy, progressive myoclonus type 2A, Lafora disease (laforin)	-44.728
PRKAA2	protein kinase, AMP-activated, alpha 2 catalytic subunit	-40.409
PFKM	phosphofructokinase, muscle	-30.145
EGF	epidermal growth factor	-29.058
PCDH12	protocadherin 12	-27.343
GHR	growth hormone receptor	-26.417
MGAT4A	mannosyl (alpha-1,3-)-glycoprotein beta-1,4-N-acetylglucosaminyltransferase,	-26.112
PARK2	parkinson protein 2, E3 ubiquitin protein ligase (parkin)	-23.64
FABP3	fatty acid binding protein 3, muscle and heart (mammary-derived growth	-23.068
ACADM	acyl-CoA dehydrogenase, C-4 to C-12 straight chain	-20.62
IMPA2	inositol(myo)-1(or 4)-monophosphatase 2	-20.385
PTPRC	protein tyrosine phosphatase, receptor type, C	-20.365
GYG1	glycogenin 1	-20.24
S1PR1	sphingosine-1-phosphate receptor 1	-19.637
SORBS1	sorbin and SH3 domain containing 1	-19.187
ACACB	acetyl-CoA carboxylase beta	-18.902
AKR1B10	aldo-keto reductase family 1, member B10 (aldose reductase)	-18.726
POMC	proopiomelanocortin	-17.947
ABCC9	ATP-binding cassette, sub-family C (CFTR/MRP), member 9	-17.736

Table 1: (Continued)

Symbol	Entrez Gene Name	Fold Change
CSF1R	colony stimulating factor 1 receptor	-17.608
APOD	apolipoprotein D	-16.216
PGM1	phosphoglucomutase 1	-16.089
RRAD	Ras-related associated with diabetes	-16.073
GOT1	glutamic-oxaloacetic transaminase 1, soluble (aspartate aminotransferase 1)	-15.991
PDGFB	platelet-derived growth factor beta polypeptide	-15.917
USF2	upstream transcription factor 2, c-fos interacting	-13.867
USP2	ubiquitin specific peptidase 2	-13.449
CEBPB	CCAAT/enhancer binding protein (C/EBP), beta	-12.894
PIK3R1	phosphoinositide-3-kinase, regulatory subunit 1 (alpha)	-12.874
HADH	hydroxyacyl-CoA dehydrogenase	-12.683
HFE	hemochromatosis	-12.505
SLC2A8	solute carrier family 2 (facilitated glucose transporter), member 8	-12.337
IL18	interleukin 18 (interferon-gamma-inducing factor)	-12.335
ALDH2	aldehyde dehydrogenase 2 family (mitochondrial)	-12.246
INPP5D	inositol polyphosphate-5-phosphatase, 145kDa	-12.031
PRKG1	protein kinase, cGMP-dependent, type I	-11.739
TLR2	toll-like receptor 2	-11.465
SEPP1	selenoprotein P, plasma, 1	-11.444
PPP1R3C	protein phosphatase 1, regulatory subunit 3C	-11.32
LYVE1	lymphatic vessel endothelial hyaluronan receptor 1	-11.257
PLA2G4C	phospholipase A2, group IVC (cytosolic, calcium-independent)	-11.253
ACSL1	acyl-CoA synthetase long-chain family member 1	-11.063
NOS3	nitric oxide synthase 3 (endothelial cell)	-10.848
NPY1R	neuropeptide Y receptor Y1	-10.842
LIPE	lipase, hormone-sensitive	-10.644
VDAC1	voltage-dependent anion channel 1	-10.367
CSGALNACT1	chondroitin sulfate N-acetylgalactosaminyltransferase 1	-10.262
SERP1	stress-associated endoplasmic reticulum protein 1	-10.134
NT5C1A	5'-nucleotidase, cytosolic IA	-10.024
ESRRA	estrogen-related receptor alpha	-9.987
NR4A1	nuclear receptor subfamily 4, group A, member 1	-9.941
CRY2	cryptochrome 2 (photolyase-like)	-9.745
LTF	lactotransferrin	-9.532
PANK1	pantothenate kinase 1	-9.394
FABP4	fatty acid binding protein 4, adipocyte	-9.354
CS	citrate synthase	-9.071
GBP5	guanylate binding protein 5	-8.982
ACTA1	actin, alpha 1, skeletal muscle	-8.961
ABCC8	ATP-binding cassette, sub-family C (CFTR/MRP), member 8	-8.861
PRKCB	protein kinase C, beta	-8.791
ACVR2B	activin A receptor, type IIB	-8.528
ATP8A1	ATPase, aminophospholipid transporter (APLT), class I, type 8A, member 1	-8.502
ZBTB20	zinc finger and BTB domain containing 20	-8.361
CRYAB	crystallin, alpha B	-8.196
SCP2	sterol carrier protein 2	-8.134
RTN2	reticulon 2	-8.074
AK1	adenylate kinase 1	-8.052
ARPP19	cAMP-regulated phosphoprotein, 19kDa	-8.035
LIFR	leukemia inhibitory factor receptor alpha	-7.467
FOXO4	forkhead box O4	-7.382
TLR5	toll-like receptor 5	-7.337

Table 1: (Continued)

Symbol	Entrez Gene Name	Fold Change
ALDOA	aldolase A, fructose-bisphosphate	-7.33
ABCB4	ATP-binding cassette, sub-family B (MDR/TAP), member 4	-7.187
HYAL4	hyaluronoglucosaminidase 4	-7.115
MLYCD	malonyl-CoA decarboxylase	-7.045
SLC37A4	solute carrier family 37 (glucose-6-phosphate transporter), member 4	-6.909
BAG1	BCL2-associated athanogene	-6.864
NR1I3	nuclear receptor subfamily 1, group I, member 3	-6.849
ACADVL	acyl-CoA dehydrogenase, very long chain	-6.586
MFN2	mitofusin 2	-6.385
PRKAG3	protein kinase, AMP-activated, gamma 3 non-catalytic subunit	-6.383
PPARA	peroxisome proliferator-activated receptor alpha	-6.153
COQ2	coenzyme Q2 homolog, prenyltransferase (yeast)	-6.149
NR4A3	nuclear receptor subfamily 4, group A, member 3	-6.032
TNF	tumor necrosis factor	-5.997
PPP1CB	protein phosphatase 1, catalytic subunit, beta isozyme	-5.903
PHKB	phosphorylase kinase, beta	-5.899
PLIN2	perilipin 2	-5.836
GPLD1	glycosylphosphatidylinositol specific phospholipase D1	-5.824
CRAT	carnitine O-acetyltransferase	-5.58
HIF1AN	hypoxia inducible factor 1, alpha subunit inhibitor	-5.506
CEBPA	CCAAT/enhancer binding protein (C/EBP), alpha	-5.429
RHOQ	ras homolog family member Q	-5.354
LNPEP	leucyl/cystinyl aminopeptidase	-5.155
IP6K3	inositol hexakisphosphate kinase 3	-5.098
FABP5	fatty acid binding protein 5 (psoriasis-associated)	-4.991
DGKZ	diacylglycerol kinase, zeta	-4.964
UGP2	UDP-glucose pyrophosphorylase 2	-4.963
MAPK14	mitogen-activated protein kinase 14	-4.926
PRDX2	peroxiredoxin 2	-4.926
PRKAB2	protein kinase, AMP-activated, beta 2 non-catalytic subunit	-4.918
PLD1	phospholipase D1, phosphatidylcholine-specific	-4.905
FCGR2A	Fc fragment of IgG, low affinity IIa, receptor (CD32)	-4.812
PGR	progesterone receptor	-4.689
APPL1	adaptor protein, phosphotyrosine interaction, PH domain and leucine zipper	-4.633
PPM1A	protein phosphatase, Mg2+/Mn2+ dependent, 1A	-4.623
PPARG	peroxisome proliferator-activated receptor gamma	-4.579
AKR1B1	aldo-keto reductase family 1, member B1 (aldose reductase)	-4.567
CPE	carboxypeptidase E	-4.558
SIRT3	sirtuin 3	-4.53
B4GALNT1	beta-1,4-N-acetyl-galactosaminyl transferase 1	-4.479
ADCY5	adenylate cyclase 5	-4.381
ST3GAL5	ST3 beta-galactoside alpha-2,3-sialyltransferase 5	-4.339
ASPN	asporin	-4.33
SNRPN	small nuclear ribonucleoprotein polypeptide N	-4.288
PFKFB3	6-phosphofructo-2-kinase/fructose-2,6-biphosphatase 3	-4.239
MLXIP	MLX interacting protein	-4.217
WDTC1	WD and tetratricopeptide repeats 1	-4.185
CDO1	cysteine dioxygenase, type I	-4.185
DECR1	2,4-dienoyl CoA reductase 1, mitochondrial	-4.162
DAB2IP	DAB2 interacting protein	-4.151
PLA1A	phospholipase A1 member A	-4.125
FITM2	fat storage-inducing transmembrane protein 2	-3.94

Table 1: (Continued)

Symbol	Entrez Gene Name	Fold Change
PIK3CB	phosphatidylinositol-4,5-bisphosphate 3-kinase, catalytic subunit beta	-3.899
CIDEA	cell death-inducing DFFA-like effector a	-3.886
RGS3	regulator of G-protein signaling 3	-3.844
APLN	apelin	-3.842
PITPNC1	phosphatidylinositol transfer protein, cytoplasmic 1	-3.82
SSTR2	somatostatin receptor 2	-3.796
SLC27A1	solute carrier family 27 (fatty acid transporter), member 1	-3.768
S1PR2	sphingosine-1-phosphate receptor 2	-3.738
TEK	TEK tyrosine kinase, endothelial	-3.734
ADRB2	adrenoceptor beta 2, surface	-3.707
TFF1	trefoil factor 1	-3.702
NR1H4	nuclear receptor subfamily 1, group H, member 4	-3.695
PLEK	pleckstrin	-3.695
SH2B2	SH2B adaptor protein 2	-3.677
GYS1	glycogen synthase 1 (muscle)	-3.65
HEXA	hexosaminidase A (alpha polypeptide)	-3.583
APOE	apolipoprotein E	-3.538
CAT	catalase	-3.532
PPP1CC	protein phosphatase 1, catalytic subunit, gamma isozyme	-3.474
ADIPOQ	adiponectin, C1Q and collagen domain containing	-3.45
ADIPOR2	adiponectin receptor 2	-3.401
PGK1	phosphoglycerate kinase 1	-3.365
IL1RN	interleukin 1 receptor antagonist	-3.328
PBX1	pre-B-cell leukemia homeobox 1	-3.322
SPI1	spleen focus forming virus (SFFV) proviral integration oncogene spi1	-3.284
O3FAR1	omega-3 fatty acid receptor 1	-3.274
TIRAP	toll-interleukin 1 receptor (TIR) domain containing adaptor protein	-3.257
GAPDH	glyceraldehyde-3-phosphate dehydrogenase	-3.254
BCAT2	branched chain amino-acid transaminase 2, mitochondrial	-3.225
PPIP5K1	diphosphoinositol pentakisphosphate kinase 1	-3.178
TPI1	triosephosphate isomerase 1	-3.178
IGFBP5	insulin-like growth factor binding protein 5	-3.094
H6PD	hexose-6-phosphate dehydrogenase (glucose 1-dehydrogenase)	-3.086
AKT2	v-akt murine thymoma viral oncogene homolog 2	-3.056
PARP1	poly (ADP-ribose) polymerase 1	-3.049
NPHS1	nephrosis 1, congenital, Finnish type (nephrin)	-3.008
B3GALNT2	beta-1,3-N-acetylgalactosaminyltransferase 2	-2.951
OMA1	OMA1 zinc metallopeptidase homolog (S. cerevisiae)	-2.884
TXNIP	thioredoxin interacting protein	-2.854
AGK	acylglycerol kinase	-2.821
IRS2	insulin receptor substrate 2	-2.787
RBP4	retinol binding protein 4, plasma	-2.74
ATF3	activating transcription factor 3	-2.722
IGF2	insulin-like growth factor 2 (somatomedin A)	-2.715
PPP3R2	protein phosphatase 3, regulatory subunit B, beta	-2.713
ERN1	endoplasmic reticulum to nucleus signaling 1	-2.706
NRIP1	nuclear receptor interacting protein 1	-2.696
GALT	galactose-1-phosphate uridylyltransferase	-2.685
GRK5	G protein-coupled receptor kinase 5	-2.681
ATXN2	ataxin 2	-2.646
SRF	serum response factor (c-fos serum response element-binding transcription	-2.644
CCL5	chemokine (C-C motif) ligand 5	-2.637

Table 1: (Continued)

Symbol	Entrez Gene Name	Fold Change
PTGER4	prostaglandin E receptor 4 (subtype EP4)	-2.631
SOD2	superoxide dismutase 2, mitochondrial	-2.61
MTRR	5-methyltetrahydrofolate-homocysteine methyltransferase reductase	-2.569
PNPLA8	patatin-like phospholipase domain containing 8	-2.557
IKBKB	inhibitor of kappa light polypeptide gene enhancer in B-cells, kinase beta	-2.548
TACR1	tachykinin receptor 1	-2.542
PLCH2	phospholipase C, eta 2	-2.506
LARGE	like-glycosyltransferase	-2.498
TNKS2	tankyrase, TRF1-interacting ankyrin-related ADP-ribose polymerase 2	-2.494
CXADR	coxsackie virus and adenovirus receptor	-2.488
SQSTM1	sequestosome 1	-2.479
PRKD3	protein kinase D3	-2.478
FGF23	fibroblast growth factor 23	-2.43
IL10	interleukin 10	-2.416
CCRN4L	CCR4 carbon catabolite repression 4-like (S. cerevisiae)	-2.413
PCCA	propionyl CoA carboxylase, alpha polypeptide	-2.411
CAV3	caveolin 3	-2.405
NR2C2	nuclear receptor subfamily 2, group C, member 2	-2.397
PCYT1A	phosphate cytidylyltransferase 1, choline, alpha	-2.387
SRGN	serglycin	-2.384
ONECUT1	one cut homeobox 1	-2.382
SOCS7	suppressor of cytokine signaling 7	-2.379
G6PC	glucose-6-phosphatase, catalytic subunit	-2.376
ADRA1A	adrenoceptor alpha 1A	-2.375
IRS4	insulin receptor substrate 4	-2.372
IGF1R	insulin-like growth factor 1 receptor	-2.37
BTC	betacellulin	-2.37
CYP19A1	cytochrome P450, family 19, subfamily A, polypeptide 1	-2.369
ASIP	agouti signaling protein	-2.368
CYP3A5	cytochrome P450, family 3, subfamily A, polypeptide 5	-2.362
IL6ST	interleukin 6 signal transducer (gp130, oncostatin M receptor)	-2.362
INSRR	insulin receptor-related receptor	-2.362
PCK1	phosphoenolpyruvate carboxykinase 1 (soluble)	-2.36
ABCB1	ATP-binding cassette, sub-family B (MDR/TAP), member 1	-2.359
ABCB1	ATP-binding cassette, sub-family B (MDR/TAP), member 1	-2.359
ALDOB	aldolase B, fructose-bisphosphate	-2.348
PKLR	pyruvate kinase, liver and RBC	-2.346
F2	coagulation factor II (thrombin)	-2.345
UGT2B28	UDP glucuronosyltransferase 2 family, polypeptide B28	-2.344
TAT	tyrosine aminotransferase	-2.341
HRH3	histamine receptor H3	-2.339
APOC3	apolipoprotein C-III	-2.338
IL17F	interleukin 17F	-2.336
HTR2C	5-hydroxytryptamine (serotonin) receptor 2C, G protein-coupled	-2.335
ST8SIA4	ST8 alpha-N-acetyl-neuraminide alpha-2,8-sialyltransferase 4	-2.334
MTNR1B	melatonin receptor 1B	-2.334
LRAT	lecithin retinol acyltransferase (phosphatidylcholine--retinol O-acyltransferase)	-2.333
B3GAT1	beta-1,3-glucuronyltransferase 1 (glucuronosyltransferase P)	-2.322
ESR2	estrogen receptor 2 (ER beta)	-2.321
CD22	CD22 molecule	-2.317
CYP3A4	cytochrome P450, family 3, subfamily A, polypeptide 4	-2.316
GRB10	growth factor receptor-bound protein 10	-2.316

Table 1: (Continued)

Symbol	Entrez Gene Name	Fold Change
IL4	interleukin 4	-2.312
GPRC6A	G protein-coupled receptor, family C, group 6, member A	-2.312
RPS6KB1	ribosomal protein S6 kinase, 70kDa, polypeptide 1	-2.31
SLC30A8	solute carrier family 30 (zinc transporter), member 8	-2.309
IL1R2	interleukin 1 receptor, type II	-2.308
LEP	leptin	-2.306
CNR2	cannabinoid receptor 2 (macrophage)	-2.305
PRLR	prolactin receptor	-2.303
SOD1	superoxide dismutase 1, soluble	-2.303
SLC13A1	solute carrier family 13 (sodium/sulfate symporters), member 1	-2.292
NTRK1	neurotrophic tyrosine kinase, receptor, type 1	-2.289
PLA2G10	phospholipase A2, group X	-2.289
POFUT1	protein O-fucosyltransferase 1	-2.289
OBP2A	odorant binding protein 2A	-2.282
ACP1	acid phosphatase 1, soluble	-2.279
SLC12A1	solute carrier family 12 (sodium/potassium/chloride transporters), member 1	-2.278
ERBB2	v-erb-b2 erythroblastic leukemia viral oncogene homolog 2, neuro/glioblastoma	-2.277
CA5A	carbonic anhydrase VA, mitochondrial	-2.269
INPP5E	inositol polyphosphate-5-phosphatase, 72 kDa	-2.268
ERBB3	v-erb-b2 erythroblastic leukemia viral oncogene homolog 3 (avian)	-2.253
GCNT3	glucosaminyl (N-acetyl) transferase 3, mucin type	-2.247
NEU3	sialidase 3 (membrane sialidase)	-2.245
FGF10	fibroblast growth factor 10	-2.238
UCP1	uncoupling protein 1 (mitochondrial, proton carrier)	-2.236
THRA	thyroid hormone receptor, alpha	-2.228
ABCB11	ATP-binding cassette, sub-family B (MDR/TAP), member 11	-2.225
CEL	carboxyl ester lipase (bile salt-stimulated lipase)	-2.222
TSHR	thyroid stimulating hormone receptor	-2.221
C1QBP	complement component 1, q subcomponent binding protein	-2.206
AGER	advanced glycosylation end product-specific receptor	-2.203
PTPRE	protein tyrosine phosphatase, receptor type, E	-2.198
MC2R	melanocortin 2 receptor (adrenocorticotropic hormone)	-2.174
PPP1R3D	protein phosphatase 1, regulatory subunit 3D	-2.124
TRHR	thyrotropin-releasing hormone receptor	-2.119
ARNT	aryl hydrocarbon receptor nuclear translocator	-2.117
DGAT1	diacylglycerol O-acyltransferase 1	-2.107
POMT1	protein-O-mannosyltransferase 1	-2.088
DGAT2	diacylglycerol O-acyltransferase 2	-2.068
PEX11B	peroxisomal biogenesis factor 11 beta	-2.067
TRPC3	transient receptor potential cation channel, subfamily C, member 3	-2.065
UCP2	uncoupling protein 2 (mitochondrial, proton carrier)	-2.063
PPP3CA	protein phosphatase 3, catalytic subunit, alpha isozyme	-2.049
MECP2	methyl CpG binding protein 2 (Rett syndrome)	-2.047
RELA	v-rel reticuloendotheliosis viral oncogene homolog A (avian)	-2.043

Table 2: List of Low expressed genes in myotube compared to skeletal muscle tissue related to lipid metabolism.

Symbol	Entrez Gene Name	Fold Change
GPIHBP1	glycosylphosphatidylinositol anchored high density lipoprotein binding protein 1	-4606.449
SLC2A4	solute carrier family 2 (facilitated glucose transporter), member 4	-3329.179
LPL	lipoprotein lipase	-2198.27
ANKRD23	ankyrin repeat domain 23	-1097.932
PLIN5	perilipin 5	-410.365
HRASLS	HRAS-like suppressor	-217.855
PDK4	pyruvate dehydrogenase kinase, isozyme 4	-176.367
CD36	CD36 molecule (thrombospondin receptor)	-165.23
UCP3	uncoupling protein 3 (mitochondrial, proton carrier)	-156.344
MLXIPL	MLX interacting protein-like	-113.783
FGR	Gardner-Rasheed feline sarcoma viral (v-fgr) oncogene homolog	-106.935
CPT1B	carnitine palmitoyltransferase 1B (muscle)	-97.448
CNTFR	ciliary neurotrophic factor receptor	-96.53
ERBB4	v-erb-a erythroblastic leukemia viral oncogene homolog 4 (avian)	-67.807
CD74	CD74 molecule, major histocompatibility complex, class II invariant chain	-59.088
PPARGC1A	peroxisome proliferator-activated receptor gamma, coactivator 1 alpha	-51.108
PPARGC1B	peroxisome proliferator-activated receptor gamma, coactivator 1 beta	-49.366
ESR1	estrogen receptor 1	-48.794
ABCC6	ATP-binding cassette, sub-family C (CFTR/MRP), member 6	-46.906
ABCG1	ATP-binding cassette, sub-family G (WHITE), member 1	-44.984
PRKAA2	protein kinase, AMP-activated, alpha 2 catalytic subunit	-40.409
ACSS1	acyl-CoA synthetase short-chain family member 1	-36.598
EGF	epidermal growth factor	-29.058
ACSL6	acyl-CoA synthetase long-chain family member 6	-26.642
GHR	growth hormone receptor	-26.417
THRB	thyroid hormone receptor, beta	-25.103
FABP3	fatty acid binding protein 3, muscle and heart (mammary-derived growth	-23.068
ACADS	acyl-CoA dehydrogenase, C-2 to C-3 short chain	-21.627
ACADM	acyl-CoA dehydrogenase, C-4 to C-12 straight chain	-20.62
ADH1C	alcohol dehydrogenase 1C (class I), gamma polypeptide	-20.238
PHYH	phytanoyl-CoA 2-hydroxylase	-20.072
S1PR1	sphingosine-1-phosphate receptor 1	-19.637
GOT2	glutamic-oxaloacetic transaminase 2, mitochondrial (aspartate	-19.42
ACACB	acetyl-CoA carboxylase beta	-18.902
POMC	proopiomelanocortin	-17.947
OSBPL1A	oxysterol binding protein-like 1A	-17.945
APOD	apolipoprotein D	-16.216
CEBPB	CCAAT/enhancer binding protein (C/EBP), beta	-12.894
LPIN1	lipin 1	-12.73
HADH	hydroxyacyl-CoA dehydrogenase	-12.683
PRKAR2B	protein kinase, cAMP-dependent, regulatory, type II, beta	-12.425
IL18	interleukin 18 (interferon-gamma-inducing factor)	-12.335
LRPPRC	leucine-rich pentatricopeptide repeat containing	-11.873
CADM1	cell adhesion molecule 1	-11.814
TLR2	toll-like receptor 2	-11.465
PLA2G4C	phospholipase A2, group IVC (cytosolic, calcium-independent)	-11.253
SUCLA2	succinate-CoA ligase, ADP-forming, beta subunit	-11.067
ACSL1	acyl-CoA synthetase long-chain family member 1	-11.063
SUCLG1	succinate-CoA ligase, alpha subunit	-11.005
MDH2	malate dehydrogenase 2, NAD (mitochondrial)	-10.709
LIPE	lipase, hormone-sensitive	-10.644
ACADL	acyl-CoA dehydrogenase, long chain	-10.286
SDHA	succinate dehydrogenase complex, subunit A, flavoprotein (Fp)	-10.212
ESRRA	estrogen-related receptor alpha	-9.987
KL	klotho	-9.957

Table 2: (Continued)

Symbol	Entrez Gene Name	Fold Change
MITF	microphthalmia-associated transcription factor	-9.7
PDHA1	pyruvate dehydrogenase (lipoamide) alpha 1	-9.535
LTF	lactotransferrin	-9.532
FABP4	fatty acid binding protein 4, adipocyte	-9.354
CS	citrate synthase	-9.071
CYCS	cytochrome c, somatic	-9.063
PEX5	peroxisomal biogenesis factor 5	-8.753
ATP8A1	ATPase, aminophospholipid transporter (APLT), class I, type 8A, member 1	-8.502
SDHB	succinate dehydrogenase complex, subunit B, iron sulfur (Ip)	-8.425
ACSBG1	acyl-CoA synthetase bubblegum family member 1	-8.361
SCP2	sterol carrier protein 2	-8.134
SMPD3	sphingomyelin phosphodiesterase 3, neutral membrane (neutral	-8.13
ABCB4	ATP-binding cassette, sub-family B (MDR/TAP), member 4	-7.187
MLYCD	malonyl-CoA decarboxylase	-7.045
OGDH	oxoglutarate (alpha-ketoglutarate) dehydrogenase (lipoamide)	-6.993
ACSL5	acyl-CoA synthetase long-chain family member 5	-6.667
ACADVL	acyl-CoA dehydrogenase, very long chain	-6.586
NUDT7	nudix (nucleoside diphosphate linked moiety X)-type motif 7	-6.508
IL16	interleukin 16	-6.484
IL33	interleukin 33	-6.448
FAAH	fatty acid amide hydrolase	-6.399
CNR1	cannabinoid receptor 1 (brain)	-6.398
TEF	thyrotrophic embryonic factor	-6.389
NTRK2	neurotrophic tyrosine kinase, receptor, type 2	-6.337
IL18RAP	interleukin 18 receptor accessory protein	-6.301
DLAT	dihydrolipoamide S-acetyltransferase	-6.267
EDNRB	endothelin receptor type B	-6.243
PPARA	peroxisome proliferator-activated receptor alpha	-6.153
CYP27A1	cytochrome P450, family 27, subfamily A, polypeptide 1	-6.109
NR4A3	nuclear receptor subfamily 4, group A, member 3	-6.032
TNF	tumor necrosis factor	-5.997
PLIN2	perilipin 2	-5.836
CRAT	carnitine O-acetyltransferase	-5.58
SLC10A2	solute carrier family 10 (sodium/bile acid cotransporter family), member 2	-5.565
SUCLG2	succinate-CoA ligase, GDP-forming, beta subunit	-5.432
ATP5J	ATP synthase, H+ transporting, mitochondrial Fo complex, subunit F6	-5.321
PLA2G4F	phospholipase A2, group IVF	-5.286
IMMT	inner membrane protein, mitochondrial	-5.162
PLA2G16	phospholipase A2, group XVI	-5.099
FABP5	fatty acid binding protein 5 (psoriasis-associated)	-4.991
HOXA10	homeobox A10	-4.987
SLC22A5	solute carrier family 22 (organic cation/carnitine transporter), member 5	-4.978
FH	fumarate hydratase	-4.961
HADHB	hydroxyacyl-CoA dehydrogenase/3-ketoacyl-CoA thiolase/enoyl-CoA hydratase	-4.935
MAPK14	mitogen-activated protein kinase 14	-4.926
SLC36A1	solute carrier family 36 (proton/amino acid symporter), member 1	-4.877
TECR	trans-2,3-enoyl-CoA reductase	-4.851
FCGR2A	Fc fragment of IgG, low affinity IIa, receptor (CD32)	-4.812
ECI1	enoyl-CoA delta isomerase 1	-4.794
PGR	progesterone receptor	-4.689
APPL1	adaptor protein, phosphotyrosine interaction, PH domain and leucine zipper	-4.633
DBP	D site of albumin promoter (albumin D-box) binding protein	-4.618

Table 2: (Continued)

Symbol	Entrez Gene Name	Fold Change
PPARG	peroxisome proliferator-activated receptor gamma	-4.579
AKR1B1	aldo-keto reductase family 1, member B1 (aldose reductase)	-4.567
ECI2	enoyl-CoA delta isomerase 2	-4.485
B4GALNT1	beta-1,4-N-acetyl-galactosaminyl transferase 1	-4.479
ST3GAL5	ST3 beta-galactoside alpha-2,3-sialyltransferase 5	-4.339
HADHA	hydroxyacyl-CoA dehydrogenase/3-ketoacyl-CoA thiolase/enoyl-CoA hydratase	-4.295
IL15	interleukin 15	-4.269
DLD	dihydrolipoamide dehydrogenase	-4.198
MID1IP1	MID1 interacting protein 1	-4.191
WDTC1	WD and tetratricopeptide repeats 1	-4.185
ACOT1	acyl-CoA thioesterase 1	-4.18
DECR1	2,4-dienoyl CoA reductase 1, mitochondrial	-4.162
FITM2	fat storage-inducing transmembrane protein 2	-3.94
PIK3CB	phosphatidylinositol-4,5-bisphosphate 3-kinase, catalytic subunit beta	-3.899
PITPNC1	phosphatidylinositol transfer protein, cytoplasmic 1	-3.82
SLC27A1	solute carrier family 27 (fatty acid transporter), member 1	-3.768
ADRB2	adrenoceptor beta 2, surface	-3.707
NFKBIA	nuclear factor of kappa light polypeptide gene enhancer in B-cells inhibitor,	-3.702
NR1H4	nuclear receptor subfamily 1, group H, member 4	-3.695
B4GALT6	UDP-Gal:betaGlcNAc beta 1,4- galactosyltransferase, polypeptide 6	-3.662
STAT5B	signal transducer and activator of transcription 5B	-3.662
ME2	malic enzyme 2, NAD(+)-dependent, mitochondrial	-3.575
ME3	malic enzyme 3, NADP(+)-dependent, mitochondrial	-3.574
APOE	apolipoprotein E	-3.538
CAT	catalase	-3.532
PTGES2	prostaglandin E synthase 2	-3.462
ADIPOQ	adiponectin, C1Q and collagen domain containing	-3.45
ADIPOR2	adiponectin receptor 2	-3.401
B3GALT4	UDP-Gal:betaGlcNAc beta 1,3-galactosyltransferase, polypeptide 4	-3.379
NFATC2	nuclear factor of activated T-cells, cytoplasmic, calcineurin-dependent 2	-3.371
IL1RN	interleukin 1 receptor antagonist	-3.328
OSBP	oxysterol binding protein	-3.282
PEBP1	phosphatidylethanolamine binding protein 1	-3.171
CASP8	caspase 8, apoptosis-related cysteine peptidase	-3.082
AKT2	v-akt murine thymoma viral oncogene homolog 2	-3.056
CLEC7A	C-type lectin domain family 7, member A	-3.051
NR5A2	nuclear receptor subfamily 5, group A, member 2	-3.035
QKI	QKI, KH domain containing, RNA binding	-2.865
VEGFA	vascular endothelial growth factor A	-2.858
AGK	acylglycerol kinase	-2.821
IRS2	insulin receptor substrate 2	-2.787
ALOX5AP	arachidonate 5-lipoxygenase-activating protein	-2.75
RBP4	retinol binding protein 4, plasma	-2.74
IGF2	insulin-like growth factor 2 (somatomedin A)	-2.715
IDE	insulin-degrading enzyme	-2.684
CCL5	chemokine (C-C motif) ligand 5	-2.637
MECR	mitochondrial trans-2-enoyl-CoA reductase	-2.599
PNPLA8	patatin-like phospholipase domain containing 8	-2.557
TACR1	tachykinin receptor 1	-2.542
PCCB	propionyl CoA carboxylase, beta polypeptide	-2.52
MGLL	monoglyceride lipase	-2.513
LARGE	like-glycosyltransferase	-2.498

Table 2: (Continued)

Symbol	Entrez Gene Name	Fold Change
HMGCL	3-hydroxymethyl-3-methylglutaryl-CoA lyase	-2.463
ARV1	ARV1 homolog (S. cerevisiae)	-2.444
IL10	interleukin 10	-2.416
CCRN4L	CCR4 carbon catabolite repression 4-like (S. cerevisiae)	-2.413
PLA2G2D	phospholipase A2, group IID	-2.412
PCCA	propionyl CoA carboxylase, alpha polypeptide	-2.411
PCYT1A	phosphate cytidylyltransferase 1, choline, alpha	-2.387
SLCO1A2	solute carrier organic anion transporter family, member 1A2	-2.371
IGF1R	insulin-like growth factor 1 receptor	-2.37
CYP19A1	cytochrome P450, family 19, subfamily A, polypeptide 1	-2.369
CYP3A5	cytochrome P450, family 3, subfamily A, polypeptide 5	-2.362
ABCB1	ATP-binding cassette, sub-family B (MDR/TAP), member 1	-2.359
F2	coagulation factor II (thrombin)	-2.345
FASLG	Fas ligand (TNF superfamily, member 6)	-2.341
APOC3	apolipoprotein C-III	-2.338
ST8SIA4	ST8 alpha-N-acetyl-neuraminide alpha-2,8-sialyltransferase 4	-2.334
ESR2	estrogen receptor 2 (ER beta)	-2.321
ABCD2	ATP-binding cassette, sub-family D (ALD), member 2	-2.32
CYP3A4	cytochrome P450, family 3, subfamily A, polypeptide 4	-2.316
IL4	interleukin 4	-2.312
IL1R2	interleukin 1 receptor, type II	-2.308
LEP	leptin	-2.306
SLCO6A1	solute carrier organic anion transporter family, member 6A1	-2.304
SOD1	superoxide dismutase 1, soluble	-2.303
KLF2	Kruppel-like factor 2 (lung)	-2.292
PLA2G10	phospholipase A2, group X	-2.289
MAP3K1	mitogen-activated protein kinase kinase kinase 1, E3 ubiquitin protein ligase	-2.286
OBP2A	odorant binding protein 2A	-2.282
CYP2C19	cytochrome P450, family 2, subfamily C, polypeptide 19	-2.279
ERBB2	v-erb-b2 erythroblastic leukemia viral oncogene homolog 2, neuro/glioblastoma	-2.277
MAP2K1	mitogen-activated protein kinase kinase 1	-2.269
UCP1	uncoupling protein 1 (mitochondrial, proton carrier)	-2.236
FA2H	fatty acid 2-hydroxylase	-2.228
THRA	thyroid hormone receptor, alpha	-2.228
PLA2G3	phospholipase A2, group III	-2.226
ABCB11	ATP-binding cassette, sub-family B (MDR/TAP), member 11	-2.225
CEL	carboxyl ester lipase (bile salt-stimulated lipase)	-2.222
CYP46A1	cytochrome P450, family 46, subfamily A, polypeptide 1	-2.219
AGER	advanced glycosylation end product-specific receptor	-2.203
GSN	gelsolin	-2.198
HSPA8	heat shock 70kDa protein 8	-2.177
ALOX15	arachidonate 15-lipoxygenase	-2.173
SLCO2A1	solute carrier organic anion transporter family, member 2A1	-2.134
DBI	diazepam binding inhibitor (GABA receptor modulator, acyl-CoA binding	-2.113
DGAT1	diacylglycerol O-acyltransferase 1	-2.107
ACAA1	acetyl-CoA acyltransferase 1	-2.082
HSD17B4	hydroxysteroid (17-beta) dehydrogenase 4	-2.075
NAA40	N(alpha)-acetyltransferase 40, NatD catalytic subunit, homolog (S. cerevisiae)	-2.075
ME1	malic enzyme 1, NADP(+)-dependent, cytosolic	-2.068
MAP2K4	mitogen-activated protein kinase kinase 4	-2.067
UCP2	uncoupling protein 2 (mitochondrial, proton carrier)	-2.063
SLC16A1	solute carrier family 16, member 1 (monocarboxylic acid transporter 1)	-2.058
ABCG5	ATP-binding cassette, sub-family G (WHITE), member 5	-2.053
RELA	v-rel reticuloendotheliosis viral oncogene homolog A (avian)	-2.043
RASGRP4	RAS guanyl releasing protein 4	-2.037
EPAS1	endothelial PAS domain protein 1	-2.018

Table 3: List of Low expressed genes in myotube compared to skeletal muscle tissue related to energy production.

Symbol	Entrez Gene Name	Fold Change
SLC2A4	solute carrier family 2 (facilitated glucose transporter), member 4	-3329.179
LPL	lipoprotein lipase	-2198.27
PLIN5	perilipin 5	-410.365
S100A1	S100 calcium binding protein A1	-374.526
NOS1	nitric oxide synthase 1 (neuronal)	-245.532
PDK4	pyruvate dehydrogenase kinase, isozyme 4	-176.367
CD36	CD36 molecule (thrombospondin receptor)	-165.23
UCP3	uncoupling protein 3 (mitochondrial, proton carrier)	-156.344
MAPT	microtubule-associated protein tau	-141.057
MLXIPL	MLX interacting protein-like	-113.783
SLC25A12	solute carrier family 25 (aspartate/glutamate carrier), member 12	-88.9
PPARGC1A	peroxisome proliferator-activated receptor gamma, coactivator 1 alpha	-51.108
PPARGC1B	peroxisome proliferator-activated receptor gamma, coactivator 1 beta	-49.366
ABCG1	ATP-binding cassette, sub-family G (WHITE), member 1	-44.984
EPM2A	epilepsy, progressive myoclonus type 2A, Lafora disease (laforin)	-44.728
RYR1	ryanodine receptor 1 (skeletal)	-43.562
PRKAA2	protein kinase, AMP-activated, alpha 2 catalytic subunit	-40.409
EGF	epidermal growth factor	-29.058
ACSL6	acyl-CoA synthetase long-chain family member 6	-26.642
THRB	thyroid hormone receptor, beta	-25.103
PARK2	parkinson protein 2, E3 ubiquitin protein ligase (parkin)	-23.64
FABP3	fatty acid binding protein 3, muscle and heart (mammary-derived growth	-23.068
ACADS	acyl-CoA dehydrogenase, C-2 to C-3 short chain	-21.627
ACADM	acyl-CoA dehydrogenase, C-4 to C-12 straight chain	-20.62
ADH1C	alcohol dehydrogenase 1C (class I), gamma polypeptide	-20.238
SOX6	SRY (sex determining region Y)-box 6	-20.137
PHYH	phytanoyl-CoA 2-hydroxylase	-20.072
GOT2	glutamic-oxaloacetic transaminase 2, mitochondrial (aspartate	-19.42
ACACB	acetyl-CoA carboxylase beta	-18.902
POMC	proopiomelanocortin	-17.947
CREB5	cAMP responsive element binding protein 5	-14.264
LPIN1	lipin 1	-12.73
HADH	hydroxyacyl-CoA dehydrogenase	-12.683
IL18	interleukin 18 (interferon-gamma-inducing factor)	-12.335
LRPPRC	leucine-rich pentatricopeptide repeat containing	-11.873
ACSL1	acyl-CoA synthetase long-chain family member 1	-11.063
NOS3	nitric oxide synthase 3 (endothelial cell)	-10.848
NPY1R	neuropeptide Y receptor Y1	-10.842
LIPE	lipase, hormone-sensitive	-10.644
NDUFS1	NADH dehydrogenase (ubiquinone) Fe-S protein 1, 75kDa (NADH-coenzyme Q	-10.521
VDAC1	voltage-dependent anion channel 1	-10.367
ACADL	acyl-CoA dehydrogenase, long chain	-10.286
ESRRA	estrogen-related receptor alpha	-9.987
KL	klotho	-9.957
NR4A1	nuclear receptor subfamily 4, group A, member 1	-9.941
CYCS	cytochrome c, somatic	-9.063
PINK1	PTEN induced putative kinase 1	-8.965
ABCC8	ATP-binding cassette, sub-family C (CFTR/MRP), member 8	-8.861
PEX5	peroxisomal biogenesis factor 5	-8.753
ATP6	ATP synthase F0 subunit 6	-8.66

Table 3: (Continued)

Symbol	Entrez Gene Name	Fold Change
CRYAB	crystallin, alpha B	-8.196
ATP5B	ATP synthase, H+ transporting, mitochondrial F1 complex, beta polypeptide	-7.735
ALDOA	aldolase A, fructose-bisphosphate	-7.33
DES	desmin	-7.084
MLYCD	malonyl-CoA decarboxylase	-7.045
ACSL5	acyl-CoA synthetase long-chain family member 5	-6.667
COQ7	coenzyme Q7 homolog, ubiquinone (yeast)	-6.59
ACADVL	acyl-CoA dehydrogenase, very long chain	-6.586
MFN2	mitofusin 2	-6.385
ATP5G1	ATP synthase, H+ transporting, mitochondrial Fo complex, subunit C1 (subunit	-6.265
PPARA	peroxisome proliferator-activated receptor alpha	-6.153
CYP27A1	cytochrome P450, family 27, subfamily A, polypeptide 1	-6.109
NR4A3	nuclear receptor subfamily 4, group A, member 3	-6.032
TNF	tumor necrosis factor	-5.997
COX8A	cytochrome c oxidase subunit VIIIA (ubiquitous)	-5.717
ATP5D	ATP synthase, H+ transporting, mitochondrial F1 complex, delta subunit	-5.679
RXRA	retinoid X receptor, alpha	-5.604
CRAT	carnitine O-acetyltransferase	-5.58
COX3	cytochrome c oxidase III	-5.537
HIF1AN	hypoxia inducible factor 1, alpha subunit inhibitor	-5.506
IMMT	inner membrane protein, mitochondrial	-5.162
SLC22A5	solute carrier family 22 (organic cation/carnitine transporter), member 5	-4.978
HADHB	hydroxyacyl-CoA dehydrogenase/3-ketoacyl-CoA thiolase/enoyl-CoA hydratase	-4.935
MAPK14	mitogen-activated protein kinase 14	-4.926
ECI1	enoyl-CoA delta isomerase 1	-4.794
NDUFAF1	NADH dehydrogenase (ubiquinone) complex I, assembly factor 1	-4.768
EEF2K	eukaryotic elongation factor-2 kinase	-4.656
APPL1	adaptor protein, phosphotyrosine interaction, PH domain and leucine zipper	-4.633
PPARG	peroxisome proliferator-activated receptor gamma	-4.579
SIRT3	sirtuin 3	-4.53
ECI2	enoyl-CoA delta isomerase 2	-4.485
HADHA	hydroxyacyl-CoA dehydrogenase/3-ketoacyl-CoA thiolase/enoyl-CoA hydratase	-4.295
PFKFB3	6-phosphofructo-2-kinase/fructose-2,6-biphosphatase 3	-4.239
TH	tyrosine hydroxylase	-4.206
NAMPT	nicotinamide phosphoribosyltransferase	-4.186
DECR1	2,4-dienoyl CoA reductase 1, mitochondrial	-4.162
FITM2	fat storage-inducing transmembrane protein 2	-3.94
NDUFS6	NADH dehydrogenase (ubiquinone) Fe-S protein 6, 13kDa (NADH-coenzyme Q	-3.887
SLC27A1	solute carrier family 27 (fatty acid transporter), member 1	-3.768
ADRB2	adrenoceptor beta 2, surface	-3.707
APOE	apolipoprotein E	-3.538
CAT	catalase	-3.532
ADIPOQ	adiponectin, C1Q and collagen domain containing	-3.45
ADIPOR2	adiponectin receptor 2	-3.401
IL1RN	interleukin 1 receptor antagonist	-3.328
AKT2	v-akt murine thymoma viral oncogene homolog 2	-3.056
PARP1	poly (ADP-ribose) polymerase 1	-3.049
MNF1	mitochondrial nucleoid factor 1	-3.019
TYR	tyrosinase (oculocutaneous albinism IA)	-2.934
MEF2D	myocyte enhancer factor 2D	-2.906

Table 3: (Continued)

Symbol	Entrez Gene Name	Fold Change
OMA1	OMA1 zinc metallopeptidase homolog (S. cerevisiae)	-2.884
NMNAT1	nicotinamide nucleotide adenylyltransferase 1	-2.873
TXNIP	thioredoxin interacting protein	-2.854
LDHA	lactate dehydrogenase A	-2.79
IRS2	insulin receptor substrate 2	-2.787
NRIP1	nuclear receptor interacting protein 1	-2.696
IDE	insulin-degrading enzyme	-2.684
PNPLA8	patatin-like phospholipase domain containing 8	-2.557
MSRA	methionine sulfoxide reductase A	-2.544
SQSTM1	sequestosome 1	-2.479
NR2C2	nuclear receptor subfamily 2, group C, member 2	-2.397
IGF1R	insulin-like growth factor 1 receptor	-2.37
CYP19A1	cytochrome P450, family 19, subfamily A, polypeptide 1	-2.369
CYP3A5	cytochrome P450, family 3, subfamily A, polypeptide 5	-2.362
PKLR	pyruvate kinase, liver and RBC	-2.346
HRH3	histamine receptor H3	-2.339
ESR2	estrogen receptor 2 (ER beta)	-2.321
ABCD2	ATP-binding cassette, sub-family D (ALD), member 2	-2.32
CYP3A4	cytochrome P450, family 3, subfamily A, polypeptide 4	-2.316
IL4	interleukin 4	-2.312
RBL1	retinoblastoma-like 1 (p107)	-2.307
LEP	leptin	-2.306
SOD1	superoxide dismutase 1, soluble	-2.303
ADK	adenosine kinase	-2.292
KRAS	v-Ki-ras2 Kirsten rat sarcoma viral oncogene homolog	-2.284
OBP2A	odorant binding protein 2A	-2.282
CYP2C19	cytochrome P450, family 2, subfamily C, polypeptide 19	-2.279
ERBB2	v-erb-b2 erythroblastic leukemia viral oncogene homolog 2, neuro/glioblastoma	-2.277
UCP1	uncoupling protein 1 (mitochondrial, proton carrier)	-2.236
THRA	thyroid hormone receptor, alpha	-2.228
WNT3A	wingless-type MMTV integration site family, member 3A	-2.216
AGER	advanced glycosylation end product-specific receptor	-2.203
PTPMT1	protein tyrosine phosphatase, mitochondrial 1	-2.191
TFAM	transcription factor A, mitochondrial	-2.14
SLCO2A1	solute carrier organic anion transporter family, member 2A1	-2.134
DNM1L	dynamin 1-like	-2.125
DGAT1	diacylglycerol O-acyltransferase 1	-2.107
ACAA1	acetyl-CoA acyltransferase 1	-2.082
HSD17B4	hydroxysteroid (17-beta) dehydrogenase 4	-2.075
UCP2	uncoupling protein 2 (mitochondrial, proton carrier)	-2.063
RELA	v-rel reticuloendotheliosis viral oncogene homolog A (avian)	-2.043
EPAS1	endothelial PAS domain protein 1	-2.018

Table 4: List of Low expressed genes in myotube compared to skeletal muscle tissue related to protein metabolism.

Symbol	Entrez Gene Name	Fold Change
SLC2A4	solute carrier family 2 (facilitated glucose transporter), member 4	-3329.179
CKMT2	creatine kinase, mitochondrial 2 (sarcomeric)	-985.349
NOS1	nitric oxide synthase 1 (neuronal)	-245.532
PDK4	pyruvate dehydrogenase kinase, isozyme 4	-176.367
SLC25A4	solute carrier family 25 (mitochondrial carrier; adenine nucleotide translocator),	-69.464
CKM	creatine kinase, muscle	-50.899
PRKAA2	protein kinase, AMP-activated, alpha 2 catalytic subunit	-40.409
EGF	epidermal growth factor	-29.058
GHR	growth hormone receptor	-26.417
ASPA	aspartoacylase	-25.332
THRB	thyroid hormone receptor, beta	-25.103
FABP3	fatty acid binding protein 3, muscle and heart (mammary-derived growth	-23.068
GAMT	guanidinoacetate N-methyltransferase	-20.568
GOT2	glutamic-oxaloacetic transaminase 2, mitochondrial (aspartate	-19.42
RXRG	retinoid X receptor, gamma	-18.255
POMC	proopiomelanocortin	-17.947
GOT1	glutamic-oxaloacetic transaminase 1, soluble (aspartate aminotransferase 1)	-15.991
CD34	CD34 molecule	-15.361
HOMER2	homer homolog 2 (Drosophila)	-14.36
DDC	dopa decarboxylase (aromatic L-amino acid decarboxylase)	-14.194
HADH	hydroxyacyl-CoA dehydrogenase	-12.683
NOS3	nitric oxide synthase 3 (endothelial cell)	-10.848
GATM	glycine amidinotransferase (L-arginine:glycine amidinotransferase)	-9.61
PANK1	pantothenate kinase 1	-9.394
ABCC8	ATP-binding cassette, sub-family C (CFTR/MRP), member 8	-8.861
SMPD3	sphingomyelin phosphodiesterase 3, neutral membrane (neutral	-8.13
GLUL	glutamate-ammonia ligase	-7.788
NR1I3	nuclear receptor subfamily 1, group I, member 3	-6.849
ACADVL	acyl-CoA dehydrogenase, very long chain	-6.586
LIAS	lipoic acid synthetase	-6.533
FAAH	fatty acid amide hydrolase	-6.399
PPARA	peroxisome proliferator-activated receptor alpha	-6.153
TNF	tumor necrosis factor	-5.997
SLC6A8	solute carrier family 6 (neurotransmitter transporter, creatine), member 8	-5.689
CEBPA	CCAAT/enhancer binding protein (C/EBP), alpha	-5.429
PRODH	proline dehydrogenase (oxidase) 1	-5.34
DDO	D-aspartate oxidase	-5.282
SLC22A5	solute carrier family 22 (organic cation/carnitine transporter), member 5	-4.978
HOMER1	homer homolog 1 (Drosophila)	-4.765
SLC7A8	solute carrier family 7 (amino acid transporter light chain, L system), member 8	-4.25
TH	tyrosine hydroxylase	-4.206
CDO1	cysteine dioxygenase, type I	-4.185
SPR	sepiapterin reductase (7,8-dihydrobiopterin:NADP+ oxidoreductase)	-4.129
FOS	FBJ murine osteosarcoma viral oncogene homolog	-4.026
PCYOX1	prenylcysteine oxidase 1	-3.72
CD86	CD86 molecule	-3.63
ME2	malic enzyme 2, NAD(+)-dependent, mitochondrial	-3.575
APOE	apolipoprotein E	-3.538
BCKDHA	branched chain keto acid dehydrogenase E1, alpha polypeptide	-3.467
MCCC2	methylcrotonoyl-CoA carboxylase 2 (beta)	-3.415

Table 4: (Continued)

Symbol	Entrez Gene Name	Fold Change
GSTZ1	glutathione S-transferase zeta 1	-3.321
BCAT2	branched chain amino-acid transaminase 2, mitochondrial	-3.225
MUT	methylmalonyl CoA mutase	-3.002
EFNA5	ephrin-A5	-2.785
MTRR	5-methyltetrahydrofolate-homocysteine methyltransferase reductase	-2.569
MSRA	methionine sulfoxide reductase A	-2.544
PCCB	propionyl CoA carboxylase, beta polypeptide	-2.52
IL10	interleukin 10	-2.416
PCCA	propionyl CoA carboxylase, alpha polypeptide	-2.411
DBT	dihydrolipoamide branched chain transacylase E2	-2.391
PCYT1A	phosphate cytidylyltransferase 1, choline, alpha	-2.387
IGF1R	insulin-like growth factor 1 receptor	-2.37
PCK1	phosphoenolpyruvate carboxykinase 1 (soluble)	-2.36
CGA	glycoprotein hormones, alpha polypeptide	-2.345
TAT	tyrosine aminotransferase	-2.341
IL4	interleukin 4	-2.312
MCHR1	melanin-concentrating hormone receptor 1	-2.309
LEP	leptin	-2.306
PRLR	prolactin receptor	-2.303
PRKCE	protein kinase C, epsilon	-2.259
CD80	CD80 molecule	-2.259
UCP1	uncoupling protein 1 (mitochondrial, proton carrier)	-2.236
THRA	thyroid hormone receptor, alpha	-2.228
TSHR	thyroid stimulating hormone receptor	-2.221
NFS1	NFS1 nitrogen fixation 1 homolog (S. cerevisiae)	-2.181
TRHR	thyrotropin-releasing hormone receptor	-2.119
MTHFR	methylenetetrahydrofolate reductase (NAD(P)H)	-2.087
MECP2	methyl CpG binding protein 2 (Rett syndrome)	-2.047
PSPH	phosphoserine phosphatase	-2.043
BCKDHB	branched chain keto acid dehydrogenase E1, beta polypeptide	-2.032
MTHFD1	methylenetetrahydrofolate dehydrogenase (NADP+ dependent) 1,	-2.032
PICK1	protein interacting with PRKCA 1	-2.001

Table 5: List of Low expressed genes in myotube compared to skeletal muscle tissue related to mitochondria dysfunction.

Symbol	Entrez Gene Name	Fold Change
MAOB	monoamine oxidase B	-2484.776
CPT1B	carnitine palmitoyltransferase 1B (muscle)	-97.448
MAPK12	mitogen-activated protein kinase 12	-46.432
COX7B	cytochrome c oxidase subunit VIIb	-24.49
PARK2	parkinson protein 2, E3 ubiquitin protein ligase (parkin)	-23.64
COX7A1	cytochrome c oxidase subunit VIIa polypeptide 1 (muscle)	-22.431
COX4I2	cytochrome c oxidase subunit IV isoform 2 (lung)	-20.916
MAOA	monoamine oxidase A	-15.857
COX6A2	cytochrome c oxidase subunit VIa polypeptide 2	-13.739
NDUFB10	NADH dehydrogenase (ubiquinone) 1 beta subcomplex, 10, 22kDa	-12.022
NDUFS7	NADH dehydrogenase (ubiquinone) Fe-S protein 7, 20kDa (NADH-coenzyme Q	-11.716
NDUFS1	NADH dehydrogenase (ubiquinone) Fe-S protein 1, 75kDa (NADH-coenzyme Q	-10.521
SDHA	succinate dehydrogenase complex, subunit A, flavoprotein (Fp)	-10.212
UQCRFS1	ubiquinol-cytochrome c reductase, Rieske iron-sulfur polypeptide 1	-9.909
NDUFS3	NADH dehydrogenase (ubiquinone) Fe-S protein 3, 30kDa (NADH-coenzyme Q	-9.536
PDHA1	pyruvate dehydrogenase (lipoamide) alpha 1	-9.535
ATP5A1	ATP synthase, H+ transporting, mitochondrial F1 complex, alpha subunit 1,	-9.496
NDUFS2	NADH dehydrogenase (ubiquinone) Fe-S protein 2, 49kDa (NADH-coenzyme Q	-9.197
CYCS	cytochrome c, somatic	-9.063
PINK1	PTEN induced putative kinase 1	-8.965
COX5A	cytochrome c oxidase subunit Va	-8.902
COX5B	cytochrome c oxidase subunit Vb	-8.764
SDHB	succinate dehydrogenase complex, subunit B, iron sulfur (Ip)	-8.425
COX1	cytochrome c oxidase subunit I	-8.379
UQCRC1	ubiquinol-cytochrome c reductase core protein I	-8.298
LRRK2	leucine-rich repeat kinase 2	-8.038
ND5	NADH dehydrogenase, subunit 5 (complex I)	-7.88
NDUFA10	NADH dehydrogenase (ubiquinone) 1 alpha subcomplex, 10, 42kDa	-7.744
ATP5B	ATP synthase, H+ transporting, mitochondrial F1 complex, beta polypeptide	-7.735
NDUFV2	NADH dehydrogenase (ubiquinone) flavoprotein 2, 24kDa	-7.692
NDUFB9	NADH dehydrogenase (ubiquinone) 1 beta subcomplex, 9, 22kDa	-7.566
CYC1	cytochrome c-1	-7.474
NDUFA6	NADH dehydrogenase (ubiquinone) 1 alpha subcomplex, 6, 14kDa	-7.393
NDUFB3	NADH dehydrogenase (ubiquinone) 1 beta subcomplex, 3, 12kDa	-7.188
CYTB	cytochrome b	-7.149
OGDH	oxoglutarate (alpha-ketoglutarate) dehydrogenase (lipoamide)	-6.993
NDUFA5	NADH dehydrogenase (ubiquinone) 1 alpha subcomplex, 5, 13kDa	-6.663
SDHD	succinate dehydrogenase complex, subunit D, integral membrane protein	-6.624
NDUFV3	NADH dehydrogenase (ubiquinone) flavoprotein 3, 10kDa	-6.212
ATP5C1	ATP synthase, H+ transporting, mitochondrial F1 complex, gamma polypeptide	-6.051
COX8A	cytochrome c oxidase subunit VIIIA (ubiquitous)	-5.717
NDUFA12	NADH dehydrogenase (ubiquinone) 1 alpha subcomplex, 12	-5.695
NDUFA9	NADH dehydrogenase (ubiquinone) 1 alpha subcomplex, 9, 39kDa	-5.598
COX3	cytochrome c oxidase III	-5.537
COX2	cytochrome c oxidase subunit II	-5.47
COX4I1	cytochrome c oxidase subunit IV isoform 1	-5.378
ATP5J	ATP synthase, H+ transporting, mitochondrial Fo complex, subunit F6	-5.321
NDUFA7	NADH dehydrogenase (ubiquinone) 1 alpha subcomplex, 7, 14.5kDa	-5.227
NDUFB7	NADH dehydrogenase (ubiquinone) 1 beta subcomplex, 7, 18kDa	-4.947
NDUFB5	NADH dehydrogenase (ubiquinone) 1 beta subcomplex, 5, 16kDa	-4.932

Table 5: (Continued)

Symbol	Entrez Gene Name	Fold Change
NDUFS4	NADH dehydrogenase (ubiquinone) Fe-S protein 4, 18kDa (NADH-coenzyme Q	-4.819
COX6B1	cytochrome c oxidase subunit VIb polypeptide 1 (ubiquitous)	-4.811
UQCRC2	ubiquinol-cytochrome c reductase core protein II	-4.799
NDUFV1	NADH dehydrogenase (ubiquinone) flavoprotein 1, 51kDa	-4.77
NDUFAF1	NADH dehydrogenase (ubiquinone) complex I, assembly factor 1	-4.768
PRDX3	peroxiredoxin 3	-4.695
NDUFA2	NADH dehydrogenase (ubiquinone) 1 alpha subcomplex, 2, 8kDa	-4.652
UQCR11	ubiquinol-cytochrome c reductase, complex III subunit XI	-4.543
UQCRH	ubiquinol-cytochrome c reductase hinge protein	-4.452
NDUFA8	NADH dehydrogenase (ubiquinone) 1 alpha subcomplex, 8, 19kDa	-4.394
COX7C	cytochrome c oxidase subunit VIIc	-4.391
NDUFS6	NADH dehydrogenase (ubiquinone) Fe-S protein 6, 13kDa (NADH-coenzyme Q	-3.887
NDUFA3	NADH dehydrogenase (ubiquinone) 1 alpha subcomplex, 3, 9kDa	-3.871
NDUFB4	NADH dehydrogenase (ubiquinone) 1 beta subcomplex, 4, 15kDa	-3.66
COX6C	cytochrome c oxidase subunit VIc	-3.636
CAT	catalase	-3.532
NDUFS8	NADH dehydrogenase (ubiquinone) Fe-S protein 8, 23kDa (NADH-coenzyme Q	-3.481
AIFM1	apoptosis-inducing factor, mitochondrion-associated, 1	-3.425
COX17	COX17 cytochrome c oxidase assembly homolog (S. cerevisiae)	-3.199
NDUFB6	NADH dehydrogenase (ubiquinone) 1 beta subcomplex, 6, 17kDa	-3.11
CASP8	caspase 8, apoptosis-related cysteine peptidase	-3.082
NDUFS5	NADH dehydrogenase (ubiquinone) Fe-S protein 5, 15kDa (NADH-coenzyme Q	-2.945
NDUFA13	NADH dehydrogenase (ubiquinone) 1 alpha subcomplex, 13	-2.851
SOD2	superoxide dismutase 2, mitochondrial	-2.61
FIS1	fission 1 (mitochondrial outer membrane) homolog (S. cerevisiae)	-2.446
COX6A1	cytochrome c oxidase subunit VIa polypeptide 1	-2.225
MAP2K4	mitogen-activated protein kinase kinase 4	-2.067
UCP2	uncoupling protein 2 (mitochondrial, proton carrier)	-2.063

Table 6: List of Low expressed genes in myotube compared to skeletal muscle tissue related to calcium signalling.

Symbol	Entrez Gene Name	Fold Change
CASQ1	calsequestrin 1 (fast-twitch, skeletal muscle)	-3128.116
MYL3	myosin, light chain 3, alkali; ventricular, skeletal, slow	-2435.062
ATP2A1	ATPase, Ca++ transporting, cardiac muscle, fast twitch 1	-672.378
TRDN	triadin	-308.202
TNNI2	troponin I type 2 (skeletal, fast)	-135.175
TNNI3	troponin I type 3 (cardiac)	-87.453
MYH11	myosin, heavy chain 11, smooth muscle	-80.244
MYL2	myosin, light chain 2, regulatory, cardiac, slow	-63.976
CAMK2A	calcium/calmodulin-dependent protein kinase II alpha	-62.127
ATP2A2	ATPase, Ca++ transporting, cardiac muscle, slow twitch 2	-61.947
TPM3	tropomyosin 3	-49.685
RYR3	ryanodine receptor 3	-44.983
RYR1	ryanodine receptor 1 (skeletal)	-43.562
MYH2	myosin, heavy chain 2, skeletal muscle, adult	-40.062
TNNT3	troponin T type 3 (skeletal, fast)	-27.717
TNNC2	troponin C type 2 (fast)	-22.838
MYL1	myosin, light chain 1, alkali; skeletal, fast	-20.491
TNNC1	troponin C type 1 (slow)	-19.648
TNNT1	troponin T type 1 (skeletal, slow)	-14.543
CREB5	cAMP responsive element binding protein 5	-14.264
TP63	tumor protein p63	-12.987
MYH7	myosin, heavy chain 7, cardiac muscle, beta	-12.585
PRKAR2B	protein kinase, cAMP-dependent, regulatory, type II, beta	-12.425
MYH1	myosin, heavy chain 1, skeletal muscle, adult	-12.397
ACTA1	actin, alpha 1, skeletal muscle	-8.961
HDAC9	histone deacetylase 9	-8.74
CAMK2G	calcium/calmodulin-dependent protein kinase II gamma	-7.294
PRKAR2A	protein kinase, cAMP-dependent, regulatory, type II, alpha	-5.954
PPP3CB	protein phosphatase 3, catalytic subunit, beta isozyme	-5.865
ASPH	aspartate beta-hydroxylase	-5.802
NFATC1	nuclear factor of activated T-cells, cytoplasmic, calcineurin-dependent 1	-5.798
TNNI1	troponin I type 1 (skeletal, slow)	-5.744
MEF2C	myocyte enhancer factor 2C	-4.756
ACTC1	actin, alpha, cardiac muscle 1	-4.724
HDAC5	histone deacetylase 5	-4.65
CHRNA5	cholinergic receptor, nicotinic, alpha 5 (neuronal)	-4.114
ACTA2	actin, alpha 2, smooth muscle, aorta	-3.836
NFATC3	nuclear factor of activated T-cells, cytoplasmic, calcineurin-dependent 3	-3.765
HDAC10	histone deacetylase 10	-3.672
HDAC4	histone deacetylase 4	-3.585
NFATC2	nuclear factor of activated T-cells, cytoplasmic, calcineurin-dependent 2	-3.371
HDAC11	histone deacetylase 11	-3.103
MEF2D	myocyte enhancer factor 2D	-2.906
MYH14	myosin, heavy chain 14, non-muscle	-2.898
PRKAG1	protein kinase, AMP-activated, gamma 1 non-catalytic subunit	-2.803
PPP3R2	protein phosphatase 3, regulatory subunit B, beta	-2.713
PRKACA	protein kinase, cAMP-dependent, catalytic, alpha	-2.634
CALM1	calmodulin 1 (phosphorylase kinase, delta)	-2.532
HDAC8	histone deacetylase 8	-2.418
GRIN2A	glutamate receptor, ionotropic, N-methyl D-aspartate 2A	-2.359
CAMK1G	calcium/calmodulin-dependent protein kinase IG	-2.34
TRPV6	transient receptor potential cation channel, subfamily V, member 6	-2.313
ATP2A3	ATPase, Ca++ transporting, ubiquitous	-2.298
TRPC2	transient receptor potential cation channel, subfamily C, member 2	-2.298
TRPC6	transient receptor potential cation channel, subfamily C, member 6	-2.29
CALML5	calmodulin-like 5	-2.28
MYH4	myosin, heavy chain 4, skeletal muscle	-2.231
TRPC3	transient receptor potential cation channel, subfamily C, member 3	-2.065
PPP3CA	protein phosphatase 3, catalytic subunit, alpha isozyme	-2.049

Appendix 4: List of up regulated genes in mytube vs skeletal muscle tissue.

Table 1: List of up regulated genes in MT vs skeletal muscle TIS related to skeletal muscle proliferation.

ID	Prediction (based on expression direction)	Fold Change	Findings	Entrez Gene Name
POSTN	Increased	2432.253	Increases (1)	periostin, osteoblast specific factor
IL6	Increased	456.32	Increases (6)	interleukin 4 receptor
GATA6	Increased	198.633	Increases (2)	GATA binding protein 6
RGS4	Decreased	131.933	Decreases (1)	regulator of G-protein signaling 4
IGFBP3	Decreased	98.432	Decreases (1)	insulin-like growth factor binding protein 3
FN1	Increased	73.187	Increases (1)	fibronectin 1
MMP14	Increased	60.372	Increases (1)	matrix metallopeptidase 14 (membrane-inserted)
TNC	Increased	47.24	Increases (1)	tenascin C
VCAN	Increased	39.177	Increases (1)	versican
HMGA2	Increased	37.237	Increases (2)	high mobility group AT-hook 2
PAPPA	Increased	30.67	Increases (2)	pregnancy-associated plasma protein A, pappalysin 1
CDKN1A	Decreased	30.432	Decreases (4)	cyclin-dependent kinase 2 associated protein 2
NRG1	Increased	28.718	Increases (1)	neuregulin 1
IL1B	Increased	25.016	Increases (4)	inhibitor of kappa light polypeptide gene enhancer in B-cells, kinase gamma
HIF1A	Increased	23.93	Increases (2)	hypoxia inducible factor 1, alpha subunit (basic helix-loop-helix transcription factor)
ELN	Decreased	21.355	Decreases (4)	elastin
FGF2	Increased	20.559	Increases (29)	fibroblast growth factor 2 (basic)
FGF1	Increased	19.66	Increases (1)	fibroblast growth factor 1 (acidic)
LRP1	Decreased	17.488	Decreases (1)	low density lipoprotein receptor-related protein 1
KLF5	Increased	17.369	Increases (2)	Kruppel-like factor 5 (intestinal)
FGFR2	Increased	12.255	Increases (2)	fibroblast growth factor receptor 2
TNFRSF12A	Increased	10.952	Increases (1)	tumor necrosis factor receptor superfamily, member 12A
IGFBP4	Increased	10.278	Increases (1)	insulin-like growth factor binding protein 4
ID2	Increased	10.192	Increases (3)	inhibitor of DNA binding 2, dominant negative helix-loop-helix protein
PTGS2	Increased	9.967	Increases (1)	prostaglandin-endoperoxide synthase 2 (prostaglandin G/H synthase and cyclooxygenase)
SPARC	Decreased	9.857	Decreases (1)	secreted protein, acidic, cysteine-rich (osteonectin)
MYF5	Affected	9.234	Affects (1)	myogenic factor 5
GJA1	Affected	8.995	Affects (1)	gap junction protein, alpha 1, 43kDa
MIF	Increased	8.941	Increases (2)	macrophage migration inhibitory factor (glycosylation-inhibiting factor)
MYC	Affected	7.943	Affects (5)	v-myc myelocytomatosis viral oncogene homolog (avian)
TNFRSF10B	Affected	6.99	Affects (1)	tumor necrosis factor receptor superfamily, member 10b
NQO1	Decreased	6.5	Decreases (1)	NAD(P)H dehydrogenase, quinone 1
TFPI2	Decreased	6.439	Decreases (1)	tissue factor pathway inhibitor 2
SLC9A1	Increased	6.422	Increases (1)	solute carrier family 9, subfamily A (NHE1, cation proton antiporter 1),
F3	Increased	6.409	Increases (1)	coagulation factor II (thrombin) receptor-like 2
SOCS3	Decreased	5.694	Decreases (4)	suppressor of cytokine signaling 3
SHC1	Increased	5.685	Increases (3)	SHC (Src homology 2 domain containing) transforming protein 1
IRAK4	Increased	5.475	Increases (1)	interleukin-1 receptor-associated kinase 4
TP53	Decreased	4.933	Decreases (5)	tumor protein p53
TGFBR2	Affected	4.882	Affects (2)	transforming growth factor, beta receptor II (70/80kDa)
ATP2B1	Decreased	4.779	Decreases (1)	ATPase, Ca++ transporting, plasma membrane 1
CTNNB1	Increased	4.767	Increases (3)	catenin (cadherin-associated protein), beta 1, 88kDa
PLAT	Increased	4.667	Increases (1)	plasminogen activator, tissue
S1PR2	Increased	4.538	Increases (3)	sphingosine-1-phosphate receptor 2
HEYL	Affected	4.375	Affects (1)	hairy/enhancer-of-split related with YRPW motif-like
BDNF	Increased	4.198	Increases (1)	brain-derived neurotrophic factor
FOXP1	Decreased	3.958	Decreases (3)	forkhead box P1
ITGB1	Decreased	3.865	Decreases (2)	integrin, beta 1 (fibronectin receptor, beta polypeptide, antigen CD29 includes MDF2, MSK12)
TXN	Decreased	3.849	Decreases (1)	thioredoxin
DNAJB6	Decreased	3.693	Decreases (2)	DnaJ (Hsp40) homolog, subfamily B, member 11
PRNP	Increased	3.661	Increases (1)	prion protein
MYD88	Increased	3.517	Increases (1)	myeloid differentiation primary response gene (88)
IGFBP1	Increased	3.414	Increases (1)	insulin-like growth factor binding protein 1
GNAQ	Increased	3.138	Increases (2)	guanine nucleotide binding protein (G protein), q polypeptide
ABCC2	Decreased	3.024	Decreases (1)	ATP-binding cassette, sub-family C (CFTR/MRP), member 2
GSK3B	Decreased	3.019	Decreases (5)	glycogen synthase kinase 3 beta
CREB1	Decreased	2.988	Decreases (1)	cAMP responsive element binding protein 1
FBLN5	Affected	2.978	Affects (2)	fibulin 5
ROCK1	Increased	2.976	Increases (1)	Rho-associated, coiled-coil containing protein kinase 1
PPIA	Increased	2.899	Increases (6)	peptidylprolyl isomerase A (cyclophilin A)
TGM2	Increased	2.889	Increases (1)	transglutaminase 2 (C polypeptide, protein-glutamine-gamma-
TNFRSF1A	Decreased	2.883	Decreases (2)	tumor necrosis factor receptor superfamily, member 1A
H19	Affected	2.833	Affects (1)	H19, imprinted maternally expressed transcript (non-protein coding)
EDN1	Increased	2.827	Increases (10)	endothelin 1
IRAK1	Increased	2.724	Increases (1)	interleukin-1 receptor-associated kinase 1
ITGA6	Decreased	2.695	Decreases (1)	integrin, alpha 11
BMPR2	Decreased	2.652	Decreases (2)	bone morphogenetic protein receptor, type II (serine/threonine kinase)
RAB1A	Increased	2.636	Increases (7)	RAB13, member RAS oncogene family
NFE2L2	Decreased	2.576	Decreases (1)	nuclear factor (erythroid-derived 2)-like 2
PTPN11	Increased	2.485	Increases (1)	protein tyrosine phosphatase-like (proline instead of catalytic arginine), member b
KRAS	Affected	2.418	Affects (1)	v-Ki-ras2 Kirsten rat sarcoma viral oncogene homolog
ABCC4	Increased	2.232	Increases (1)	ATP-binding cassette, sub-family C (CFTR/MRP), member 4
TLR4	Increased	2.216	Increases (1)	toll-like receptor 4
NOG	Decreased	2.168	Decreases (3)	noggin
YAP1	Increased	2.113	Increases (3)	Yes-associated protein 1
PLCE1	Increased	2.103	Increases (9)	phospholipase C, epsilon 1
EPC1	Affected	2.1	Affects (1)	enhancer of polycomb homolog 1 (Drosophila)
MYOG	Increased	2.096	Increases (1)	myogenin (myogenic factor 4)
TNFAIP3	Decreased	2.05	Decreases (1)	tumor necrosis factor, alpha-induced protein 3
CCDC88A	Increased	2.048	Increases (1)	coiled-coil domain containing 88A
PTEN	Decreased	2.048	Decreases (1)	phosphatase and tensin homolog
HMGB1	Increased	2.034	Increases (1)	high mobility group box 1
MKL1	Affected	2.02	Affects (1)	megakaryoblastic leukemia (translocation) 1
PRKCA	Increased	2.001	Increases (4)	protein kinase C, alpha

Appendix 5: RNA Electorpherogram Summary.

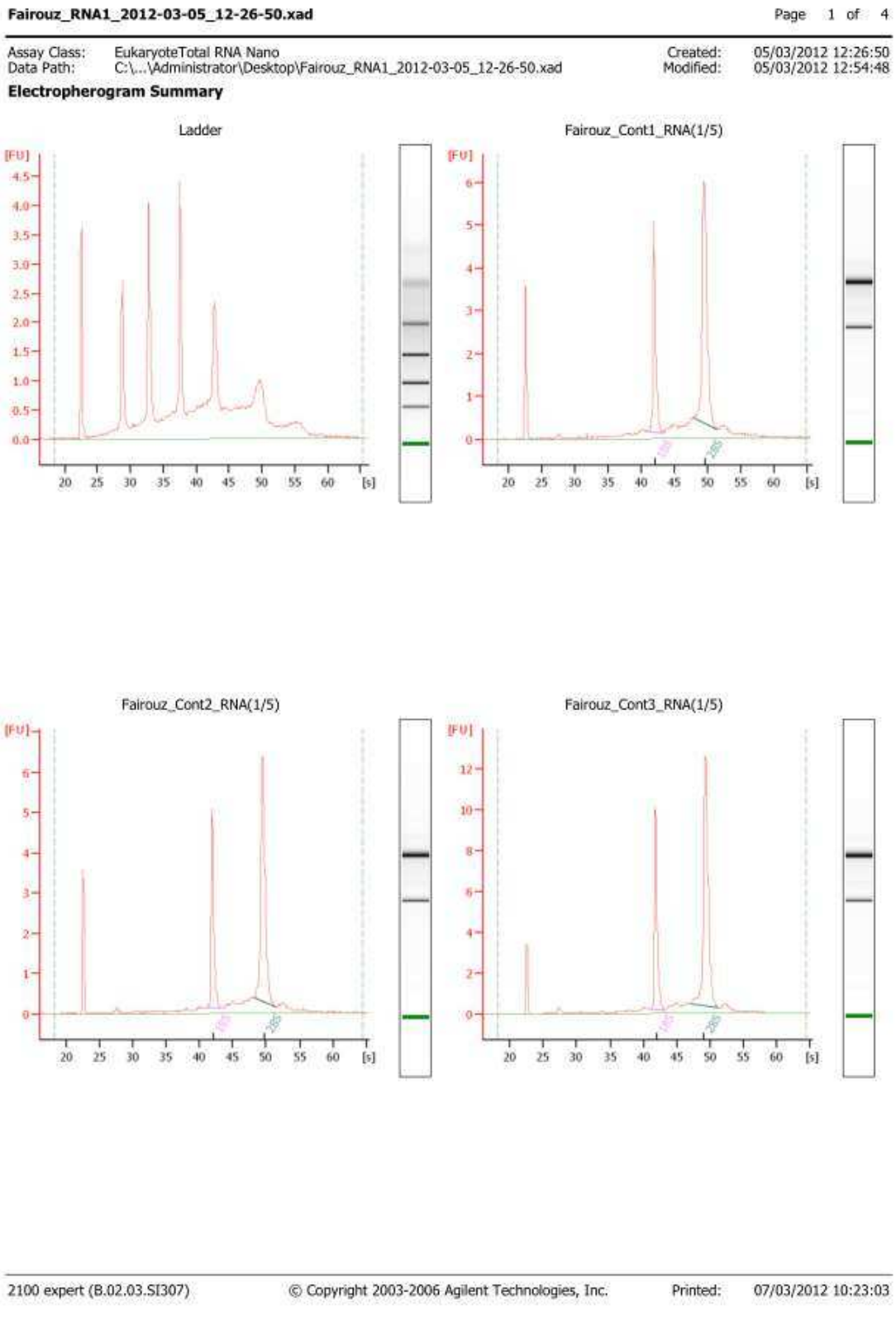

Appendix 6: List of genes regulated by GPR40 agonist.

Table 1: The effect of GPR40 agonist (100nM AZ921) on mRNA expression in himan myotubes

ID	Fold Change	Entrez Gene Name
PCSK1	3.702	proprotein convertase subtilisin/kexin type 1
BMP6	3.049	bone morphogenetic protein 6
CENPF	2.390	centromere protein F, 350/400kDa (mitosin)
LOC100131564	2.086	uncharacterized LOC100131564
MALAT1	2.063	metastasis associated lung adenocarcinoma transcript 1 (non-protein coding)
HNRNPA2B1	2.057	heterogeneous nuclear ribonucleoprotein A2/B1
PDE4D	2.057	phosphodiesterase 4D, cAMP-specific
AHSA2	2.001	AHA1, activator of heat shock 90kDa protein ATPase homolog 2 (yeast)
RPL10	1.999	ribosomal protein L10
ASPM	1.971	asp (abnormal spindle) homolog, microcephaly associated (Drosophila)
FGF7	1.951	fibroblast growth factor 7
SFRS3	1.911	serine/arginine-rich splicing factor 3
P4HA3	1.907	prolyl 4-hydroxylase, alpha polypeptide III
ZBTB20	1.893	zinc finger and BTB domain containing 20
HES1	1.869	hairy and enhancer of split 1, (Drosophila)
NEAT1	1.846	nuclear paraspeckle assembly transcript 1 (non-protein coding)
RBM25	1.843	RNA binding motif protein 25
ATRX	1.842	alpha thalassemia/mental retardation syndrome X-linked
SFRS18	1.840	PNN-interacting serine/arginine-rich protein
PLD1	1.805	phospholipase D1, phosphatidylcholine-specific
PHIP	1.799	pleckstrin homology domain interacting protein
COL3A1	1.789	collagen, type III, alpha 1
DST	1.784	dystonin
PNN	1.779	pinin, desmosome associated protein
HNRNPD	1.756	heterogeneous nuclear ribonucleoprotein D (AU-rich element RNA binding protein 1, 37kDa)
BNC2	1.754	basonuclin 2
TOP2A	1.739	topoisomerase (DNA) II alpha 170kDa
EFHC1	1.735	EF-hand domain (C-terminal) containing 1
NOTCH2NL	1.724	notch 2 N-terminal like
DTWD1	1.722	DTW domain containing 1
PDK3	1.711	pyruvate dehydrogenase kinase, isozyme 3
MEG3	1.696	maternally expressed 3 (non-protein coding)
RASEF	1.691	RAS and EF-hand domain containing
MIR214	1.684	microRNA 214
ANGPTL2	1.680	angiopoietin-like 2
REV3L	1.661	REV3-like, polymerase (DNA directed), zeta, catalytic subunit
OBSL1	1.645	obscurin-like 1
ABCA1	1.644	ATP-binding cassette, sub-family A (ABC1), member 1
NKTR	1.644	natural killer-tumor recognition sequence
CCNL1	1.639	cyclin L1
RBBP6	1.635	retinoblastoma binding protein 6
EML4	1.632	echinoderm microtubule associated protein like 4
CCNL2	1.631	cyclin L2
C7orf63	1.628	chromosome 7 open reading frame 63
NFIA	1.624	nuclear factor I/A
PDE7B	1.624	phosphodiesterase 7B
ZNF696	1.619	zinc finger protein 696
ARGLU1	1.605	arginine and glutamate rich 1

Data have fold changes ≥ 1.5 and P value ≤ 0.05 (analysed with Unpaired TTest followed by Benjamini-Hochberg test)

Table 1: (Continued)

ID	Fold Change	Entrez Gene Name
CADM4	1.605	cell adhesion molecule 4
CRYBG3	1.601	beta-gamma crystallin domain containing 3
EIF3B	1.599	eukaryotic translation initiation factor 3, subunit B
SNHG12	1.597	small nucleolar RNA host gene 12 (non-protein coding)
AHI1	1.587	Abelson helper integration site 1
ARID4B	1.582	AT rich interactive domain 4B (RBP1-like)
PPAP2B	1.579	phosphatidic acid phosphatase type 2B
CCDC14	1.573	coiled-coil domain containing 14
SF3B1	1.567	splicing factor 3b, subunit 1, 155kDa
TMEM161B	1.560	transmembrane protein 161B
ZNF638	1.560	zinc finger protein 638
ZSCAN5A	1.559	zinc finger and SCAN domain containing 5A
PLEKHN1	1.555	pleckstrin homology domain containing, family N member 1
RPL18	1.555	ribosomal protein L18
SRSF7	1.552	serine/arginine-rich splicing factor 7
GOLGA8A	1.550	golgin A8 family, member B
LUC7L3	1.546	LUC7-like 3 (S. cerevisiae)
ITGA8	1.545	integrin, alpha 8
SLK	1.545	STE20-like kinase
LRCH4	1.540	leucine-rich repeats and calponin homology (CH) domain containing 4
FAM176B	1.538	eva-1 homolog B (C. elegans)
SMC4	1.529	structural maintenance of chromosomes 4
NIPBL	1.528	Nipped-B homolog (Drosophila)
NCRNA00107	1.524	long intergenic non-protein coding RNA 685
ZFC3H1	1.523	zinc finger, C3H1-type containing
CEP350	1.522	centrosomal protein 350kDa
RORA	1.519	RAR-related orphan receptor A
FLJ44342	1.517	uncharacterized LOC645460
DYNC2H1	1.516	dynein, cytoplasmic 2, heavy chain 1
PLAGL1	1.516	pleiomorphic adenoma gene-like 1
ABCC5	1.515	ATP-binding cassette, sub-family C (CFTR/MRP), member 5
KTN1	1.512	kinectin 1 (kinesin receptor)
EIF5B	1.505	eukaryotic translation initiation factor 5B
RRP9	1.503	ribosomal RNA processing 9, small subunit (SSU) processome component, homolog (yeast)
SIP1	-1.501	gem (nuclear organelle) associated protein 2
FAM43A	-1.502	family with sequence similarity 43, member A
MRS2	-1.502	MRS2 magnesium homeostasis factor homolog (S. cerevisiae)
CDK8	-1.503	cyclin-dependent kinase 8
CARS	-1.504	cysteinyl-tRNA synthetase
SMEK1	-1.514	SMEK homolog 1, suppressor of mek1 (Dictyostelium)
BRAP	-1.520	BRCA1 associated protein
MEGF6	-1.531	multiple EGF-like-domains 6
CLIC3	-1.534	chloride intracellular channel 3
SIGLEC15	-1.535	sialic acid binding Ig-like lectin 15
NHLRC3	-1.537	NHL repeat containing 3
CMKLR1	-1.540	chemokine-like receptor 1
KCND3	-1.544	potassium voltage-gated channel, Shal-related subfamily, member 3
C16orf72	-1.550	chromosome 16 open reading frame 72
HS6ST2	-1.553	heparan sulfate 6-O-sulfotransferase 2

Table 1: (Continued)

ID	Fold Change	Entrez Gene Name
MYO5B	-1.554	myosin VB
CXorf38	-1.555	chromosome X open reading frame 38
IL32	-1.556	interleukin 32
ZNF599	-1.560	zinc finger protein 599
PDGFA	-1.568	platelet-derived growth factor alpha polypeptide
DKK2	-1.578	dickkopf 2 homolog (Xenopus laevis)
ANXA3	-1.590	annexin A3
ARHGAP26	-1.590	Rho GTPase activating protein 26
CHST7	-1.593	carbohydrate (N-acetylglucosamine 6-O) sulfotransferase 7
NEDD9	-1.598	neural precursor cell expressed, developmentally down-regulated 9
ATP8B1	-1.603	ATPase, aminophospholipid transporter, class I, type 8B, member 1
BCAT1	-1.610	branched chain amino-acid transaminase 1, cytosolic
CCBE1	-1.613	collagen and calcium binding EGF domains 1
APBB2	-1.617	amyloid beta (A4) precursor protein-binding, family B, member 2
SUMO1	-1.620	SMT3 suppressor of mif two 3 homolog 1 (S. cerevisiae)
JAG1	-1.621	jagged 1
DOPEY2	-1.623	dopey family member 2
PCDH19	-1.626	protocadherin 19
INHBE	-1.629	inhibin, beta E
PAQR5	-1.632	progestin and adipoQ receptor family member V
C5orf46	-1.639	chromosome 5 open reading frame 46
HDAC9	-1.639	histone deacetylase 9
PRR16	-1.639	proline rich 16
SDPR	-1.649	serum deprivation response
FRMD4B	-1.654	FERM domain containing 4B
SRD5A1	-1.656	steroid-5-alpha-reductase, alpha polypeptide 1 (3-oxo-5 alpha-steroid delta 4-dehydrogenase alpha 1)
HERPUD2	-1.686	HERPUD family member 2
ADRA2A	-1.728	adrenoceptor alpha 2A
EHD1	-1.729	EH-domain containing 1
COL13A1	-1.737	collagen, type XIII, alpha 1
MKX	-1.742	mohawk homeobox
LPXN	-1.746	leupaxin
LYPD6B	-1.752	LY6/PLAUR domain containing 6B
DTX4	-1.754	deltex homolog 4 (Drosophila)
KLF5	-1.755	Kruppel-like factor 5 (intestinal)
CDC42EP5	-1.764	CDC42 effector protein (Rho GTPase binding) 5
COL11A1	-1.764	collagen, type XI, alpha 1
TGFB2	-1.769	transforming growth factor, beta 2
C14orf28	-1.777	chromosome 14 open reading frame 28
LASS6	-1.810	ceramide synthase 6
SLC24A3	-1.876	solute carrier family 24 (sodium/potassium/calcium exchanger), member 3
C1orf85	-1.892	chromosome 1 open reading frame 85
CITED2	-1.914	Cbp/p300-interacting transactivator, with Glu/Asp-rich carboxy-terminal domain, 2
NRXN3	-1.930	neurexin 3
RGS4	-1.958	regulator of G-protein signaling 4
OPCML	-2.047	opioid binding protein/cell adhesion molecule-like